DYNAMIC MODELIGN AND CONTROL OF A ZETA CONVERTER

VUTHCHHAY ENG

A THESIS SUBMITTED IN PARTIAL FULFILLMENT
OF THE REQUIREMENT FOR THE DEGREE OF
MASTER OF ENGINEERING IN CONTROL ENGINEERING
FACULTY OF ENGINEERING
KING MONGKUT'S INSTITUTE OF TECHNOLOGY LADKRABANG
2009

KMITL 2009-EN-M-080-025

หัวข้อวิทยานิพนธ์	การจำลองแบบและควบคุมวงจรซีต้าคอนเวอร์เตอร์
นักศึกษา	วุธชาย อิง
รหัสนักศึกษา	50060551
ปริญญา	วิศวกรรมศาสตร์มหาบัณฑิต
สาขาวิชา	วิศวกรรมระบบควบคุม
พ.ศ.	2552
อาจารย์ที่ปรึกษาวิทยานิพนธ์	รศ. ดร. ชนินทร์ บุญลักษณานุสรณ์

บทคัดย่อ

วงจรดีซี-ดีซีคอนเวอร์เตอร์ซึ่งประกอบด้วย วงจรชุค ซีปีค และซีต้าคอนเวอร์เตอร์ สามารถทำงานได้ทั้งแบบเพิ่มและลดแรงดันไฟฟ้าอินพุท คุณสมบัตินี้ทำให้วงจรมีความเหมาะสมในการใช้งานที่แบตเตอรี่เป็นแรงดันอินพุท แรงดันโหลดเป็นดีซีคงที่ โดยแรงดันแบตเตอร์รี่อาจมีค่าสูงกว่าหรือต่ำกว่าแรงดันโหลด เมื่อเทียบกับวงจรชุคและซีปีคคอนเวอร์เตอร์ วงจรซีต้าคอนเวอร์เตอร์ได้รับความสนใจน้อยมาก และยังไม่พบว่ามีการศึกษาการจำลองแบบและการควบคุมวงจรชนิดนี้มาก่อน ดังนั้นวิทยานิพนธ์จึงทำการศึกษาการจำลองแบบและควบคุมวงจรซีต้าคอนเวอร์เตอร์ เทคนิคการจำลองแบบวงจรดีซี-ดีซีคอนเวอร์เตอร์ที่เป็นที่รู้จักดี 3 วิธีซึ่งประกอบไปด้วย วิธี สเตทสเปซเฉลี่ย วิธีแบบจำลองสวิทช์พีดับเบิวเอ็ม วิธีแบบจำลองสวิทช์เฉลี่ย ได้ถูกนำมาใช้เพื่อหาแบบจำลองที่สภาวะคงตัวและแบบจำลองเชิงเส้นสัญญาณขนาดเล็กของวงจร ซีต้าคอนเวอร์เตอร์แบบจำลองสัญญาณขนาดเล็กนี้สามารถนำไปหาฟังชั่นถ่ายโอนต่างของวงจรคอนเวอร์เตอร์ซึ่งจะถูกนำมาใช้ในการออกแบบตัวชดเชยป้อนกลับสำหรับการควบคุมแบบแรงดันและการควบคุมแบบกระแส ในตอนท้ายของวิทยานิพนธ์จะนำเสนอผลการเปรียบเทียบระหว่างการสร้างแบบจำลองและผลการทดลองจริงเพื่อยืนยันความถูกต้องของแบบจำลองที่หาได้และแสดงสมรรถนะในการควบคุมแรงดันเอาพุทโดยตัวชดเชยป้อนกลับที่ได้ออกแบบ

Thesis Title	Dynamic Modeling and Control of a Zeta converter
Student	Mr. Vuthchhay Eng
Student ID.	50060551
Degree	Master of Engineering
Program	Control Engineering
Year	2009
Thesis Advisor	Assoc. Prof. Dr. Chanin Bunlaksananusorn

ABSTRACT

Forth-order DC-DC converters, which include Cuk, SEPIC (Single-Ended Primary Inductor Converter), and Zeta converters, are capable of operating in either step-up or step-down mode. This property makes them attractive in the battery-operated applications, where the battery voltage can be higher or lower than the load voltage. Compared with Cuk and SEPIC converters, Zeta converter has received the least attention and, most importantly, its dynamic modeling and control have never been reported before in the literature. This thesis presents dynamic modeling and control of Zeta converters in both Continuous Conduction Mode (CCM) and Discontinuous Conduction Mode (DCM). Three well-known modeling methods: State-Space Averaging (SSA), PWM-switch model, and averaged switch model are applied to find steady state and linear small-signal models of the converter. Based on the small-signal models, various transfer functions of the converter are derived and used in feedback compensator design for Voltage Mode Control (VMC) and Peak Current Mode Control (PCMC) schemes. The validity of the derived models, as well as the control performance, is verified by simulated and experimental results.

Acknowledgements

I am deeply indebted to my supervisor, Dr. Chanin Bunlaksananusorn, for his encouragement and guidance, combined with the good leadership and teaching; that is, all lead me to my academic and professional development.

I would like to express my sincere thank to all the professors, lecturers, and staffs of Control Engineering Department, who always continuously encouraged, helped, and provided me facilities during the whole period of my study.

My deep thanks go to ASEAN University Network/Southeast Asia Engineering Education Development Network (AUN/Seed-Net) for awarding me the scholarship to study in Thailand where I can produce this thesis. AUN/Seed-Net also provides me all the financial support for the research and study.

I would like to thank to Institute of Technology of Cambodia (ITC) that gave me the opportunity to pursue my study.

I am grateful for all my friends in both Cambodia and Thailand who always encouraged and helped me during the time of my study. Throughout my years at KMITL, I can earn and enrich my life with companion and friendship.

I would like to express all my gratitude to my parents for their emotional and financial support, as well as encouragement and guidance. More importantly, they have been always providing continuous encouragement, love, guidance, and support. They were the first to teach me the beauty and value of life, art, and science.

Contents

Contents (Continued)

Contents (Continued)

List of Tables

List of Figures

Contents (Continued)

Contents (Continued)

Contents (Continued)

Contents (Continued)

Chapter 1

Introduction

1.1 Overview

Nowadays, the use of a DC-DC converter is widespread in modern portable electronic equipment and systems. In the battery-operated portable devices, when not connected to the AC mains, the battery provides an input voltage to the converter, which then converts it into the output voltage suitable for use by the electronic load. The battery voltage can vary over a wide range, depending on a charge level. At the low charge level, it may drop below the load voltage. Hence, to continue supplying the constant load voltage over the entire battery voltage range, the converter must be able to work in both buck and boost modes. The DC-DC converters that meet this operational requirement are buck-boost, Cuk, SEPIC (Single-Ended Primary Inductor Converter), and Zeta converters. However, the buck-boost and Cuk converters, in their basic form, produce the output voltage, whose polarity is reversed from the input voltage. The problem can be corrected by incorporating an isolation transformer into the circuits, but this will inevitably lead to the increased size and cost of the converters. On the other hand, SEPIC (Single-Ended Primary Inductor Converter) and Zeta converters are capable of operating in both step-up and step-down modes and do not suffer from the polarity reversal problem. They are therefore attractive for the aforementioned application.

Both SEPIC and Zeta converter circuits consist of an active power switch (e.g. MOSFET), a diode, two inductors, and two capacitors and thus are a fourth-order nonlinear system. There are two possible modes of operation in the SEPIC and Zeta converters: Continuous Conduction Mode (CCM) and Discontinuous Conduction Mode (DCM). Although the converters are usually designed for the CCM operation, they can plunge into DCM at light loads. In some cases, the converters are even intentionally designed to operate in DCM, because of the faster dynamic response. It is therefore essential to understand the characteristics of the converters in both operational modes. Furthermore, Pulse Width Modulation (PWM) control is usually incorporated into the converter circuit to regulate its output voltage. In this regard, a dynamic model of the converters is required to facilitate the feedback control design.

1.2 Literature review and research objective

Modeling plays a key role in revealing the insight of the converters' dynamic behavior as well as providing a basis for feedback control design. Three well-known modeling techniques for DC-DC converters include State Space Averaging (SSA) technique [1-10], PWM-switch model [11-17], and Averaged switch model [18-20]. The SEPIC converter has been extensively studied by many groups of researchers. Modeling of the SEPIC converter by the SSA technique has been published in [3, 6-8], by the PWM-switch model in [14-16], and by the averaged switch model in [18, 20]. On the contrary, the Zeta converter is the least known converter as compared to its fourth-order counterparts such as Cuk or SEPIC converter. More importantly, unlike the SEPIC converter, modeling of the Zeta converter has never been performed and reported before in the literature.

Therefore, the objective of this thesis is to study dynamic modeling and control of a Zeta converter. The three abovementioned modeling techniques are applied to find steady-state and linear small-signal models of Zeta converter operating in CCM and DCM. Voltage Mode Control (VMC) and Peak Current Mode Control (PCMC) [18, 21-23] are the two control methods adopted to regulate an output voltage of the converter. Based on these control schemes and the small-signal models of Zeta converter, a variety of the feedback compensators are designed to provide the converter good stability, tight output regulation and fast transient response.

1.3 Assumption of this study

The converter's model derivation and feedback compensator design are carried out for four circuit categories: (1) CCM Zeta converter with VMC, (2) DCM Zeta converter with VMC, (3) CCM Zeta converter with PCMC, and (4) DCM Zeta converter with PCMC. To evaluate the performance of the designed feedback compensators, the Zeta converter in category (1) is simulated using SIMULINK, and the performances of the Zeta converter in categories (2), (3), and (4) are simulated and tested by step responses in MATLAB. The prototype Zeta converter in category (1) is then built and tested to allow the performance of the designed feedback compensator to be evaluated experimentally.

1.4 Thesis structure

The thesis is organized as follows:

Chapter 2 – Modeling of Zeta Converters In Continuous Conduction Mode (CCM) – Three modeling methods for DC-DC converters in CCM, i.e. SSA technique, PWM-switch model, and averaged switch model, are reviewed and applied to model the Zeta converter. The converter's models obtained from the three methods are compared.

Chapter 3 – Modeling of Zeta Converters In Discontinuous Conduction Mode (DCM) – The organization is the same as in Chapter 2 in that the three modeling methods in DCM are reviewed and applied to model the Zeta converter, with the comparison of modeling results concluded the Chapter.

Chapter 4 – Control of Zeta Converter – Operation of Voltage Mode Control (VMC) and Peak Current Mode Control (PCMC) are described. Block diagrams of Zeta converter with VMC and PCMC are given, which will be used for feedback compensator design in Chapter 5.

Chapter 5 – Design of Feedback Compensator – Feedback compensator design is performed for CCM/DCM Zeta converters with VMC and PCMC, based on the small-signal models obtained in Chapters 2 and 3, and the control block diagrams in Chapter 4.

Chapter 6 – Results – Simulated and experimental results are presented.

Chapter 7 – Conclusion – This chapter provides a summary of the thesis's outcomes.

Chapter 2

Modeling of Zeta Converter Operating in Continuous Conduction Mode (CCM)

This chapter first describes basic operation of CCM Zeta converter. State-Space Averaging (SSA) technique is then reviewed and applied to model Zeta converter [1-10]. Modeling of Zeta converter by other well-known techniques such as PWM-switch model [11-17] and Averaged switch model [18-20] is also presented.

2.1 Zeta Converter in CCM

Fig. 2.1(a) shows a Zeta converter which is comprised of the MOSFET switch (Q), diode (D), two capacitors (C_1 and C_2), and two inductors (L_1 and L_2). The resistor, R, represents a standing load, and the current source, I_Z, models the load current. The resistors, r_{C1}, r_{C2}, r_{L1}, and r_{L2}, are Equivalent Series Resistances (ESRs) of the capacitors and inductors respectively. Although their values are practically very small compared to R, these ESRs cannot be neglected in the modeling process as they can affect the accuracy of the final model. In the ideal converter, these ESRs are assumed to be zero.

In CCM, the converter exhibits two circuit states. The first state is when the MOSFET switch is turned on (Fig. 2.1(b)). During this interval (dT), L_1 is charged by the source, V_g, and L_2 by the capacitor C_1. Hence i_{L1} and i_{L2} increase linearly, as shown in Fig. 2.2. The second state is when the MOSFET switch is turned off (Fig. 2.1(c)). During this interval ($(1-d)T$), L_1 and L_2 are in a discharging phase; L_1 and L_2 release the stored energy to the capacitors and load respectively. Thus, i_{L1} and i_{L2} decrease linearly as shown in Fig. 2.2. The output voltage, V_O, is a DC voltage that contains small ripple due to the switching action. For ideal Zeta converter, the relationship between V_O and V_g is given by:

$$M = \frac{V_O}{V_g} = \frac{d}{1-d} \tag{2.1-1}$$

where M is a voltage conversion ratio. It should be noted that V_O could be larger or smaller than V_g, depending on the duty cycle, d ($0< d <1$). From Fig. 2.2, the averaged inductor currents, I_{L1} and I_{L2}, must be greater than one-half of their ripple components, Δi_{L1} and Δi_{L2}, for the circuit to remain in CCM [24]. It can be found that for CCM Zeta converter, L_1 and L_2 must satisfy the following conditions (**Appendix A**):

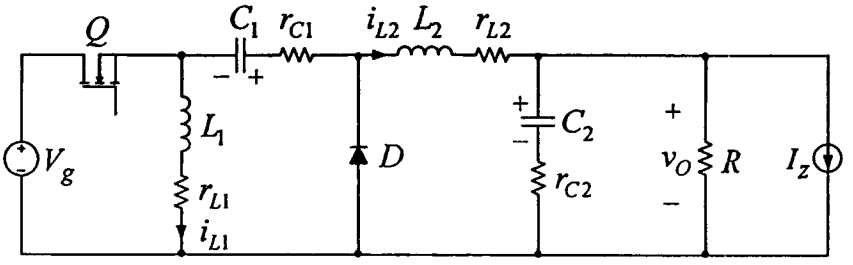

(a) Zeta converter.

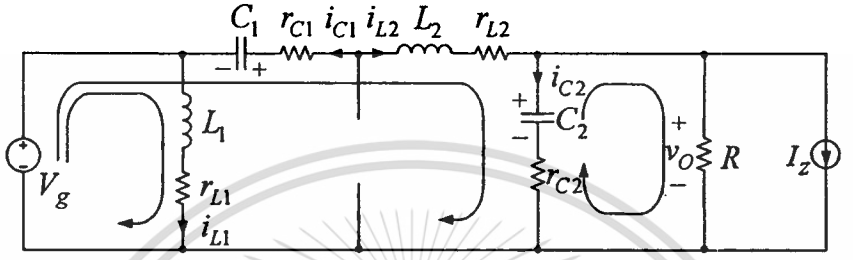

(b) Zeta converter when MOSFET is turned on.

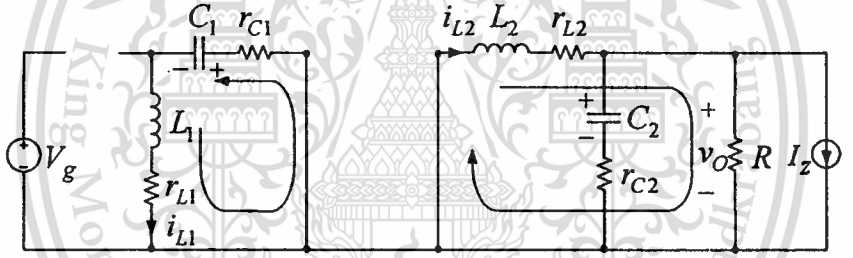

(c) Zeta converter when MOSFET is turned off.

Fig. 2.1. Operation of Zeta converter.

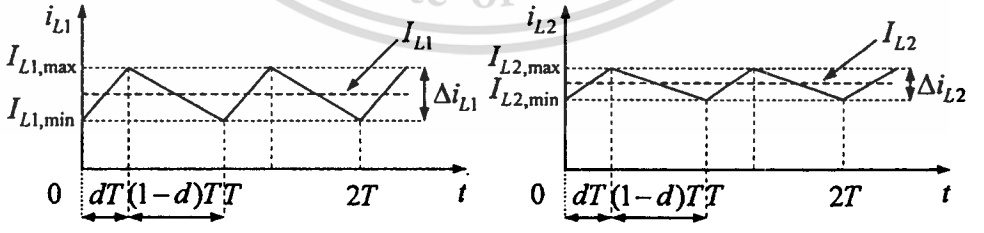

(a) i_{L1} waveform. (b) i_{L2} waveform.

Fig. 2.2. Inductor Current waveforms of Zeta converter.

$$\begin{cases} L_1 > \dfrac{(1-D)^2 R}{2Df}\left(1+\dfrac{r_{L2}}{R}+\dfrac{r_{C1}}{R}\dfrac{D}{1-D}\right) \\ L_2 > \dfrac{(1-D)R}{2f}\left(1+\dfrac{r_{L2}}{R}\right) \end{cases} \quad (2.1\text{-}2)$$

2.2 Modeling of CCM Zeta Converter with State-Space Averaging (SSA) Technique

2.2.1 Overview of SSA Technique in CCM

The State-Space Averaging (SSA) technique [1-10] is an effective method of modeling DC-DC converters. It is a matrix-based technique in that all steps in the modeling are performed in a matrix form. Hence, formal matrix treatment can be applied to facilitate the modeling process. The SSA modeling consists of three steps: (1) Formulation of state-space equations of the converter for each subinterval in a switching cycle, (2) Average of these equations to get a single averaged state-space equation, and (3) Perturbation of the averaged equation to get a linear small-signal state-space equation, from which various transfer functions can be determined.

For the DC-DC converters operating in CCM, there exist two power circuit states within one switching period, *T*. One is when the MOSFET is turned on for an interval *dT*, and another is when the MOSFET is turned off for an interval *(1-d)T*, where *d* is a duty cycle. The state-space equations for these two circuit states are:

$$\begin{cases} \dfrac{d\mathbf{x}(t)}{dt} = \mathbf{A}_1\mathbf{x}(t) + \mathbf{B}_1\mathbf{u}(t) \\ \mathbf{y}(t) = \mathbf{C}_1\mathbf{x}(t) + \mathbf{E}_1\mathbf{u}(t) \end{cases} \quad (2.2.1\text{-}1)$$

$$\begin{cases} \dfrac{d\mathbf{x}(t)}{dt} = \mathbf{A}_2\mathbf{x}(t) + \mathbf{B}_2\mathbf{u}(t) \\ \mathbf{y}(t) = \mathbf{C}_2\mathbf{x}(t) + \mathbf{E}_2\mathbf{u}(t) \end{cases} \quad (2.2.1\text{-}2)$$

To find the averaged behavior of the converter over one switching period, (2.2.1-1) and (2.2.1-2) are weighed average by the duty cycle, *d*:

$$\begin{cases} \dfrac{d<\mathbf{x}(t)>}{dt} = \mathbf{A}_s<\mathbf{x}(t)> + \mathbf{B}_s<\mathbf{u}(t)> \\ <\mathbf{y}(t)> = \mathbf{C}_s<\mathbf{x}(t)> + \mathbf{E}_s<\mathbf{u}(t)> \end{cases} \quad (2.2.1\text{-}3)$$

where $\mathbf{A}_s = \mathbf{A}_1 d_1 + \mathbf{A}_2(1-d)$, $\mathbf{B}_s = \mathbf{B}_1 d_1 + \mathbf{B}_2(1-d)$, $\mathbf{C}_s = \mathbf{C}_1 d + \mathbf{C}_2(1-d)$, and $\mathbf{E}_s = \mathbf{E}_1 d + \mathbf{E}_2(1-d)$.

Note that the variables with bracket < > represent the average value. Equation (2.2.1-3) is a nonlinear continuous-time equation. It can be linearized by small-signal perturbation with $<\mathbf{x}>=\mathbf{X}+\tilde{\mathbf{x}}$, $<\mathbf{y}>=\mathbf{Y}+\tilde{\mathbf{y}}$, $<\mathbf{u}>=\mathbf{U}+\tilde{\mathbf{u}}$, and $d=D+\tilde{d}$, where the tilde symbol, $\tilde{\ }$, represents a small signal value and the capital letter a DC value. It should be noted that $\mathbf{X} \gg \tilde{\mathbf{x}}$, $\mathbf{Y} \gg \tilde{\mathbf{y}}$, $\mathbf{U} \gg \tilde{\mathbf{u}}$, and $D \gg \tilde{d}$. Substituting the perturbation above into (2.2.1-3) gives:

$$\begin{cases} \dfrac{d}{dt}(\mathbf{X}+\tilde{\mathbf{x}}) = [\mathbf{A}_1(D+\tilde{d}) + \mathbf{A}_2(1-D-\tilde{d})](\mathbf{X}+\tilde{\mathbf{x}}) + [\mathbf{B}_1(D+\tilde{d}) + \mathbf{B}_2(1-D-\tilde{d})](\mathbf{U}+\tilde{\mathbf{u}}) \\ \mathbf{Y}+\tilde{\mathbf{y}} = [\mathbf{C}_1(D+\tilde{d}) + \mathbf{C}_2(1-D-\tilde{d})](\mathbf{X}+\tilde{\mathbf{x}}) + [\mathbf{E}_1(D+\tilde{d}) + \mathbf{E}_2(1-D-\tilde{d})](\mathbf{U}+\tilde{\mathbf{u}}) \end{cases} \quad (2.2.1\text{-}4\text{-a})$$

Rearranging (2.2.1-4-a) yields:

$$\begin{cases} \dfrac{d}{dt}(\mathbf{X}+\tilde{\mathbf{x}}) = [\mathbf{A}_1 D + \mathbf{A}_2(1-D)]\mathbf{X} + [\mathbf{B}_1 D + \mathbf{B}_2(1-D)]\mathbf{U} + [\mathbf{A}_1 D + \mathbf{A}_2(1-D)]\tilde{\mathbf{x}} \\ \quad + [\mathbf{B}_1\tilde{d} + \mathbf{B}_2(1-D)]\tilde{\mathbf{u}} + [(\mathbf{A}_1 - \mathbf{A}_2)\mathbf{X} + (\mathbf{B}_1 - \mathbf{B}_2)\mathbf{U}]\tilde{d} + [(\mathbf{A}_1 - \mathbf{A}_2)\tilde{\mathbf{x}} + (\mathbf{B}_1 - \mathbf{B}_2)\tilde{\mathbf{u}}]\tilde{d} \\ \mathbf{Y} + \tilde{\mathbf{y}} = [\mathbf{C}_1 D + \mathbf{C}_2(1-D)]\mathbf{X} + [\mathbf{E}_1 D + \mathbf{E}_2(1-D)]\mathbf{U} + [\mathbf{C}_1 D + \mathbf{C}_2(1-D)]\tilde{\mathbf{x}} \\ \quad + [\mathbf{E}_1 D + \mathbf{E}_2(1-D)]\tilde{\mathbf{u}} + [(\mathbf{C}_1 - \mathbf{C}_2)\mathbf{X} + (\mathbf{E}_1 - \mathbf{E}_2)\mathbf{U}]\tilde{d} + [(\mathbf{C}_1 - \mathbf{C}_2)\tilde{\mathbf{x}} + (\mathbf{E}_1 - \mathbf{E}_2)\tilde{\mathbf{u}}]\tilde{d} \end{cases} \quad (2.1.1\text{-}4\text{-b})$$

Steady-state equation is obtained by collecting the DC terms from (2.2.1-4-b):

$$\begin{cases} \dfrac{d\mathbf{X}}{dt} = \mathbf{AX} + \mathbf{BU} = 0 \\ \mathbf{Y} = \mathbf{CX} + \mathbf{EU} \end{cases} \quad (2.2.1\text{-}5\text{-a})$$

where $\mathbf{A} = \mathbf{A}_1 D + \mathbf{A}_2(1-D)$, $\mathbf{B} = \mathbf{B}_1 D + \mathbf{B}_2(1-D)$, $\mathbf{C} = \mathbf{C}_1 D + \mathbf{C}_2(1-D)$, and $\mathbf{E} = \mathbf{E}_1 D + \mathbf{E}_2(1-D)$.

The steady-state solution can be found by solving (2.2.1-5-a), which gives:

$$\begin{cases} \mathbf{X} = -\mathbf{A}^{-1}\mathbf{BU} \\ \mathbf{Y} = (-\mathbf{CA}^{-1}\mathbf{B} + \mathbf{E})\mathbf{U} \end{cases} \quad (2.2.1\text{-}5\text{-b})$$

Collecting small-signal or AC terms from (2.2.1-4-b) and neglecting the product of the two small-signal terms (e.g. $\tilde{d}.\tilde{u}=0$), the linear small-signal state-space equation is obtained as:

$$\begin{cases} \dfrac{d\tilde{\mathbf{x}}(t)}{dt} = \mathbf{A}\tilde{\mathbf{x}}(t) + \mathbf{B}\tilde{\mathbf{u}}(t) + \mathbf{B}_d\tilde{d}(t) \\ \tilde{\mathbf{y}}(t) = \mathbf{C}\tilde{\mathbf{x}}(t) + \mathbf{E}\tilde{\mathbf{u}}(t) + \mathbf{E}_d\tilde{d}(t) \end{cases} \quad (2.2.1\text{-}6\text{-a})$$

where $\mathbf{B}_d = (\mathbf{A}_1 - \mathbf{A}_2)\mathbf{X} + (\mathbf{B}_1 - \mathbf{B}_2)\mathbf{U}$ and $\mathbf{E}_d = (\mathbf{C}_1 - \mathbf{C}_2)\mathbf{X} + (\mathbf{E}_1 - \mathbf{E}_2)\mathbf{U}$.

The small-signal transfer function of the converter can be found by applying the Laplace transform to (2.2.1-6-a). In a matrix form, we get:

$$\begin{cases} \tilde{\mathbf{x}}(s) = \begin{bmatrix} (s\mathbf{I}-\mathbf{A})^{-1}\mathbf{B} & (s\mathbf{I}-\mathbf{A})^{-1}\mathbf{B}_d \end{bmatrix} \begin{bmatrix} \tilde{\mathbf{u}}(s) \\ \tilde{d}(s) \end{bmatrix} \\ \tilde{\mathbf{y}}(s) = \begin{bmatrix} \mathbf{C}(s\mathbf{I}-\mathbf{A})^{-1}\mathbf{B} + \mathbf{E} & \mathbf{C}(s\mathbf{I}-\mathbf{A})^{-1}\mathbf{B}_d + \mathbf{E}_d \end{bmatrix} \begin{bmatrix} \tilde{\mathbf{u}}(s) \\ \tilde{d}(s) \end{bmatrix} \end{cases} \quad (2.2.1\text{-}6\text{-b})$$

In DC-DC converters, the input variable $\tilde{\boldsymbol{u}}$ usually contains input voltage and load current. Hence, $\tilde{\boldsymbol{u}}$ is expressed as $\tilde{\boldsymbol{u}} = [u_1\ u_2]^T$, the matrix **B** as $\mathbf{B}=[\mathbf{B}_{u1}\ \mathbf{B}_{u2}]$, and the matrix **E** as $\mathbf{E}=[\mathbf{E}_{u1}\ \mathbf{E}_{u2}]$. Therefore, equation (2.2.1-6-b) is expressed as:

$$\begin{cases} \tilde{\mathbf{x}}(s) = \begin{bmatrix} (s\mathbf{I}-\mathbf{A})^{-1}\mathbf{B}_{u1} & (s\mathbf{I}-\mathbf{A})^{-1}\mathbf{B}_{u2} & (s\mathbf{I}-\mathbf{A})^{-1}\mathbf{B}_d \end{bmatrix} \begin{bmatrix} \tilde{u}_1(s) \\ \tilde{u}_2(s) \\ \tilde{d}(s) \end{bmatrix} \\ \tilde{\mathbf{y}}(s) = \begin{bmatrix} \mathbf{C}(s\mathbf{I}-\mathbf{A})^{-1}\mathbf{B}_{u1} + \mathbf{E}_{u1} & \mathbf{C}(s\mathbf{I}-\mathbf{A})^{-1}\mathbf{B}_{u2} + \mathbf{E}_{u2} & \mathbf{C}(s\mathbf{I}-\mathbf{A})^{-1}\mathbf{B}_d + \mathbf{E}_d \end{bmatrix} \begin{bmatrix} \tilde{u}_1(s) \\ \tilde{u}_2(s) \\ \tilde{d}(s) \end{bmatrix} \end{cases} \quad (2.2.1\text{-}6\text{-c})$$

For the fourth-order converter, $(s\mathbf{I}-\mathbf{A})^{-1}\mathbf{B}_{u1}$, $(s\mathbf{I}-\mathbf{A})^{-1}\mathbf{B}_{u2}$, and $(s\mathbf{I}-\mathbf{A})^{-1}\mathbf{B}_d$ are the matrices that have four rows and one column. So, the equations above can be extended into:

$$\begin{cases} \tilde{\mathbf{x}}(s) = \begin{bmatrix} G_{vi_1}(s) & G_{zi_1}(s) & G_{di_1}(s) \\ G_{vi_2}(s) & G_{zi_2}(s) & G_{di_2}(s) \\ G_{vv_1}(s) & G_{zv_1}(s) & G_{dv_1}(s) \\ G_{vv_2}(s) & G_{zv_2}(s) & G_{dv_2}(s) \end{bmatrix} \begin{bmatrix} \tilde{u}_1(s) \\ \tilde{u}_2(s) \\ \tilde{d}(s) \end{bmatrix} \\ \tilde{\mathbf{y}}(s) = \begin{bmatrix} G_{vv}(s) & G_{zv}(s) & G_{dv}(s) \end{bmatrix} \begin{bmatrix} \tilde{u}_1(s) \\ \tilde{u}_2(s) \\ \tilde{d}(s) \end{bmatrix} \end{cases} \quad (2.2.1\text{-}6\text{-}d)$$

where

$$G_{vi_1}(s) = [(s\mathbf{I} - \mathbf{A})^{-1}\mathbf{B}_{u1}]_{11},\ G_{zi_1}(s) = [(s\mathbf{I} - \mathbf{A})^{-1}\mathbf{B}_{u2}]_{11},\ G_{di_1}(s) = [(s\mathbf{I} - \mathbf{A})^{-1}\mathbf{B}_{d}]_{11},$$

$$G_{vi_2}(s) = [(s\mathbf{I} - \mathbf{A})^{-1}\mathbf{B}_{u1}]_{21},\ G_{zi_2}(s) = [(s\mathbf{I} - \mathbf{A})^{-1}\mathbf{B}_{u2}]_{21},\ G_{di_2}(s) = [(s\mathbf{I} - \mathbf{A})^{-1}\mathbf{B}_{d}]_{21},$$

$$G_{vv_1}(s) = [(s\mathbf{I} - \mathbf{A})^{-1}\mathbf{B}_{u1}]_{31},\ G_{zv_1}(s) = [(s\mathbf{I} - \mathbf{A})^{-1}\mathbf{B}_{u2}]_{31},\ G_{dv_1}(s) = [(s\mathbf{I} - \mathbf{A})^{-1}\mathbf{B}_{d}]_{31},$$

$$G_{vv_2}(s) = [(s\mathbf{I} - \mathbf{A})^{-1}\mathbf{B}_{u1}]_{41},\ G_{zv_2}(s) = [(s\mathbf{I} - \mathbf{A})^{-1}\mathbf{B}_{u2}]_{41},\ G_{dv_2}(s) = [(s\mathbf{I} - \mathbf{A})^{-1}\mathbf{B}_{d}]_{41},$$

$$G_{vv}(s) = \mathbf{C}(s\mathbf{I} - \mathbf{A})^{-1}\mathbf{B}_{u1} + \mathbf{E}_{u1},\quad G_{zv}(s) = \mathbf{C}(s\mathbf{I} - \mathbf{A})^{-1}\mathbf{B}_{u2} + \mathbf{E}_{u2},\quad \text{and}$$

$$G_{dv}(s) = \mathbf{C}(s\mathbf{I} - \mathbf{A})^{-1}\mathbf{B}_{d} + \mathbf{E}_{d}.$$

2.2.2 Application of SSA Technique to model CCM Zeta Converter

A - State-Space Description of Zeta Converter

The state-space equations of the Zeta converter when the switch is on and off can be written from Fig. 2.1(b) and (c) respectively, and is given in (2.2.2-1):

$$\begin{cases} \dfrac{di_{L1}}{dt} = \dfrac{r_{C1}}{L_1}(\delta - 1)i_{L1} - \dfrac{r_{L1}}{L_1} + \dfrac{v_{C1}}{L_1}(\delta - 1) + \dfrac{V_g}{L_1}\delta \\ \dfrac{di_{L2}}{dt} = \dfrac{-1}{L_2}(r_{L2} + r_{C1}\delta + \dfrac{r_{C2}R}{r_{C2}+R})i_{L2} + \dfrac{v_{C1}}{L_2}\delta - \dfrac{R}{L_2(r_{C2}+R)}v_{C2} + \dfrac{V_g}{L_2}\delta + \dfrac{r_{C2}R}{L_2(r_{C2}+R)}I_z \\ \dfrac{dv_{C1}}{dt} = \dfrac{i_{L1}}{C_1}(1-\delta) - \dfrac{i_{L2}}{C_1}\delta \\ \dfrac{dv_{C2}}{dt} = \dfrac{R}{C_2(r_{C2}+R)}i_{L2} - \dfrac{1}{C_2(r_{C2}+R)}v_{C2} - \dfrac{R}{C_2(r_{C2}+R)}I_z \\ v_O = \dfrac{r_{C2}R}{r_{C2}+R}i_{L2} + \dfrac{R}{r_{C2}+R}v_{C2} - \dfrac{r_{C2}R}{r_{C2}+R}I_z \end{cases} \quad (2.2.2\text{-}1)$$

Note that the equations are expressed in a compact form using the switching function, δ. The derivation of this equation is detailed in **Appendix B**. When the switch is on, δ=1, (2.2.2-1) will become the on-state equation. When the switch is off, δ=0, (2.2.2-1) will become the off-state equation. The matrices $\mathbf{A}_1$, $\mathbf{A}_2$, $\mathbf{B}_1$, $\mathbf{B}_2$, $\mathbf{C}_1$, $\mathbf{C}_2$, $\mathbf{E}_1$, and $\mathbf{E}_2$ are thus given by:

$$\mathbf{A}_1=\begin{bmatrix} \frac{-r_{L1}}{L_1} & 0 & 0 & 0 \\ 0 & \frac{-1}{L_2}(r_{L2}+r_{C1}+\frac{r_{C2}R}{r_{C2}+R}) & \frac{1}{L_2} & \frac{-R}{L_2(r_{C2}+R)} \\ 0 & \frac{-1}{C_1} & 0 & 0 \\ 0 & \frac{R}{C_2(r_{C2}+R)} & 0 & \frac{-1}{C_2(r_{C2}+R)} \end{bmatrix} \quad \text{(2.2.2-2-a)}$$

$$\mathbf{B}_1=\begin{bmatrix} \frac{1}{L_1} & 0 \\ \frac{1}{L_2} & \frac{r_{C2}R}{L_2(r_{C2}+R)} \\ 0 & 0 \\ 0 & \frac{-R}{C_2(r_{C2}+R)} \end{bmatrix} \quad \text{(2.2.2-2-b)}$$

$$\mathbf{C}_1=\begin{bmatrix} 0 & \frac{r_{C2}R}{r_{C2}+R} & 0 & \frac{R}{r_{C2}+R} \end{bmatrix} \quad \text{(2.2.2-2-c)}$$

$$\mathbf{E}_1=\begin{bmatrix} 0 & \frac{-r_{C2}R}{r_{C2}+R} \end{bmatrix} \quad \text{(2.2.2-2-d)}$$

$$\mathbf{A}_2=\begin{bmatrix} \frac{-r_{L1}+r_{C1}}{L_1} & 0 & \frac{-1}{L_1} & 0 \\ 0 & \frac{-1}{L_2}(r_{L2}+\frac{r_{C2}R}{r_{C2}+R}) & 0 & \frac{-R}{L_2(r_{C2}+R)} \\ \frac{1}{C_1} & 0 & 0 & 0 \\ 0 & \frac{R}{C_2(r_{C2}+R)} & 0 & \frac{-1}{C_2(r_{C2}+R)} \end{bmatrix} \quad \text{(2.2.3-2-e)}$$

$$\mathbf{B}_2=\begin{bmatrix} 0 & 0 \\ 0 & \frac{r_{C2}R}{L_2(r_{C2}+R)} \\ 0 & 0 \\ 0 & \frac{-R}{C_2(r_{C2}+R)} \end{bmatrix} \quad \text{(2.2.2-2-e)}$$

$$\mathbf{C}_2=\begin{bmatrix} 0 & \frac{r_{C2}R}{r_{C2}+R} & 0 & \frac{R}{r_{C2}+R} \end{bmatrix} \quad \text{(2.2.3-2-f)}$$

$$\mathbf{E}_2=\begin{bmatrix} 0 & \frac{-r_{C2}R}{r_{C2}+R} \end{bmatrix} \quad \text{(2.2.2-2-g)}$$

The averaged matrices for the steady-state and the linear small-signal state-space equations can be written according to (2.2.1-5-a) and (2.2.1-6-a).

$$\mathbf{A}=\mathbf{A}_1D+\mathbf{A}_2(1-D)=\begin{bmatrix} -\frac{r_{C1}(1-D)+r_{L1}}{L_1} & 0 & -\frac{1-D}{L_1} & 0 \\ 0 & -\frac{(r_{C2}+R)(Dr_{C1}+r_{L2})+r_{C2}R}{L_2(r_{C2}+R)} & \frac{D}{L_2} & \frac{-R}{L_2(r_{C2}+R)} \\ \frac{1-D}{C_1} & \frac{-D}{C_1} & 0 & 0 \\ 0 & \frac{R}{C_2(r_{C2}+R)} & 0 & \frac{-1}{C_2(r_{C2}+R)} \end{bmatrix} \quad \text{(2.2.2-3-a)}$$

$$\mathbf{B}=\mathbf{B}_1 D+\mathbf{B}_2(1-D)=\begin{bmatrix} \frac{D}{L_1} & 0 \\ \frac{D}{L_2} & \frac{r_{C2}R}{L_2(r_{C2}+R)} \\ 0 & 0 \\ 0 & \frac{-R}{C_2(r_{C2}+R)} \end{bmatrix} \quad (2.2.2\text{-}3\text{-b})$$

$$\mathbf{C}=\mathbf{C}_1 D+\mathbf{C}_2(1-D)=\begin{bmatrix} 0 & \frac{r_{C2}R}{r_{C2}+R} & 0 & \frac{r_{C2}R}{r_{C2}+R} \end{bmatrix} \quad (2.2.2\text{-}3\text{-c})$$

$$\mathbf{E}=\mathbf{E}_1 D+\mathbf{E}_2(1-D)=\begin{bmatrix} 0 & \frac{-r_{C2}R}{r_{C2}+R} \end{bmatrix} \quad (2.2.2\text{-}3\text{-d})$$

$$\mathbf{B}_d=(\mathbf{A}_1-\mathbf{A}_2)\mathbf{X}+(\mathbf{B}_1-\mathbf{B}_2)\mathbf{U}=\frac{\eta}{R(1-D)^2}\begin{bmatrix} [V_g[(1-D)(R+r_{L2})+Dr_{C1}]-I_z Dr_{L1}R]/L_1 \\ [V_g(r_{L2}+R)(1-D)-I_z R[r_{C1}(1-D)+Dr_{L1}]]/L_2 \\ -[DV_g+RI_z(1-D)]/C_1 \\ 0 \end{bmatrix} \quad (2.2.2\text{-}3\text{-e})$$

$$\mathbf{E}_d=(\mathbf{C}_1-\mathbf{C}_2)\mathbf{X}+(\mathbf{E}_1-\mathbf{E}_2)\mathbf{U}=[0] \quad (2.2.2\text{-}3\text{-f})$$

B - Steady-State Equation

Given the averaged matrices in (2.2.2-3), the steady-state solution of converter is obtained, following (2.2.1-5-b):

$$\begin{cases} \begin{bmatrix} I_{L1} \\ I_{L2} \\ V_{C1} \\ V_{C2} \end{bmatrix} = m\eta \begin{bmatrix} D/[R(1-D)] & 1 \\ 1/R & 1/n \\ 1+r_{L2}/R-nr_{L1}/R & -[r_{C1}+r_{L1}/(1-D)] \\ 1 & -(r_{C1}+r_{L1}n+r_{L2}/n) \end{bmatrix} \begin{bmatrix} V_g \\ I_z \end{bmatrix} \\ V_o = m\eta[V_g - I_z(r_{C1}+r_{L1}n+r_{L2}/n)] \end{cases} \quad (2.2.2\text{-}4)$$

where $\eta=\dfrac{1}{1+\frac{r_{L2}}{R}+\frac{r_{L1}}{R}n^2+\frac{r_{C1}}{R}n}$ and $n=\dfrac{D}{1-D}$.

Notice that if r_{C1}, r_{C2}, r_{L1}, and r_{L2} are assumed to be zero, the output equation in (2.2.2-4) will be become $M=V_O/V_g=D/(1-D)$, the same as the expression for the ideal Zeta converter in (2.1-1).

C - Linear Small-Signal State-Space Equation

Given the averaged matrices (2.2.2-3), the linear small-signal state-space equations of the Zeta converter can be formulated in accordance with (2.2.1-6-a):

$$\frac{d}{dt}\begin{bmatrix}\tilde{i}_{L1}(t)\\ \tilde{i}_{L2}(t)\\ \tilde{v}_{C1}(t)\\ \tilde{v}_{C2}(t)\end{bmatrix}=\begin{bmatrix}\frac{r_{C1}(1-D)+r_{L1}}{L_1} & 0 & -\frac{1-D}{L_1} & 0\\ 0 & -\frac{(r_{C2}+R)(Dr_{C1}+r_{L2})+r_{C2}R}{L_2(r_{C2}+R)} & \frac{D}{L_2} & \frac{-R}{L_2(r_{C2}+R)}\\ \frac{1-D}{C_1} & \frac{-D}{C_1} & 0 & 0\\ 0 & \frac{R}{C_2(r_{C2}+R)} & 0 & \frac{-1}{C_2(r_{C2}+R)}\end{bmatrix}\begin{bmatrix}\tilde{i}_{L1}(t)\\ \tilde{i}_{L2}(t)\\ \tilde{v}_{C1}(t)\\ \tilde{v}_{C2}(t)\end{bmatrix}+$$

$$\begin{bmatrix}\frac{D}{L_1} & 0 & \frac{\eta[V_g[(1-D)(R+r_{L2})+Dr_{C1}]-I_Z Dr_{L1}R]}{L_1R(1-D)^2}\\ \frac{D}{L_2} & \frac{r_{C2}R}{L_2(r_{C2}+R)} & \frac{\eta[V_g(r_{L2}+R)(1-D)-I_Z R[r_{C1}(1-D)+Dr_{L1}]]}{L_2R(1-D)^2}\\ 0 & 0 & \frac{-\eta[DV_g+RI_Z(1-D)]}{C_1R(1-D)^2}\\ 0 & -\frac{R}{C_2(r_{C2}+R)} & 0\end{bmatrix}\begin{bmatrix}\tilde{v}_g(t)\\ \tilde{i}_Z(t)\\ \tilde{d}(t)\end{bmatrix} \qquad (2.2.2\text{-}5)$$

$$\tilde{v}_O(t)=\begin{bmatrix}0 & \frac{r_{C2}R}{r_{C2}+R} & 0 & \frac{r_{C2}R}{r_{C2}+R}\end{bmatrix}\begin{bmatrix}\tilde{i}_{L1}(t)\\ \tilde{i}_{L2}(t)\\ \tilde{v}_{C1}(t)\\ \tilde{v}_{C2}(t)\end{bmatrix}+\begin{bmatrix}0 & \frac{-r_{C2}R}{r_{C2}+R} & 0\end{bmatrix}\begin{bmatrix}\tilde{v}_g(t)\\ \tilde{i}_Z(t)\\ \tilde{d}(t)\end{bmatrix}$$

D - Finding Transfer Functions

Referring to (2.2.1-6-d), fifteen transfer functions can be determined from (2.2.2-5). However, only those useful for feedback control design are derived and given here. These transfer functions are:

The duty ratio-to-inductor-L_1-current transfer function

$$G_{di_1}=\tilde{i}_{L1}(s)/\tilde{d}(s)=\left[(s\mathbf{I}-\mathbf{A})^{-1}\mathbf{B}_d\right]_{11}=\mathbf{C}_1(s\mathbf{I}-\mathbf{A})^{-1}\mathbf{B}_d$$
$$=\frac{1}{(1-D)^2(R+r_{L2})+r_{C1}D(1-D)+r_{L1}D^2}\frac{a_{di1}s^3+b_{di1}s^2+c_{di1}s+d_{di1}}{as^4+bs^3+cs^2+ds+e} \qquad (2.2.2\text{-}6\text{-a})$$

The duty ratio-to-inductor-L_2-current transfer function

$$G_{di_2}=\tilde{i}_{L2}(s)/\tilde{d}(s)=\left[(s\mathbf{I}-\mathbf{A})^{-1}\mathbf{B}_d\right]_{21}=\mathbf{C}_2(s\mathbf{I}-\mathbf{A})^{-1}\mathbf{B}_d$$
$$=\frac{1}{(1-D)^2(R+r_{L2})+r_{C1}D(1-D)+r_{L1}D^2}\frac{(a_{di2}s^2+b_{di2}s+c_{di2})(d_{di2}s+1)}{as^4+bs^3+cs^2+ds+e} \qquad (2.2.2\text{-}6\text{-b})$$

The input voltage-to-inductor-L_1-current transfer function

$$\mathrm{G}_{vi1}=\tilde{i}_{L1}(s)/\tilde{v}_g(s)=\left[(s\mathbf{I}-\mathbf{A})^{-1}\mathbf{B}_d\right]_{11}=\mathbf{C}_1(s\mathbf{I}-\mathbf{A})^{-1}\mathbf{B}_d=D\frac{a_{vi1}s^3+b_{vi1}s^2+c_{vi1}s+d_{vi1}}{as^4+bs^3+cs^2+ds+e} \qquad (2.2.2\text{-}6\text{-c})$$

The input voltage-to-inductor-L_2-current transfer function

$$\mathrm{G}_{vi2}=\tilde{i}_{L2}/\tilde{v}_g=\left[(s\mathbf{I}-\mathbf{A})^{-1}\mathbf{B}_d\right]_{21}=\mathbf{C}_2(s\mathbf{I}-\mathbf{A})^{-1}\mathbf{B}_d=D\frac{(a_{vi2}s^2+b_{vi2}s+c_{vi2})(d_{vi2}s+1)}{as^4+bs^3+cs^2+ds+e} \qquad (2.2.2\text{-}6\text{-d})$$

The duty ratio-to-output voltage transfer function

$$\mathrm{G}_{dv}(s)=\tilde{v}_O(s)/\tilde{d}(s)=\mathbf{C}(s\mathbf{I}-\mathbf{A})^{-1}\mathbf{B}_d+\mathbf{E}_d$$
$$=\frac{1}{(1-D)^2(1+\frac{r_{L2}}{R}+\frac{r_{L1}}{R}n^2+\frac{r_{C1}}{R}n)}\frac{(a_{dv}s^2+b_{dv}s+c_{dv})(d_{dv}s+1)}{as^4+bs^3+cs^2+ds+e} \qquad (2.2.2\text{-}6\text{-e})$$

where $n=D/(1-D)$.

The input voltage-to-output voltage transfer function

$$G_{vv}(s)=\tilde{v}_O(s)/\tilde{v}_g(s)=\mathbf{C(sI-A)^{-1}B_{u1}+E_{u1}}=DR\frac{(a_{vv}s^2+b_{vv}s+c_{vv})(d_{vv}s+1)}{as^4+bs^3+cs^2+ds+e} \quad (2.2.2\text{-}6\text{-f})$$

The output impedance transfer function

$$G_{zv}(s)=\tilde{v}_O(s)/\tilde{v}_g(s)=\mathbf{C(sI-A)^{-1}B_{u2}+E_{u2}}=-R\frac{(a_{zv}s^2+b_{zv}s+c_{zv})(d_{zv}s+1)}{as^4+bs^3+cs^2+ds+e} \quad (2.2.2\text{-}6\text{-g})$$

where the coefficients of (2.2.2-6-a) to (2.2.2-6-g) are listed in TABLE 2.1.

TABLE 2.1

Coefficients of $G_{di1}(s)$, $G_{di2}(s)$, $G_{vi1}(s)$, $G_{vi2}(s)$, $G_{dv}(s)$, $G_{zv}(s)$, and $G_{vv}(s)$ of CCM Zeta converter.

$a_{di1}=V_g[C_1L_2C_2(1-D)(R+r_{L2})(R+r_{C2})+(r_{C2}+R)C_1L_2C_2Dr_{C1}]-I_zC_1L_2C_2DRr_{L1}(r_{C2}+R)$ $b_{di1}=V_g[(1-D)[C_2(R+r_{C2})(L_2D+C_1r_{L2}^2)+(R+r_{L2})C_1L_2+C_1C_2R(r_{C2}R+r_{L2}R+Dr_{C1}R+2r_{C2}r_{L2})]$ $-C_1C_2Dr_{C1}(D-2)[(R+r_{C2})r_{L2}+Rr_{C2}]+C_1Dr_{C1}[L_2+(R+r_{C2})C_2Dr_{C1}]]$ $+I_zR[L_2C_2(1-D)^2(R+r_{C2})-C_1C_2Dr_{L1}[(Dr_{C1}+r_{L2})(r_{C2}+R)+r_{C2}R]-C_1L_2Dr_{L1}]$ $c_{di1}=V_g[(1-D)[L_2D+R^2(C_1+C_2D)+C_1r_{L2}(2R+r_{L2})+2C_2D(r_{C2}R+r_{C2}r_{L2}+Rr_{L2})]$ $+r_{C1}D[C_1(2-D)(R+r_{L2})+D[C_2(R+r_{C2})+C_1r_{C1}]]]$ $+I_zR[(1-D)^2[L_2+C_2(r_{C2}R+r_{L2}R+r_{C2}r_{L2})]-Dr_{L1}[C_1(R+r_{L2}+Dr_{C1})+DC_2(R+r_{C2})]]$ $d_{di1}=V_g[2D(1-D)(R+r_{L2})+D^2r_{C1}]-I_zR[D^2r_{L1}-(1-D)^2(r_{L2}+R)]]$
$a_{di2}=V_g(1-D)(r_{L2}+R)L_1C_1-I_zL_1C_1R[(1-D)r_{C1}+Dr_{L1}]$ $b_{di2}=-V_g[L_1D^2-C_1(1-D)(r_{L2}+R)[r_{L1}+(1-D)r_{C1}]]-I_zR[(1-D)[L_1D+r_{C1}^2C_1(1-D)]+r_{L1}C_1(r_{C1}+r_{L1}D-r_{C1}D^2)]$ $c_{di2}=V_g[(1-D)^2(R+r_{L2})-D^2r_{L1}]-I_zR(1-D)[2Dr_{L1}+r_{C1}(1-D)]$ $d_{di2}=C_2(r_{C2}+R)$
$a_{vi1}=(r_{C2}+R)C_1L_2C_2$, $b_{vi1}=L_2C_1+C_1C_2[r_{C2}R+r_{L2}R+r_{C2}r_{L2}+(r_{C2}+R)Dr_{C1}]$ $c_{vi1}=(C_1r_{C1}+C_2r_{C2}+C_2R)D+(r_{L2}+R)C_1$, $d_{vi1}=D$
$a_{vi2}=L_1C_1$, $b_{vi2}=[r_{L1}+(1-D)r_{C1}]C_1$, $c_{vi2}=1-D$, $d_{vi2}=(r_{C2}+R)C_2$
$a_{dv}=L_1C_1[V_g(1-D)(R+r_{L2})-I_zR[(1-D)r_{C1}+Dr_{L1}]$ $b_{dv}=-V_g[L_1D^2-C_1(1-D)(R+r_{L2})[(1-D)r_{C1}+r_{L1}]]-I_zR[L_1D(1-D)+r_{C1}^2C_1(1-D)^2+r_{L1}C_1(r_{C1}+r_{L1}D-D^2r_{C1})]$ $c_{dv}=V_g[(1-D)^2(R+r_{L2})-D^2r_{L1}]-I_zR(1-D)[2Dr_{L1}+r_{C1}(1-D)]$ $d_{dv}=C_2r_{C2}$
$a_{vv}=C_1L_1$, $b_{vv}=C_1[r_{L1}+r_{C1}(1-D)]$, $c_{vv}=1-D$, $d_{vv}=C_2r_{C2}$
$a_{zv}=L_1L_2C_1C_2r_{C2}$, $b_{zv}=L_1C_1(L_2+Dr_{C2}r_{C1}C_2)+(1-D)r_{C1}r_{C2}L_2C_1C_2+(L_1r_{L2}+L_2r_{L1})r_{C2}C_1C_2$ $c_{zv}=(1-D)[(1-D)r_{C2}L_2C_2+r_{C1}C_1(L_2+Dr_{C1}r_{C2}C_2+r_{C2}r_{L2}C_2)]+L_1D(Dr_{C2}C_2+r_{C1}C_1)$ $+C_1[r_{L1}r_{C2}C_2(r_{C1}D+r_{L2})+r_{L1}L_2+r_{L2}L_1]$ $d_{zv}=L_1D^2+(1-D)[(1-D)(L_2+r_{C2}r_{L2}C_2)+Dr_{C1}(r_{C1}C_1+r_{C2}C_2)+r_{C1}r_{L2}C_1]+r_{L1}(C_1r_{L2}+C_1Dr_{C1}+r_{C2}D^2C_2)$ $e_{zv}=r_{C1}D(1-D)+r_{L1}D^2+r_{L2}(1-D)^2$
$a=L_1C_1L_2C_2(R+r_{C2})$ $b=L_1C_1(L_2+r_{C2}C_2R)+C_1(R+r_{C2})[r_{C1}L_2C_2(1-D)+Dr_{C1}L_1C$ $c=(1-D)[[(1-D)L_2+(Dr_{C1}+r_{L2})r_{C1}C_1](r_{C2}+R)C_2+r_{C1}C_1(r_{C2}C_2R+L_2)]$ $+C_2(r_{C2}+R)[L_1D^2+(Dr_{C1}+r_{L2})r_{L1}C_1]+C_1[L_1(Dr_{C1}+R)+r_{L1}L_2+r_{L2}L_1+r_{L1}r_{C2}C_2R]_2+C_2(r_{L2}L_1+r_{L1}L_2)]$ $d=(1-D)^2[L_2+r_{C2}C_2R+r_{L2}C_2(R+r_{C2})]+[r_{C1}(1-D)+r_{L1}D](R+r_{C2})DC_2+[(1-D)r_{C1}+r_{L1}](r_{L2}+Dr_{C1}+R)C_1$ $+L_1D^2$ $e=(1-D)^2(R+r_{L2})+r_{C1}D(1-D)+r_{L1}D^2$

The coefficients in (2.2.2-6) are listed in TABLE 2.1. The derivation of these coefficients is given in the **Appendix F**. The following chapters will discuss some control methods applied with Zeta converter, and $G_{dv}(s)$ will be used in the control scheme. Due to this reason, it is worthwhile to firstly examine the transfer function $G_{dv}(s)$. The transfer function has three zeros and four poles. It can be proved by the Routh-Hurwitz criterion [25] that all the poles of $G_{dv}(s)$ are located on the Left-Half Plane (LHP) (**Appendix D**). The $d_{dv}s+1$ term on the numerator always gives the LHP zero since d_{dv} is positive. However, there is a possibility that the quadratic term, $a_{dv}s^2+b_{dv}s+c_{dv}$, can yield a pair of Right-Half-Plane (RHP) zeros. The pair of RHP zeros are undesirable because they cause additional 180 degrees phase-lag to $G_{dv}(s)$, making feedback loop compensation very difficult. In order to avoid the RHP zeros, the zeros of the quadratic term must satisfy the following condition:

$$s_{z1,2}=(-b_{dv}\pm\sqrt{b_{dv}^2-4a_{dv}c_{dv}})/(2a_{dv})<0 \qquad (2.2.2\text{-}7\text{-a})$$

That is,

$$\begin{cases} b_{dv}^2<4a_{dv}c_{dv} \\ b_{dv}>0 \end{cases} \qquad (2.2.2\text{-}7\text{-b})$$

where $a_{dv}=L_1C_1V_g(1-D)(R+r_{L2})$, $b_{dv}=-V_g[L_1D^2-C_1(1-D)(R+r_{L2})[(1-D)r_{C1}+r_{L1}]]$, and $c_{dv}=V_g[(1-D)^2(R+r_{L2})-D^2r_{L1}]$.

2.3 Modeling of CCM Zeta Converter with PWM-Switch Model

2.3.1 Overview of PWM-Switch Model in CCM

The concept of the PWM-switch model [11-17] focuses on modeling the behavior of the PWM-switch block, comprising of the active switch and diode, since it is responsible for the nonlinearity in DC-DC converters. The modeling process first begins with averaging the terminal voltages and currents of the PWM-switch block and finding their relationships. The resulting equations that relate the averaged terminal voltages and currents are then perturbed with a small signal around a DC operating point. The perturbation yields both DC and small-signal terms, and by separating them, the DC and linear small-signal equations (or models) of the PWM-switch block are obtained. Substitution of the DC and small-signal models for the switching block in the DC-DC converters will result in the DC and small-signal equivalent circuits of the converters respectively. The DC model is used to find the converter's steady state solutions. The small-signal model is used to determine the converter's transfer function. The PWM-switch block is shown in Fig. 2.3 where *a*, *c*, and *p* are active, common, and passive terminals respectively. The relationship between average terminal voltages and currents is:

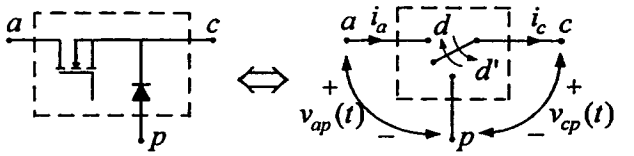

(a)

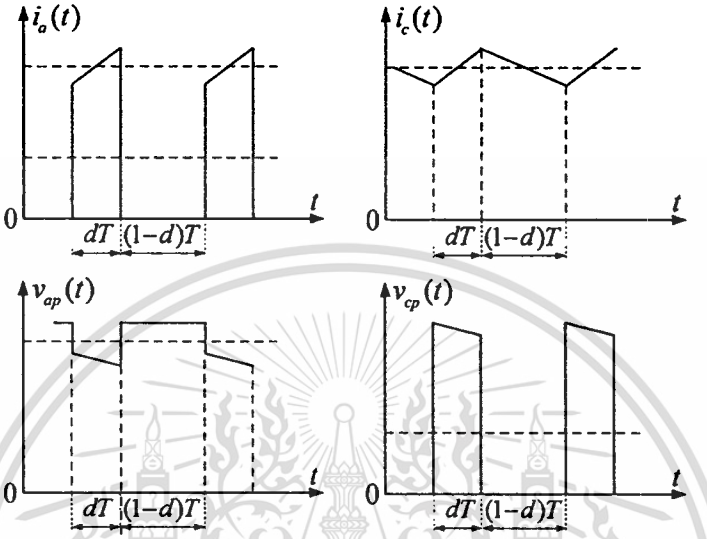

(b)

Fig. 2.3. (a) PWM-switch block and (b) Terminal voltage and current waveforms.

$$\begin{cases} <i_a> = d<i_c> \\ <v_{cp}> = d<v_{ap}> \end{cases} \quad (2.3.1\text{-}1\text{-a})$$

From (2.3.1-1-a), the average model of PWM switch is obtained as shown in Fig. 2.4(a). Equation (2.3.1-1-a) is a nonlinear equation and can be linearized by small-signal perturbation with $<i_a> = I_a+\tilde{i}_a$, $<i_p> = I_p+\tilde{i}_p$, $<v_{ac}> = V_{ac}+\tilde{v}_{ac}$, $<v_{cp}> = V_{cp}+\tilde{v}_{cp}$, and $d = D+\tilde{d}$, where the tilde symbol, $\tilde{}$, represents a small-signal value and the capital letter a DC value. It should be noted that $I_a >> \tilde{i}_a$, $I_p >> \tilde{i}_p$, $V_{ac} >> \tilde{v}_{ac}$, $V_{cp} >> \tilde{v}_{cp}$, and $D >> \tilde{d}$. Substituting the perturbation into (2.3.1-1-a) yields:

$$\begin{cases} I_a+\tilde{i}_a = (D+\tilde{d})(I_c+\tilde{i}_c) \\ V_{cp}+\tilde{v}_{cp} = (D+\tilde{d})(V_{ap}+\tilde{v}_{ap}) \end{cases} \quad (2.3.1\text{-}1\text{-b})$$

$$\begin{cases} I_a+\tilde{i}_a = DI_c+D\tilde{i}_c+I_c\tilde{d}+\tilde{i}_c\tilde{d} \\ V_{cp}+\tilde{v}_{cp} = DV_{ap}+D\tilde{v}_{ap}+V_{ap}\tilde{d}+\tilde{v}_{ap}\tilde{d} \end{cases} \quad (2.3.1\text{-}1\text{-c})$$

Collecting the DC terms from (2.3.1-1-c), DC equation is given by:

$$\begin{cases} I_a = DI_c \\ V_{cp} = DV_{ap} \end{cases} \quad (2.3.1\text{-}1\text{-d})$$

Collecting the small-signal terms from (2.3.1-1-c) and neglecting the product of the two small-signal terms (e.g. $\tilde{d}.\tilde{u}=0$), linear small-signal equation is given by:

$$\begin{cases} \tilde{i}_a = D\tilde{i}_c + I_c\tilde{d} \\ \tilde{v}_{cp} = D\tilde{v}_{ap} + V_{ap}\tilde{d} \end{cases} \qquad (2.3.1\text{-}1\text{-}e)$$

From (2.3.1-1-d) and (2.3.1-1-e), the DC and small-signal PWM-switch models are developed as depicted Fig. 2.4(b) and Fig. 2.4(c) respectively.

2.3.2 Application of PWM-Switch Model to CCM Zeta Converter

Fig. 2.5(a) depicts a Zeta converter. To use PWM-switch model, the circuit elements of the converter must first be rearranged as shown in Fig. 2.5(b) and Fig. 2.5(c) respectively. Then, the PWM-switch section is inserted by its AC model, yielding the small-signal model of the CCM Zeta converter as shown in Fig. 2.6. The DC solution can be solved from the circuit in Fig. 2.6, by assuming the small-signal terms to be zero, short circuiting L, and open circuiting C. It should be noted that the obtained DC solution serves as a DC operating point for the AC analysis. Given the DC operating point, the AC model in Fig. 2.6 can be solved by using circuit analysis techniques to determine the converter's transfer functions. Nevertheless, the aforementioned DC and AC analysis will be tedious and lengthy. For this reason, in this work PSPICE is employed to simulate the Zeta converter's model in Fig. 2.6 to obtain the desired transfer functions numerically. The results are presented in following section.

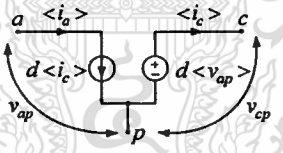

(a)

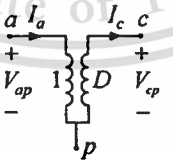

(b)

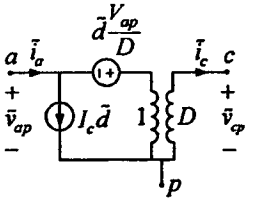

(c)

Fig. 2.4. (a) Average model of PWM switch in CCM,
(b) DC model of PWM switch and (c) AC model of PWM switch

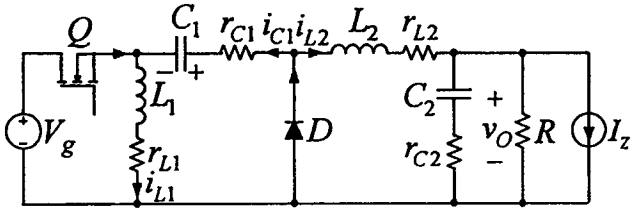

(a)

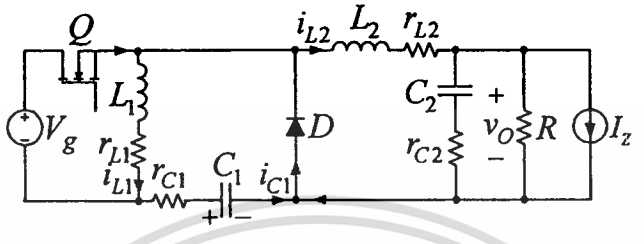

(b)

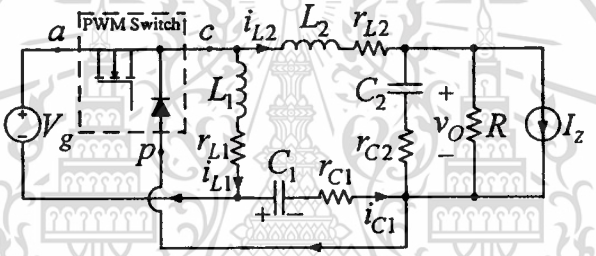

(c)

Fig. 2.5 (a) Zeta converter, (b) Equivalent circuit schematic of Zeta converter, and (c) Equivalent circuit schematic of PWM-switch Zeta converter.

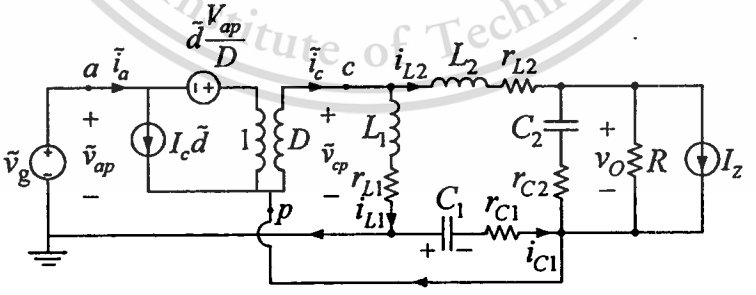

Fig. 2.6. Small-signal circuit model of the Zeta converter in CCM.

2.4 Modeling of CCM Zeta Converter with Averaged Switch Model

2.4.1 Overview of Averaged Switch Model in CCM

Similar to the PWM switch model, the averaged switch model [18-20] is a circuit-based model which represents the averaged equivalent circuit of power switch and diode. However,

the way the switch network is identified, and the terminal quantities assigned in the averaged switch model is different from that in the PWM switch model, as illustrated in Fig. 2.7(a). It can be shown that the relationship between averaged terminal voltages ($<v_1>$ and $<v_2>$) and currents ($<i_1>$ and $<i_2>$) is given by:

$$<v_1(t)>=\frac{1-d(t)}{d(t)}<v_2(t)> \quad (2.4.1\text{-}1\text{-a})$$

$$<i_2(t)>=\frac{1-d(t)}{d(t)}<i_1(t)> \quad (2.4.1\text{-}1\text{-b})$$

From (2.4.1-1), the averaged switch model in CCM is drawn as shown in Fig. 2.7(b). Equation (2.4.1-1) is nonlinear and can be linearized by small-signal perturbation with $<i_1> = I_1+\tilde{i}_1$, $<i_2> = I_2+\tilde{i}_2$, $<v_1> = V_1+\tilde{v}_1$, $<v_2> = V_2+\tilde{v}_2$, and $d= D+\tilde{d}$, where the tilde symbol, $\tilde{}$, represents a small-signal value and the capital letter a DC value. It should be noted that $I_1 >> \tilde{i}_1$, $I_2 >> \tilde{i}_2$, $V_1 >> \tilde{v}_1$, $V_2 >> \tilde{v}_2$, and $D >> \tilde{d}$. Substituting the perturbation into (2.4.1-1) and neglecting the product of two small-signal terms produce:

$$V_1+\tilde{v}_1=\frac{1-D-\tilde{d}}{D+\tilde{d}}(V_2+\tilde{v}_2) \quad (2.4.1\text{-}2\text{-a})$$

$$D(V_1+\tilde{v}_1)=(1-D)(V_2+\tilde{v}_2)-\tilde{d}(V_2+\tilde{v}_2)-(V_1+\tilde{v}_1)\tilde{d} \quad (2.4.1\text{-}2\text{-b})$$

$$D(V_1+\tilde{v}_1)=(1-D)(V_2+\tilde{v}_2)-(V_1+V_2)\tilde{d}-\tilde{v}_2\tilde{d}-\tilde{v}_1\tilde{d} \quad (2.4.1\text{-}2\text{-c})$$

$$(V_1+\tilde{v}_1)=\frac{1-D}{D}(V_2+\tilde{v}_2)-\frac{V_1+\frac{V_1D}{1-D}}{D}\tilde{d} \quad (2.4.1\text{-}2\text{-d})$$

$$(V_1+\tilde{v}_1)=\frac{1-D}{D}(V_2+\tilde{v}_2)-\frac{V_1}{D(1-D)}\tilde{d} \quad (2.4.1\text{-}2\text{-e})$$

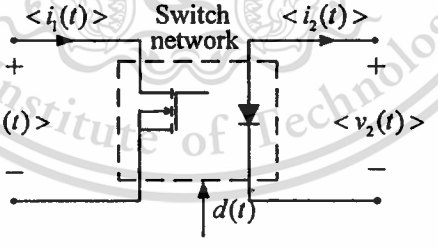

(a)

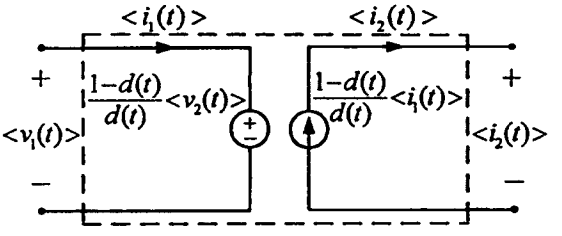

(b)

Fig. 2.7. (a) General averaged switch network and (b) Averaged switch model.

$$I_2+\tilde{i}_2=\frac{1-D-\tilde{d}}{D+\tilde{d}}(I_1+\tilde{i}_1) \tag{2.4.1-3-a}$$

$$D(I_2+\tilde{i}_2)=(1-D)(I_1+\tilde{i}_1)-\tilde{d}(I_1+\tilde{i}_1)-\tilde{d}(I_2+\tilde{i}_2) \tag{2.4.1-3-b}$$

$$D(I_2+\tilde{i}_2)=(1-D)(I_1+\tilde{i}_1)-(I_1+I_2)\tilde{d}-\tilde{i}_1\tilde{d}-\tilde{i}_2\tilde{d} \tag{2.4.1-3-c}$$

$$I_2+\tilde{i}_2=\frac{1-D}{D}(I_1+\tilde{i}_1)-\frac{I_2\frac{1-D}{D}+I_2}{D}\tilde{d} \tag{2.4.1-3-d}$$

$$I_2+\tilde{i}_2=\frac{1-D}{D}(I_1+\tilde{i}_1)-\frac{I_2}{D(1-D)}\tilde{d} \tag{2.4.1-3-e}$$

Separating the DC from the AC terms in (2.4.1-2-e) and (2.4.1-3-e), the steady and small-signal equations are given by:

$$\begin{cases} V_1=V_2(1-D)/D \\ I_2=I_1(1-D)/D \end{cases} \tag{2.4.1-4-a}$$

$$\begin{cases} \tilde{v}_1=\tilde{v}_2(1-D)/D-\tilde{d}V_1/[D(1-D)] \\ \tilde{i}_2=\tilde{i}_1(1-D)/D-\tilde{d}I_2/[D(1-D)] \end{cases} \tag{2.4.1-4-b}$$

From (2.4.1-4-a) and (2.4.1-4-b), the DC and AC averaged switch models are drawn as shown in Fig. 2.8(a) and 2.8(b) respectively.

2.4.2 Application of Averaged Switch Model to CCM Zeta Converter

Fig. 2.9(a) shows a Zeta converter with the identified averaged switch network. Substituting the switch network with the DC averaged switch model in Fig. 2.8(a) yields the DC model of the Zeta converter as shown in Fig. 2.9(b).

Note that in DC analysis *L*'s are short circuited and *C*'s open circuited. The DC solution found from Fig. 2.9(b) serves as a DC operating point for the subsequent AC analysis. The AC analysis is performed by inserting the AC averaged switch model in Fig. 2.8(b) for the switch network, giving the AC model of the Zeta converter as depicted in Fig. 2.9(c).

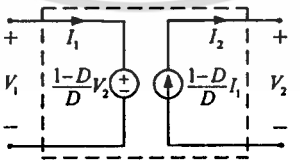

(a)

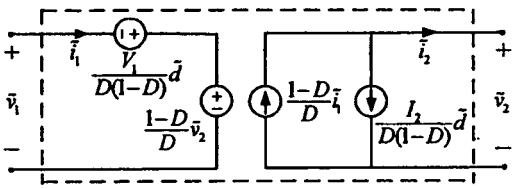

(b)

Fig. 2.8. (a) DC averaged switch model and (b) AC averaged switch model.

To determine the converter's transfer functions, Fig. 2.9(c) is manipulated and solved using circuit analysis techniques. However, the process can be tedious and time-consuming. As with the PWM-switch model, the desired transfer functions are numerically computed by means of PSPICE simulation of the converter in Fig. 2.9. The results will be presented in the subsequent section.

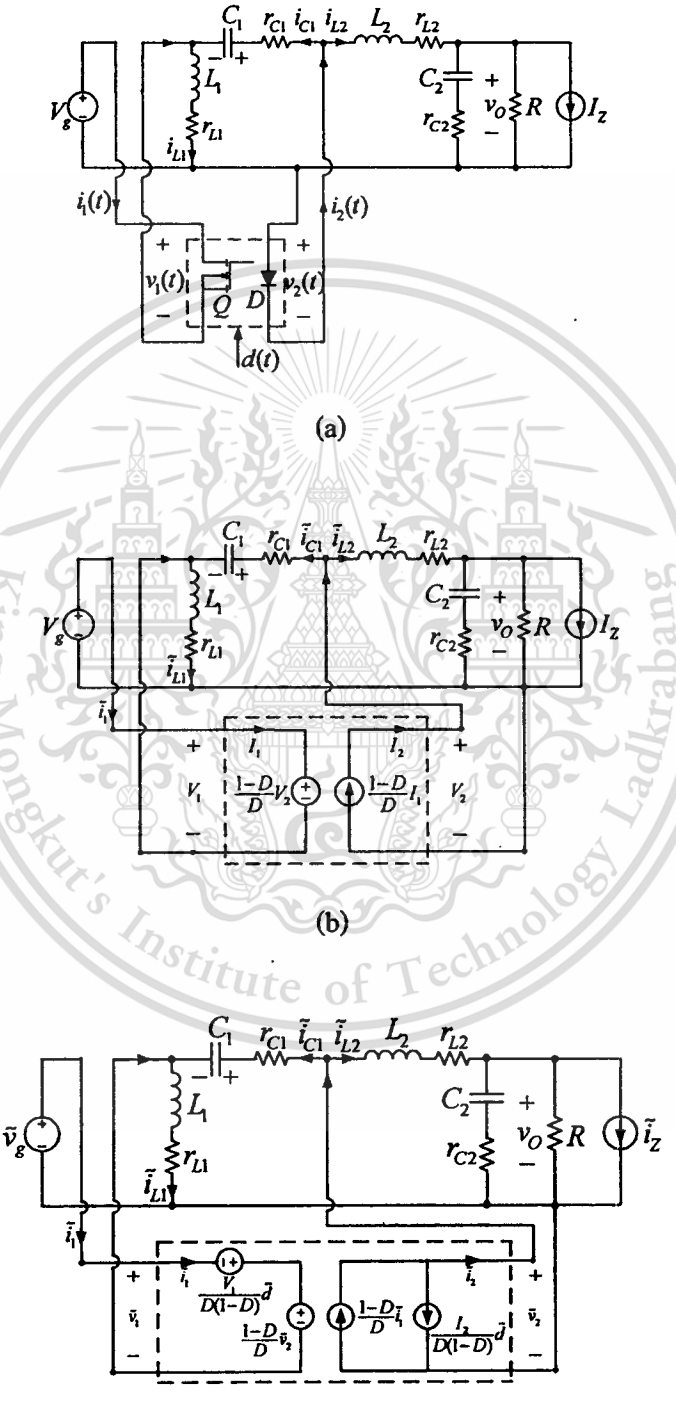

Fig. 2.9. Zeta converter with (a) the identified switch network,
(b) the switch network substituted by DC averaged switch model, and
(c) the switch network substituted by AC averaged switch model.

2.5 Duty ratio-to-Output Voltage Transfer Function, $G_{dv}(s)$

In this section, the transfer functions derived earlier from three different modeling methods, i.e., SSA technique, PWM-switch model, and averaged switch model are plotted and compared. The component values of the Zeta converter are given in TABLE 2.2. It should be noted that these values satisfy both condition for CCM in (2.1-2) and Left-Half Plane (LHP) zeros in (2.2.2-7-b). The transfer function $G_{dv}(s)$ from the SSA technique expressed in (2.2.2-6-e) is compared with that from the other two methods. MATLAB is used to plot the Bode plot of $G_{dv}(s)$ in (2.2.2-6-e). To generate the Bode plot of $G_{dv}(s)$ from PWM-switch and averaged switch models, the Zeta converter circuits shown in Fig. 2.9 are simulated by PSPICE using AC simulation (.AC). The active switch and diode of the converter are replaced by PWM-switch mode in Fig. 2.10(a) and averaged switch model in Fig. 2.10(b). Bode plots of $G_{dv}(s)$ from the three modeling methods are illustrated in Fig. 2.11. It can be seen that $G_{dv}(s)$ from the SSA technique in Fig. 2.11(a) closely agrees with those from the PWM-switch and averaged switch models in Fig. 2.11(b) and Fig. 2.11(c) respectively. This verifies that the three modeling methods accurately give the identical results.

TABLE 2.2.

Circuit Parameters for CCM Zeta converter

Circuit Parameters	Values
V_g / V_o	15-20/ 5V
C_1 / C_2	100/ 200μF
L_1 / L_2	100/ 55μH
r_{C1} / r_{C2}	0.19/ 0.095Ω
r_{L1} / r_{L2}	1/ 0. 55mΩ
R	1-5Ω
I_z	0
$T=1/f$	10μs

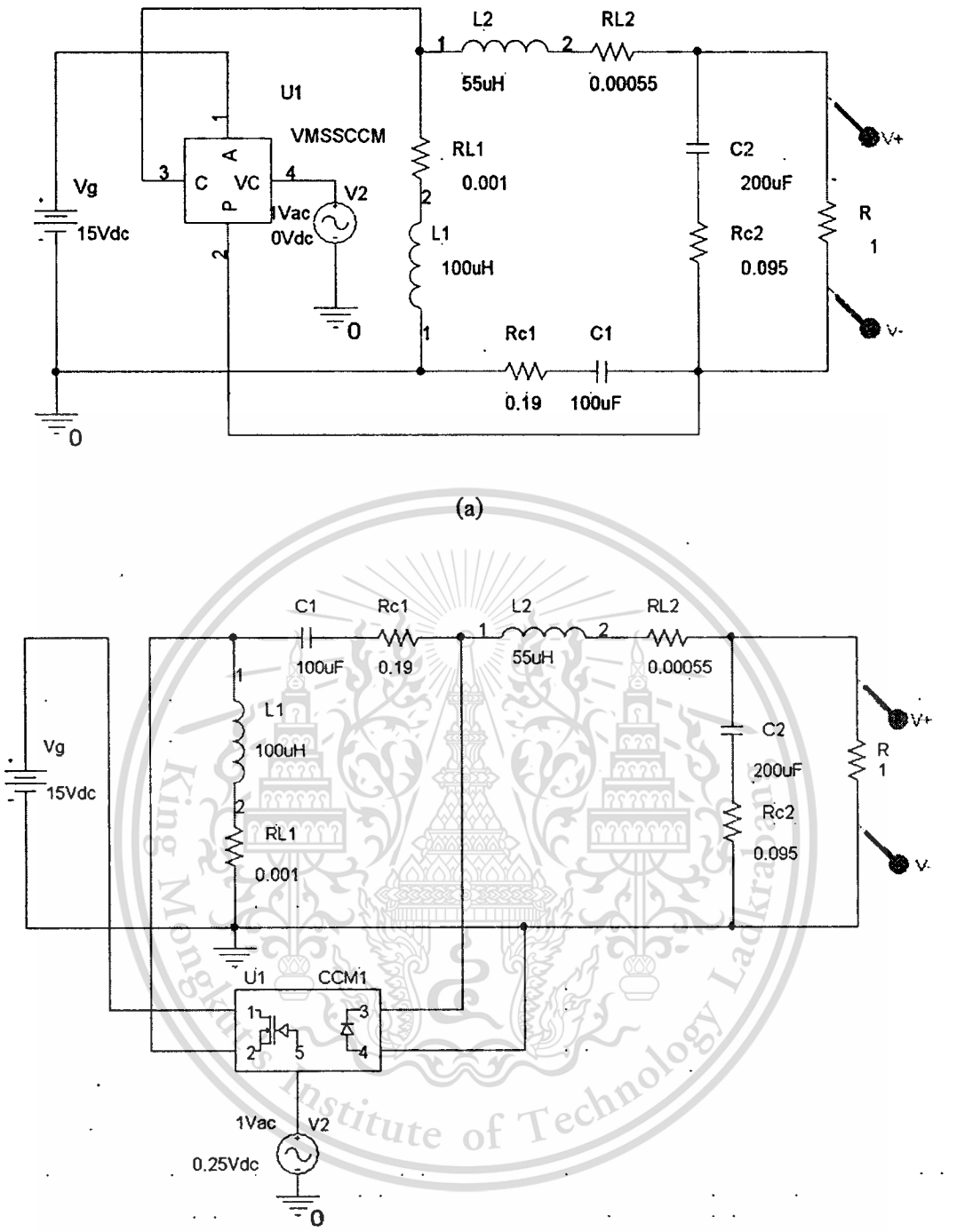

Fig. 2.10. PSPICE circuit schematic of CCM Zeta converter:

(a) PWM-switch model and (b) Averaged switch model.

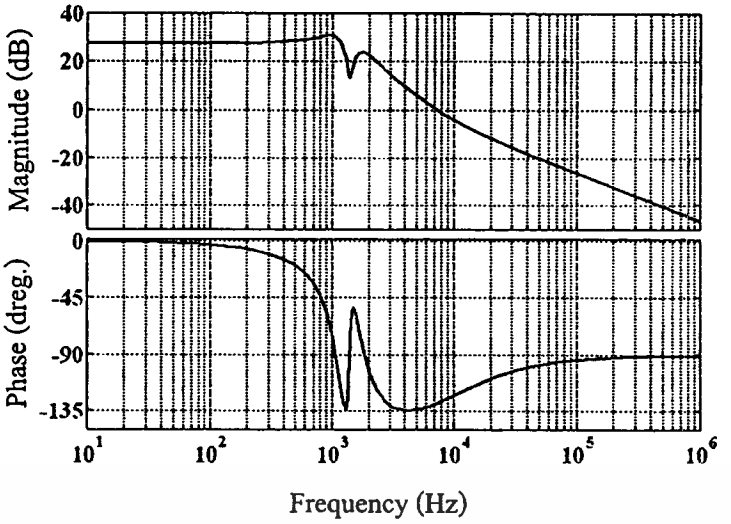

(a)

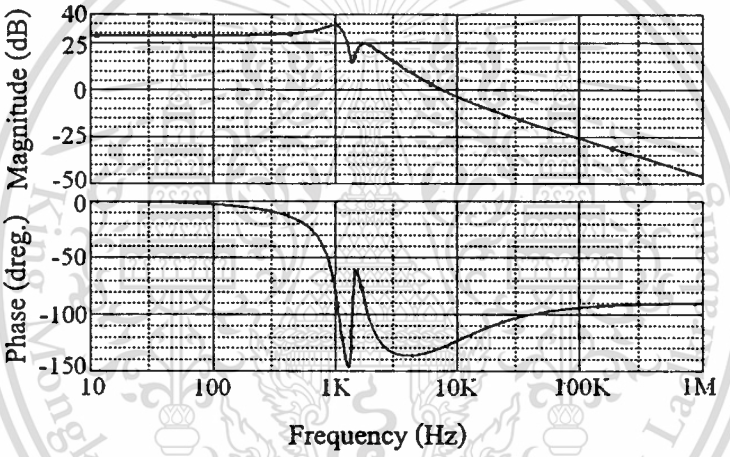

(b)

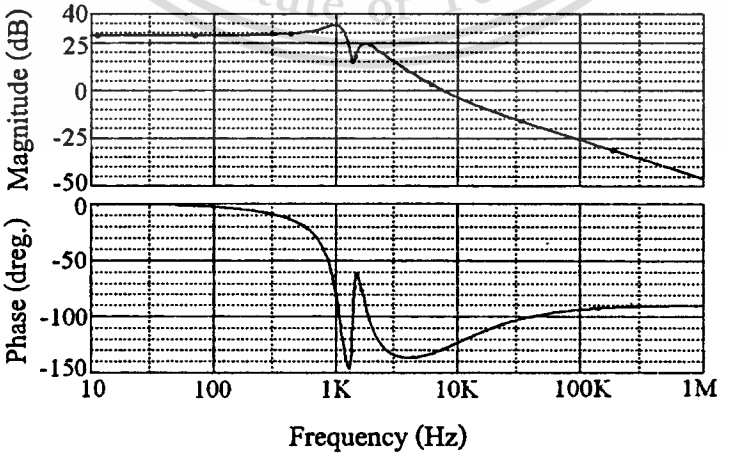

(c)

Fig. 2.11. Bode plot of $G_{dv}(s)$ of CCM Zeta converter (V_g = 15V and R = 1Ω):
(a) SSA technique, (b) PWM-switch model, and (c) Averaged switch model.

Chapter 3

Modeling of Zeta Converters Operating in Discontinuous Conduction Mode (DCM)

The outline of this chapter is similar to chapter 2, but emphasis here is on Discontinuous Conduction Mode (DCM). The chapter begins with the basic operation of DCM Zeta converter followed by modeling of the converter by State-Space Averaging (SSA) technique [1-10], PWM-switch model [11-17], and Averaged switch model [18-20]. It is found that the SSA technique yields the model whose accuracy is limited to one-tenth of the switching frequency as compared with those from PWM-switch and averaged switch modeling.

3.1 Zeta Converter in DCM

There are two possible operation modes of the DC-DC converter: Continuous Conduction Mode (CCM) and Discontinuous Conduction Mode (DCM). Operation in DCM can occurs when the converter operates at light load condition. In some cases, the converter is even intentionally designed for DCM operation because of its faster dynamic response compared to CCM.

The Zeta converter in Fig. 3.1(a) will exhibit three different circuit states in one switching period, T, when operating in DCM. The first state exists when Q is turned on for a time interval d_1T, and the currents i_{L1} and i_{L2} are increasing, as shown in Fig. 3.2. The second state occurs when Q is turned off (i.e. D turned on) for a time interval d_2T, and i_{L1} and i_{L2} are decreasing. The third state happens when both Q and D are turned off for the rest of the time period d_3T. During the time interval d_3T, these currents have a constant value, with the amplitude of i_{L1} and i_{L2} being equal but flowing on the opposite direction (Fig. 3.1(d)), i.e., $i_{L1} = -i_{L2}$. The equality in the amplitude of i_{L1} and i_{L2} is always true during the time interval d_3T, and this essentially makes i_{L1} and i_{L2} depend on each other. The relationship between V_O and V_g is given by:

$$M = \frac{V_O}{V_g} = \frac{d_1}{d_2} \tag{3.1-1}$$

where $d_2 = \sqrt{2L_E/(RT)}$ and $L_E = L_1L_2/(L_1+L_2)$.

It can be shown that for DCM operation, the values of L_1 and L_2 must satisfy the following conditions (**Appendix A**):

$$\begin{cases} L_1 < \dfrac{(1-D)^2 R}{2Df}\left(1+\dfrac{r_{L2}}{R}+\dfrac{r_{C1}}{R}\dfrac{D}{1-D}\right) \\ L_2 < \dfrac{(1-D)R}{2f}\left(1+\dfrac{r_{L2}}{R}\right) \end{cases} \tag{3.1-2}$$

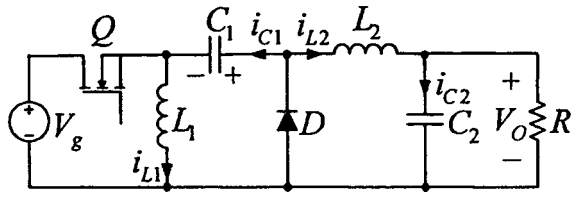

(a) Zeta converter.

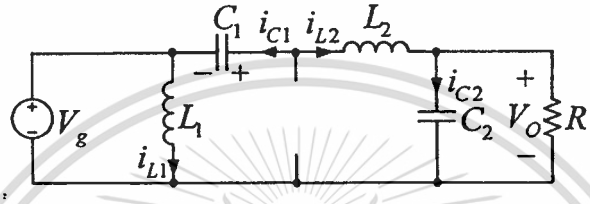

(b) Zeta converter during the first state d_1T.

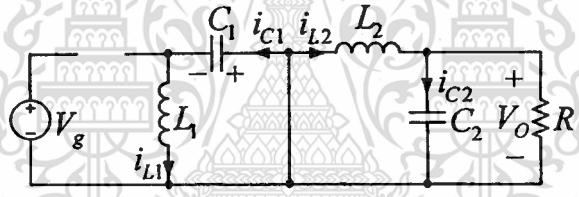

(c) Zeta converter during the second state d_2T.

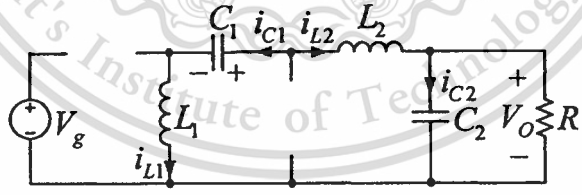

(d) Zeta converter during the third state d_3T.

Fig. 3.1. Operation of the Zeta converter in DCM.

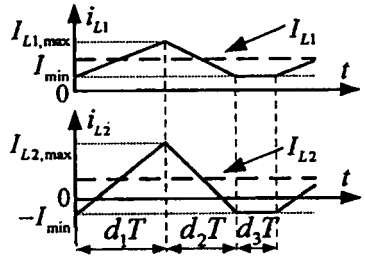

Fig. 3.2. Current waveform of i_{L1} and i_{L2}.

3.2 Modeling of DCM Zeta Converter with State-Space Averaging (SSA) Technique

3.2.1 Overview of SSA Technique in DCM

As stated earlier, DCM has one more circuit state than CCM, i.e., the third state when both MOSFET and diode are turned off. During this interval (d_3T), $i_{L1} = -i_{L2}$ and hence the summation of the two inductor current, $i(t)$, is equal to zero. Fig. 3.3 shows the waveform, $i(t)$, over one switching period. It is discontinuous similar to the inductor current of the second-order converters operating in DCM. Note that $i(t)$ does not really exist in the Zeta converter's circuit; this fictitious current is useful for modeling purpose. The general state-space equations for the three circuit states are:

$$\begin{cases} \dfrac{d\mathbf{x}}{dt} = \mathbf{A}_1\mathbf{x} + \mathbf{B}_1\mathbf{u} \\ \mathbf{y} = \mathbf{C}_1\mathbf{x} + \mathbf{E}_1\mathbf{u} \end{cases} \quad \text{for an interval } d_1T \qquad (3.2.1\text{-}1\text{-a})$$

$$\begin{cases} \dfrac{d\mathbf{x}}{dt} = \mathbf{A}_2\mathbf{x} + \mathbf{B}_2\mathbf{u} \\ \mathbf{y} = \mathbf{C}_2\mathbf{x} + \mathbf{E}_2\mathbf{u} \end{cases} \quad \text{for an interval } d_2T \qquad (3.2.1\text{-}1\text{-b})$$

$$\begin{cases} \dfrac{d\mathbf{x}}{dt} = \mathbf{A}_3\mathbf{x} + \mathbf{B}_3\mathbf{u} \\ \mathbf{y} = \mathbf{C}_3\mathbf{x} + \mathbf{E}_3\mathbf{u} \end{cases} \quad \text{for an interval } d_3T \qquad (3.2.1\text{-}1\text{-c})$$

Since the Zeta converter is made up of two inductors (L_1 and L_2) and two capacitors (C_1 and C_2) the state vector, $\mathbf{x}$, thus comprises of i_{L1}, i_{L2}, v_{C1}, and v_{C2}. The input voltage, v_g, is typically assigned as the input vector, $\mathbf{u}$, and the output voltage, v_O, as the output vector, $\mathbf{y}$. To find the averaged behavior of the converter over one switching period, T, equations (3.2.1-1-a) to (3.2.1-1-c) are weighed average by the duty cycles as:

$$\begin{cases} \dfrac{d\langle \mathbf{x} \rangle}{dt} = \mathbf{A}_s\langle \mathbf{x} \rangle + \mathbf{B}_s\langle \mathbf{u} \rangle \\ \langle \mathbf{y} \rangle = \mathbf{C}_s\langle \mathbf{x} \rangle + \mathbf{E}_s\langle \mathbf{u} \rangle \end{cases} \qquad (3.2.1\text{-}2)$$

where

$$\mathbf{A}_s = \mathbf{A}_1d_1 + \mathbf{A}_2d_2 + \mathbf{A}_3d_3, \qquad (3.2.1\text{-}3\text{-a})$$

$$\mathbf{B}_s = \mathbf{B}_1d_1 + \mathbf{B}_2d_2 + \mathbf{B}_3d_3, \qquad (3.2.1\text{-}3\text{-b})$$

$$\mathbf{C}_s = \mathbf{C}_1d_1 + \mathbf{C}_2d_2 + \mathbf{C}_3d_3, \text{ and} \qquad (3.2.1\text{-}3\text{-c})$$

$$\mathbf{E}_s = \mathbf{E}_1d_1 + \mathbf{E}_2d_2 + \mathbf{E}_3d_3. \qquad (3.2.1\text{-}3\text{-d})$$

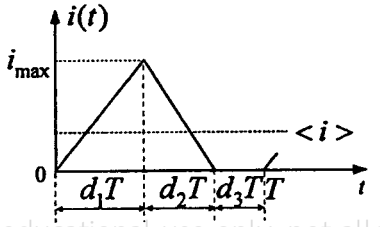

Fig. 3.3. Summation of i_{L1} and i_{L2}.

Equation (3.2.1-2) is a nonlinear continuous-time equation. It can be linearized by small-signal perturbation with $\langle \mathbf{x} \rangle = \mathbf{X} + \tilde{\mathbf{x}}$, $\langle \mathbf{y} \rangle = \mathbf{Y} + \tilde{\mathbf{y}}$, $\langle \mathbf{u} \rangle = \mathbf{U} + \tilde{\mathbf{u}}$, $d_1 = D_1 + \tilde{d}_1$, $d_2 = D_2 + \tilde{d}_2$, and $d_3 = D_3 - \tilde{d}_1 - \tilde{d}_2$ where the tilde symbol, $\tilde{}$, represents a small-signal value, and the capital letter a DC value. It should be noted that $\mathbf{X} \gg \tilde{\mathbf{x}}$, $\mathbf{Y} \gg \tilde{\mathbf{y}}$, $\mathbf{U} \gg \tilde{\mathbf{u}}$, $D_1 \gg \tilde{d}_1$, and $D_2 \gg \tilde{d}_2$. Substituting all perturbation into (3.2.1-2) gives:

$$\begin{cases} (d/dt)(\mathbf{X}+\tilde{\mathbf{x}}) = [\mathbf{A}_1(D_1+\tilde{d}_1) + \mathbf{A}_2(D_2+\tilde{d}_2) + \mathbf{A}_3(D_3-\tilde{d}_1-\tilde{d}_2)](\mathbf{X}+\tilde{\mathbf{x}}) \\ \qquad\qquad + [\mathbf{B}_1(D_1+\tilde{d}_1) + \mathbf{B}_2(D_2+\tilde{d}_2) + \mathbf{B}_3(D_3-\tilde{d}_1-\tilde{d}_2)](\mathbf{U}+\tilde{\mathbf{u}}) \\ \mathbf{Y}+\tilde{\mathbf{y}} = [\mathbf{C}_1(D_1+\tilde{d}_1) + \mathbf{C}_2(D_2+\tilde{d}_2) + \mathbf{C}_3(D_3-\tilde{d}_1-\tilde{d}_2)](\mathbf{X}+\tilde{\mathbf{x}}) \\ \qquad + [\mathbf{E}_1(D_1+\tilde{d}_1) + \mathbf{E}_2(D_2+\tilde{d}_2) + \mathbf{E}_3(D_3-\tilde{d}_1-\tilde{d}_2)](\mathbf{U}+\tilde{\mathbf{u}}) \end{cases} \quad (3.2.1\text{-}4\text{-a})$$

$$\begin{cases} (d/dt)(\mathbf{X}+\tilde{\mathbf{x}}) = [(\mathbf{A}_1D_1 + \mathbf{A}_2D_2 + \mathbf{A}_3D_3) + (\mathbf{A}_1-\mathbf{A}_3)\tilde{d}_1 + (\mathbf{A}_2-\mathbf{A}_3)\tilde{d}_2](\mathbf{X}+\tilde{\mathbf{x}}) \\ \qquad\qquad + [(\mathbf{B}_1D_1 + \mathbf{B}_2D_2 + \mathbf{B}_3D_3) + (\mathbf{B}_1-\mathbf{B}_3)\tilde{d}_1 + (\mathbf{B}_2-\mathbf{B}_3)\tilde{d}_2](\mathbf{U}+\tilde{\mathbf{u}}) \\ \mathbf{Y}+\tilde{\mathbf{y}} = [(\mathbf{C}_1D_1 + \mathbf{C}_2D_2 + \mathbf{C}_3D_3) + (\mathbf{C}_1-\mathbf{C}_3)\tilde{d}_1 + (\mathbf{C}_2-\mathbf{C}_3)\tilde{d}_2](\mathbf{X}+\tilde{\mathbf{x}}) \\ \qquad + [(\mathbf{E}_1D_1 + \mathbf{E}_2D_2 + \mathbf{E}_3D_3) + (\mathbf{E}_1-\mathbf{E}_3)\tilde{d}_1 + (\mathbf{E}_2-\mathbf{E}_3)\tilde{d}_2](\mathbf{U}+\tilde{\mathbf{u}}) \end{cases} \quad (3.2.1\text{-}4\text{-b})$$

$$\begin{cases} (d/dt)(\mathbf{X}+\tilde{\mathbf{x}}) = \mathbf{AX} + \mathbf{BU} + \mathbf{A}\tilde{\mathbf{x}} + \mathbf{B}\tilde{\mathbf{u}} + [(\mathbf{A}_1-\mathbf{A}_3)\mathbf{X} + (\mathbf{B}_1-\mathbf{B}_3)\mathbf{U}]\tilde{d}_1 + [(\mathbf{A}_2-\mathbf{A}_3)\mathbf{X} + (\mathbf{B}_2-\mathbf{B}_3)\mathbf{U}]\tilde{d}_2 \\ \qquad\qquad + [(\mathbf{A}_1-\mathbf{A}_3)\tilde{d}_1 + (\mathbf{A}_2-\mathbf{A}_3)\tilde{d}_2]\tilde{\mathbf{x}} + [(\mathbf{B}_1-\mathbf{B}_3)\tilde{d}_1 + (\mathbf{B}_2-\mathbf{B}_3)\tilde{d}_2]\tilde{\mathbf{u}} \\ \mathbf{Y}+\tilde{\mathbf{y}} = \mathbf{CX} + \mathbf{EU} + \mathbf{C}\tilde{\mathbf{x}} + \mathbf{E}\tilde{\mathbf{u}} + [(\mathbf{C}_1-\mathbf{C}_3)\mathbf{X} + (\mathbf{E}_1-\mathbf{E}_3)\mathbf{U}]\tilde{d}_1 + [(\mathbf{C}_2-\mathbf{C}_3)\mathbf{X} + (\mathbf{E}_2-\mathbf{E}_3)\mathbf{U}]\tilde{d}_2 \\ \qquad + [(\mathbf{C}_1-\mathbf{C}_3)\tilde{d}_1 + (\mathbf{C}_2-\mathbf{C}_3)\tilde{d}_2]\tilde{\mathbf{x}} + [(\mathbf{E}_1-\mathbf{E}_3)\tilde{d}_1 + (\mathbf{E}_2-\mathbf{E}_3)\tilde{d}_2]\tilde{\mathbf{u}} \end{cases} \quad (3.2.1\text{-}4\text{-c})$$

$$\begin{cases} (d/dt)(\mathbf{X}+\tilde{\mathbf{x}}) = \mathbf{AX} + \mathbf{BU} + \mathbf{A}\tilde{\mathbf{x}} + \mathbf{B}\tilde{\mathbf{u}} + [(\mathbf{A}_1-\mathbf{A}_3)\mathbf{X} + (\mathbf{B}_1-\mathbf{B}_3)\mathbf{U}]\tilde{d}_1 + [(\mathbf{A}_2-\mathbf{A}_3)\mathbf{X} + (\mathbf{B}_2-\mathbf{B}_3)\mathbf{U}]\tilde{d}_2 \\ \mathbf{Y}+\tilde{\mathbf{y}} = \mathbf{CX} + \mathbf{EU} + \mathbf{C}\tilde{\mathbf{x}} + \mathbf{E}\tilde{\mathbf{u}} + [(\mathbf{C}_1-\mathbf{C}_3)\mathbf{X} + (\mathbf{E}_1-\mathbf{E}_3)\mathbf{U}]\tilde{d}_1 + [(\mathbf{C}_2-\mathbf{C}_3)\mathbf{X} + (\mathbf{E}_2-\mathbf{E}_3)\mathbf{U}]\tilde{d}_2 \end{cases} \quad (3.2.1\text{-}4\text{-d})$$

$$\begin{cases} (d/dt)(\mathbf{X}+\tilde{\mathbf{x}}) = \mathbf{AX} + \mathbf{BU} + \mathbf{A}\tilde{\mathbf{x}} + \mathbf{B}\tilde{\mathbf{u}} + \mathbf{B}_{d1}\tilde{d}_1 + \mathbf{B}_{d2}\tilde{d}_2 \\ \mathbf{Y}+\tilde{\mathbf{y}} = \mathbf{CX} + \mathbf{EU} + \mathbf{C}\tilde{\mathbf{x}} + \mathbf{E}\tilde{\mathbf{u}} + \mathbf{E}_{d1}\tilde{d}_1 + \mathbf{E}_{d2}\tilde{d}_2 \end{cases} \quad (3.2.1\text{-}4\text{-e})$$

From (3.2.1-4-e), the DC terms can be separated from AC terms; consequently, the steady-state (DC) and linear small-signal state-space (AC) equations can be defined in (3.2.1-5) and (3.2.1-6) respectively.

$$\begin{cases} d\mathbf{X}/dt = \mathbf{AX} + \mathbf{BU} = 0 \\ \mathbf{Y} = \mathbf{CX} + \mathbf{EU} \end{cases} \quad (3.2.1\text{-}5)$$

$$\begin{cases} d\tilde{\mathbf{x}}/dt = \mathbf{A}\tilde{\mathbf{x}} + \mathbf{B}\tilde{\mathbf{u}} + \mathbf{B}_{d1}\tilde{d}_1 + \mathbf{B}_{d2}\tilde{d}_2 \\ \tilde{\mathbf{y}} = \mathbf{C}\tilde{\mathbf{x}} + \mathbf{E}\tilde{\mathbf{u}} + \mathbf{E}_{d1}\tilde{d}_1 + \mathbf{E}_{d2}\tilde{d}_2 \end{cases} \quad (3.2.1\text{-}6)$$

The averaged matrices to solve (3.2.1-5) and (3.2.1-6) are given by:

$$\mathbf{A} = \mathbf{A}_1D_1 + \mathbf{A}_2D_2 + \mathbf{A}_3D_3 \quad (3.2.1\text{-}7\text{-a})$$

$$\mathbf{B} = \mathbf{B}_1D_1 + \mathbf{B}_2D_2 + \mathbf{B}_3D_3 \quad (3.2.1\text{-}7\text{-b})$$

$$\mathbf{C} = \mathbf{C}_1D_1 + \mathbf{C}_2D_2 + \mathbf{C}_3D_3 \quad (3.2.1\text{-}7\text{-c})$$

$$\mathbf{E} = \mathbf{E}_1D_1 + \mathbf{E}_2D_2 + \mathbf{E}_3D_3 \quad (3.2.1\text{-}7\text{-d})$$

$$\mathbf{B}_{d1} = (\mathbf{A}_1 - \mathbf{A}_3)\mathbf{X} + (\mathbf{B}_1 - \mathbf{B}_3)\mathbf{U} \quad (3.2.1\text{-}7\text{-e})$$

$$\mathbf{B}_{d2} = (\mathbf{A}_2 - \mathbf{A}_3)\mathbf{X} + (\mathbf{B}_2 - \mathbf{B}_3)\mathbf{U} \quad (3.2.1\text{-}7\text{-f})$$

$$\mathbf{E}_{d1} = (\mathbf{C}_1 - \mathbf{C}_3)\mathbf{X} + (\mathbf{E}_1 - \mathbf{E}_3)\mathbf{U} \quad (3.2.1\text{-}7\text{-g})$$

$$\mathbf{E}_{d2} = (\mathbf{C}_2 - \mathbf{C}_3)\mathbf{X} + (\mathbf{E}_2 - \mathbf{E}_3)\mathbf{U} \quad (3.2.1\text{-}7\text{-h})$$

Referring to equation (3.2.1-2), the state vector, **x**, is comprised of i_{L1}, i_{L2}, v_{C1}, and v_{C2}. The state-space representation requires that all state variables be independent from each other. But, as seen in section 3.1, i_{L1} and i_{L2} are actually not independent from each other since they must add up to zero in the third interval (d_3T). Hence, only one of these currents can be said to be a true state variable. Due to the dependency between i_{L1} and i_{L2}, the direct solution of (3.2.1-5) and (3.2.1-6) will not produce correct results. If both i_{L1} and i_{L2} are to remain as state variables, the following constraints [1] must be imposed on equations (3.2.1-5) and (3.2.1-6) respectively:

$$I=I(V_g,V_O,D,L_1,L_2,T) \tag{3.2.1-8-a}$$

Where $I = I_{L1} + I_{L2}$.

$$\begin{cases} d\tilde{i}/dt = 0 \\ \tilde{i} = (\partial\tilde{i}/\partial v_g)\tilde{v}_g + (\partial\tilde{i}/\partial v_O)\tilde{v}_O + (\partial\tilde{i}/\partial d)\tilde{d}_1 \end{cases} \tag{3.2.1-8-b}$$

where $\tilde{i} = \tilde{i}_{L1} + \tilde{i}_{L2}$.

To find the steady-state solution, the relationship between I_{L1} and I_{L2} must be first established. Once it is known, other unknowns, such as V_{C1} V_{C2}, and V_O, can be found by solving (3.2.1-5):

$$\begin{cases} \mathbf{X} = -\mathbf{A}^{-1}\mathbf{B}\mathbf{U} \\ \mathbf{Y} = (-\mathbf{C}\mathbf{A}^{-1}\mathbf{B} + \mathbf{E})\mathbf{U} \end{cases} \tag{3.2.1-9}$$

When applied, the constraints in (3.2.1-8) will result in $\tilde{d}_2$ and one inductor current being eliminated from the linear small-signal state-space equations in (3.2.1-6). The disappearance of one inductor current means that the system's order has been reduced by one. For this reason, the DC-DC converter model derived by the SSA technique in DCM is known as a reduced-order model [20]. The disappearance of $\tilde{d}_2$ and one inductor current allows (3.2.1-6) to be rewritten as:

$$\begin{cases} d\tilde{\mathbf{x}}/dt = \mathbf{A}_m\tilde{\mathbf{x}} + \mathbf{B}_m\tilde{v}_g + \mathbf{B}_{md1}\tilde{d}_1 \\ \tilde{\mathbf{y}} = \mathbf{C}_m\tilde{\mathbf{x}} + \mathbf{E}_m\tilde{v}_g + \mathbf{E}_{md1}\tilde{d}_1 \end{cases} \tag{3.2.1-10}$$

Finally, by applying the Laplace transform to the linear small-signal state-space equations in (3.2.1-10), various transfer functions of the converter can be determined.

3.2.2 Application of SSA Technique to model DCM Zeta Converter

A - State-Space Description of DCM Zeta Converter

The state-space equations are written for each of the three circuit states in Fig. 3.1. The matrices $\mathbf{A}_1$, $\mathbf{A}_2$, $\mathbf{A}_3$, $\mathbf{B}_1$, $\mathbf{B}_2$, $\mathbf{B}_3$, $\mathbf{C}_1$, $\mathbf{C}_2$, $\mathbf{C}_3$, $\mathbf{E}_1$, $\mathbf{E}_2$, and $\mathbf{E}_3$ of the DCM Zeta converter are given by (**Appendix C**):

$$\mathbf{A}_1 = \begin{bmatrix} 0 & 0 & 0 & 0 \\ 0 & 0 & 1/L_2 & -1/L_2 \\ 0 & -1/C_1 & 0 & 0 \\ 0 & 1/C_2 & 0 & -1/(C_2R) \end{bmatrix}, \tag{3.2.2-1-a}$$

$$\mathbf{B}_1 = \begin{bmatrix} 1/L_1 & 1/L_2 & 0 & 0 \end{bmatrix}^T, \tag{3.2.2-1-b}$$

$$\mathbf{C}_1 = [0 \quad 0 \quad 0 \quad 1], \tag{3.2.2-1-c}$$

$$\mathbf{A}_2 = \begin{bmatrix} 0 & 0 & -1/L_1 & 0 \\ 0 & 0 & 0 & -1/L_2 \\ 1/C_1 & 0 & 0 & 0 \\ 0 & 1/C_2 & 0 & -1/(C_2R) \end{bmatrix}, \tag{3.2.2-1-d}$$

$$\mathbf{B}_2 = [0 \quad 0 \quad 0 \quad 0]^T, \tag{3.2.2-1-e}$$

$$\mathbf{C}_2 = [0 \quad 0 \quad 0 \quad 1], \tag{3.2.3-1-f}$$

$$\mathbf{A}_3 = \begin{bmatrix} 0 & 0 & -1/(L_1+L_2) & 1/(L_1+L_2) \\ 0 & 0 & 1/(L_1+L_2) & -1/(L_1+L_2) \\ 1/C_1 & 0 & 0 & 0 \\ 0 & 1/C_2 & 0 & -1/(C_2R) \end{bmatrix}, \tag{3.2.2-1-g}$$

$$\mathbf{B}_3 = [0 \quad 0 \quad 0 \quad 0]^T, \tag{3.2.2-1-h}$$

$$\mathbf{C}_3 = [0 \quad 0 \quad 0 \quad 1], \text{ and} \tag{3.2.2-1-i}$$

$$\mathbf{E}_1 = \mathbf{E}_2 = \mathbf{E}_3 = [0] \tag{3.2.2-1-j}$$

Referring to (3.2.1-5) and (3.2.1-6), the matrices for the steady-state and linear small-signal state-space equations are determined from (3.2.1-7):

$$\mathbf{A} = \begin{bmatrix} 0 & 0 & -D_2/L_1 - D_3/(L_1+L_2) & D_3/(L_1+L_2) \\ 0 & 0 & D_1/L_2 + D_3/(L_1+L_2) & -(D_1+D_2)/L_2 - D_3/(L_1+L_2) \\ (D_2+D_3)/C_1 & -D_1/C_1 & 0 & 0 \\ 0 & 1/C_2 & 0 & -1/(RC_2) \end{bmatrix} \tag{3.2.2-2-a}$$

$$\mathbf{B} = \begin{bmatrix} D_1/L_1 \\ D_1/L_2 \\ 0 \\ 0 \end{bmatrix} \tag{3.2.2-2-b}$$

$$\mathbf{C} = [0 \quad 0 \quad 0 \quad 1] \tag{3.2.2-2-c}$$

$$\mathbf{E} = [0] \tag{3.2.2-2-d}$$

$$\mathbf{B}_{d1} = \begin{bmatrix} V_g/L_1 \\ V_g/L_2 \\ -(I_{L1}+I_{L2})/C_1 \\ 0 \end{bmatrix} \tag{3.2.2-2-e}$$

$$\mathbf{B}_{d2} = \begin{bmatrix} -V_{C1}/L_1 \\ -V_{C1}/L_2 \\ 0 \\ 0 \end{bmatrix} \tag{3.2.2-2-f}$$

$$\mathbf{E}_{d1} = \mathbf{E}_{d2} = [0] \tag{3.2.2-2-g}$$

B - Steady-State (DC) Equations

As mentioned above, the relationship between the steady-state inductor currents, I_{L1} and I_{L2}, must be defined before other steady-state variables can be found. This is realized by averaging the capacitor current, i_{C1}, in Fig. 3.4 over a switching period, T.

In Fig. 3.4, i_{C1} can be expressed as:

$$i_{C1} = -i_{L2} \quad \text{for time interval } d_1T \tag{3.2.2-3-a}$$

$i_{C1} = i_{L1}$ for time interval d_2T (3.2.2-3-b)

$i_{C1} = i_{L1} = -i_{L2}$ for time interval d_3T (3.2.2-3-c)

The average capacitor current, I_{C1}, is found by averaging the waveform in Fig. 3.4:

$$I_{C1} = I_{min} - \Delta i_{L1}\frac{D_2}{2} + \Delta i_{L2}\frac{D_1}{2} \quad (3.2.2\text{-}4)$$

From Fig 3.2, the average values of I_{L1} and I_{L2} can be expressed as:

$$I_{L1} = \frac{1}{T}(\Delta i_{L1}\frac{D_1T}{2} + D_1TI_{min} + \Delta i_{L1}\frac{D_2T}{2} + D_2TI_{min} + D_3TI_{min}) = \frac{\Delta i_{L1}}{2}(D_1 + D_2) + I_{min} \quad (3.2.2\text{-}5\text{-a})$$

$$I_{L2} = \frac{1}{T}(\Delta i_{L2}\frac{D_1T}{2} + \Delta i_{L2}\frac{D_2T}{2} - TI_{min}) = \frac{\Delta i_{L2}}{2}(D_1 + D_2) - I_{min} \quad (3.2.2\text{-}5\text{-b})$$

Equation (3.2.2-5) can be written as:

$$\frac{\Delta i_{L1}}{2} = \frac{I_{L1} - I_{min}}{D_1 + D_2} \quad (3.2.2\text{-}6\text{-a})$$

$$\frac{\Delta i_{L1}}{2} = \frac{I_{L2} + I_{min}}{D_1 + D_2} \quad (3.2.2\text{-}6\text{-b})$$

Substituting (3.2.2-6) into (3.2.2-4),

$$I_{C1} = I_{min} - \frac{I_{L2} + I_{min}}{D_1 + D_2}D_1 + \frac{I_{L1} - I_{min}}{D_1 + D_2}D_2 \quad (3.2.2\text{-}7)$$

In steady state, I_{C1} is equal to zero. Thus, the relationship between I_{L1} and I_{L2} is obtained as:

$$I_{C1} = I_{min} - \frac{I_{L2} + I_{min}}{D_1 + D_2}D_1 + \frac{I_{L1} - I_{min}}{D_1 + D_2}D_2 = 0 \quad (3.2.2\text{-}8\text{-a})$$

$$\frac{I_{L2}}{I_{L1}} = \frac{D_2}{D_1} \quad (3.2.2\text{-}8\text{-b})$$

Given the average matrices in (3.2.2-2-a) to (3.2.2-2-d) and the relationship in (3.2.2-8-b), the steady-state solution of converter can now be solved through (3.2.1-9).

$$\begin{bmatrix} I_{L1} \\ I_{L2} \\ V_{C1} \\ V_{C2} \end{bmatrix} = V_g \begin{bmatrix} \frac{1}{R}\left(\frac{D_1}{D_2}\right)^2 \\ \frac{1}{R}\frac{D_1}{D_2} \\ \frac{D_1}{D_2} \\ \frac{D_1}{D_2} \end{bmatrix} \quad (3.2.2\text{-}9)$$

The diode's duty cycle, D_2, is unknown in the above steady-state solution. The procedure to find D_2 is given as follows:

From Fig 3.1(b), in steady state, the inductor current ripple can be written as:

$$\Delta i_{L1} = \frac{V_g}{L_1}D_1T \quad (3.2.2\text{-}10\text{-a})$$

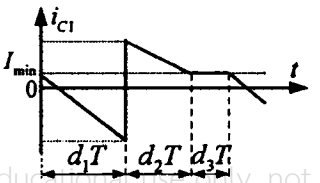

Fig. 3.4. Current waveform of i_{C1}.

$$\Delta i_{L2} = (V_{C1} - V_{C2} + V_g)D_1T / L_2 = V_g D_1 T / L_2 \quad (3.2.2\text{-}10\text{-}b)$$

Substitution of (3.2.2-10) into (3.2.2-5) yields:

$$I_{L1} = \frac{V_g}{2L_1} D_1 T(D_1 + D_2) + I_{min} \quad (3.2.2\text{-}11\text{-}a)$$

$$I_{L2} = \frac{V_g}{2L_2} D_1 T(D_1 + D_2) - I_{min} \quad (3.2.2\text{-}11\text{-}b)$$

Matching the summation of I_{L1} and I_{L2} in (3.2.2-9) to those in (3.2.2-11), D_2 is defined as:

$$\frac{V_g D_1}{RD_2}\left(\frac{D_1}{D_2}+1\right) = \frac{V_g}{2L_E} D_1 T(D_1 + D_2) \quad (3.2.2\text{-}12\text{-}a)$$

$$D_2 = \sqrt{2L_E/(RT)} \quad (3.2.2\text{-}12\text{-}b)$$

where $L_E = L_1 L_2/(L_1 + L_2)$.

C- Linear Small-Signal State-Space (AC) Equations

Given the averaged matrices (3.2.2-2), the linear small-signal state-space equations of the DCM Zeta converter can be formulated in accordance with (3.2.1-6):

$$\frac{d\tilde{i}_{L1}}{dt} = \left(\frac{-D_2}{L_1} - \frac{D_3}{L_1+L_2}\right)\tilde{v}_{C1} + \frac{D_3}{L_1+L_2}\tilde{v}_{C2} + \frac{D_1}{L_1}\tilde{v}_g + \frac{V_g}{L_1}\tilde{d}_1 - \frac{V_{C1}}{L_1}\tilde{d}_2 \quad (3.2.2\text{-}13\text{-}a)$$

$$\frac{d\tilde{i}_{L2}}{dt} = \left(\frac{D_1}{L_2} + \frac{D_3}{L_1+L_2}\right)\tilde{v}_{C1} + \left(\frac{-D_1-D_2}{L_2} - \frac{D_3}{L_1+L_2}\right)\tilde{v}_{C2} + \frac{D_1}{L_2}\tilde{v}_g + \frac{V_g}{L_2}\tilde{d}_1 - \frac{V_{C2}}{L_2}\tilde{d}_2 \quad (3.2.2\text{-}13\text{-}b)$$

$$\frac{d\tilde{v}_{C1}}{dt} = \frac{D_2+D_3}{C_1}\tilde{i}_{L1} + \frac{-D_1}{C_1}\tilde{i}_{L2} + \frac{-1}{C_1}(I_{L1}+I_{L2})\tilde{d}_1 \quad (3.2.2\text{-}13\text{-}c)$$

$$\frac{d\tilde{v}_{C2}}{dt} = \frac{1}{C_2}\tilde{i}_{L2} - \frac{1}{RC_2}\tilde{v}_{C2} \quad (3.2.2\text{-}13\text{-}d)$$

Adding (3.2.2-13-a) to (3.2.2-13-b) and applying the constraint in (3.2.1-8-b),

$$\frac{d\tilde{i}}{dt} = \frac{d\tilde{i}_{L1}}{dt} + \frac{d\tilde{i}_{L2}}{dt} = 0 \quad (3.2.2\text{-}14\text{-}a)$$

$$\frac{-D_1-D_2}{L_2}\tilde{v}_{C2} + \frac{D_1}{L_E}\tilde{v}_g + \frac{V_g}{L_E}\tilde{d}_1 - \frac{V_{C1}}{L_E}\tilde{d}_2 = 0 \quad (3.2.2\text{-}14\text{-}b)$$

$$\tilde{d}_2 = \frac{L_E}{V_{C1}}\left(\frac{D_1}{L_2} - \frac{D_2}{L_1}\right)\tilde{v}_{C1} + \frac{-L_E(D_1+D_2)}{L_2 V_{C1}}\tilde{v}_{C2} + \frac{D_1}{V_{C1}}\tilde{v}_g + \frac{V_g}{V_{C1}}\tilde{d}_1 \quad (3.2.2\text{-}14\text{-}c)$$

From Fig. 3.3,

$$<i> = \frac{i_{max}}{2} = \frac{\Delta i_{L1} + \Delta i_{L2}}{2} \quad (3.2.2\text{-}15\text{-}a)$$

Substituting $\Delta i_{L1} = \frac{v_g}{L_1} d_1 T$ and $\Delta i_{L2} = \frac{v_g + v_{C1} - v_{C2}}{L_2} d_1 T$ into (3.2.2-15-a),

$$<i> = \frac{1}{2}\left(\frac{1}{L_E} v_g d_1 T + \frac{1}{L_2} v_{C1} d_1 T - \frac{1}{L_2} v_{C2} d_1 T\right) \quad (3.2.2\text{-}15\text{-}b)$$

Applying Taylor series expansion to (3.2.2-15-b),

$$\tilde{i} = \frac{DT}{2L_E}\tilde{v}_g + \frac{DT}{2L_2}\tilde{v}_{C1} - \frac{DT}{2L_2}\tilde{v}_{C2} + \frac{VT}{2L_E}\tilde{d}_1 = \tilde{i}_{L1} + \tilde{i}_{L2} \quad (3.2.2\text{-}16\text{-}a)$$

$$\tilde{i}_{L2} = \frac{DT}{2L_E}\tilde{v}_g + \frac{DT}{2L_2}\tilde{v}_{C1} - \frac{DT}{2L_2}\tilde{v}_{C2} + \frac{VT}{2L_E}\tilde{d}_1 - \tilde{i}_{L1} \quad (3.2.2\text{-}16\text{-}b)$$

Here, $\tilde{d}_2$ and $\tilde{i}_{L2}$ get eliminated from the linear small-signal state-space equations by substituting (3.2.2-14-c) and (3.2.2-16-b) into (3.2.2-13).

$$\frac{d\tilde{i}_{L1}}{dt}=\frac{-1}{L_1+L_2}\tilde{v}_{C1}+\frac{1}{L_1+L_2}\tilde{v}_{C2} \quad (3.2.2\text{-}17\text{-a})$$

$$\frac{d\tilde{i}_{L2}}{dt}=\frac{1}{L_1+L_2}\tilde{v}_{C1}-\frac{1}{L_1+L_2}\tilde{v}_{C2} \quad (3.2.2\text{-}17\text{-b})$$

$$\frac{d\tilde{v}_{C1}}{dt}=\frac{1}{C_1}\tilde{i}_{L1}-\frac{D_1^2T}{2C_1L_2}\tilde{v}_{C1}+\frac{D_1^2T}{2C_1L_2}\tilde{v}_{C2}-\frac{D_1^2T}{2C_1L_e}\tilde{v}_g-\frac{D_1V_gT}{C_1L_E}\tilde{d}_1 \quad (3.2.2\text{-}17\text{-c})$$

$$\frac{d\tilde{v}_{C2}}{dt}=-\frac{1}{C_2}\tilde{i}_{L1}+\frac{D_1T}{2C_2L_2}\tilde{v}_{C1}-\frac{1}{C_2}(\frac{D_1T}{2L_2}+\frac{1}{R})\tilde{v}_{C2}+\frac{D_1T}{2C_2L_E}\tilde{v}_g+\frac{V_gT}{2C_2L_E}\tilde{d}_1 \quad (3.2.2\text{-}17\text{-d})$$

Equation (3.2.2-17) can be arranged in the form of:

$$\begin{cases}d\tilde{\mathbf{x}}/dt=\mathbf{A}_m\tilde{\mathbf{x}}+\mathbf{B}_m\tilde{v}_g+\mathbf{B}_{md1}\tilde{d}_1\\ \tilde{\mathbf{y}}=\mathbf{C}_m\tilde{\mathbf{x}}+\mathbf{E}_m\tilde{v}_g+\mathbf{E}_{md1}\tilde{d}_1\end{cases} \quad (3.2.2\text{-}18)$$

where

$$\mathbf{A}_m=\begin{bmatrix}0 & 0 & \frac{-1}{L_1+L_2} & \frac{1}{L_1+L_2}\\ 0 & 0 & \frac{1}{L_1+L_2} & \frac{-1}{L_1+L_2}\\ \frac{1}{C_1} & 0 & \frac{-D_1^2T}{2C_1L_2} & \frac{D_1^2T}{2C_1L_2}\\ \frac{-1}{C_2} & 0 & \frac{D_1T}{2C_2L_2} & \frac{-1}{C_2}(\frac{D_1T}{2L_2}+\frac{1}{R})\end{bmatrix}, \quad (3.2.2\text{-}19\text{-a})$$

$$\mathbf{B}_m=\begin{bmatrix}0\\0\\\frac{-D_1^2T}{2C_1L_E}\\\frac{D_1T}{2C_2L_E}\end{bmatrix}, \quad (3.2.2\text{-}19\text{-b})$$

$$\mathbf{C}_m=\begin{bmatrix}0 & 0 & 0 & 1\end{bmatrix}, \quad (3.2.2\text{-}19\text{-c})$$

$$\mathbf{E}_m=[0], \quad (3.2.2\text{-}19\text{-d})$$

$$\mathbf{B}_{md1}=\begin{bmatrix}0\\0\\\frac{-D_1V_gT}{C_1L_e}\\\frac{V_gT}{2C_2L_e}\end{bmatrix}, \text{ and} \quad (3.2.2\text{-}19\text{-e})$$

$$\mathbf{E}_{md1}=[0]. \quad (3.2.2\text{-}19\text{-f})$$

D- Finding Transfer Functions

Various transfer functions of the converter can be determined from (3.2.2-18). Only two importance ones are given here.

The control-to-output transfer function:

$$G_{d1v}(s)=\frac{\tilde{v}_o(s)}{\tilde{d}_1(s)}=\mathbf{C}_m(s\mathbf{I}-\mathbf{A}_m)^{-1}\mathbf{B}_{md1}+\mathbf{E}_{md1}=\frac{RTV_g}{2L_E}\frac{a_{d1v}s^2+b_{d1v}s+c_{d1v}}{as^3+bs^2+cs+d} \quad (3.2.2\text{-}20\text{-a})$$

The input-to-output transfer function:

$$G_{vv}(s)=\frac{\tilde{v}_o(s)}{\tilde{v}_g(s)}=\mathbf{C}_m(s\mathbf{I}-\mathbf{A}_m)^{-1}\mathbf{B}_m=\frac{D_1TRL_2}{L_E}\frac{a_{vv}s^2+b_{vv}}{as^3+bs^2+cs+d} \quad (3.2.2\text{-}20\text{-b})$$

Coefficients of $G_{d1v}(s)$ and $G_{vv}(s)$ are listed in the TABLE 3.1. The derivation of these coefficients is given in the **Appendix F**.

3.3 Modeling of DCM Zeta Converter with PWM-Switch Model

3.3.1 Overview of PWM-Switch Model in DCM

The PWM-switch block in DCM is shown in Fig. 3.5 where *a*, *c*, and *p* are active, common, and passive terminals [11]. Terminal currents of the PWM switch block in DCM are depicted in Fig. 3.6, where the average terminal currents and voltages can be expressed as:

$$\langle i_a\rangle=\frac{i_{pk}d_1}{2} \quad (3.3.1\text{-}1\text{-a})$$

$$\langle i_p\rangle=\frac{i_{pk}d_2}{2} \quad (3.3.1\text{-}1\text{-b})$$

$$\langle v_{ac}\rangle=\frac{Li_{pk}}{d_1T} \quad (3.3.1\text{-}1\text{-c})$$

$$\langle v_{cp}\rangle=\frac{Li_{pk}}{d_2T} \quad (3.3.1\text{-}1\text{d})$$

From (3.3.1-1), the relationship between the average terminal voltages and currents is given by:

$$\langle i_a\rangle=\frac{\langle i_p\rangle d_1}{d_2} \quad (3.3.1\text{-}2\text{-a})$$

$$\langle v_{ac}\rangle=\frac{\langle v_{cp}\rangle d_2}{d_1} \quad (3.3.1\text{-}2\text{-b})$$

$$i_{pk}=\frac{2\langle i_a\rangle}{d_1} \quad (3.3.1\text{-}2\text{-c})$$

$$d_2=\frac{Li_{pk}}{\langle v_{cp}\rangle T} \quad (3.3.1\text{-}2\text{-d})$$

From (3.3.1-2), d_2 can be written as:

$$d_2=\frac{2Lf\langle i_a\rangle}{d_1\langle v_{cp}\rangle}=\frac{2Lf\langle i_p\rangle}{d_1\langle v_{ac}\rangle} \quad (3.3.1\text{-}3)$$

Substituting (3.3.1-3) into (3.3.1-2-a) and (3.3.1-2-b), the average PWM-switch model can be defined:

$$\langle i_a\rangle=\mu\langle i_p\rangle \quad (3.3.1\text{-}4\text{-a})$$

$$\langle v_{cp}\rangle=\mu\langle v_{ac}\rangle \quad (3.3.1\text{-}4\text{-b})$$

TABLE 3.1

Coefficients of $G_{d1v}(s)$ and $G_{vv}(s)$ of DCM Zeta converter.

$a_{d1v}=2C_1L_2(L_1+L_2)$, $b_{d1v}=-D_1^2T(L_1+L_2)$, and $c_{d1v}=2L_2(1-2D_1)$.
$a_{vv}=C_1$ and $b_{vv}=\frac{1-D_1}{L_1+L_2}$.
$a=2L_2C_1C_2R(L_1+L_2)$, $b=(L_1+L_2)(2C_1L_2+C_1D_1TR+D_1^2TC_2R)$, $c=D_1^2T(L_1+L_2)+2L_2R(C_1+C_2)$, and $d=2L_2$.

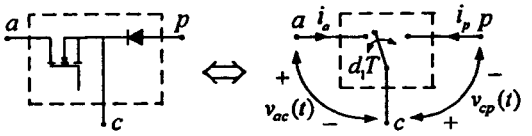

(a) (b)

Fig. 3.5 (a) General power switch and diode and

(b) Voltage and currents of the PWM switch in DCM.

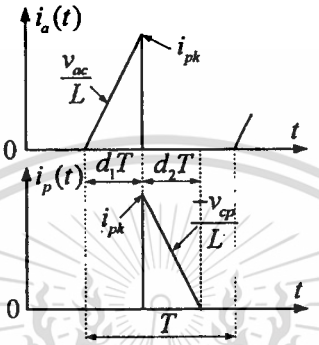

Fig. 3.6. Terminal currents of PWM switch in DCM.

$$\mu=\frac{d_1^2<v_{cp}>}{2Lf<i_a>}=\frac{d_1^2<v_{ac}>}{2Lf<i_p>} \qquad (3.3.1\text{-}4\text{-c})$$

Fig. 3.7 depicts the average PWM-switch model in DCM. Equation (3.3.1-4) is nonlinear and can be linearized by small-signal perturbation with $<i_a> = I_a+\tilde{i}_a$, $<i_p> = I_p+\tilde{i}_p$, $<v_{ac}> = V_{ac}+\tilde{v}_{ac}$, $<v_{cp}> = V_{cp}+\tilde{v}_{cp}$, $d_1 = D_1+\tilde{d}_1$, and $d_2 = D_2+\tilde{d}_2$, where the $\tilde{}$ symbol represents a small-signal value and the capital letter a DC value. It should be noted that $I_a >> \tilde{i}_a$, $I_p >> \tilde{i}_p$, $V_{ac} >> \tilde{v}_{ac}$, $V_{cp} >> \tilde{v}_{cp}$, $D_1 >> \tilde{d}_1$, and $D_2 >> \tilde{d}_2$. Substituting the perturbation into (3.3.1-4-a) and (3.3.1-4-b) and separating the DC from the AC terms, the steady-state and small-signal equations are respectively obtained:

$$V_{cp}=\mu V_{ac} \qquad (3.3.1\text{-}5\text{-a})$$

$$I_a=\mu I_p \qquad (3.3.1\text{-}5\text{-b})$$

$$\mu=\frac{d_1^2}{2L_E f}\frac{V_{cp}}{I_a}=\frac{d_1^2}{2L_E f}\frac{V_{ac}}{I_p}. \qquad (3.3.1\text{-}5\text{-c})$$

$$\tilde{i}_a=g_1\tilde{v}_{ac}+k_1\tilde{d}_1 \qquad (3.3.1\text{-}6\text{-a})$$

$$\tilde{i}_p=g_1\tilde{v}_{ac}+k_o\tilde{d}_1-g_o\tilde{v}_{cp} \qquad (3.3.1\text{-}6\text{-b})$$

where $g_1=\frac{I_a}{V_{ac}}$, $k_1=\frac{2I_a}{D_1}$, $k_O=\frac{2I_p}{D_1}$, $g_O=\frac{I_p}{V_{cp}}$, and $g_1=\frac{2I_p}{V_{ac}}$. (3.3.1-6-c)

From (3.3.1-5) and (3.3.1-6), the DC and small-signal PWM-switch model are drawn as illustrated in Fig. 3.8(a) and Fig. 3.8(b) respectively.

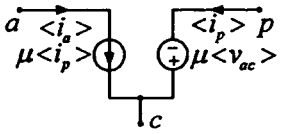

Fig. 3.7. Average model of PWM switch in DCM.

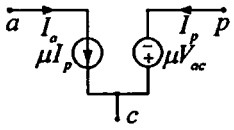

(a)

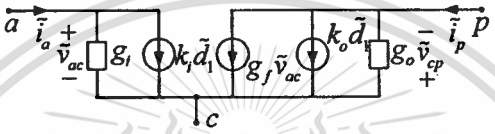

(b)

Fig. 3.8. PWM-switch model in DCM: (a) DC model and (b) AC model.

3.3.2 Application of PWM-Switch Model to DCM Zeta Converter

As shown earlier in chapter 2, the Zeta converter must be rearranged before PWM-switch modeling can be preceded. The rearrangement results in the circuit shown in Fig. 3.9.

A- Steady-State (DC) Analysis

Fig. 3.10(a) shows the Zeta converter substituted with the DC model of the PWM switch. For DC analysis, L_1 and L_2 are short circuited, and C_1 and C_2 open circuited. Simplified circuit for DC analysis is depicted in Fig. 3.10(b), from which the following relationships are observed:

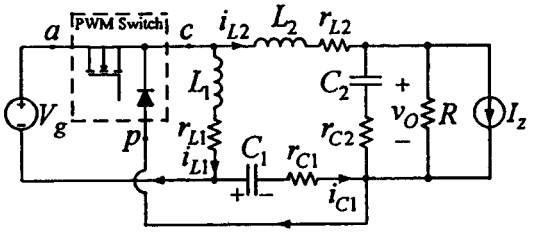

Fig. 3.9. Rearrangement of Zeta converter for PWM-switch modeling.

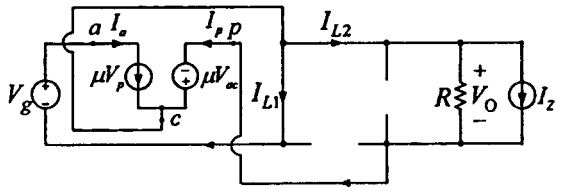

(a)

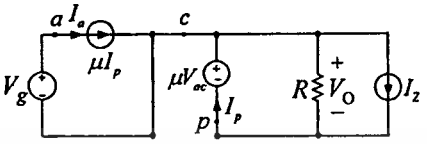

(b)

Fig. 3.10 (a) Zeta converter for dc analysis and

(b) Simplified Circuit of Zeta converter for DC analysis.

$$\mu=\frac{V_{cp}}{V_{oc}}=\frac{V_O}{V_g}=M \tag{3.3.2-1}$$

$$I_p=\frac{V_O}{R}+I_Z=\frac{MV_g+RI_Z}{R} \tag{3.3.2-2}$$

$$I_a=\mu I_p=\frac{M^2V_g+MRI_Z}{R} \tag{3.3.2-3}$$

From (3.3.1-4),

$$\mu=\frac{D_1^2}{2L_Ef}\frac{V_{cp}}{I_a}=\frac{D_1^2}{2L_Ef}\frac{V_{oc}}{I_p} \tag{3.3.2-4-a}$$

$$\mu=\frac{D_1^2}{2L_Ef}\frac{V_g}{I_p}=\frac{D_1^2}{R\frac{2L_Ef}{R}}\frac{V_g}{I_p}=\frac{D_1^2}{\frac{2L_Ef}{R}}\frac{V_g}{V_O+RI_Z} \tag{3.3.2-4-b}$$

$$\mu=\frac{D_1^2}{KM}\frac{1}{1+\frac{I_ZR}{V_O}}=M \tag{3.3.2-4-c}$$

where $K=\frac{2L_Ef}{R}$, $M=\frac{V_O}{V_g}$, and $L_E=\frac{L_1L_2}{L_1+L_2}$.

Equation (3.3.2-4-c) can be rewritten as:

$$M=\frac{D_1}{\sqrt{K(1+\frac{I_ZR}{V_O})}} \tag{3.3.2-5}$$

From (3.3.1-2-b),

$$I_a=\frac{D_1}{D_2}I_p \tag{3.3.2-6-a}$$

$$V_{oc}=\frac{D_2}{D_1}V_{cp} \tag{3.3.2-6-b}$$

$$\frac{D_1}{D_2}=\frac{I_a}{I_p}=\frac{V_{cp}}{V_{oc}}=\mu=M \tag{3.3.2-6-c}$$

From (3.3.2-5) and (3.3.2-6-c), D_2 can be defined as:

$$D_2=\frac{D_1}{M}=\frac{D_1}{\mu}=\sqrt{K(1+\frac{I_ZR}{V_O})} \tag{3.3.2-7}$$

B- Small-Signal (AC) Analysis

Fig. 3.11 illustrates the Zeta converter substituted with the small-signal model of the PWM switch, where the coefficients of the small-signal model are defined from the above DC analysis:

$$g_i=\frac{M^2}{R},\ g_f=\frac{2M}{R},\ g_o=\frac{1}{R},\ k_i=\frac{2M^2V_g}{RD_1},\ \text{and}\ k_o=\frac{2MV_g}{RD_1}. \tag{3.3.2-8}$$

Applying KVL and KCL to Fig. 3.11; voltage and current equations are obtained as follows.

KVL on loop containing $\tilde{v}_g$, v_{ac}, and L_1:

$$\tilde{v}_g-\tilde{v}_{ac}-\tilde{i}_{L1}(sL_1+r_{L1})=0 \tag{3.3.2-9-a}$$

$$\tilde{i}_{L1}=\frac{1}{sL_1+r_{L1}}(\tilde{v}_g-\tilde{v}_{ac}) \tag{3.3.2-9-b}$$

KVL on loop containing $\tilde{v}_{cp}$, L_2, and C_2:

$$\tilde{v}_{cp}-(\tilde{i}_{L2}sL_2+r_{L2}\tilde{i}_{L2})-(\tilde{v}_{C2}+r_{C2}\tilde{i}_{C2})=0 \tag{3.3.2-10-a}$$

$$\tilde{v}_{cp}-\tilde{i}_{L2}(sL_2+r_{L2})-\tilde{v}_{C2}(sC_2r_{C2}+1)=0 \tag{3.3.2-10-b}$$

$$\tilde{i}_{L2}=\frac{1}{sL_2+r_{L2}}[\tilde{v}_{cp}-\tilde{v}_{C2}(sC_2r_{C2}+1)] \tag{3.3.2-10-c}$$

where $\tilde{i}_{C2}=sC_2\tilde{v}_{C2}$.

KVL on loop containing $\tilde{v}_{cp}$, L_1, and C_1:

$$\tilde{v}_{cp}-(\tilde{i}_{L1}sL_1+r_{L1}\tilde{i}_{L1})-(\tilde{v}_{C1}+r_{C1}\tilde{i}_{C1})=0 \tag{3.3.2-11-a}$$

$$\tilde{v}_{cp}-\tilde{i}_{L1}(sL_1+r_{L1})-\tilde{v}_{C1}(sC_1r_{C1}+1)=0 \tag{3.3.2-11-b}$$

$$\tilde{v}_{C1}=\frac{1}{sC_1r_{C1}+1}[\tilde{v}_{cp}-\tilde{i}_{L1}(sL_1+r_{L1})] \tag{3.3.2-11-c}$$

where $\tilde{i}_{C1}=sC_1\tilde{v}_{C1}$.

KVL on loop containing C_1, L_1, L_2, and C_2:

$$\tilde{v}_{C1}(sC_2r_{C1}+1)+\tilde{i}_{L1}(sL_1+r_{L1})-\tilde{i}_{L2}(sL_2+r_{L2})-\tilde{v}_{C2}(sC_2r_{C2}+1)=0 \tag{3.3.2-12}$$

KVL on loop containing C_2 and R:

$$\tilde{v}_O=\tilde{v}_{C2}+r_{C2}\tilde{i}_{C2}=\tilde{v}_{C2}(sC_2r_{C2}+1) \tag{3.3.2-13}$$

KCL on node 1:

$$\tilde{i}_a+\tilde{i}_p=\tilde{i}_{L1}+\tilde{i}_{L2}=(g_i+g_f)\tilde{v}_{ac}+(k_i+k_o)\tilde{d}-g_o\tilde{v}_{cp} \tag{3.3.2-14}$$

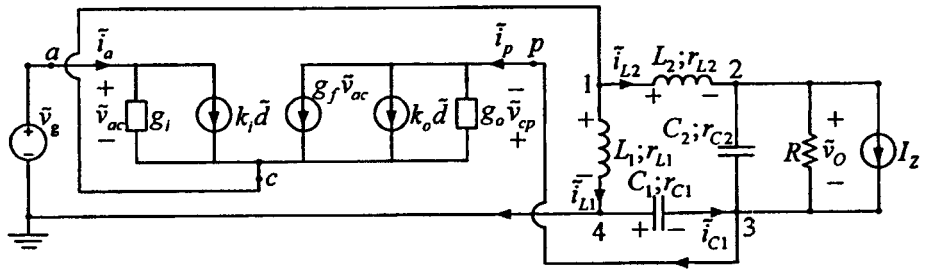

Fig. 3.11. Small-signal model of the DCM Zeta converter.

KCL on node 2 and 3:

$$\tilde{i}_{C2}+\frac{\tilde{v}_o}{R}+\tilde{i}_z=\tilde{i}_p-\tilde{i}_{C1}=\tilde{i}_{L2} \tag{3.3.2-15}$$

KCL on node 4:

$$\tilde{i}_{L1}=\tilde{i}_a+\tilde{i}_{C1}=g_i\tilde{v}_{ac}+k_i\tilde{d}+sC_1\tilde{v}_{C1} \tag{3.3.2-16-a}$$

Substitution of (3.3.2-11-c) into (3.3.2-16-a) produces:

$$\tilde{i}_{L1}=g_i\tilde{v}_{ac}+k_i\tilde{d}+sC_1\frac{1}{sC_1r_{C1}+1}[\tilde{v}_{cp}-\tilde{i}_{L1}(sL_1+r_{L1})] \tag{3.3.2-16-b}$$

$$\tilde{i}_{L1}[1+\frac{sC_1(sL_1+r_{L1})}{sC_1r_{C1}+1}]=g_i\tilde{v}_{ac}+k_i\tilde{d}+\frac{sC_1}{sC_1r_{C1}+1}\tilde{v}_{cp} \tag{3.3.2-16-c}$$

Substitution of (3.3.2-9-b) into (3.3.2-16-c) results in:

$$\frac{1}{sL_1+r_{L1}}(\tilde{v}_g-\tilde{v}_{ac})[1+\frac{sC_1(sL_1+r_{L1})}{sC_1r_{C1}+1}]=g_i\tilde{v}_{ac}+k_i\tilde{d}+\frac{sC_1}{sC_1r_{C1}+1}\tilde{v}_{cp} \tag{3.3.2-16-d}$$

$$\{g_i+\frac{1}{sL_1+r_{L1}}[1+\frac{sC_1(sL_1+r_{L1})}{sC_1r_{C1}+1}]\}\tilde{v}_{ac}+\frac{sC_1}{sC_1r_{C1}+1}\tilde{v}_{cp}=\frac{1}{sL_1+r_{L1}}[1+\frac{sC_1(sL_1+r_{L1})}{sC_1r_{C1}+1}]\tilde{v}_g-k_i\tilde{d} \tag{3.3.2-16-e}$$

Rewriting (3.3.2-11-b),

$$\tilde{v}_{C1}(sC_1r_{C1}+1)=\tilde{v}_{cp}-\tilde{i}_{L1}(sL_1+r_{L1})=\tilde{v}_{cp}-\tilde{v}_g+\tilde{v}_{ac} \tag{3.3.2-17-a}$$

$$\tilde{v}_{C1}=\frac{1}{sC_1r_{C1}+1}(\tilde{v}_{cp}-\tilde{v}_g+\tilde{v}_{ac}) \tag{3.3.2-17-b}$$

Substitution of (3.3.2-13) into (3.3.2-15) gives:

$$sC_2\tilde{v}_{C2}+\frac{\tilde{v}_{C2}(sC_2r_{C2}+1)}{R}+\tilde{i}_z=g_f\tilde{v}_{ac}+k_a\tilde{d}-g_o\tilde{v}_{cp}-sC_1\tilde{v}_{C1} \tag{3.3.2-18-a}$$

$$\tilde{v}_{C2}=\frac{R}{sC_2(R+r_{C2})+1}(g_f\tilde{v}_{ac}+k_o\tilde{d}-g_o\tilde{v}_{cp}-sC_1\tilde{v}_{C1}-\tilde{i}_z) \tag{3.3.2-18-b}$$

Substitution of (3.3.2-17-b) into (3.3.2-18-b) yields:

$$\tilde{v}_{C2}=\frac{R}{sC_2(R+r_{C2})+1}[g_f\tilde{v}_{ac}+k_o\tilde{d}-g_o\tilde{v}_{cp}-sC_1\frac{1}{sC_1r_{C1}+1}(\tilde{v}_{cp}-\tilde{v}_g+\tilde{v}_{ac})-\tilde{i}_z] \tag{3.3.2-19-a}$$

$$\tilde{v}_{C2}=\frac{R}{sC_2(R+r_{C2})+1}[(g_f-\frac{sC_1}{sC_1r_{C1}+1})\tilde{v}_{ac}-(g_o+\frac{sC_1}{sC_1r_{C1}+1})\tilde{v}_{cp}+\frac{sC_1}{sC_1r_{C1}+1}\tilde{v}_g+k_o\tilde{d}-\tilde{i}_z] \tag{3.3.2-19-b}$$

Substitution of (3.3.2-9-b) and (3.3.2-10-c) into (3.3.2-14) yields:

$$\frac{1}{sL_1+r_{L1}}(\tilde{v}_g-\tilde{v}_{ac})+\frac{1}{sL_2+r_{L2}}[\tilde{v}_{cp}-\tilde{v}_{C2}(sC_2r_{C2}+1)]=(g_i+g_f)\tilde{v}_{ac}+(k_i+k_o)\tilde{d}-g_o\tilde{v}_{cp} \tag{3.3.2-20-a}$$

$$\frac{1}{sL_1+r_{L1}}\tilde{v}_g-(k_i+k_o)\tilde{d}-\tilde{v}_{C2}\frac{sC_2r_{C2}+1}{sL_2+r_{L2}}=(g_i+g_f+\frac{1}{sL_1+r_{L1}})\tilde{v}_{ac}-(g_o+\frac{1}{sL_2+r_{L2}})\tilde{v}_{cp} \tag{3.3.2-20-b}$$

Inserting (3.3.2-19-b) into (3.3.2-20-b),

$$\frac{1}{sL_1+r_{L1}}\tilde{v}_g-\frac{R}{sC_2(R+r_{C2})+1}[(g_f-\frac{sC_1}{sC_1r_{C1}+1})\tilde{v}_{ac}-(g_o+\frac{sC_1}{sC_1r_{C1}+1})\tilde{v}_{cp}+\frac{sC_1}{sC_1r_{C1}+1}\tilde{v}_g+k_o\tilde{d}-\tilde{i}_z]\frac{sC_2r_{C2}+1}{sL_2+r_{L2}} \tag{3.3.2-21-a}$$

$$-(k_i+k_o)\tilde{d}=(g_i+g_f+\frac{1}{sL_1+r_{L1}})\tilde{v}_{ac}-(g_o+\frac{1}{sL_2+r_{L2}})\tilde{v}_{cp}$$

$$[(g_i+g_f+\frac{1}{sL_1+r_{L1}})+\frac{R(sC_2r_{C2}+1)}{[sC_2(R+r_{C2})+1](sL_2+r_{L2})}(g_f-\frac{sC_1}{sC_1r_{C1}+1})]\tilde{v}_{ac}-[(g_o+\frac{1}{sL_2+r_{L2}})$$

$$+\frac{R(sC_2r_{C2}+1)}{[sC_2(R+r_{C2})+1](sL_2+r_{L2})}(g_o+\frac{sC_1}{sC_1r_{C1}+1})]\tilde{v}_{cp}=[\frac{1}{sL_1+r_{L1}}-\frac{R(sC_2r_{C2}+1)}{[sC_2(R+r_{C2})+1](sL_2+r_{L2})}\frac{sC_1}{sC_1r_{C1}+1}]\tilde{v}_g \tag{3.3.2-21-b}$$

$$-[(k_i+k_o)+\frac{R(sC_2r_{C2}+1)}{[sC_2(R+r_{C2})+1](sL_2+r_{L2})}k_o]\tilde{d}+\frac{R(sC_2r_{C2}+1)}{[sC_2(R+r_{C2})+1](sL_2+r_{L2})}\tilde{i}_z$$

$$[(g_i+g_f+\frac{1}{sL_1+r_{L1}})+\frac{R(sC_2r_{C2}+1)}{[sC_2(R+r_{C2})+1](sL_2+r_{L2})}(g_f-\frac{sC_1}{sC_1r_{C1}+1})]\tilde{v}_{oc}-B\tilde{v}_{cp}=[\frac{1}{sL_1+r_{L1}}-$$
$$\frac{R(sC_2r_{C2}+1)}{[sC_2(R+r_{C2})+1](sL_2+r_{L2})}\frac{sC_1}{sC_1r_{C1}+1}]\tilde{v}_g-[(k_i+k_o)+\frac{R(sC_2r_{C2}+1)}{[sC_2(R+r_{C2})+1](sL_2+r_{L2})}k_o]\tilde{d} \quad (3.3.2\text{-}21\text{-}c)$$
$$+\frac{R(sC_2r_{C2}+1)}{[sC_2(R+r_{C2})+1](sL_2+r_{L2})}\tilde{i}_Z$$

Where $B=(g_o+\frac{1}{sL_2+r_{L2}})+\frac{R(sC_2r_{C2}+1)}{[sC_2(R+r_{C2})+1](sL_2+r_{L2})}(g_o+\frac{sC_1}{sC_1r_{C1}+1})$

From (3.3.2-16-e),

$$\tilde{v}_{cp}=\frac{sC_1r_{C1}+1}{sC_1}\{\frac{1}{sL_1+r_{L1}}[1+\frac{sC_1(sL_1+r_{L1})}{sC_1r_{C1}+1}]\tilde{v}_g-k_i\tilde{d}-\{g_i+\frac{1}{sL_1+r_{L1}}[1+\frac{sC_1(sL_1+r_{L1})}{sC_1r_{C1}+1}]\}\tilde{v}_{oc}\} \quad (3.3.2\text{-}22\text{-}a)$$

$$\tilde{v}_{cp}=\frac{sC_1r_{C1}+1}{sC_1(sL_1+r_{L1})}[1+\frac{sC_1(sL_1+r_{L1})}{sC_1r_{C1}+1}]\tilde{v}_g-\frac{sC_1r_{C1}+1}{sC_1}k_i\tilde{d}-\frac{sC_1r_{C1}+1}{sC_1}\{g_i+\frac{1}{sL_1+r_{L1}}[1+\frac{sC_1(sL_1+r_{L1})}{sC_1r_{C1}+1}]\}\tilde{v}_{oc} \quad (3.3.2\text{-}22\text{-}b)$$

$$\tilde{v}_{cp}=\frac{sC_1r_{C1}+1}{sC_1(sL_1+r_{L1})}[1+\frac{sC_1(sL_1+r_{L1})}{sC_1r_{C1}+1}]\tilde{v}_g-\frac{sC_1r_{C1}+1}{sC_1}k_i\tilde{d}-A\tilde{v}_{oc} \quad (3.3.2\text{-}22\text{-}c)$$

where $A=\frac{sC_1r_{C1}+1}{sC_1}\{g_i+\frac{1}{sL_1+r_{L1}}[1+\frac{sC_1(sL_1+r_{L1})}{sC_1r_{C1}+1}]\}$.

Substitution of (3.3.2-22-c) into (3.3.2-21-c) produces:

$$[(g_i+g_f+\frac{1}{sL_1+r_{L1}})+\frac{R(sC_2r_{C2}+1)}{[sC_2(R+r_{C2})+1](sL_2+r_{L2})}(g_f-\frac{sC_1}{sC_1r_{C1}+1})]\tilde{v}_{oc}-B[\frac{sC_1r_{C1}+1}{sC_1(sL_1+r_{L1})}[1+$$
$$\frac{sC_1(sL_1+r_{L1})}{sC_1r_{C1}+1}]\tilde{v}_g-\frac{sC_1r_{C1}+1}{sC_1}k_i\tilde{d}-A\tilde{v}_{oc}]=[\frac{1}{sL_1+r_{L1}}-\frac{R(sC_2r_{C2}+1)}{[sC_2(R+r_{C2})+1](sL_2+r_{L2})}\frac{sC_1}{sC_1r_{C1}+1}]\tilde{v}_g \quad (3.3.2\text{-}22\text{-}d)$$
$$-[(k_i+k_o)+\frac{R(sC_2r_{C2}+1)}{[sC_2(R+r_{C2})+1](sL_2+r_{L2})}k_o]\tilde{d}+\frac{R(sC_2r_{C2}+1)}{[sC_2(R+r_{C2})+1](sL_2+r_{L2})}\tilde{i}_Z$$

$$\{[(g_i+g_f+\frac{1}{sL_1+r_{L1}})+\frac{R(sC_2r_{C2}+1)}{[sC_2(R+r_{C2})+1](sL_2+r_{L2})}(g_f-\frac{sC_1}{sC_1r_{C1}+1})]+BA\}\tilde{v}_{oc}=$$
$$\{[\frac{1}{sL_1+r_{L1}}-\frac{R(sC_2r_{C2}+1)}{[sC_2(R+r_{C2})+1](sL_2+r_{L2})}\frac{sC_1}{sC_1r_{C1}+1}]+B\frac{sC_1r_{C1}+1}{sC_1(sL_1+r_{L1})}[1+\frac{sC_1(sL_1+r_{L1})}{sC_1r_{C1}+1}]\}\tilde{v}_g \quad (3.3.2\text{-}22\text{-}e)$$
$$-\{[(k_i+k_o)+\frac{R(sC_2r_{C2}+1)}{[sC_2(R+r_{C2})+1](sL_2+r_{L2})}k_o]+B\frac{sC_1r_{C1}+1}{sC_1}k_i\}\tilde{d}+\frac{R(sC_2r_{C2}+1)}{[sC_2(R+r_{C2})+1](sL_2+r_{L2})}\tilde{i}_Z$$

$$A_{oc}\tilde{v}_{oc}=A_{ocg}\tilde{v}_g-A_{ocd}\tilde{d}+A_{ocz}\tilde{i}_Z \quad (3.3.2\text{-}22\text{-}f)$$

$$\tilde{v}_{oc}=\frac{A_{ocg}}{A_{oc}}\tilde{v}_g-\frac{A_{ocd}}{A_{oc}}\tilde{d}+\frac{A_{ocz}}{A_{oc}}\tilde{i}_Z \quad (3.3.2\text{-}22\text{-}g)$$

where $A_{oc}=[(g_i+g_f+\frac{1}{sL_1+r_{L1}})+\frac{R(sC_2r_{C2}+1)}{[sC_2(R+r_{C2})+1](sL_2+r_{L2})}(g_f-\frac{sC_1}{sC_1r_{C1}+1})]+BA$,

$A_{ocg}=[\frac{1}{sL_1+r_{L1}}-\frac{R(sC_2r_{C2}+1)}{[sC_2(R+r_{C2})+1](sL_2+r_{L2})}\frac{sC_1}{sC_1r_{C1}+1}]+B\frac{sC_1r_{C1}+1}{sC_1(sL_1+r_{L1})}[1+\frac{sC_1(sL_1+r_{L1})}{sC_1r_{C1}+1}]$,

$A_{ocZ}=\frac{R(sC_2r_{C2}+1)}{[sC_2(R+r_{C2})+1](sL_2+r_{L2})}$,

and $A_{ocd}=[(k_i+k_o)+\frac{R(sC_2r_{C2}+1)}{[sC_2(R+r_{C2})+1](sL_2+r_{L2})}k_o]+B\frac{sC_1r_{C1}+1}{sC_1}k_i$.

Substitution of (3.3.2-22-g) into (3.3.2-22-c) yields:

$$\tilde{v}_{cp}=\frac{sC_1r_{C1}+1}{sC_1(sL_1+r_{L1})}[1+\frac{sC_1(sL_1+r_{L1})}{sC_1r_{C1}+1}]\tilde{v}_g-\frac{sC_1r_{C1}+1}{sC_1}k_i\tilde{d}-A(\frac{A_{ocg}}{A_{oc}}\tilde{v}_g-\frac{A_{ocd}}{A_{oc}}\tilde{d}+\frac{A_{ocz}}{A_{oc}}\tilde{i}_z) \quad (3.3.2\text{-}23\text{-}a)$$

$$\tilde{v}_{cp}=\{\frac{sC_1r_{C1}+1}{sC_1(sL_1+r_{L1})}[1+\frac{sC_1(sL_1+r_{L1})}{sC_1r_{C1}+1}]-A\frac{A_{ocg}}{A_{oc}}\}\tilde{v}_g+\{A\frac{A_{ocd}}{A_{oc}}-\frac{sC_1r_{C1}+1}{sC_1}k_i\}\tilde{d}-A\frac{A_{ocz}}{A_{oc}}\tilde{i}_Z \quad (3.3.2\text{-}23\text{-}b)$$

$$\tilde{v}_{cp}=A_{cpg}\tilde{v}_g+A_{cpd}\tilde{d}-A_{cpz}\tilde{i}_Z \quad (3.3.2\text{-}23\text{-}c)$$

where $A_{cpg}=\frac{sC_1r_{C1}+1}{sC_1(sL_1+r_{L1})}[1+\frac{sC_1(sL_1+r_{L1})}{sC_1r_{C1}+1}]-A\frac{A_{ocg}}{A_{oc}}$, $A_{cpd}=A\frac{A_{ocd}}{A_{oc}}-\frac{sC_1r_{C1}+1}{sC_1}k_i$, and $A_{cpz}=A\frac{A_{ocz}}{A_{oc}}$.

Substitution of (3.3.2-19-b) into (3.3.2-13) gives:

$$\tilde{v}_o=(sC_2r_{C2}+1)\tilde{v}_{C2}=\frac{(sC_2r_{C2}+1)R}{sC_2(R+r_{C2})+1}[(g_f-\frac{sC_1}{sC_1r_{C1}+1})\tilde{v}_{ac}-(g_o+\frac{sC_1}{sC_1r_{C1}+1})\tilde{v}_{cp}+\frac{sC_1}{sC_1r_{C1}+1}\tilde{v}_g+k_o\tilde{d}-\tilde{i}_z] \quad (3.3.2\text{-}24\text{-}a)$$

Substitution (3.3.2-22-g) and (3.3.2-23-c) into (3.3.2-24-a) yields:

$$\tilde{v}_O=\frac{(sC_2r_{C2}+1)R}{sC_2(R+r_{C2})+1}[(g_f-\frac{sC_1}{sC_1r_{C1}+1})(\frac{A_{acg}}{A_{ac}}\tilde{v}_g-\frac{A_{acd}}{A_{ac}}\tilde{d}+\frac{A_{acZ}}{A_{ac}}\tilde{i}_2)-(g_o+\frac{sC_1}{sC_1r_{C1}+1})(A_{cpg}\tilde{v}_g+A_{cpd}\tilde{d}-A_{cpZ}\tilde{i}_2) \quad (3.3.2\text{-}24\text{-}b)$$
$$+\frac{sC_1}{sC_1r_{C1}+1}\tilde{v}_g+k_o\tilde{d}]$$

$$\tilde{v}_O=\frac{(sC_2r_{C2}+1)R}{sC_2(R+r_{C2})+1}[\{(g_f-\frac{sC_1}{sC_1r_{C1}+1})\frac{A_{acg}}{A_{ac}}-(g_o+\frac{sC_1}{sC_1r_{C1}+1})A_{cpg}+\frac{sC_1}{sC_1r_{C1}+1}\}\tilde{v}_g \quad (3.3.2\text{-}24\text{-}c)$$
$$+\{k_o-(g_f-\frac{sC_1}{sC_1r_{C1}+1})\frac{A_{acd}}{A_{ac}}-(g_o+\frac{sC_1}{sC_1r_{C1}+1})A_{cpd}\}\tilde{d}+\{(g_f-\frac{sC_1}{sC_1r_{C1}+1})\frac{A_{acZ}}{A_{ac}}+(g_o+\frac{sC_1}{sC_1r_{C1}+1})A_{cpZ}\}\tilde{i}_Z]$$

$$\tilde{v}_O=\frac{(sC_2r_{C2}+1)R}{sC_2(R+r_{C2})+1}\{(g_f-\frac{sC_1}{sC_1r_{C1}+1})\frac{A_{acg}}{A_{ac}}-(g_o+\frac{sC_1}{sC_1r_{C1}+1})A_{cpg}+\frac{sC_1}{sC_1r_{C1}+1}\}\tilde{v}_g$$
$$+\frac{(sC_2r_{C2}+1)R}{sC_2(R+r_{C2})+1}\{k_o-(g_f-\frac{sC_1}{sC_1r_{C1}+1})\frac{A_{acd}}{A_{ac}}-(g_o+\frac{sC_1}{sC_1r_{C1}+1})A_{cpd}\}\tilde{d} \quad (3.3.2\text{-}24\text{-}d)$$
$$+\frac{(sC_2r_{C2}+1)R}{sC_2(R+r_{C2})+1}\{(g_f-\frac{sC_1}{sC_1r_{C1}+1})\frac{A_{acZ}}{A_{ac}}+(g_o+\frac{sC_1}{sC_1r_{C1}+1})A_{cpZ}\}\tilde{i}_Z$$

where $G_{vv}=\frac{\tilde{v}_O}{\tilde{v}_g}=\frac{(sC_2r_{C2}+1)R}{sC_2(R+r_{C2})+1}\{(g_f-\frac{sC_1}{sC_1r_{C1}+1})\frac{A_{acg}}{A_{ac}}-(g_o+\frac{sC_1}{sC_1r_{C1}+1})A_{cpg}+\frac{sC_1}{sC_1r_{C1}+1}\}$ (3.3.2-25-a)

$$G_{dv}=\frac{\tilde{v}_O}{\tilde{d}}=\frac{(sC_2r_{C2}+1)R}{sC_2(R+r_{C2})+1}\{k_o-(g_f-\frac{sC_1}{sC_1r_{C1}+1})\frac{A_{acd}}{A_{ac}}-(g_o+\frac{sC_1}{sC_1r_{C1}+1})A_{cpd}\} \quad (3.3.2\text{-}25\text{-}b)$$

$$G_{zv}=\frac{\tilde{v}_O}{\tilde{i}_Z}=\frac{(sC_2r_{C2}+1)R}{sC_2(R+r_{C2})+1}\{(g_f-\frac{sC_1}{sC_1r_{C1}+1})\frac{A_{acZ}}{A_{ac}}+(g_o+\frac{sC_1}{sC_1r_{C1}+1})A_{cpZ}\} \quad (3.3.2\text{-}25\text{-}c)$$

The above transfer functions can be rewritten as:

$$G_{vv}=\frac{R(sC_2r_{C2}+1)}{sC_2(R+r_{C2})+1}\frac{a_{vv}s^6+b_{vv}s^5+c_{dv}s^4+d_{vv}s^3+e_{vv}s^2+f_{vv}s+g_{vv}}{as^4+bs^3+cs^2+ds+e} \quad (3.3.2\text{-}26\text{-}a)$$

$$G_{dv}=R(sC_2r_{C2}+1)\frac{a_{dv}s^2+b_{dv}s+c_{dv}}{as^4+bs^3+cs^2+ds+e} \quad (3.3.2\text{-}26\text{-}b)$$

$$G_{zv}=\frac{R^2(sC_2r_{C2}+1)^2}{sC_2(R+r_{C2})+1}\frac{a_{zv}s^2+b_{zv}s+c_{zv}}{as^4+bs^3+cs^2+ds+e} \quad (3.3.2\text{-}26\text{-}c)$$

Coefficient of these transfer functions are listed in TABLE 3.2. The derivation of these coefficients is given in the **Appendix F**.

3.4 Modeling of DCM Zeta Converter with Averaged Switch Model

3.4.1 Overview of Averaged Switch Model in DCM

Like the CCM case, the switch network in DCM is identified as shown in Fig 3.12(a). From [18], it can be shown that the relationship between averaged terminal quantities in Fig. 3.12(a) is given by:

$$\langle i_1(t)\rangle=\frac{d_1^2(t)T}{2L_E}\langle v_1(t)\rangle \quad (3.4.1\text{-}a)$$

$$\langle i_2(t)\rangle=\frac{d_1^2(t)T}{2L_E}\frac{\langle v_1(t)\rangle^2}{\langle v_2(t)\rangle} \quad (3.4.1\text{-}b)$$

TABLE 3.2

Coefficient of $G_{d1v}(s)$, $G_{vv}(s)$, and $G_{zv}(s)$ of DCM Zeta converter.

$a_{dv}=C_1L_1[(k_Og_i-g_fk_i)r_{C1}+k_i+k_O]$, $b_{dv}=C_1r_{L1}[(k_Og_i-g_fk_i)r_{C1}+k_i+k_O]+k_OC_1r_{C1}-(g_fk_i-k_Og_i)L_1$, $c_{dv}=(k_Og_i-g_fk_i)r_{L1}-k_O$
$a_w=g_Og_iL_1L_2C_1^3C_2r_{C1}^2(R+r_{C2})$ $b_w=C_1^2r_{C1}[C_2(R+r_{C2})[g_Og_iC_1r_{C1}(L_2r_{L1}+L_1r_{L2})+C_1r_{C1}(g_iL_1-g_fL_2)+2g_Og_iL_1L_2]+g_Og_iL_1C_1r_{C1}(C_2Rr_{C2}+L_2)]$ $c_{dv}=C_1^2r_{C1}[(r_{L2}+R)[g_ig_oC_1r_{C1}(C_2r_{L2}r_{L1}+L_1)+2g_ig_oC_2(L_2r_{L1}+L_1r_{L2})+C_1C_2r_{C1}(gr_{L1}-g_fr_{L2})]$ $+g_ig_O(C_1r_{C1}r_{L1}+2L_1)(C_2Rr_{C2}+L_2)+[C_1r_{C1}+2C_2(r_{C2}+R)](g_iL_1-g_fL_2)-g_fC_1C_2Rr_{C2}r_{C1}]$ $d_w=C_1[g_iC_1r_{C1}(g_or_{L2}+1)[C_1r_{C1}r_{L1}+2C_2r_{L1}(r_{C2}+R)+2L_1]+2C_1r_{C1}(g_og_ir_{L1}-g_f)(L_2+C_2Rr_{C2})+g_ig_oC_1r_{C1}R(C_1r_{C1}r_{L1}+2L_1)$ $+\{L_1C_2(g_f+g_i)-g_fC_1r_{C1}(C_1r_{C1}+2C_2r_{L2})\}(R+r_{C2})]$ $e_w=C_1[2C_1r_{C1}[g_ir_{L1}+(g_ig_or_{L1}-g_f)(R+r_{L2})]+C_2(R+r_{C2})(g_fr_{L1}+g_ir_{L1}+g_fr_{C1})+L_1(g_f+g_i)]$ $f_w=C_1r_{L1}(g_i+g_f)+g_f(C_1r_{C1}+C_2r_{C2}+C_2R)$ $g_w=g_f$
$a_{zv}=L_1C_1(g_O+g_i+g_f+g_Or_{C1}g_i)$, $b_{zv}=C_1r_{L1}(g_O+g_i+g_f+g_Og_ir_{C1})+C_1(g_Or_{C1}+1)+g_Og_iL_1$, $c_{zv}=g_O(1+g_ir_{L1})$
$a=L_1L_2C_1C_2(g_f+g_O+g_i+g_Or_{C1}g_i)(r_{C2}+R)$ $b=C_1C_2(g_f+g_O+g_i+g_Og_ir_{C1})(r_{C2}+R)(L_2r_{L1}+L_1r_{L2})+g_Og_iL_1(L_2C_1r_{C1}+L_2C_2r_{C2}+L_2C_2R+C_1C_2Rr_{C2}r_{C1})$ $+C_1C_2(g_iL_1+g_OL_2)(Rr_{C1}+r_{C1}r_{C2})+L_1C_1(C_2Rr_{C2}+L_2)(g_f+g_i+g_O)+C_1C_2(r_{C2}+R)(L_1+L_2)$ $c=[C_2r_{L2}r_{L1}(r_{C2}+R)+L_1(r_{L2}+R)+r_{L1}(C_2Rr_{C2}+L_2)](g_f+g_i+g_O)C_1+[g_ig_OC_2(L_2r_{L1}+L_1r_{L2}+C_1r_{L2}r_{L1}r_{C1})$ $+C_1C_2(g_ir_{C1}+1)(r_{L1}+r_{L2})+C_2C_1r_{C1}](r_{C2}+R)+g_Og_i[C_1r_{C1}(L_2r_{L1}+L_1r_{L2})+C_1C_2Rr_{C2}r_{C1}r_{L1}+L_1L_2]$ $+C_1C_2Rr_{C2}(g_Or_{C1}+1)+(g_iL_1+g_OL_2+g_Og_iL_1R)(C_1r_{C1}+C_2r_{C2})+(g_iC_2R+C_1)(L_1+L_2)$ $d=(g_Og_fr_{L2}r_{L1}+g_fr_{L1}+1)(R+r_{C2})C_2+[C_1r_{L1}(g_f+g_O+g_i)+g_Og_i(L_1+C_1r_{C1}r_{L1})+g_OC_2r_{L2}](R+r_{L2})+C_1r_{C1}(g_ir_{L1}+g_Or_{L2})$ $+g_Og_fr_{L1}(L_2+C_2Rr_{C2})+g_OR(C_1r_{C1}+C_2r_{C2})+g_OL_2+g_iL_1+C_1(R+r_{L2}+r_{L1}+r_{C1})$ $e=(1+g_fr_{L1})(Rg_O+1+g_Or_{L2})$

The averaged switch model corresponding with (3.4.1-a) and (3.4.1-b) is drawn as shown in Fig. 3.12(b). Equation (3.4.1) is a nonlinear function of $<v_1(t)>$, $<v_2(t)>$, and $d_1(t)$ and rewritten as:

$$<i_1(t)>=\frac{d_1^2(t)T}{2L_E}<v_1(t)>=f_1(<v_1(t)>,<v_2(t)>,d_1(t)) \tag{3.4.2-a}$$

$$<i_2(t)>=\frac{d_1^2(t)T}{2L_E}\frac{<v_1(t)>^2}{<v_2(t)>}=f_2(<v_1(t)>,<v_2(t)>,d_1(t)) \tag{3.4.2-b}$$

The small-signal equations can be found by applying Taylor series expansion [18] to (3.4.2), which gives:

$$I_1+\tilde{i}_1(t)=f_1(V_1,V_2,D_1)+\tilde{v}_1(t)\frac{\partial f_1(v_1,V_2,D_1)}{\partial v_1}\bigg|_{v_1=V_1}+\tilde{v}_2(t)\frac{\partial f_1(V_1,v_2,D_1)}{\partial v_2}\bigg|_{v_2=V_2}+\tilde{d}_1(t)\frac{\partial f_1(V_1,V_2,d_1)}{\partial d}\bigg|_{d_1=D_1} \tag{3.4.3-a}$$

$$I_2+\tilde{i}_2(t)=f_2(V_1,V_2,D_1)+\tilde{v}_1(t)\frac{\partial f_2(v_1,V_2,D_1)}{\partial v_1}\bigg|_{v_1=V_1}+\tilde{v}_2(t)\frac{\partial f_2(V_1,v_2,D_1)}{\partial v_2}\bigg|_{v_2=V_2}+\tilde{d}_1(t)\frac{\partial f_2(V_1,V_2,d_1)}{\partial d}\bigg|_{d_1=D_1} \tag{3.4.3-b}$$

From (3.4.3), the DC equations are:

$$I_1=f_1(V_1,V_2,D_1)=V_1/R_E \tag{3.4.4-a}$$

$$I_2=f_2(V_1,V_2,D_1)=V_1^2/(R_EV_2)\,. \tag{3.4.4-b}$$

where $R_E=2L_E/(D_1T)$.

3.5 Duty ratio-to-output voltage transfer function, $G_{d1v}(s)$

Like CCM, the transfer functions derived from three different modeling methods, i.e., SSA technique, PWM-switch model, and averaged switch model are plotted and compared here. Transfer functions $G_{d1v}(s)$ of the DCM Zeta converter from the SSA technique expressed in (3.2.2-20-a), from the PWM-switch model expressed in (3.3.2-26-b), and from averaged switch model simulated with Fig. 3.15 are compared, using the component values listed in TABLE 3.3. It should be noted that these values satisfy the condition for DCM in (3.1-2).

Fig. 3.16 shows the Bode plots of $G_{d1v}(s)$ given by the three modeling methods, in the case when the circuit parasitic is assumed to be zero. It can be seen that the result from the SSA technique (Fig. 3.16(a)) corresponds with the results from PWM-switch model (Fig. 3.16(b)) and averaged switch model (Fig. 3.16(c)), which closely agree with one another, only up to one-tenth of the switching frequency (10 kHz). Beyond that, the SSA model starts to deviate from the PWM-switch and averaged switch models. This discrepancy is due to the fact that the DCM Zeta converter modeled by the SSA technique yields a reduced-order model, while the converter modeled by PWM-switch and averaged switch models are full-order models (see (3.2.2-20-a) and (3.3.2-26-b)). Fig. 3.17 compares the Bode plots of the DCM Zeta converter modeled by PWM-switch model (Fig. 3.17(a)) and by averaged switch model (Fig. 3.17(b)), taking into account the circuit parasitic. The results from these two models are exactly the same each other.

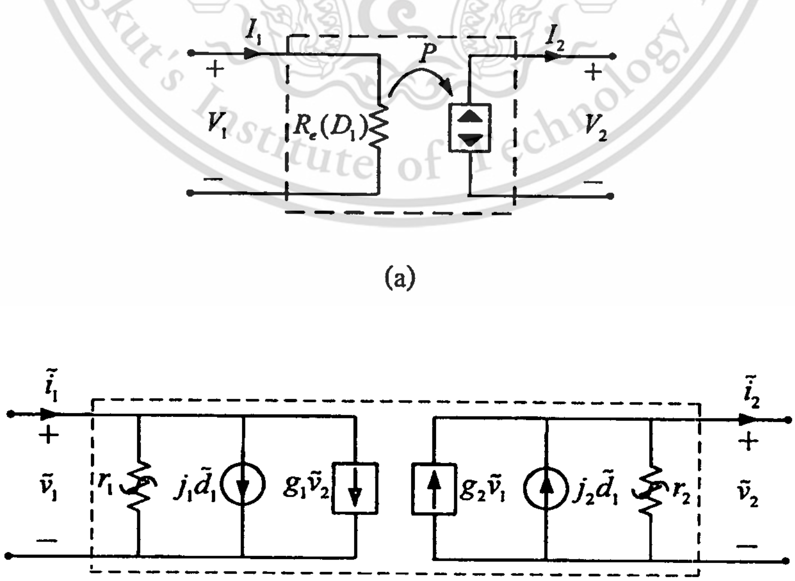

(a)

(b)

Fig. 3.13. (a) Two-port small-signal DC model and

(b) Two-port small-signal AC model of the averaged switch model.

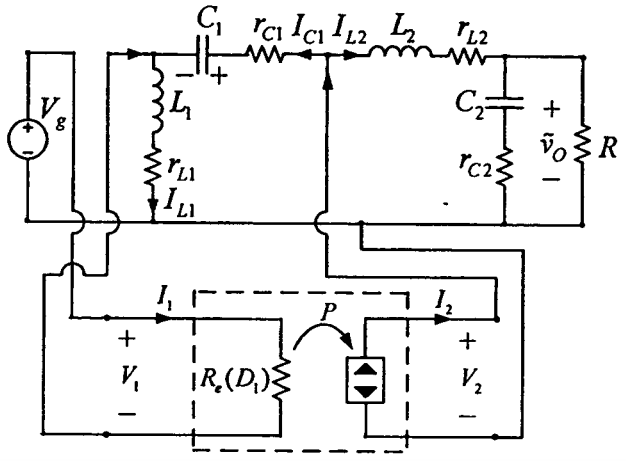

(a)

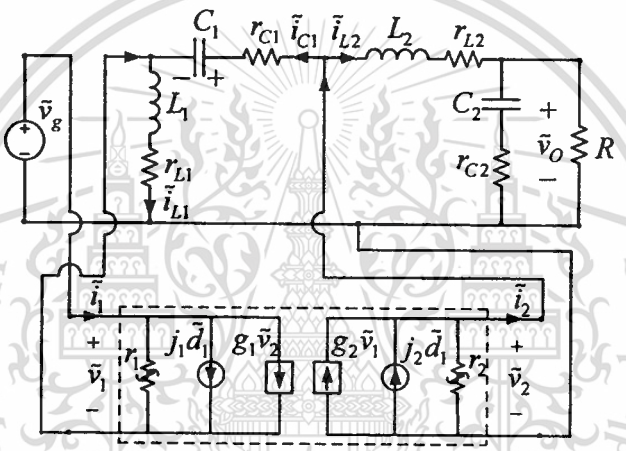

(b)

Fig. 3.14. (a) DC averaged switch model and
(b) AC averaged switch model of DCM Zeta converter.

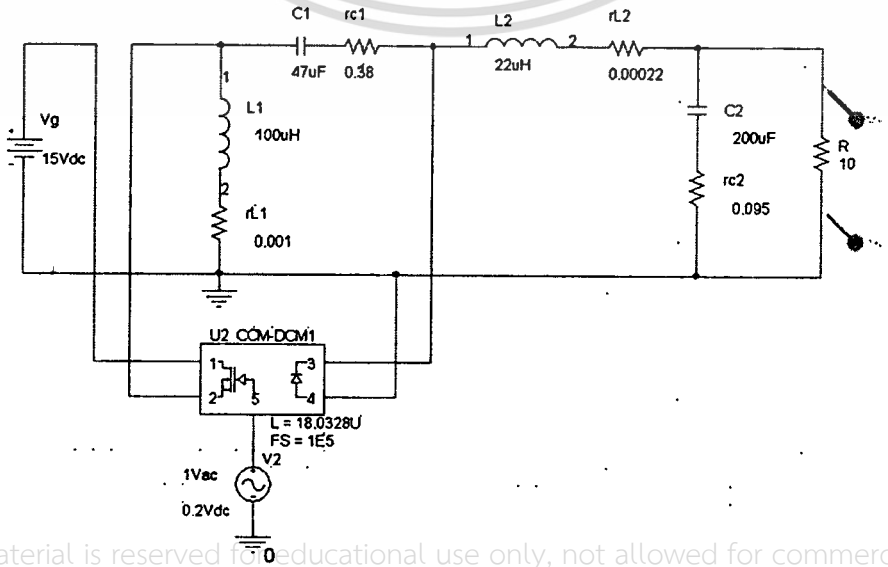

Fig. 3.15. PSPICE circuit schematic of DCM Zeta converter using averaged switch model.

TABLE 3.3

Circuit Parameters for DCM Zeta converter.

Circuit Parameters	Values
V_g / V_O	15-20 / 5V
C_1 / C_2	47 / 200μF
L_1 / L_2	100/ 22μH
$r_{C1} / r_{C2} / r_{L1} / r_{L2}$	0.38 / 0.095/0.001/0.00022Ω
R	10-38Ω

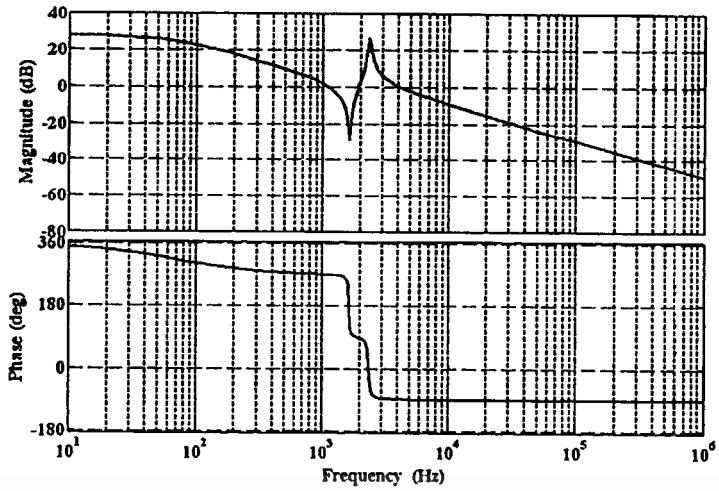

(a)

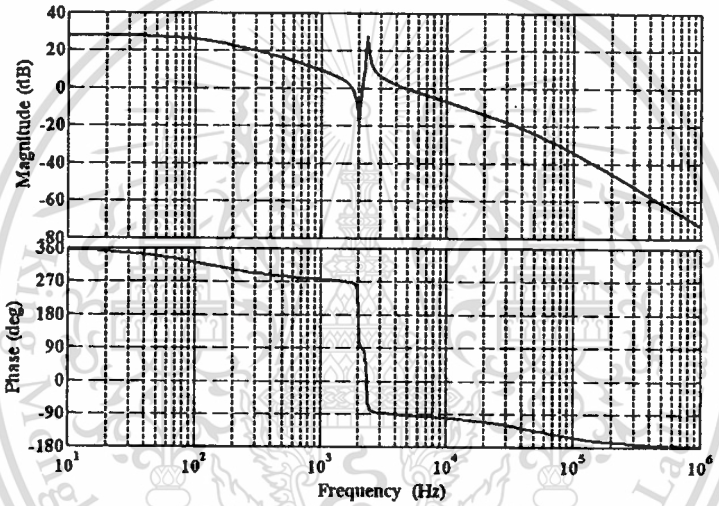

(b)

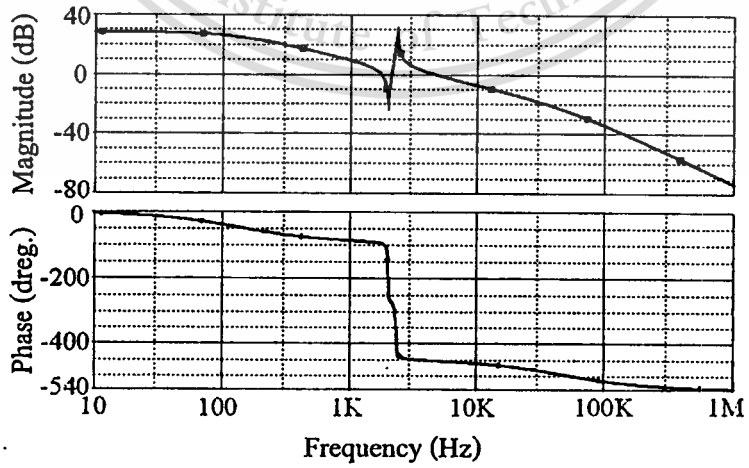

(c)

Fig.3.16. Frequency responses of $G_{d1v}(s)$ of DCM Zeta converter when circuit parasitic is zero: (a) SSA technique, (b) PWM-switch model, and (c) Averaged switch model.

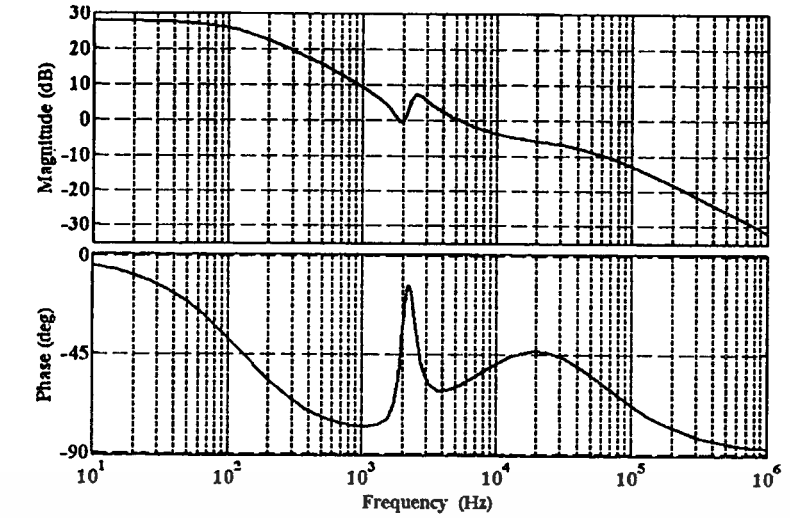

(a)

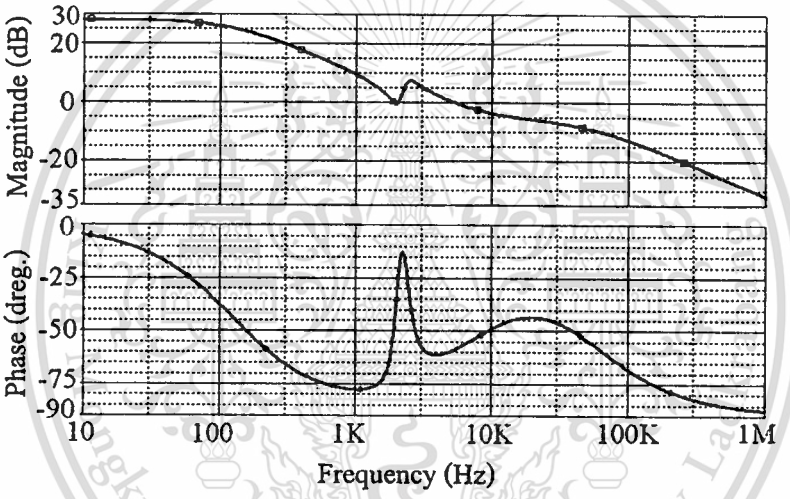

(b)

Fig. 3.17. Frequency response of $G_{d1v}(s)$ of DCM Zeta converter when circuit parasitic is included: (a) PWM-switch model and (b) Averaged switch model.

Chapter 4

Control of Zeta Converter

This chapter is divided into two parts. The first part deals with a Zeta converter whose output voltage is regulated using Voltage Mode Control (VMC). The second part covers the converter which employs Peak Current Mode Control (PCMC) scheme. Control block diagrams for each control method are presented. Based on these control block diagrams, feedback compensator can be designed to give the converter the desired regulation characteristics.

4.1 Voltage Mode Control (VMC)

4.1.1 Description of VMC

Fig. 4.1(a) shows Zeta converter with Voltage Mode Control (VMC). The power stage is the Zeta converter circuit described in the preceding chapters. The control stage consists of an error amplifier and PWM comparator. The output voltage, V_O, is fed back and compared with the reference voltage, V_{ref}. The resulting error voltage is processed by a compensator, $G_C(s)$, which produces the control voltage, v_C, to compare with the sawtooth voltage, v_{saw}, at the PWM comparator. As shown in Fig. 4.1(b), the MOSFET is turned on when v_C is larger than v_{saw}, and turned off when v_C is smaller than v_{saw}. If v_O is changed, feedback control will respond by adjusting v_C and the duty cycle of the MOSFET until v_O is again equal to V_{ref}.

A block diagram of Zeta converter with VMC in Fig. 4.1(a) is depicted in Fig. 4.2. The power stage is represented by the three transfer functions: $G_{dv}(s)$, $G_{vv}(s)$, and $G_{zv}(s)$. Note that the block diagram in Fig. 4.2 is valid for both the CCM and DCM cases. For feedback control design purpose, the input variables, v_g and i_Z, in the power stage can be assumed to be zero because the effect of the duty cycle (produce by control stage) on the output voltage is of interest here. Thus the block diagram in Fig. 4.2 is simplified into Fig. 4.3.

The transfer function of PWM comparator is derived from the waveform in Fig. 4.1(b) and given by:

$$F_M = \frac{\tilde{d}(s)}{\tilde{v}_C(s)} = \frac{1}{V_M} \qquad (4.1.1\text{-}1)$$

where V_M is amplitude of the sawtooth voltage.

From Fig. 4.3, the open-loop transfer function is defined as:

$$T(s) = G_C(s)G_{dv}(s)F_M \qquad (4.1.1\text{-}2)$$

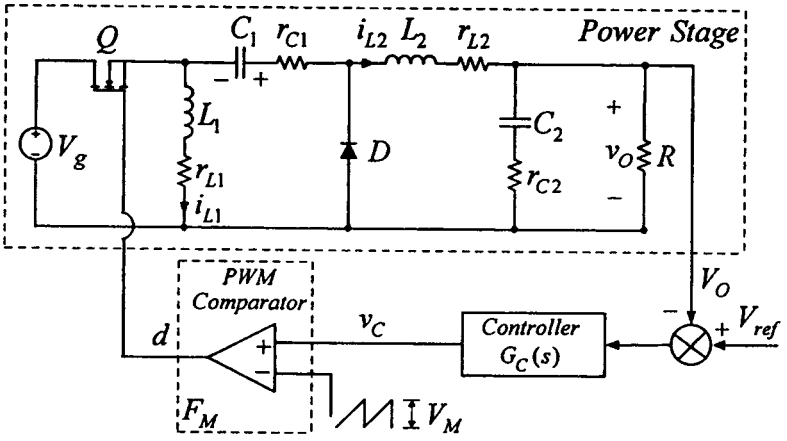

(a)

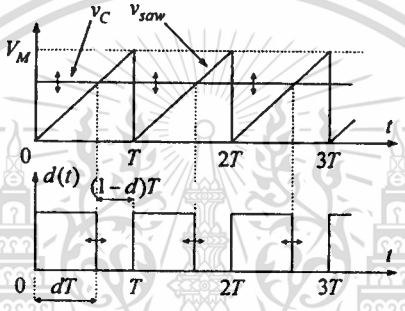

(b)

Fig. 4.1. (a) Zeta converter with VMC and (b) Operation of PWM comparator.

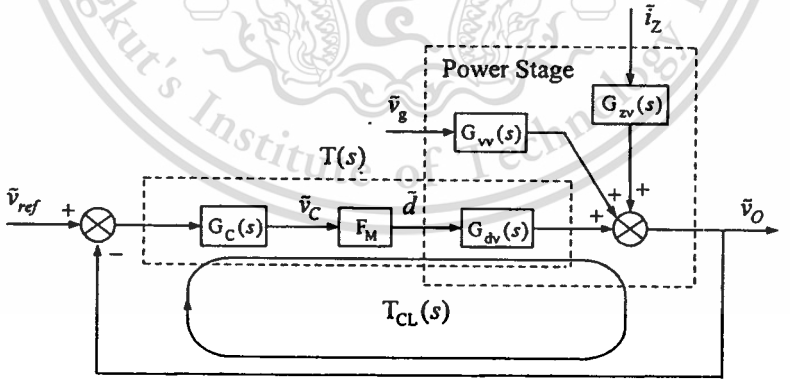

Fig. 4.2. Small-signal control block diagram of Zeta converter with VMC.

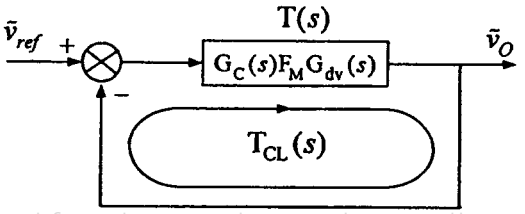

Fig. 4.3. Block diagram simplified from Fig 4.2.

The transfer function $G_{dv}(s)$ are given in (2.2.2-6-e) for CCM Zeta converter and in (3.3.2-26-b) for DCM Zeta converter. Given $G_{dv}(s)$ and F_M, the feedback compensator, $G_C(s)$, can be designed by appropriately selecting its poles and zeros so that the open-loop transfer function in (4.1.1-2) has high DC gain and reasonable crossover frequency and owns sufficient amount of phase margin [18, 21].

4.1.2 Compensator $G_C(s)$

As shown in Fig. 4.4., the feedback compensator is an operational amplifier with an input and feedback impedances, z_1 and z_2. It amplifies the difference between v_{ref} and v_O and gives the control voltage, v_C, at its output.

The control voltage, v_C, is related to reference voltage, v_{ref}, and output voltage, v_O, by:

$$v_C = v_{ref}(1+z_2/z_1) - v_O z_2/z_1 \qquad (4.1.2\text{-}1)$$

By introducing the small-signal perturbation $v_C = V_C + \tilde{v}_C$, $v_O = V_O + \tilde{v}_O$, and $v_{ref} = V_{ref}$ (V_{ref} is constant), the small-signal model of the compensator is obtained as:

$$\tilde{v}_C/\tilde{v}_O = -z_2/z_1 = -G_C(s) \qquad (4.1.2\text{-}2)$$

Below lists the some commonly used compensators and their transfer functions .

- PI compensator (Fig. 5)

$$G_C(s) = z_2/z_1 = (\omega_o/s)(s/\omega_z + 1) \qquad (4.1.2\text{-}3)$$

where $\omega_O = 1/(R_2 C_1)$ and $\omega_z = 1/(R_1 C_1)$.

- One-zero-and-two-pole compensator (Fig. 6)

$$G_C(s) = z_2/z_1 = (\omega_I/s)(s/\omega_{Z1} + 1)/(s/\omega_{P1} + 1) \qquad (4.1.2\text{-}4)$$

where $\omega_I = 1/(R_2(C_1 + C_2))$, $\omega_{Z1} = 1/(R_1 C_1)$, and $\omega_{P1} = 1/(R_1 C_1 C_2/(C_1 + C_2))$.

- Two-zero-and-two-pole compensator (Fig. 7)

$$G_C(s) = \frac{z_2}{z_1} = \omega_I \frac{(s/\omega_{Z1}+1)(s/\omega_{Z2}+1)}{(s/\omega_{P1}+1)(s/\omega_{P2}+1)} \qquad (4.1.2\text{-}5)$$

where $\omega_I = R_3/(R_1 + R_2)$, $\omega_{Z1} = 1/(R_4 C_2)$, $\omega_{P1} = 1/((R_3 + R_4)C_2)$, $\omega_{Z2} = 1/(R_2 C_1)$, and $\omega_{P2} = 1/(R_1 R_2 C_1/(R_1 + R_2))$.

- Two-zero-and-three-pole compensator (Fig. 8)

$$G_C(s) = \frac{z_2}{z_1} = \frac{\omega_I}{s} \frac{(s/\omega_{Z1}+1)(s/\omega_{Z2}+1)}{(s/\omega_{P1}+1)(s/\omega_{P2}+1)} \qquad (4.1.2\text{-}6)$$

where $\omega_I = 1/(R_1(C_1 + C_2))$, $\omega_{Z1} = 1/(R_2 C_1)$, $\omega_{P1} = 1/(R_2 C_1 C_2/(C_1 + C_2))$, $\omega_{Z2} = 1/((R_1 + R_3)C_3)$, and $\omega_{P2} = 1/(R_3 C_3)$.

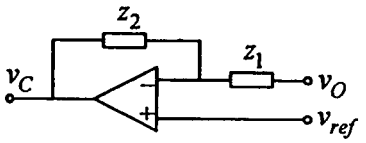

Fig. 4.4. General form of feedback compensator.

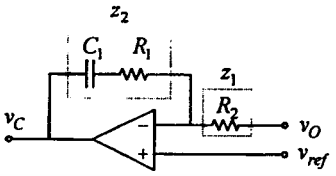

Fig. 4.5. PI compensator.

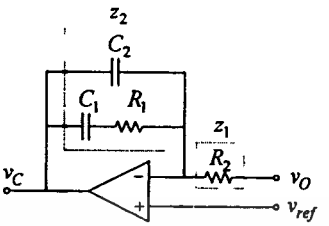

Fig. 4.6. One-zero-and-two-pole compensator.

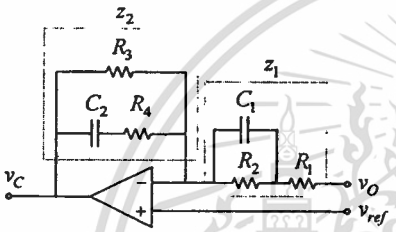

Fig. 4.7. Two-zero-and-two-pole compensator.

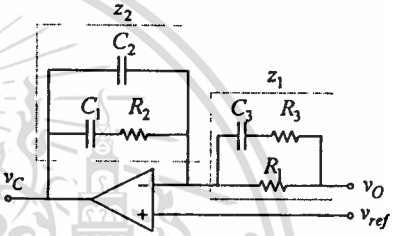

Fig. 4.8. Two-zero-and-three-pole compensator.

4.2 Peak Current Mode Control (PCMC)

4.2.1 Description of PCMC

Fig. 4.9(a) shows Zeta converter with Peak Current Mode Control (PCMC). The control principle is as follows. At the start of the switching cycle, the clock signal sets a flip-flop to 1 (Q=1), turning on the MOSFET. The MOSFET current, which is equal to summation of the inductor currents L_1 and L_2, increases linearly as shown in Fig. 4.9(b). This current is sensed as $R_S I_S$ and compared with the control voltage, v_C, from the feedback compensator. When $R_S I_S$ reaches v_C, the output of the comparator resets the flip-flop (Q=0), turning off the MOSFET. The next clock signal will turn on the MOSFET again and the same operation be repeated. If the load is increased, the output voltage will decrease and hence v_C will increase. Due to the increase in v_C, the time it takes for $R_S I_S$ to reach v_C is longer, i.e., the duty cycle is increased. The increased duty cycle will cause the MOSFET current to increase to meet the load current demand and, at the same time, restore the output voltage to the desired value set by V_{ref}.

Fig. 4.10(a) shows the fictitious inductor current waveform, $i(t)$, for $d < 0.5$. Note that the fictitious inductor current, which is a sum of i_{L1} and i_{L2}, was first introduced in chapter 3 and is used again here to describe the stability problem in PCMC. For $d < 0.5$, if there is a small

perturbation introduced to *i(t)*, it will be eventually subdued as shown in Fig. 4.10(a). Therefore, the instability does not occur for $d < 0.5$. On the other hand, the same perturbation will get amplified for $d > 0.5$; that is, the instability occurs for $d > 0.5$, as shown in Fig. 4.10(b). To avoid the instability when $d > 0.5$, a compensation ramp, V_{ramp}, is introduced to the PWM comparator. It is subtracted from the control voltage as shown in Fig. 4.11; therefore, the MOSFET will turn off when $R_S I_S$ is equal to v_C-v_{ramp}. The compensation ramp effectively provides a damping in the current loop, enhancing the loop stability [18]. With the compensation ramp, the range of the stability is extended beyond $d = 0.5$ (Fig. 4.11).

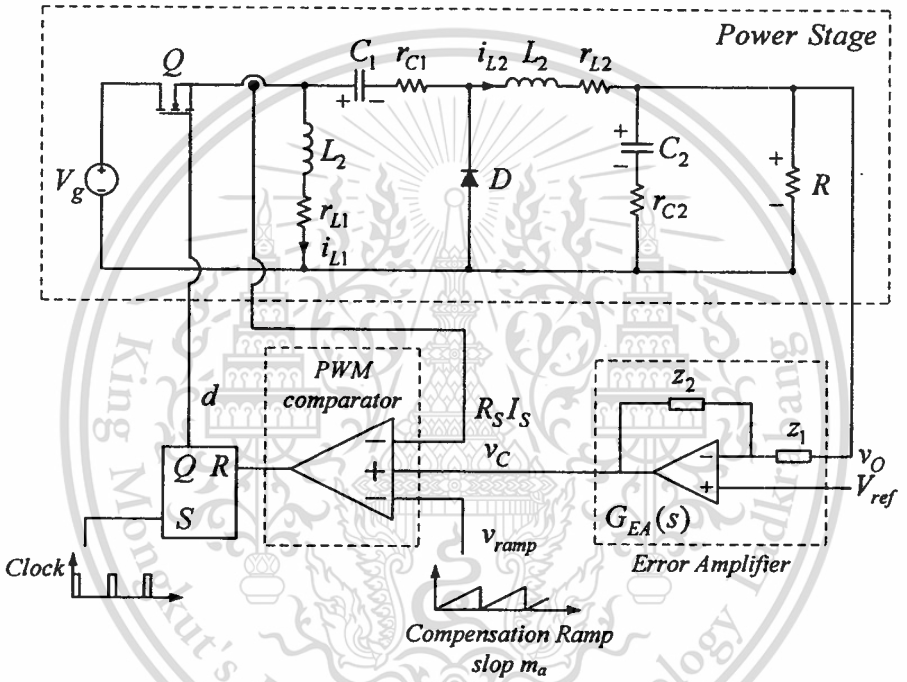

Fig. 4.9. (a) Zeta converter with Peak Current-Mode Control (PCMC) and (b) Description of its slop compensation between m_a and m_1.

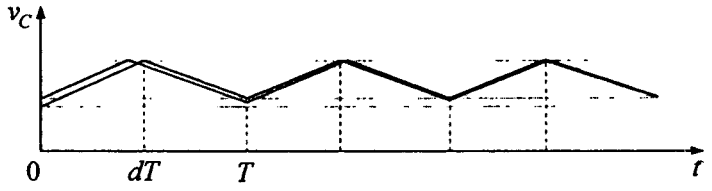

(a)

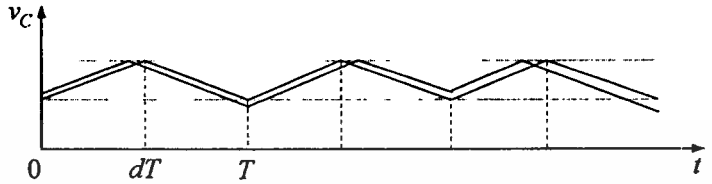

(b)

Fig. 4.10. Perturbed $i(t)$ waveform (a) $d < 0.5$ and (b) $d > 0.5$.

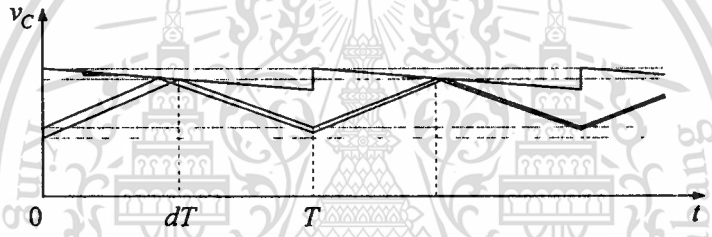

Fig. 4.11. Perturbed $i(t)$ waveform for $d > 0.5$, with compensation ramp.

4.2.2 Zeta Converter with PCMC

In PCMC, the significant transfer function for the feedback compensator design is $G_{VC}(s)$, which is the transfer function from $\tilde{v}_C$ to $\tilde{v}_O$. To obtain $G_{VC}(s)$, the control law for PCMC, which relates the duty ratio to other circuit variables, must be defined. In this thesis, the control laws proposed in [18] and [23] are adopted. From here on, the control law in [18] will be referred to as Erickson model and [23] as Ridley model.

A- CCM Zeta converter with PCMC based on Erickson model

The Zeta converter with PCMC can be drawn in a block diagram form as shown in Fig. 4.12. The power stage is represented by nine transfer function blocks, where the expression for these transfer functions is given in (2.2.1-6-d). The variables $\tilde{v}_g$, $\tilde{d}$, and $\tilde{i}_Z$ are considered to be an input to the power stage and the variables $\tilde{v}_O$, $\tilde{i}_{L1}$, and $\tilde{i}_{L2}$ an output from the power stage. The Erickson model [18] is expressed by:

$$\tilde{d} = F_m(\tilde{v}_c - R_s\tilde{i} - F_g\tilde{v}_g - F_v\tilde{v}_o) \qquad (4.2.2\text{-}1)$$

where $F_m = \frac{1}{M_a T}$, $F_g = \frac{TD^2 R_S}{2L_E}$, $F_v = \frac{TD^2 R_S}{2L_E}$, R_S is a sensing resistor, M_a is a slope of compensation ramp. The derivation of (4.2.2-1) is shown in **Appendix E**. From Fig. 4.12,

$$\tilde{i}_{L1} = G_{vi1}\tilde{v}_g + G_{di1}\tilde{d} + G_{zi1}\tilde{i}_Z \quad (4.2.2\text{-}2\text{-}a)$$

$$\tilde{i}_{L2} = G_{vi2}\tilde{v}_g + G_{di2}\tilde{d} + G_{zi2}\tilde{i}_Z \quad (4.2.2\text{-}2\text{-}b)$$

$$\tilde{v}_O = G_{vv}\tilde{v}_g + G_{dv}\tilde{d} + G_{zv}\tilde{i}_Z \quad (4.2.2\text{-}3)$$

Substitution of (4.2.2-2) and (4.2.2-3) into (4.2.2-1) yields:

$$\tilde{d} = F_m[\tilde{v}_C - (G_{vi1}\tilde{v}_g + G_{di1}\tilde{d} + G_{zi1}\tilde{i}_Z + G_{vi2}\tilde{v}_g + G_{di2}\tilde{d} + G_{zi2}\tilde{i}_Z)R_S - \tilde{v}_g F_g - \tilde{v}_O F_v] \quad (4.2.2\text{-}4\text{-}a)$$

$$\tilde{d} = F_m[\tilde{v}_C - [(G_{vi1} + G_{vi2})\tilde{v}_g + (G_{di1} + G_{di2})\tilde{d} + (G_{zi1} + G_{zi2})\tilde{i}_Z]R_S - \tilde{v}_g F_g - \tilde{v}_O F_v] \quad (4.2.2\text{-}4\text{-}b)$$

$$\tilde{d}[1 + F_m R_S(G_{di1} + G_{di2})] = F_m[\tilde{v}_C - [F_g + R_S(G_{vi1} + G_{vi2})]\tilde{v}_g - R_S(G_{zi1} + G_{zi2})\tilde{i}_Z - \tilde{v}_O F_v] \quad (4.2.2\text{-}4\text{-}c)$$

$$\tilde{d} = \frac{F_m[\tilde{v}_C - [F_g + R_S(G_{vi1} + G_{vi2})]\tilde{v}_g - R_S(G_{zi1} + G_{zi2})\tilde{i}_Z - \tilde{v}_O F_v]}{1 + F_m R_S(G_{di1} + G_{di2})} \quad (4.2.2\text{-}4\text{-}d)$$

Substitution of (4.2.2-4-d) into (4.2.2-3) gives:

$$\tilde{v}_O = G_{vv}\tilde{v}_g + \frac{G_{dv}F_m[\tilde{v}_C - [F_g + R_S(G_{vi1} + G_{vi2})]\tilde{v}_g - R_S(G_{zi1} + G_{zi2})\tilde{i}_Z - \tilde{v}_O F_v]}{1 + F_m R_S(G_{di1} + G_{di2})} + G_{zv}\tilde{i}_Z \quad (4.2.2\text{-}5\text{-}a)$$

$$\tilde{v}_O[1 + \frac{G_{dv}F_m F_v}{1 + F_m R_S(G_{di1} + G_{di2})}] = \frac{G_{dv}F_m}{1 + F_m R_S(G_{di1} + G_{di2})}\tilde{v}_C + [G_{vv} - \frac{G_{dv}F_m[F_g + R_S(G_{vi1} + G_{vi2})]}{1 + F_m R_S(G_{di1} + G_{di2})}]\tilde{v}_g + [G_{zv} - \frac{G_{dv}F_m R_S(G_{zi1} + G_{zi2})}{1 + F_m R_S(G_{di1} + G_{di2})}]\tilde{i}_Z \quad (4.2.2\text{-}5\text{-}b)$$

$$\tilde{v}_O = \frac{1}{1 + F_m[R_S(G_{di1} + G_{di2}) + G_{dv}F_v]}[G_{dv}F_m\tilde{v}_C + [G_{vv} - G_{dv}F_m F_g + F_m R_S[G_{vv}(G_{di1} + G_{di2}) - G_{dv}(G_{vi1} + G_{vi2})]]\tilde{v}_g + [G_{zv} + F_m R_S[G_{zv}(G_{di1} + G_{di2}) - G_{dv}(G_{zi1} + G_{zi2})]]\tilde{i}_Z] \quad (4.2.2\text{-}5\text{-}c)$$

$$\tilde{v}_O = G_{vc}\tilde{v}_C + G_{vv\text{-}cpm}\tilde{v}_g + G_{zv\text{-}cpm}\tilde{i}_Z \quad (4.2.2\text{-}5\text{-}d)$$

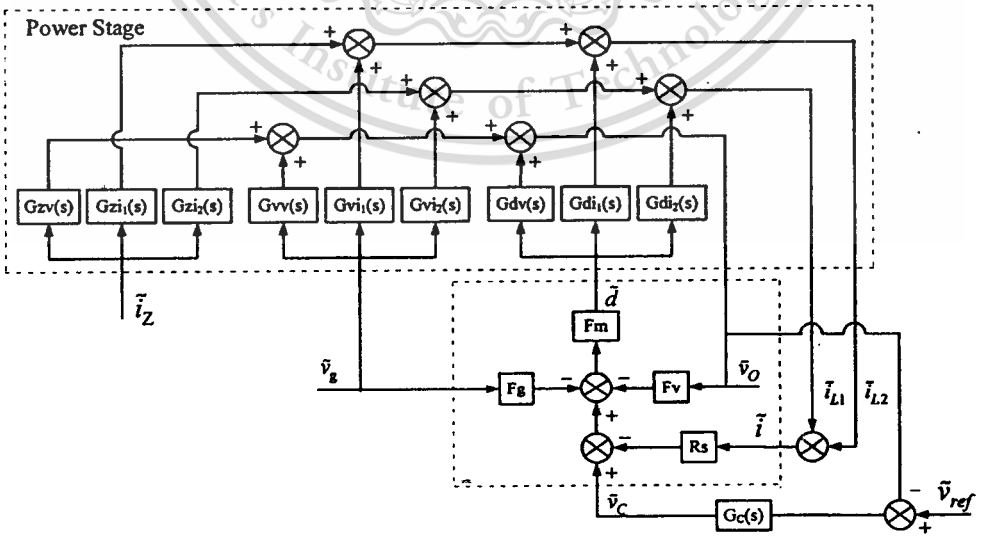

Fig. 4.12. Small-signal control block diagram of CCM Zeta converter with PCMC based on Erickson model.

where

$$G_{VC}=\frac{\tilde{v}_O}{\tilde{v}_C}=\frac{F_m G_{dv}}{1+F_m[R_S(G_{d1}+G_{d2})+G_{dv}F_V]} \quad (4.2.2\text{-}6\text{-a})$$

$$G_{VV-cpm}=\frac{\tilde{v}_O}{\tilde{v}_g}=\frac{G_{vv}-G_{dv}F_m F_g+F_m R_S[G_{vv}(G_{d1}+G_{d2})-G_{dv}(G_{v1}+G_{v2})]}{1+F_m[R_S(G_{d1}+G_{d2})+G_{dv}F_V]} \quad (4.2.2\text{-}6\text{-b})$$

$$G_{ZV-cpm}=\frac{\tilde{v}_O}{\tilde{i}_Z}=\frac{G_{zv}+F_m R_S[G_{zv}(G_{d1}+G_{d2})-G_{dv}(G_{z1}+G_{z2})]}{1+F_m[R_S(G_{d1}+G_{d2})+G_{dv}F_V]} \quad (4.2.2\text{-}6\text{-c})$$

For CCM operation, the magnitudes of F_g and F_v are typically very small; that is, $F_V=\frac{TD'^2R_S}{2L}\to 0$ and $F_g=\frac{TD^2R_S}{2L}\to 0$. Thus, (4.2.2-6-a) becomes:

$$G_{VC}=\frac{\tilde{v}_O}{\tilde{v}_C}=\frac{F_m G_{dv}}{1+F_m R_S(G_{d1}+G_{d2})} \quad (4.2.2\text{-}5)$$

Equation (4.2.2-5) is shown in the block diagram form in Fig. 4.13. If there is no artificial ramp (M_a=0), $F_m=\frac{1}{M_a T}\to\infty$ and (4.2.2-5) can be rewritten as:

$$G_{VC}=\frac{\tilde{v}_O}{\tilde{v}_C}=\frac{G_{dv}}{R_S(G_{d1}+G_{d2})} \quad (4.2.2\text{-}8)$$

$G_{VC}(s)$ is finally obtained by substituting (2.2.3-6-a), (2.2.3-6-b), and (2.2.3-6-e) into (4.2.2-8):

$$G_{VC}=\frac{\tilde{v}_O}{\tilde{v}_C}=\frac{G_{dv}}{R_S(G_{d1}+G_{d2})}=\frac{R(sC_2r_{C2}+1)(a_{VC}s^2+b_{VC}s+c_{VC})}{R_S(a_d s^3+b_d s^2+c_d s+d_d)} \quad (4.2.2\text{-}9)$$

The coefficients in (4.2.2-9) are listed in TABLE 4.1. The derivation of these coefficients is given in the **Appendix F**.

B- CCM Zeta converter with PCMC based on Ridley model

Fig. 4.14 shows the block diagram of CCM Zeta converter with PCMC based on Ridley's current mode control model. While the power stage model is the same that in Fig. 4.12, the control stage is defined by [23]:

$$\tilde{d}=F_m(\tilde{v}_C-R_S H_e(s)\tilde{i}+k'_f\tilde{v}_{on}-k'_r\tilde{v}_{off}) \quad (4.2.2\text{-}10)$$

where $F_m=\frac{1}{(M_a+M_1)T}$, $M_1=\frac{V_g R_S}{L_E}$, $k'_f=-\frac{DR_S T}{L_E}\left(1-\frac{D}{2}\right)$, $k'_r=\frac{D'^2TR_S}{2L_E}$, $L_E=\frac{L_1L_2}{L_1+L_2}$, $\tilde{v}_{on}=\tilde{v}_g$, $\tilde{v}_{off}=\tilde{v}_O$, M_a is a slope of compensation ramp, and M_1 is a upward slope of the fictitious inductor current, $i(t)$.

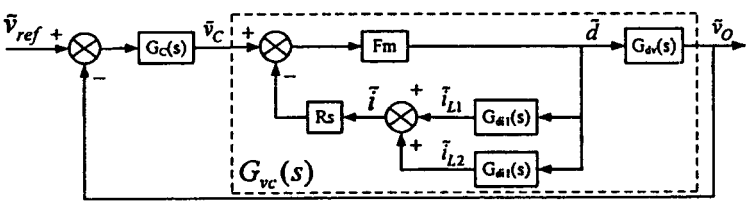

Fig. 4.13. Simplified block diagram of Fig. 4.12 when F_g=F_V=0.

TABLE 4.1

Coefficients of $G_{VC}(s)$ of CCM Zeta converter from Erickson model.

$$a_{we} = -r_{C2}L_1C_1L_2C_2[RI_Z(1-D)+DV_g](r_{C2}+R)$$

$$b_{we} = -C_1(1-D)RI_Z[(r_{C2}+R)(L_1+L_2)(r_{L1}D+r_{C1})r_{C2}C_2+C_2Rr_{C2}^2(1-D)(L_1+L_2)$$
$$+[C_2L_2r_{C2}r_{L1}-r_{C1}r_{C2}C_2L_2D+r_{L2}r_{C2}L_1C_2+L_1L_2](r_{C2}+R)]$$
$$-C_1(r_{C2}+R)[-(1-D)^2C_2r_{C2}(r_{L2}+R)(L_2+L_1)+DC_2r_{C2}(r_{L1}L_2+L_1r_{L2})+L_1D(r_{C2}r_{C1}C_2D+L_2)]V_g$$

$$c_{we} = -R(1-D)I_Z[C_1r_{C1}(C_2r_{C2}r_{L2}+C_2r_{C2}r_{C1}+L_2)(r_{C2}+R)(1-D)+C_1C_2Rr_{C2}^2(r_{L2}+r_{C1}+r_{L1})(1-D)$$
$$+(r_{C1}+r_{L2})(r_{C2}+R)[L_1+C_2r_{L1}r_{C2}(1+D)]C_1+[r_{C2}L_1C_2D+C_1C_2r_{C2}r_{L1}^2D+r_{L1}C_1L_2+C_1r_{L1}D(L_1+L_2)](r_{C2}+R)$$
$$-r_{C2}DC_1R(L_2+L_1)+r_{C2}L_1R(C_2+C_1)]$$
$$-(r_{C2}+R)[-(1-D)^2C_1[C_2r_{C2}(r_{L2}^2+r_{C1}R+r_{L2}r_{C1}+r_{L2}R)+(r_{L2}+R)(r_{L1}r_{C2}C_2+L_1+L_2)]$$
$$+C_1D(r_{L2}L_1+r_{L1}L_2)+D^2L_1(C_1r_{C1}+r_{C2}C_2)+r_{L1}r_{C2}C_1C_2D(r_{L2}+Dr_{C1})]V_g]$$

$$d_{we} = -(r_{C2}+R)[C_1r_{L2}r_{L1}D+L_1D^2-C_1(r_{L1}+r_{L2})(r_{L2}+R)(1-D)^2+(C_1r_{C1}+C_2r_{C2})[r_{L1}D^2-(r_{L2}+R)(1-D)^2]]V_g$$
$$-R(1-D)I_Z[(r_{C2}+R)[D(C_1r_{L1}^2+2r_{L1}r_{C2}C_2+L_1)+r_{L1}C_1(r_{L2}+r_{C1})(D+1)+(C_1r_{C1}+r_{C1}^2C_1+r_{C2}r_{C1}C_2)(1-D)]$$
$$+r_{C2}(r_{L1}C_1R+r_{C1}C_1R+C_2Rr_{C2}+C_1C_2r_{L2})(1-D)]$$

$$e_{we} = -(r_{C2}+R)[D^2r_{L1}-(r_{L2}+R)(1-D)^2]V_g-R(1-D)I_Z[2Dr_{L1}(r_{C2}+R)+(1-D)(r_{C2}R+Rr_{C1}+r_{C2}r_{C1})]$$

$$a_d = (r_{C2}+R)C_1C_2\{-[(r_{C2}+R)[(1-D)(L_1+L_2)r_{L2}+L_2Dr_{C1}]+R(r_{C2}+R-DR)(L_1+L_2)]V_g$$
$$+RI_Z(r_{C2}+R)[D(L_1+L_2)r_{L1}+L_1r_{C1}(1-D)]\}$$

$$b_d = [-C_1C_2(r_{C2}+R)^2[D^2r_{C1}^2+r_{L1}R-r_{L2}r_{C1}+r_{L2}(r_{L2}+r_{L1})(1-D)]$$
$$+(r_{C2}+R)[C_1C_2r_{L1}R^2D-C_1r_{C1}DL_2-RC_1C_2(r_{C1}+r_{L2})(r_{C2}+R-RD)-r_{L2}C_1(1-D)(L_1+L_2)]$$
$$+[D^2C_2r_{C2}(r_{C2}+2R)-Rr_{C2}C_1+R^2C_1(D^2-1)](L_1+L_2)-r_{C2}DL_2C_2(2R+r_{C2})+R^2L_1D^2C_2-R^2DL_2C_2(1-D)]V_g$$
$$+RI_Z[(1-D)[(1-D)[C_1C_2r_{C1}^2(r_{C2}+R)^2-R^2(L_2C_2+L_1C_1+C_1L_2)]+L_1C_1r_{C1}(r_{C2}+R)$$
$$+C_2r_{C2}(r_{C2}+2R)(DL_1+L_2D-L_2)+DL_1C_2R^2]$$
$$+C_1r_{L1}(r_{C2}+R)[C_2(Dr_{L2}+r_{C1})(r_{C2}+R)+D(L_1+L_2)]+C_1C_2Dr_{L1}^2(r_{C2}+R)^2]$$

$$c_d = [C_2(r_{L1}D^2-R)(r_{C2}+R)^2-C_1(1-D)(r_{L2}+R)r_{L2}^2$$
$$+(r_{C2}+R)[C_1r_{C1}(2r_{L2}-D^2r_{C1})+DC_2R(R-Dr_{C1})-DL_2-C_1R(r_{C1}+r_{L1})-r_{L1}r_{L2}C_1(1-D)+D^2(L_2+L_1)]$$
$$-[C_2r_{L2}r_{C2}(r_{C2}+2R)+R^2(C_1+C_2)](1-D^2)-r_{C2}^2D^2C_2r_{C1}-C_1Rr_{C2}r_{L2}+C_1R^2D^2(r_{C1}+r_{L1})]V_g$$
$$+RI_Z[(r_{C2}+R)[DC_1(r_{L1}r_{L2}+r_{L1}^2)+r_{L1}C_1r_{C1}+L_1D(1-D)]+Dr_{L1}(2-D)[r_{C2}C_2(r_{C2}+2R)+R^2(C_1+C_2)]$$
$$+(1-D)^2[C_2(r_{C1}-r_{L2})(r_{C2}+R)^2+(r_{C1}^2C_1-L_2)(r_{C2}+R)-C_1R^2(r_{L2}+r_{C1})]]$$

$$d_d = [(R+r_{C2})[D^2(r_{L1}+r_{L2}-r_{C1})-r_{L2}-R]+R^2D^2]V_g$$
$$-RI_Z[r_{L1}D(D-2)(r_{C2}+R)-[(R+r_{C2})(r_{C1}-r_{L2})-R^2](1-D)^2]$$

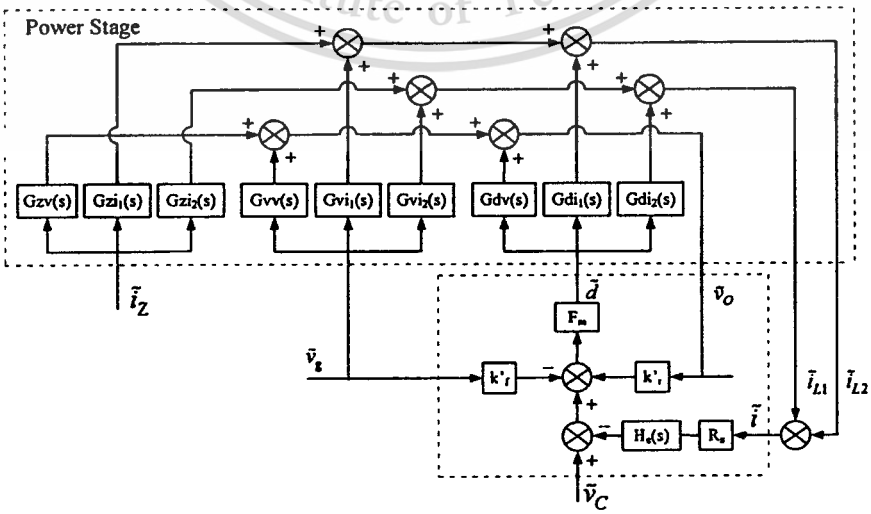

Fig. 4.14. Small-signal control block diagram of CCM Zeta converter with PCMC based on Ridley model.

$H_e(s) \approx 1 + \frac{s}{\omega_n Q_z} + \frac{s^2}{\omega_n^2}$ is an approximate sampling gain of the current loop, where $\omega_n = \frac{\pi}{T}$ and $Q_z = \frac{-2}{\pi}$. The derivation of (4.2.2-10) is shown in **Appendix E.**

For CCM operation, the magnitudes of k'_f and k'_r are typically very small and can assume to be zero. To find $G_{VC}(s)$, the input variables $\tilde{i}_z$ and $\tilde{v}_g$ in Fig 4.14 are set to zero. Thus, Fig. 4.14 is simplified into Fig. 4.15, from which $G_{VC}(s)$ is given by:

$$G_{VC} = \frac{\tilde{v}_o}{\tilde{v}_c} = \frac{F_m G_{dv}(s)}{1 + F_m R_S H_e(s)[G_{di1}(s) + G_{di2}(s)]} \quad (4.2.2\text{-}11)$$

Where $F_m = \frac{1}{(M_a + M_1)T}$. If there is no artificial ramp (M_a=0), then $F_m = \frac{1}{M_1 T}$.

Substituting of (2.2.3-6-a), (2.2.3-6-b), and (2.2.3-6-e) into (4.2.2-11) yields:

$$G_{VC} = \frac{(a_w s^2 + b_w s + c_w)(sC_2 r_{C2} + 1)RF_m}{a_e s^4 + b_e s^3 + c_e s^2 + d_e s + e_e} \quad (4.2.2\text{-}12)$$

The coefficients in (4.2.1-12) are listed in TABLE 4.2. The derivation of these coefficients is given in the **Appendix F.**

C- DCM Zeta converter with PCMC based on Ridley model

Fig. 4.16 illustrates typical slop compensation waveforms of the DCM DC-DC converter. In DCM operation, the fictitious inductor current, $\tilde{i}(t)$, is zero at the beginning of each switching period, and only the duty cycle, $\tilde{d}_1$, during the on time is required to function as control signal; that is, $\tilde{v}_{off}$ is neglected [23]. Hence, (4.2.2-10) can be rewritten as:

$$\tilde{d} = F_m(\tilde{v}_C + k'_f \tilde{v}_{on}) \quad (4.2.2\text{-}13)$$

Where F_m and v_{on} are the same as those in (4.2.2-10), $k'_f = \frac{-D_1 R_S T}{L_E}$, and $k'_r = 0$. The derivation of (4.2.2-13) is shown in the **Appendix E.**

From (4.2.2-13), the block diagram of DCM Zeta converter with PCMC based on Ridley's current mode control model is depicted in Fig. 4.17 which is hence simplified into Fig. 4.18, from which $G_{VC}(s)$ can be defined:

$$G_{VC} = \tilde{v}_O / \tilde{v}_C = F_m G_{dv}(s) \quad (4.2.2\text{-}14)$$

where $F_m = \frac{1}{(M_a + M_1)T}$. If there is no artificial ramp (M_a=0), $F_m = \frac{1}{M_1 T}$.

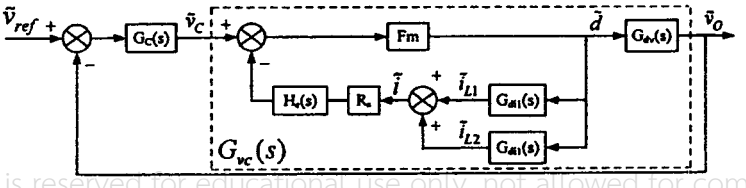

Fig. 4.15. Simplified block diagram of Fig. 4.14.

TABLE 4.2

Coefficient of $G_{VC}(s)$ of CCM Zeta converter from Ridley model.

$$a_{vc} = L_1C_1[(r_{L2}+R)(1-D)V_g + I_zR(Dr_{C1} - Dr_{L1} - r_{C1})]$$

$$b_{vc} = -[L_1D^2 - C_1(r_{L2}+R)(1-D)(r_{L1}+r_{C1}-r_{C1}D)]V_g - I_zR[r_{L1}^2C_1D + r_{L1}r_{C1}C_1(1-D^2) + (1-D)[r_{C1}^2C_1(1-D) + L_1D]]$$

$$c_{vc} = -[D^2r_{L1} - (R+r_{L2})(1-D)^2]V_g + I_zR(1-D)(Dr_{C1} - r_{C1} - 2Dr_{L1})$$

$$a_e = L_1L_2C_1C_2(r_{C2}+R)[D^2r_{L1} + r_{C1}D(1-D) + (R+r_{L2})(1-D)^2]$$

$$b_e = F_mR_SH_eC_1C_2(r_{C2}+R)\{[(r_{L2}+R)(L_1+L_2)(1-D) + L_2Dr_{C1}]V_g - I_zR[r_{L1}D(L_1+L_2) + r_{C1}L_1(1-D)]\} - C_1[D^2r_{L1} + r_{C1}D(1-D) + (R+r_{L2})(1-D)^2][C_2(r_{C2}+R)[r_{C1}(L_2D - L_1D - L_2) - r_{L1}L_2 - r_{L2}L_1] - L_1L_2 - L_1r_{C2}RC_2]$$

$$c_e = F_mR_SH_e[(1-D)(r_{C2}+R)[r_{L1}C_1(r_{L2}+R) + C_1r_{L2}^2 + L_2D]C_2 - (R+r_{C2})(L_1D^2 - r_{C1}r_{L2}C_1 - r_{C1}^2C_1D^2)C_2 + [Rr_{L2}C_1C_2(R+2r_{C2}) + C_2R^2(r_{C1}C_1 + r_{C2}C_1) + C_1(r_{L2}+R)(L_1+L_2)](1-D) + r_{C1}C_1(C_2r_{C2}R + L_2D)]V_g - F_mR_SH_eR[C_1C_2(r_{C2}+R)[r_{L1}D(r_{L1}+r_{L2}) + r_{L1}r_{C1} + r_{C1}^2(1-D)^2] + r_{L1}C_1D(C_2r_{C2}R + L_1 + L_2) + (1-D)[L_1C_1r_{C1} + (r_{C2}+R)(DL_1 + DL_2 - L_2)C_2]]I_z + [D^2r_{L1} + r_{C1}D(1-D) + (R+r_{L2})(1-D)^2][(r_{C2}+R)[C_1C_2(r_{L2}+r_{C1}D)(r_{L1}+r_{C1}-r_{C1}D) + L_1C_2D^2 + L_2C_2(1-D)^2] + C_1(L_2+r_{C2}RC_2)(r_{L1}+r_{C1}-r_{C1}D) + C_1L_1(r_{L2}+r_{C1}D+R)]$$

$$d_e = F_mR_SH_e[C_1(r_{L2}^2 + 2r_{L2}R)(1-D) + C_2(1-D^2)(r_{C2}R + r_{L2}r_{C2} + r_{L2}R) - (R+r_{C2})[(r_{L1}-r_{C1})D^2C_2 - r_{L1}C_1(1-D)] + (1-D)(C_1+C_2)R^2 + r_{C1}C_1(r_{L2}+R+D^2r_{C1}) - D^2(L_1+L_2) + L_2D]V_g + F_mR_SH_e[(1-D)^2[C_2r_{C2}R - r_{C1}^2C_1 + L_2 + C_2(r_{L2}-r_{C1})(r_{C2}+R)] - L_1D(1-D) + r_{L1}C_2D(D-2)(R+r_{C2}) - r_{L1}C_1D(R+r_{L2}) - r_{L1}C_1(r_{L1}D + r_{C1})]I_z + [D^2r_{L1} + r_{C1}D(1-D) + (R+r_{L2})(1-D)^2][C_2(r_{C2}+R)[r_{L1}D^2 + r_{L2}(1-D)^2 + Dr_{C1}(1-D)] + r_{C1}C_1(r_{L2} + Dr_{C1} + R)(1-D) + r_{L1}C_1(R+r_{L2}) + Dr_{L1}r_{C1}C_1 + L_1D^2 + (RC_2r_{C2} + L_2)(1-D)^2]$$

$$e_e = F_mR_SH_e[V_g[(1-D^2)(r_{L2}+R) + D^2(r_{C1}-r_{L1})] - [r_{L1}D(2-D) + (1-D)^2(r_{C1}-R-r_{L2})]RI_z] + [D^2r_{L1} + r_{C1}D(1-D) + (R+r_{L2})(1-D)^2]^2$$

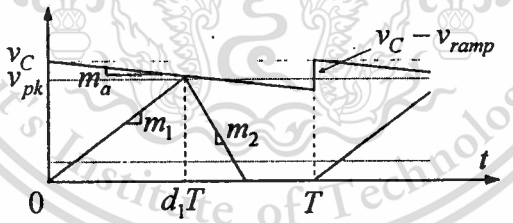

Fig. 4.16. Typical slop compensation waveforms of the DCM DC-DC converter.

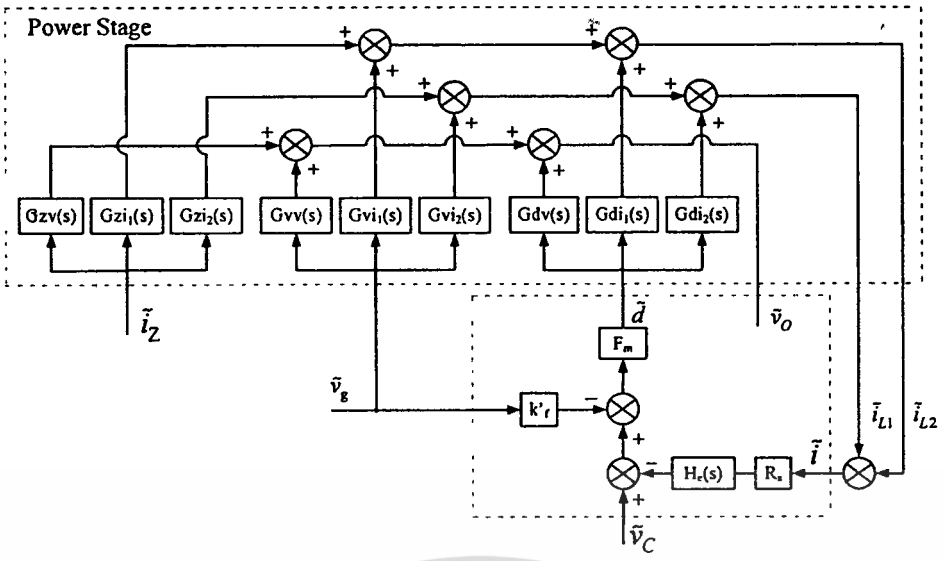

Fig. 4.17. Small-signal control block diagram of DCM Zeta converter with PCMC based on Ridley model.

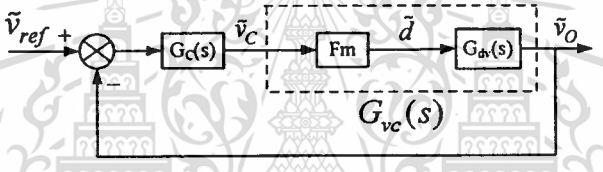

Fig. 4.18. Simplified block diagram of Fig. 4.17.

Chapter 5

Design of Feedback Compensator

This chapter illustrates feedback compensator design of Zeta converter with VMC and PCMC. The design is carried out for both CCM and DCM cases. Simulation results are given to confirm the validity of the designed compensators in regulating the output voltage.

5.1 Zeta Converter with VMC

A – Compensator Design for CCM Zeta converter with VMC

Closed-loop control of Zeta converter with VMC is shown in Fig. 5.1. A PI compensator is selected for CCM Zeta converter in Fig. 5.1(a) and a one-zero-and-two-pole compensator for DCM Zeta converter in Fig 5.1(b).

To design the compensator, a small-signal control block diagram of the converter is needed. This was developed in chapter 4 and is repeated again here in Fig. 5.2., where T(s) = $G_{dv}(s)F_M G_C(s)$ is the open-loop transfer function.

TABLE 5.1 lists circuit parameters for CCM Zeta converter. It should be noted that these parameters satisfy both the condition for CCM in (2.1-2) and the condition for LHP zeros in (2.2.2-7-b). Substituting the parameters from TABLE 5.1 into $G_{dv}(s)$ in (2.2.3-6-e) and F_m in (4.1.1-1) and multiplying them, the uncompensated open-loop transfer function, $T_U(s)=F_m G_{dv}(s)$, can be found.

$$T_U(s)=\frac{1.648\text{x}10^4 s^3+8.774\text{x}10^8 s^2+1.758\text{x}10^{12} s+6.505\text{x}10^{16}}{s^4+8452s^3+1.647\text{x}10^8 s^2+5.878\text{x}10^{11} s+4.969\text{x}10^{15}} \quad (5.1\text{-}1)$$

$T_U(s)$ has two pairs of complex poles at $\omega_{p1,2} = 9.77\text{x}10^3$ rad/s and $\omega_{p3,4} = 7.215\text{x}10^3$ rad/s, one real zero at $\omega_{z1} = 5.2632\text{x}10^4$ rad/s, and a pair of complex zero at $\omega_{z2,3} = 0.866\text{x}10^4$ rad/s. The asymptote Bode plot of $T_U(s)$ is shown in Fig. 5.3.

Next, the PI compensator is designed to compensate for $T_U(s)$ in (5.1-1). Its transfer function was given in (4.1.2-3) and is repeated again here.

$$G_C(s)=z_2/z_1=(\omega_o/s)(s/\omega_z+1) \quad (5.1\text{-}2)$$

where $\omega_o=1/(R_1C_1)$ and $\omega_z=1/(R_2C_1)$.

From (5.1-2), the pole at the origin will help increase the low frequency gain of the open-loop transfer function, $T(s)=T_U(s)G_C(s)$. The zero, ω_Z, and gain, ω_O, can be tuned to give T(s) the desirable crossover frequency and phase margin respectively. The design objective is to achieve

T(s) with the crossover frequency, ω_c, of 10 kHz and phase margin of more than 45 degrees. To achieve this, the zero of $G_c(s)$ has been set at $\omega_z=3x10^3$ rad/s and the gain at $\omega_o=8.65x10^3$ rad/s.

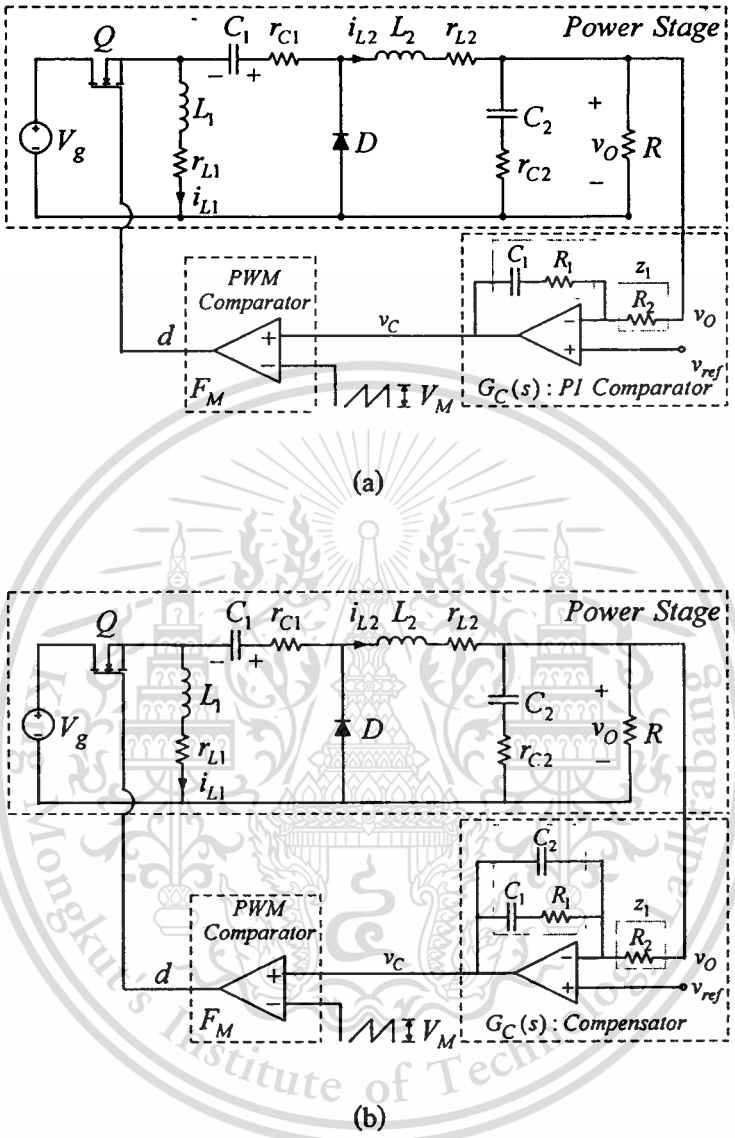

Fig. 5.1. Zeta converter with VMC in (a) CCM and (b) DCM.

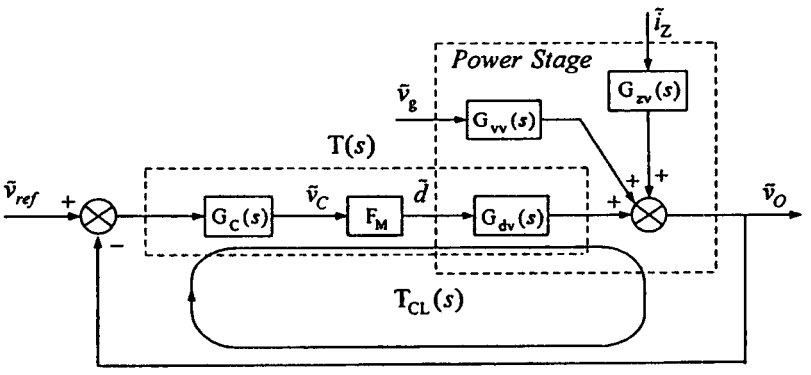

Fig. 5.2. Small-signal control block diagram of CCM/DCM Zeta converter with VMC.

TABLE 5.1.

Circuit Parameters for CCM Zeta converter.

Circuit Parameters	Values
V_g/ V_O/ V_M	15-20/ 5/ 1.8V
C_1/ C_2/ L_1/ L_2	100/200μF/ 100/ 55μH
r_{C1}/ r_{C2}/r_{L1}/ r_{L2}/ R	0.19/0.095/0.001/0.00055/1-5Ω
I_Z	0
T=1/f	10μs

Fig. 5.3 shows asymptote Bode plot of $T_U(s)$, $G_C(s)$, and T(s). Based on the selected ω_Z and ω_O, component values of the PI compensator are calculated, getting: R_1=10KΩ, R_2=3.4KΩ, and C_1=20nF. Substitution of these component values into (5.1-2) gives:

$$G_C(s)=\frac{1.47x10^4}{s}\left(\frac{s}{5x10^3}+1\right) \qquad (5.1\text{-}3)$$

To verify whether or not the design objectives have been met, $G_C(s)$ in (5.1-3), $T_U(s)$ in (5.1-1), and T(s) (the product of $G_C(s)$ and $T_U(s)$) are plotted with MATLAB, as depicted in Fig. 5.4. It can be seen that T(s) (solid line) has the phase margin of 53 degrees and crossover frequency of 10 KHz, thus satisfying the design objective.

B – Compensator Design for DCM Zeta converter with VMC

In chapter 3, $G_{d1v}(s)$ of DCM Zeta converter was derived by SSA technique and PWM-switch model. In this section, the model derived by the latter method in (3.3.2-26-b) is used in the compensator design because it is a full-order model (Recall that $G_{d1v}(s)$ derived by SSA technique is a reduced-order model) and takes into account of circuit parasitic. The small-signal block diagram for DCM Zeta converter is indicated in Fig. 5.2. The compensator design process for the DCM converter follows the same step as that for the CCM case. Substituting the converter parameters from TABLE 5.2 into $G_{d1v}(s)$ in (3.3.2-26-b) and F_m in (4.1.1-1) and multiplying them, the uncompensated open-loop transfer function, $T_U(s)=F_M G_{d1v}(s)$, is obtained:

$$T_U(s)=\frac{8.856x10^4 s^3+4.9x10^9 s^2+2.673x10^{13}s+7.463x10^{17}}{s^4+3.195x10^5 s^3+1.783x10^9 s^2+6.853x10^{13}s+5.379x10^{16}} \qquad (5.1\text{-}4)$$

$T_U(s)$ has two real poles at ω_{p1} = 0.8x10^3 rad/s, ω_{p2} = 3.145x10^5 rad/s and a pair of complex pole at $\omega_{p3,4}$ = 0.1463x10^5 rad/s, one zero at ω_{z1} = 5.2632x10^4 rad/s and a pair of complex zeros at $\omega_{z2,3}$ = 1.2654x10^4 rad/s.

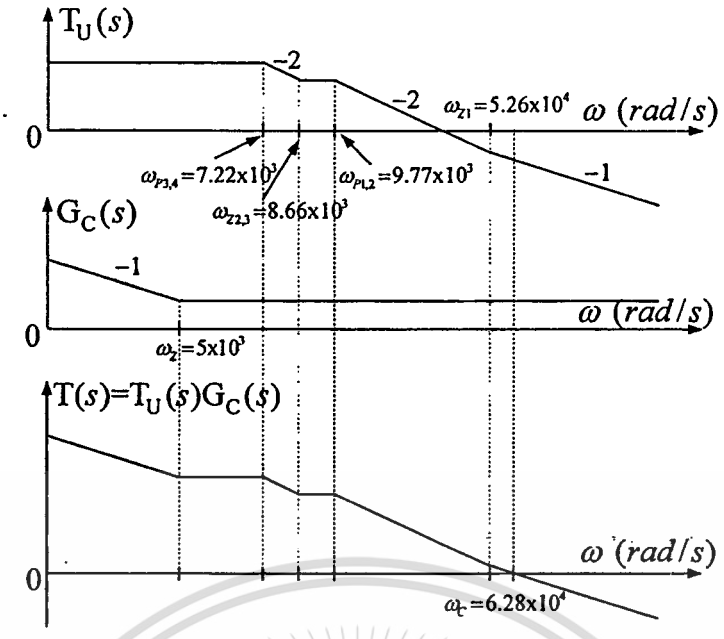

Fig. 5.3. Asymptote Bode plot of $T_U(s)$, $G_C(s)$, and T(s) of CCM VMC Zeta converter.

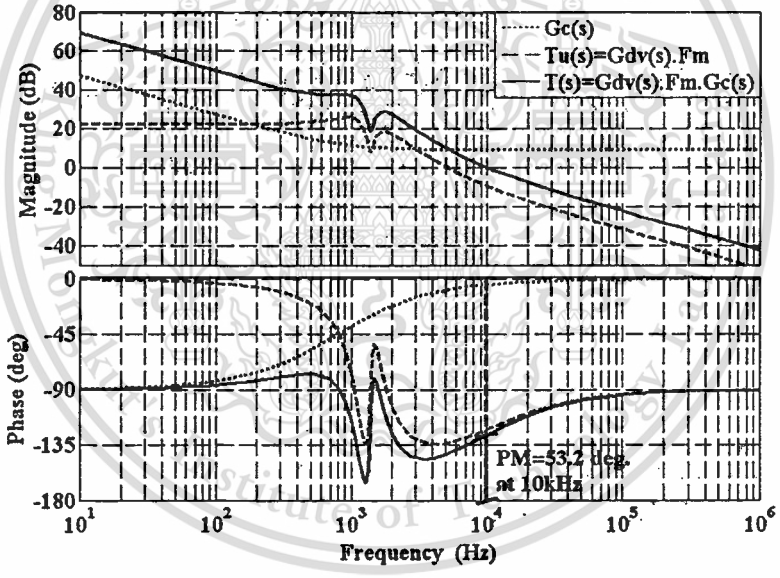

Fig. 5.4. Bode plots of $G_C(s)$, $T_U(s)$, and T(s) of CCM VMC zeta converter.

The one-zero-and-two-pole compensator is designed to compensate for $T_U(s)$ in (5.1-4). Its transfer function was given in (4.1.2-4) and is repeated again here:

$$G_C(s)=z_2/z_1=(\omega_O/s)(s/\omega_{Z1}+1)/(s/\omega_{P1}+1) \qquad (5.1\text{-}5)$$

The design objective here is the same as that in the CCM case, i.e., T(s) with the crossover frequency of 10 kHz and phase margin of more than 45 degrees. To achieve this, the zero and pole of $G_C(s)$ has been set at ω_{Z1}=18.94x10^4 rad/s, ω_{P1}=18.56x10^5 rad/s, and the gain at ω_O=1.7x10^5 rad/s. Fig. 5.5 shows asymptote Bode plot of $T_U(s)$, $G_C(s)$, and T(s). Depended on the selected ω_Z, ω_P, and ω_O, component values of the one-zero two-pole compensator are

calculated, obtaining: R_1=120Ω, R_2=120Ω, C_1=5nF, and C_2=44nF. Substitution of these component values into (5.1-5) gives:

$$G_C(s)=\frac{1.7\text{x}10^5}{s}\frac{\frac{s}{18.94\text{x}10^4}+1}{\frac{s}{18.56\text{x}10^5}+1} \qquad (5.1\text{-}6)$$

To verify that the design objective has been met, Bode plots of $G_C(s)$ (broken line), $T_U(s)$ (continuous line), and T(s) (continuous line with +) are plotted as shown in Fig. 5.6. It can be seen that T(s) has the phase margin of 58 degrees and crossover frequency of 10 KHz, satisfying the design objective.

TABLE 5.2.

Circuit Parameters for DCM Zeta converter.

Circuit Parameters	Values
V_g / V_O	15-20/ 5V
V_M	1.8V
C_1 / C_2	47/200μF
L_1 / L_2	100/22μH
$r_{C1} / r_{C2} / r_{L1} / r_{L2}$	0.38/0.095/0.001/0.00022Ω
R	10-38Ω

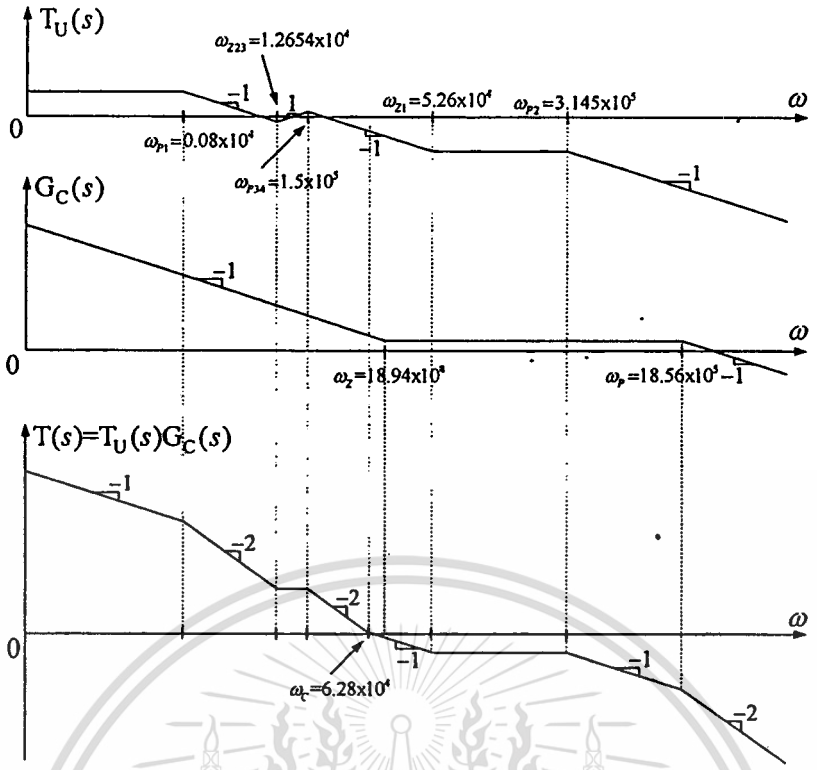

Fig. 5.5. Asymptote Bode plot of $T_U(s)$, $G_C(s)$, and T(s) of DCM VMC Zeta converter.

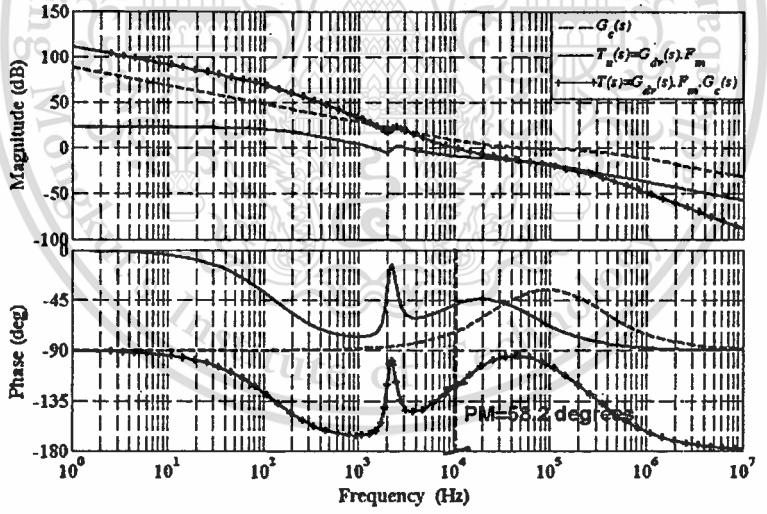

Fig. 5.6. Bode plots of $G_C(s)$, $T_U(s)$, and T(s) of DCM VMC Zeta converter.

5.2 Zeta Converter with PCMC

A – Compensator Design for CCM Zeta converter with PCMC

Closed-loop control of Zeta converter with PCMC is shown in Fig.5.7, where one-zero-and-two-pole compensator is used. Fig. 5.8 depicts the block diagram for compensator design. Recall from chapter 4 in CCM, and there are two current-mode control models, namely Erickson model and Ridley model.

- **Compensator design based on Erickson model**

$G_{VC}(s)$ of the Erickson model was derived and given in (4.2.2-9). Substituting the relevant parameters from TABLE 5.1 and a sensing resistor, R_S, of 0.1Ω into (4.2.2-9):

$$G_{VC}=\frac{0.5475s^3+2.9138\text{x}10^4s^2+5.8406\text{x}10^7s+2.1609\text{x}10^{12}}{s^3+6.719\text{x}10^3s^2+1.0328\text{x}10^8s+3.6464\text{x}10^{11}} \quad (5.2\text{-}1)$$

$G_{VC}(s)$ has one real pole at $\omega_{P1} = 3.9495\text{x}10^3$ rad/s, a pair of complex poles at $\omega_{P2,3} = 9.6093\text{x}10^3$ rad/s, one real zero at $\omega_{Z1} = 5.2632\text{x}10^4$ rad/s, and a pair of complex zeros at $\omega_{Z2,3} = 0.866\text{x}10^4$ rad/s.

The one-zero-and-two-pole compensator is selected to compensate for $G_{VC}(s)$ in (5.2-1). Its transfer function was given in (5.1-5). Like VMC, the design objective is to accomplish $G_{VC}(s)G_C(s)$ with the crossover frequency of 10 kHz and phase margin of more than 45 degrees. To achieve this, the zero and pole of $G_C(s)$ has been set at $\omega_Z = 2\pi\text{x}10^4$ rad/s, $\omega_P = 5\pi\text{x}10^4$ rad/s, and the gain at $\omega_O = 7.4\text{x}10^4$ rad/s. Fig. 5.9 shows asymptote Bode plot of $G_{VC}(s)$, $G_C(s)$, $G_{VC}(s)G_C(s)$. Based on the selected ω_Z, ω_P, and ω_O, component values of the one-zero two-pole compensator are calculated, getting: R_1=5.31 KΩ, R_2=2.7 KΩ, C_1=3 nF, and C_2=2 nF. Substitution of these component values into (5.1-5) gives:

$$G_C(s)=\frac{7.4\text{x}10^4}{s}\,\frac{s/2\pi\text{x}10^4+1}{s/5\pi\text{x}10^5+1} \quad (5.2\text{-}2)$$

To validate the design, Bode plots of $G_{VC}(s)$, $G_C(s)$, and $G_{VC}(s)G_C(s)$ are plotted as shown in Fig. 5.10. It can be seen that $G_{VC}(s)G_C(s)$ has the phase margin of 82 degrees and crossover frequency of about 10 KHz, meeting the design objective.

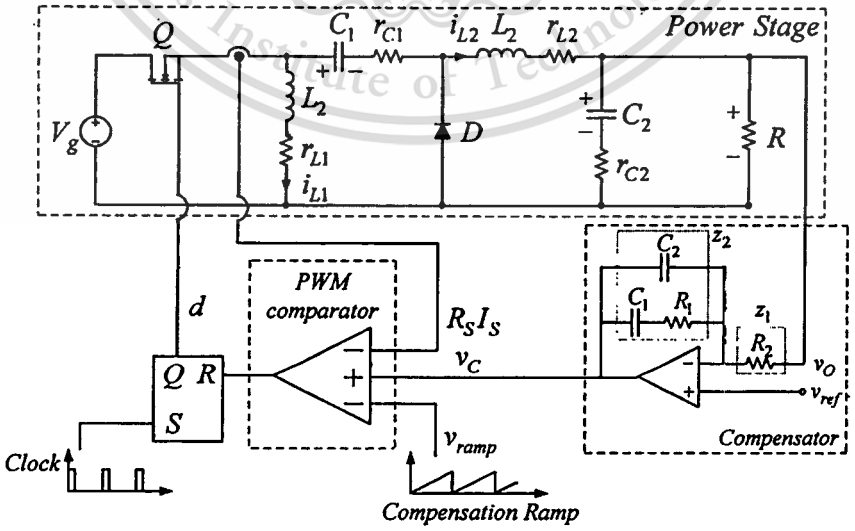

Fig. 5.7. CCM/DCM Zeta converter with PCMC.

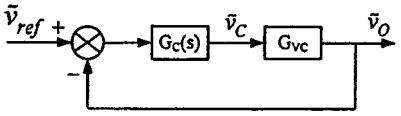

Fig. 5.8. Block diagram for compensator design for Zeta converter with PCMC.

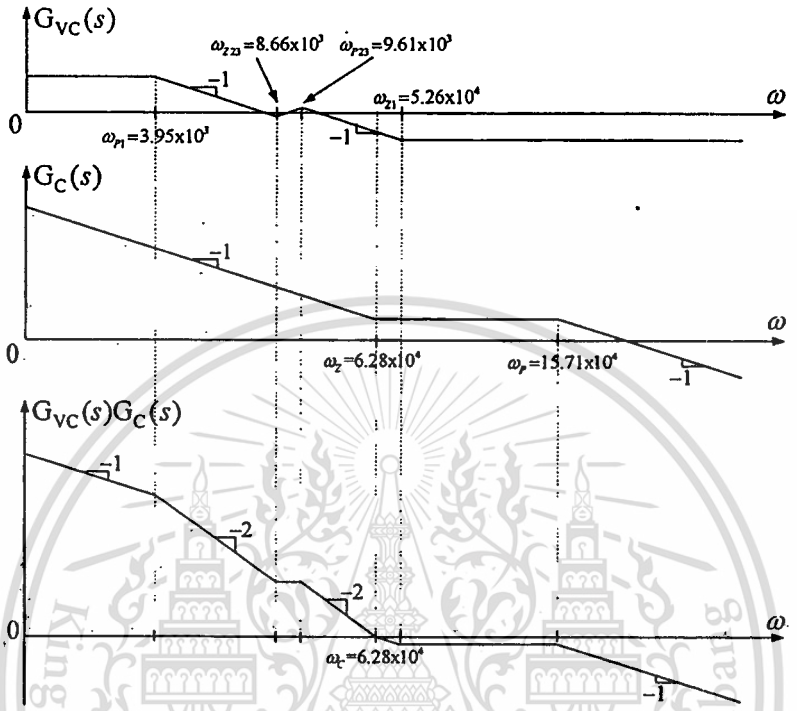

Fig. 5.9. Asymptote Bode plot of $G_{VC}(s)$, $G_C(s)$, and $G_{VC}(s)G_C(s)$.

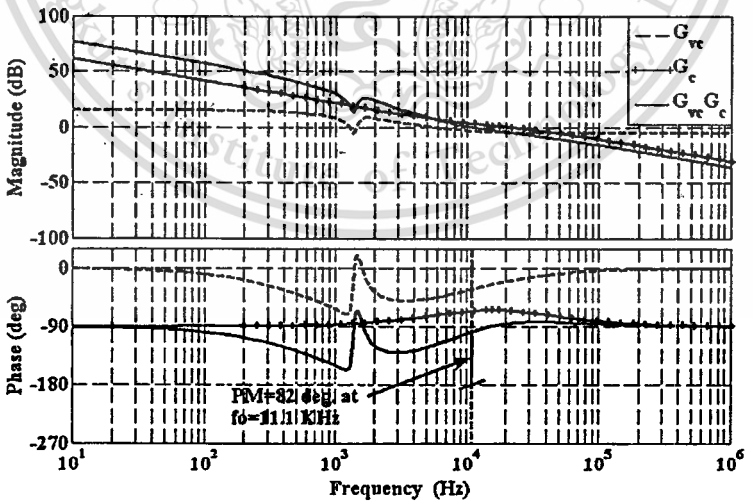

Fig. 5.10. Bode plots of $G_{vc}(s)$, $G_c(s)$, $G_{vc}(s)G_c(s)$ of CCM Zeta converter with PCMC based on Erickson model.

- **Compensator design based on Ridley model**

- **Case I**: Excluding the effect of the sampling gain $H_e(s)$

$G_{VC}(s)$ of the Ridley model was derived and given in (4.2.2-12). Substituting the relevant parameters from TABLE 5.1 into (4.2.2-12) and neglecting the sampling gain of the current loop (i.e. $H_e(s) = 1$) gives:

$$G_{VC}(s)=\frac{7.018\text{x}10^{4}s^{3}+3.736\text{x}10^{9}s^{2}+7.487\text{x}10^{12}s+2.77\text{x}10^{17}}{s^{4}+1.367\text{x}10^{5}s^{3}+1.026\text{x}10^{9}s^{2}+1.383\text{x}10^{13}s+5.172\text{x}10^{16}} \quad (5.2\text{-}3)$$

$G_{VC}(s)$ has two real poles at $\omega_{P1} = 0.0436\text{x}10^{5}$ rad/s, $\omega_{P2} = 1.2953\text{x}10^{5}$ rad/s, a pair of complex pole at $\omega_{P3,4} = 0.0957\text{x}10^{5}$ rad/s, one zero at $\omega_{Z1} = 5.2632\text{x}10^{4}$ rad/s, and a pair of complex zero at $\omega_{Z2,3} = 0.866\text{x}10^{4}$ rad/s.

The same one-zero-and-two-pole compensator, $G_C(s)$ in (5.2-2), is still used here and designed to compensate for $G_{VC}(s)$ in (5.2-3) to accomplish $G_{VC}(s)G_C(s)$ with the crossover frequency of 10 kHz and phase margin of more than 45 degrees. Fig. 5.11 shows asymptote Bode plot of $G_{VC}(s)$, $G_C(s)$, and $G_{VC}(s)G_C(s)$.

To validate the design, Bode plots of $G_{VC}(s)$ (broken line), $G_C(s)$ (continuous line with +), and $G_{VC}(s)G_C(s)$ (continuous line) are plotted as shown in Fig. 5.12. It can be seen that $G_{VC}(s)G_C(s)$ has the phase margin of 53.3 degrees and crossover frequency of around 10 KHz, meeting the design objective.

- **Case II**: Including the effect of the sampling gain $H_e(s)$

Substituting the related converter parameters from TABLE 5.1 with a sensing resistance of 0.1Ω into the derived model using Ridley's PCMC model in (4.2.2-11); equations (5.2-3) will be then defined, including sampling equation ($H_e(s)$).

$$G_{VC}=\frac{5.4026\text{x}10^{10}s^{3}+2.8761\text{x}10^{15}s^{2}+5.7637\text{x}10^{18}s+2.1324\text{x}10^{23}}{s^{5}+2.8306\text{x}10^{5}s^{4}+1.02\text{x}10^{11}s^{3}+7.3918\text{x}10^{14}s^{2}+1.0462\text{x}10^{19}s+3.9815\text{x}10^{22}} \quad (5.2\text{-}4)$$

G_{VC} has one pole at $\omega_{P1} = 0.0435\text{x}10^{5}$ rad/s, double pairs of complex pole at $\omega_{P2,3} = 0.0957\text{x}10^{5}$ rad/s, $\omega_{P4,5} = 3.1611\text{x}10^{5}$ rad/s, one zero at $\omega_{Z1} = 5.2632\text{x}10^{4}$ rad/s, and a pair of complex zero at $\omega_{Z2,3} = 0.866\text{x}10^{4}$ rad/s.

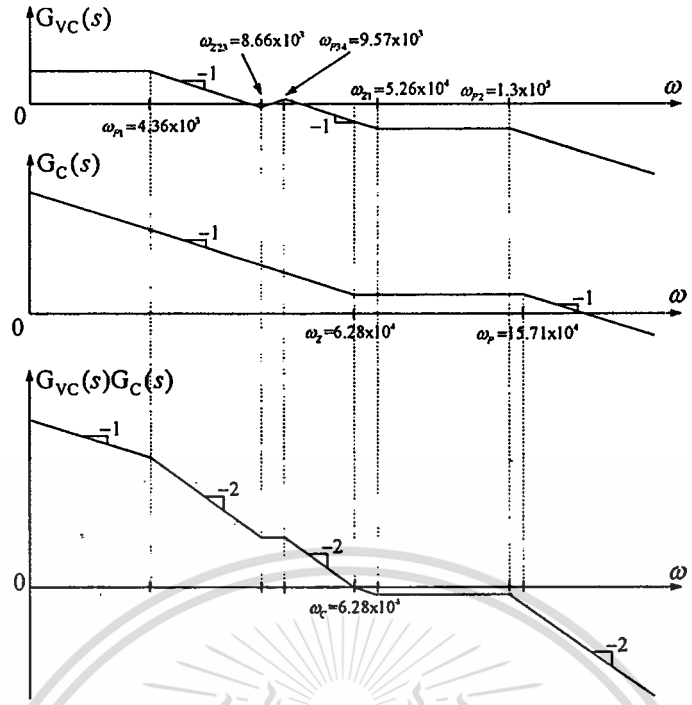

Fig. 5.11. Asymptote Bode plot of $G_{VC}(s)$, $G_C(s)$, and $G_{VC}(s)G_C(s)$.

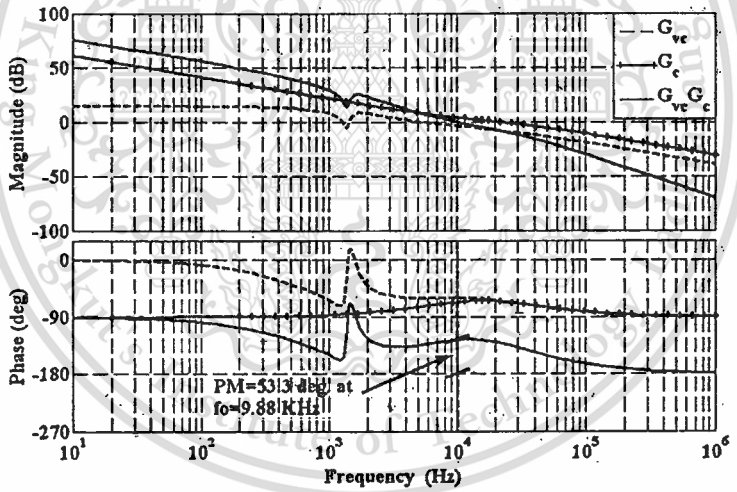

Fig. 5.12. Bode plots of $G_{VC}(s)$, $G_C(s)$, $G_{VC}(s)G_C(s)$ of CCM Zeta converter with PCMC based on Ridley model.

The same compensator $G_c(s)$ is also valid and designed to compensate for $G_{VC}(s)$ in (5.2-4), where the design objective is still met. Fig. 5.13 depicts asymptote Bode plot of $G_{VC}(s)$, $G_C(s)$, and $G_{VC}(s)G_C(s)$.

To ensure the design, the Bode plots of $G_{VC}(s)$ (broken line), $G_C(s)$ (continuous line with +), and $G_{VC}(s)G_C(s)$ (continuous line) are plotted as shown in Fig. 5.14. It can be seen that $G_{VC}(s)G_C(s)$ has the phase margin of 71.2 degrees and crossover frequency of approximately 10 KHz, meeting the design objective.

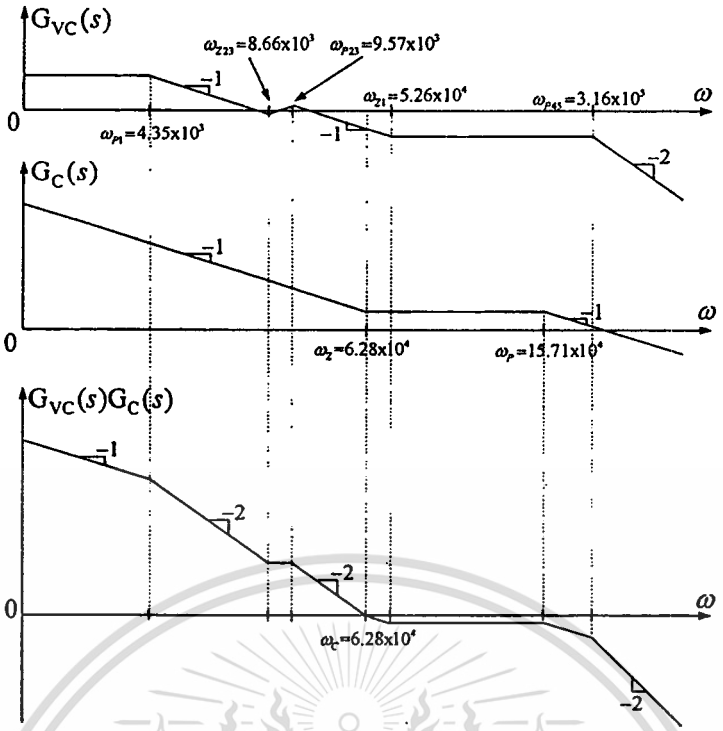

Fig. 5.13. Asymptote Bode plot of $G_{VC}(s)$, $G_C(s)$, and $G_{VC}(s)G_C(s)$.

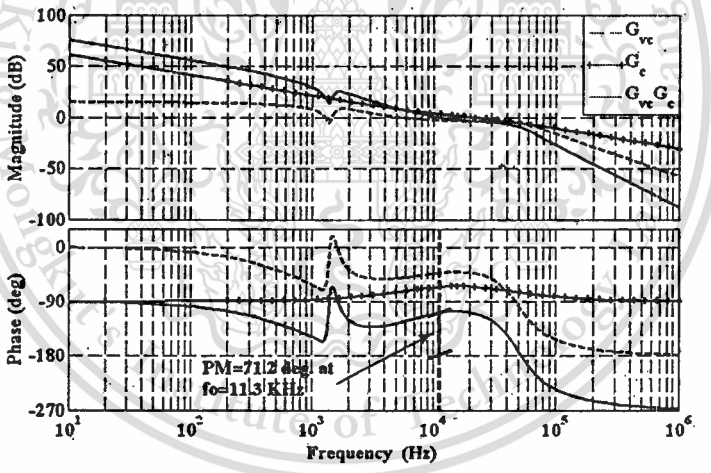

Fig. 5.14. Bode plots of $G_{VC}(s)$, $G_C(s)$, $G_{VC}(s)G_C(s)$ of CCM Zeta converter with PCMC based on Ridley model.

The comparison of CCM Zeta converter with PCMC of $G_{VC}(s)$ based on Erickson and Ridley' models (excluding and including $H_e(s)$) is illustrated in Fig. 5.15(a). It was found that the results from these models agree well each other at low frequencies, that is, below one-tenth of switching frequency or red line (Fig. 5.15(a)); this idea is proven and guaranteed by Fig. 5.15(b), that is, below the red line. Above this frequency, the results become divergent. On the other hand, the PCMC model from the Ridley's model is the accurate one [23], i.e., this model can accurately predict PCMC CCM Zeta converter at higher frequencies.

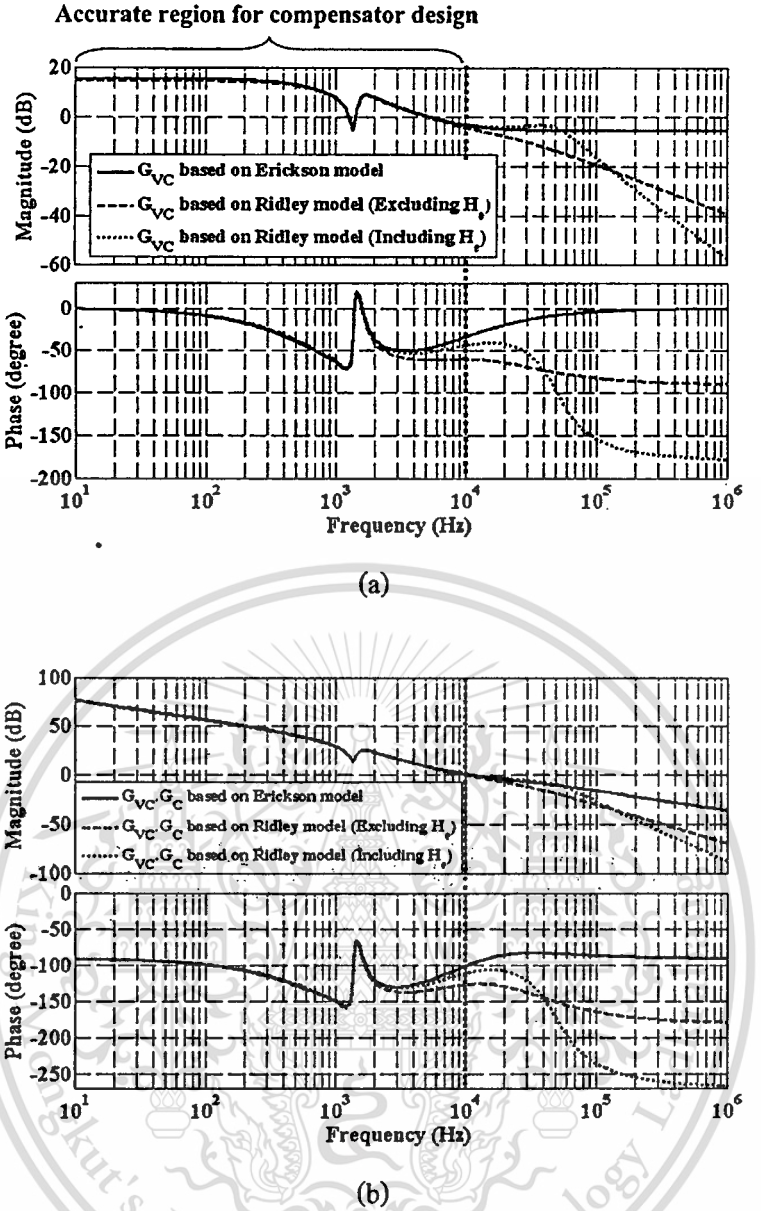

Fig. 5.15. Bode plot and (a) G_{VC} and (b) $G_{VC}(s)G_C(s)$ of CCM Zeta converter with PCMC based on Erickson and Ridley models.

B – Compensator Design of DCM Zeta converter with PCMC

In DCM, $G_{VC}(s)$ was derived and given in (4.2.2-14). Substituting the related converter parameters from TABLE 5.2 with a sensing resistance of 0.1Ω into the derived model using Ridley's PCMC model in (4.2.2-14); (5.2-5) will be then defined:

$$G_{VC}=\frac{1.202(1.5944\text{x}10^{5}s^{3}+8.8193\text{x}10^{9}s^{2}+4.8117\text{x}10^{13}s+1.3435\text{x}10^{18})}{s^{4}+3.1953\text{x}10^{5}s^{3}+1.7838\text{ex}10^{9}s^{2}+6.8531\text{x}10^{13}s+5.3792\text{x}10^{16}} \quad (5.2\text{-}5)$$

G_{VC} has one pole at $\omega_{P1} = 0.008\text{x}10^{5}$ rad/s, $\omega_{P2} = 3.1449\text{x}10^{5}$ rad/s, a pair of complex poles at $\omega_{P3,4} = 0.1463\text{x}10^{5}$ rad/s, one zero at $\omega_{Z1} = 5.2632\text{x}10^{4}$ rad/s, and a pair of complex zeros at $\omega_{Z2,3} = 1.2654\text{x}10^{4}$ rad/s.

A one-zero-and-two-pole compensator, $G_C(s)$ in (5.1-5), is necessary to compensate for $G_{VC}(s)$ in (5.2-5). The design objective is herein the same as in CCM case. To achieve this, the zero and pole of $G_C(s)$ has been set at $\omega_Z=3\pi x10^4$ rad/s, $\omega_P=\pi x10^5$ rad/s and the gain at $\omega_O=7x10^4$ rad/s. Fig. 5.15 illustrates asymptote Bode plot of $G_{VC}(s)$, $G_C(s)$, and $G_{VC}(s)G_C(s)$. Relied on the selected ω_Z, ω_P, and ω_O, the one-zero-and-two-pole compensator's component values are calculated, getting: R_1=2.2 KΩ, R_2=2 KΩ, C_1=4.7 nF, and C_2=2 nF. Substitution of these component values into (4.1.2-4) gives:

$$G_C(s)=\frac{7x10^4}{s}\frac{s/3\pi x10^4+1}{s/\pi x10^5+1} \qquad (5.2\text{-}6)$$

To ensure the design, the Bode plots of $G_{VC}(s)$ (broken line), $G_C(s)$ (continuous line with +), and $G_{VC}(s)G_C(s)$ (continuous line) are plotted as shown in Fig. 5.16. It can be seen that $G_{VC}(s)G_C(s)$ has the phase margin of 65.3 degrees and crossover frequency of about 10 KHz, meeting the design objective.

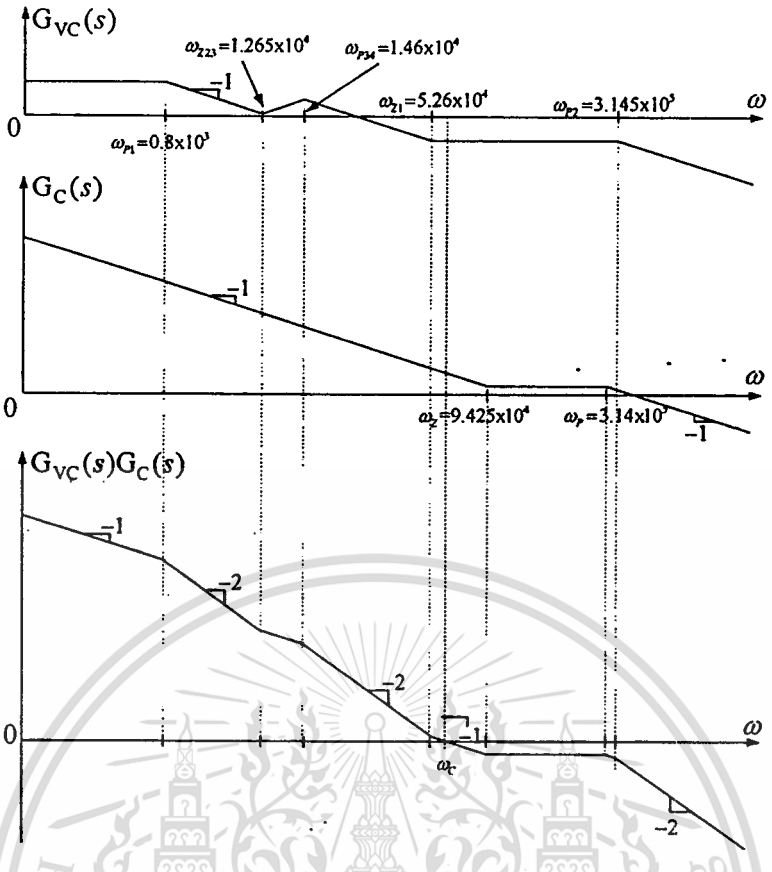

Fig. 5.16. Asymptote Bode plot of $G_{VC}(s)$, $G_C(s)$, and $G_{VC}(s)G_C(s)$.

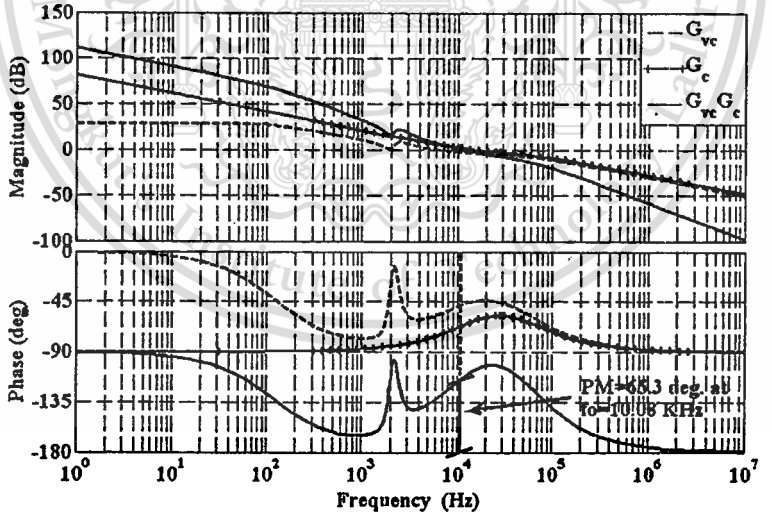

Fig. 5.17. Bode plots of $G_{VC}(s)$, $G_C(s)$, $G_{VC}(s)G_C(s)$ of DCM Zeta converter using Ridley model.

Chapter 6

Results

In the last chapter, feedback compensator design of CCM/DCM Zeta converters with VMC and PCMC was carried out. This chapter presents the performance evaluation of the Zeta converters employing the designed compensators. It is shown that the designed compensators are able to yield good performance for the Zeta converters. Finally, some experimental results are given to support the validity of theoretical design.

6.1 Simulated Results

6.1.1 CCM Zeta Converter with VMC

A SIMULINK model of a CCM Zeta converter with VMC is depicted in Fig. 6.1. The power stage is represented by the small-signal state-space equation in (2.2.2-5):

$$\frac{d}{dt}\begin{bmatrix}\tilde{i}_{L1}(t)\\ \tilde{i}_{L2}(t)\\ \tilde{v}_{C1}(t)\\ \tilde{v}_{C2}(t)\end{bmatrix}=\begin{bmatrix}\frac{r_{C1}(1-D)+r_{L1}}{L_1} & 0 & -\frac{1-D}{L_1} & 0\\ 0 & -\frac{(r_{C2}+R)(Dr_{C1}+r_{L2})+r_{C2}R}{L_2(r_{C2}+R)} & \frac{D}{L_2} & \frac{-R}{L_2(r_{C2}+R)}\\ \frac{1-D}{C_1} & -\frac{D}{C_1} & 0 & 0\\ 0 & \frac{R}{C_2(r_{C2}+R)} & 0 & \frac{-1}{C_2(r_{C2}+R)}\end{bmatrix}\begin{bmatrix}\tilde{i}_{L1}(t)\\ \tilde{i}_{L2}(t)\\ \tilde{v}_{C1}(t)\\ \tilde{v}_{C2}(t)\end{bmatrix}+$$

$$\begin{bmatrix}\frac{D}{L_1} & 0 & \frac{\eta[V_g[(1-D)(R+r_{L2})+Dr_{C1}]-I_zDr_{L1}R]}{L_1R(1-D)^2}\\ \frac{D}{L_2} & \frac{r_{C2}R}{L_2(r_{C2}+R)} & \frac{\eta[V_g(r_{L2}+R)(1-D)-I_zR[r_{C1}(1-D)+Dr_{L1}]]}{L_2R(1-D)^2}\\ 0 & 0 & \frac{-\eta[DV_g+RI_z(1-D)]}{C_1R(1-D)^2}\\ 0 & -\frac{R}{C_2(r_{C2}+R)} & 0\end{bmatrix}\begin{bmatrix}\tilde{v}_g(t)\\ \tilde{i}_z(t)\\ \tilde{d}(t)\end{bmatrix} \qquad (6.1.1\text{-}1)$$

$$\tilde{v}_o(t)=\begin{bmatrix}0 & \frac{r_{C2}R}{r_{C2}+R} & 0 & \frac{r_{C2}R}{r_{C2}+R}\end{bmatrix}\begin{bmatrix}\tilde{i}_{L1}(t)\\ \tilde{i}_{L2}(t)\\ \tilde{v}_{C1}(t)\\ \tilde{v}_{C2}(t)\end{bmatrix}+\begin{bmatrix}0 & \frac{-r_{C2}R}{r_{C2}+R} & 0\end{bmatrix}\begin{bmatrix}\tilde{v}_g(t)\\ \tilde{i}_z(t)\\ \tilde{d}(t)\end{bmatrix}$$

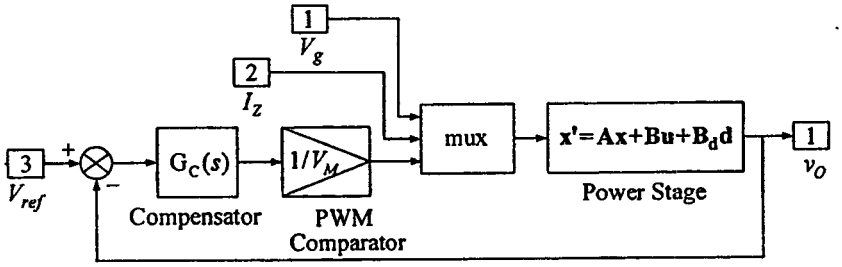

Fig. 6.1. SIMULINK model of CCM Zeta converter with VMC.

Substituting the converter parameters from TABLE 5.1 into (6.1.1-1) with V_g=15V and R=1Ω, the small-signal state-space equation used in the simulation is therefore:

$$\begin{cases} \dfrac{d}{dt}\begin{bmatrix}\tilde{i}_{L1}(t)\\ \tilde{i}_{L2}(t)\\ \tilde{v}_{C1}(t)\\ \tilde{v}_{C2}(t)\end{bmatrix} = \begin{bmatrix}-0.1435\text{x}10^4 & 0 & -0.75\text{x}10^4 & 0\\ 0 & -0.2451\text{x}10^4 & 0.4545\text{x}10^4 & -1.6604\text{x}10^4\\ 0.75\text{x}10^4 & -0.25\text{x}10^4 & 0 & 0\\ 0 & 0.4566\text{x}10^4 & 0 & -0.4566\text{x}10^4\end{bmatrix}\begin{bmatrix}\tilde{i}_{L1}(t)\\ \tilde{i}_{L2}(t)\\ \tilde{v}_{C1}(t)\\ \tilde{v}_{C2}(t)\end{bmatrix} + \\ \qquad \begin{bmatrix}2.5\text{x}10^3 & 0 & 1.9998\text{x}10^5\\ 4.5455\text{x}10^3 & 1.5774\text{x}10^3 & 3.4195\text{x}10^5\\ 0 & 0 & -0.6266\text{x}10^5\\ 0 & -4.5662\text{x}10^3 & 0\end{bmatrix}\begin{bmatrix}\tilde{v}_g(t)\\ \tilde{i}_z(t)\\ \tilde{d}(t)\end{bmatrix} \\ \tilde{v}_o(t) = \begin{bmatrix}0 & 0.0868 & 0 & 0.9132\end{bmatrix}\begin{bmatrix}\tilde{i}_{L1}(t)\\ \tilde{i}_{L2}(t)\\ \tilde{v}_{C1}(t)\\ \tilde{v}_{C2}(t)\end{bmatrix} + \begin{bmatrix}0 & -0.0868 & 0\end{bmatrix}\begin{bmatrix}\tilde{v}_g(t)\\ \tilde{i}_z(t)\\ \tilde{d}(t)\end{bmatrix} \end{cases} \quad (6.1.1\text{-}2)$$

The PWM comparator block in Fig. 6.1 is represented by transfer function in (4.1.1-1):

$$F_M = \frac{\tilde{d}(s)}{\tilde{v}_c(s)} = \frac{1}{V_M} = \frac{1}{1.8} \quad (6.1.1\text{-}3)$$

The designed compensator in (5.1-3) is used in the compensator block in Fig. 6.1:

$$G_C(s) = \frac{8.65\text{x}10^3}{s}\left(\frac{s}{3\text{x}10^3}+1\right) \quad (6.1.1\text{-}4)$$

The mux block combines three input signals (V_g, I_Z, and d) into vector form for the power stage block whose output signal is v_O. The V_{ref} block is for specifying the reference voltage which, in this case, is 5V.

Fig. 6.2 shows the simulated output voltage start-up transient. The output voltage settles to 5V after about 160μs, with the maximum voltage overshoot of 6.4V. Fig. 6.3 shows the simulated output voltage response, when the load current is switched from 1A to 4A. The maximum voltage drop during the transient is around 0.6V. The feedback control is able to keep the output voltage at 5V after the transient which lasts about 300μs.

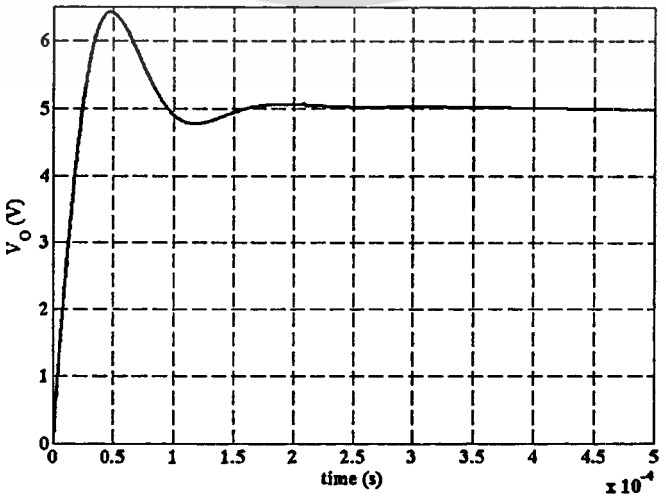

Fig. 6.2. CCM Zeta Converter with VMC: output voltage response during a start-up.

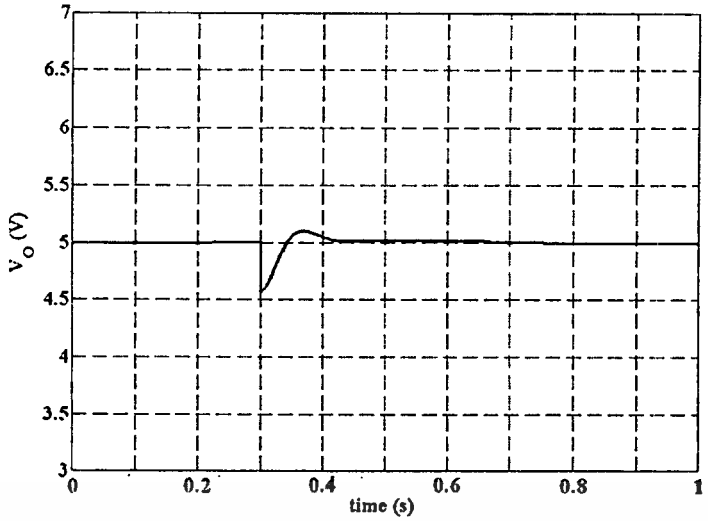

Fig. 6.3. CCM Zeta Converter with VMC: output voltage response during the load current step from 1A to 4A.

6.1.2 DCM Zeta Converter with VMC

Step response is used to test the performance of the designed compensator. A 5V step voltage is applied at the input of the open-loop transfer function, $T(s)=G_{d1v}(s)F_M G_C(s)$, and the output voltage response is measured at the output.

The transfer functions $G_{d1v}(s)$, F_m, and $G_C(s)$ used in the simulation are:

$$G_{d1v}(s)=\frac{2.967\text{x}10^4 s^3+1.579\text{x}10^9 s^2+3.165\text{x}10^{12}s+1.171\text{x}10^{17}}{s^4+8452s^3+1.647\text{x}10^8 s^2+5.878\text{x}10^{11}s+4.969\text{x}10^{15}} \quad (6.1.2\text{-}1)$$

$$F_M=\frac{\tilde{d}(s)}{\tilde{v}_C(s)}=\frac{1}{V_M}=\frac{1}{1.8} \quad (6.1.2\text{-}2)$$

$$G_C(s)=\frac{1.7\text{x}10^5}{s}\frac{\frac{s}{18.94\text{x}10^4}+1}{\frac{s}{18.56\text{x}10^5}+1} \quad (6.1.2\text{-}3)$$

The product of (6.1.2-1), (6.1.2-2), and (6.1.2-3) thus yields the open-loop transfer function $T(s)=G_{d1v}(s)F_M G_C(s)$:

$$T(s)=\frac{4.725\text{x}10^4 s^4+2.749\text{x}10^9 s^3+1.749\text{x}10^{13}s^2+2.114\text{x}10^{17}s+9.227\text{x}10^{20}}{s^5+8452s^4+1.647\text{x}10^8 s^3+5.878\text{x}10^{11}s^2+4.969\text{x}10^{15}s} \quad (6.1.2\text{-}4)$$

Fig. 6.4 shows the simulated step response or the output voltage start-up transient of the converter. The output voltage settles to 5V after about 228μs, with the maximum voltage overshoot of 6.19V or 23.7%.

6.1.3 CCM Zeta Converter with PCMC

To test the performance of the compensators designed for PCMC, a step-response method is again used, i.e. a 5V step voltage is applied at the input of the open-loop transfer

function, $G_{vc}(s)G_c(s)$, and the output voltage response is measured at the output. Recall that there are two PCMC models: Erickson and Ridley models. The performance of the designed compensator is therefore accessed for each model.

Erickson model

$$G_{vc} = \frac{0.5475s^3 + 2.9138\text{x}10^4 s^2 + 5.8406\text{x}10^7 s + 2.1609\text{x}10^{12}}{s^3 + 6.719\text{x}10^3 s^2 + 1.0328\text{x}10^8 s + 3.6464\text{x}10^{11}} \quad (6.1.3\text{-}1)$$

$$G_c(s) = \frac{7.4\text{x}10^4}{s} \frac{\frac{s}{2\pi\text{x}10^4} + 1}{\frac{s}{5\pi\text{x}10^5} + 1} \quad (6.1.3\text{-}2)$$

Fig. 6.5 shows the simulated step response or output voltage start-up transient. The output voltage settles to 5V after about 113μs, with the maximum voltage overshoot of 5.65 V or 13%.

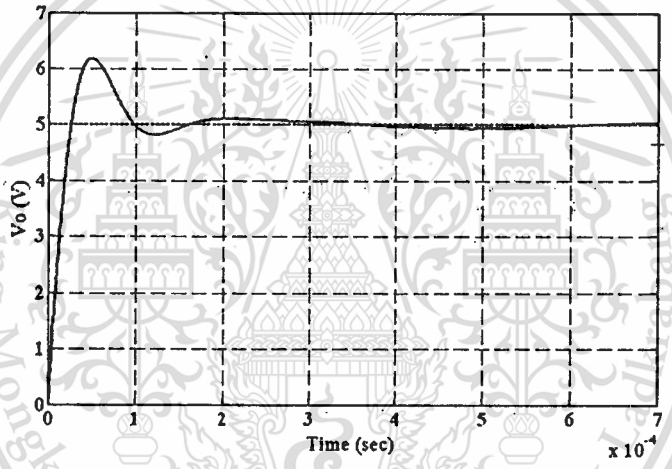

Fig. 6.4. DCM Zeta Converter with VMC: output voltage response during start-up.

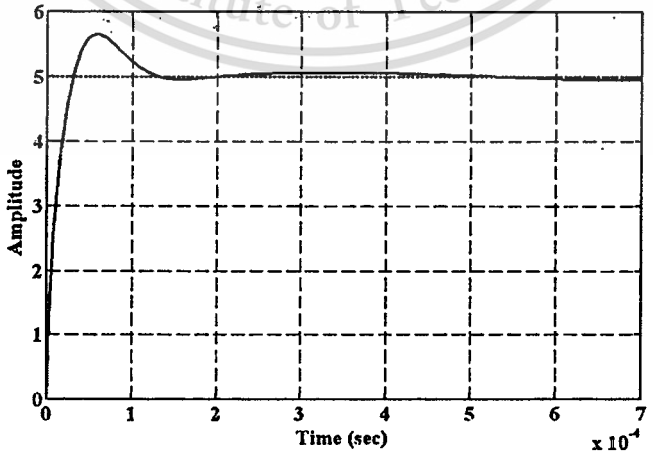

Fig. 6.5. CCM Zeta Converter with PCMC based on Erickson model: output voltage response during start-up.

Ridley model

The transfer functions $G_{VC}(s)$ (neglecting $H_e(s)$) and $G_C(s)$ used in the simulation are:

$$G_{VC}=\frac{7.018\text{x}10^4 s^3+3.736\text{x}10^9 s^2+7.487\text{x}10^{12}s+2.77\text{x}10^{17}}{s^4+1.367\text{x}10^5 s^3+1.026\text{x}10^9 s^2+1.383\text{x}10^{13}s+5.172\text{x}10^{16}} \quad (6.1.3\text{-}3)$$

$$G_C(s)=\frac{7.4\text{x}10^4}{s}\frac{\frac{s}{2\pi\text{x}10^4}+1}{\frac{s}{5\pi\text{x}10^5}+1} \quad (6.1.3\text{-}2)$$

Fig. 6.6 shows the simulated output voltage start-up transient. The output voltage settles to 5V after about 146μs, with the maximum voltage overshoot of 6.09V or 23%.

The transfer functions $G_{VC}(s)$ (including $H_e(s)$) and $G_C(s)$ used in the simulation are:

$$G_{VC}=\frac{5.4026\text{x}10^{10}s^3+2.8761\text{x}10^{15}s^2+5.7637\text{x}10^{18}s+2.1324\text{x}10^{23}}{s^5+2.8306\text{x}10^5 s^4+1.02\text{x}10^{11}s^3+7.3918\text{x}10^{14}s^2+1.0462\text{x}10^{19}s+3.9815\text{x}10^{22}} \quad (6.1.3\text{-}4)$$

$$G_C(s)=\frac{7.4\text{x}10^4}{s}\frac{\frac{s}{2\pi\text{x}10^4}+1}{\frac{s}{5\pi\text{x}10^5}+1} \quad (6.1.3\text{-}2)$$

Fig. 6.7 shows the simulated output voltage start-up transient. The output voltage settles to 5V after about 108μs, with the maximum voltage overshoot of 5.67 V or 14.6 %.

6.1.4 DCM Zeta Converter with PCMC

Like CCM, a step-response method is used to investigate the performance of the PCMC Zeta converter in the DCM, that is, the open-loop transfer function, $G_{VC}(s)G_C(s)$. Only the CMC model from Ridley is shown here.

$$G_{VC}=\frac{1.202(1.5944\text{x}10^5 s^3+8.8193\text{x}10^9 s^2+4.8117\text{x}10^{13}s+1.3435\text{x}10^{18})}{s^4+3.1953\text{x}10^5 s^3+1.7838\text{ex}10^9 s^2+6.8531\text{x}10^{13}s+5.3792\text{x}10^{16}} \quad (6.1.4\text{-}1)$$

$$G_C(s)=\frac{7\text{x}10^4}{s}\frac{s/3\pi\text{x}10^4+1}{s/\pi\text{x}10^5+1} \quad (6.1.4\text{-}2)$$

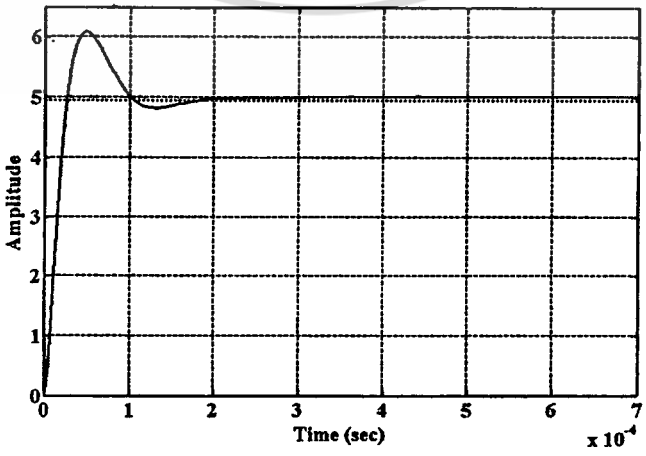

Fig. 6.6. CCM Zeta Converter with PCMC based on Ridley model ($H_e(s)$ excluded): output voltage response during start-up.

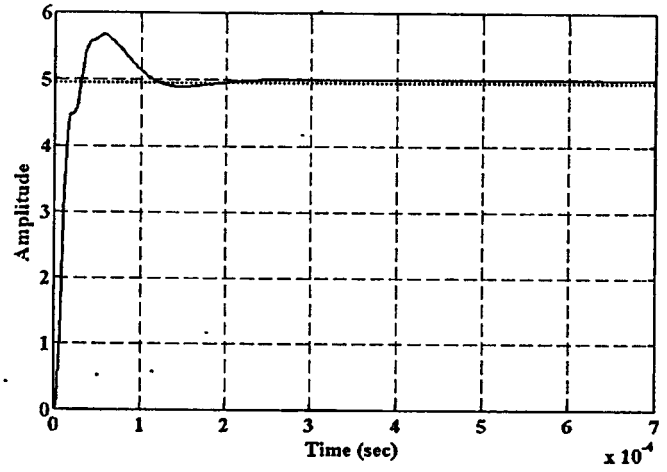

Fig. 6.7. CCM Zeta Converter with PCMC based on Ridley model ($H_c(s)$ included): output voltage response during a start-up.

Fig. 6.8 illustrates the simulated output voltage start-up transient. The output voltage settles to 5V after about 244μs, with the maximum voltage overshoot of 6.V or 20%.

6.2 Experimental Results

To verify the performance of the designed compensator, the prototype CCM Zeta converter with VMC shown in Fig. 6.9 has been designed and built. Circuit parameters of the prototype converter closely follow the values listed in TABLE 5.1. The PI compensator designed in section 5.1 is used to compensate for the feedback loop.

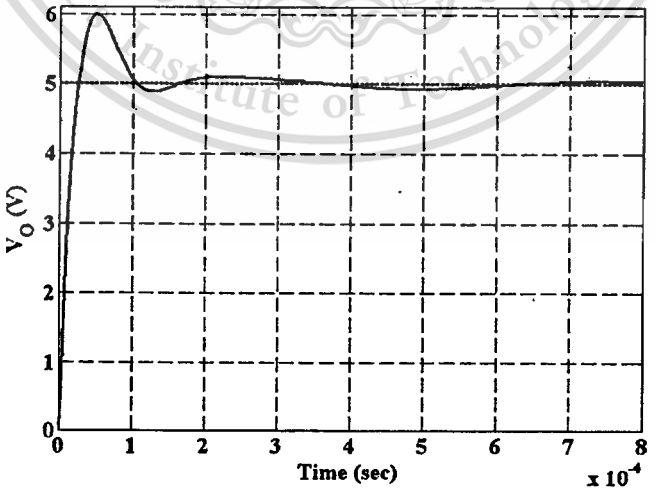

Fig. 6.8. Output voltage response of PCMC DCM Zeta converter using Ridley model.

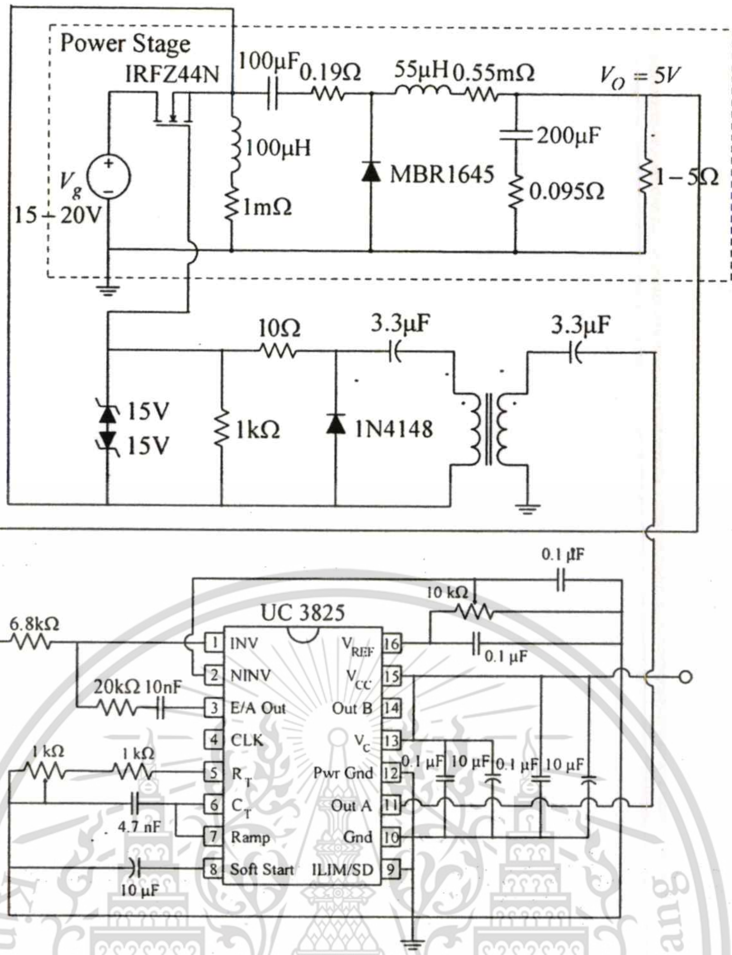

(a)

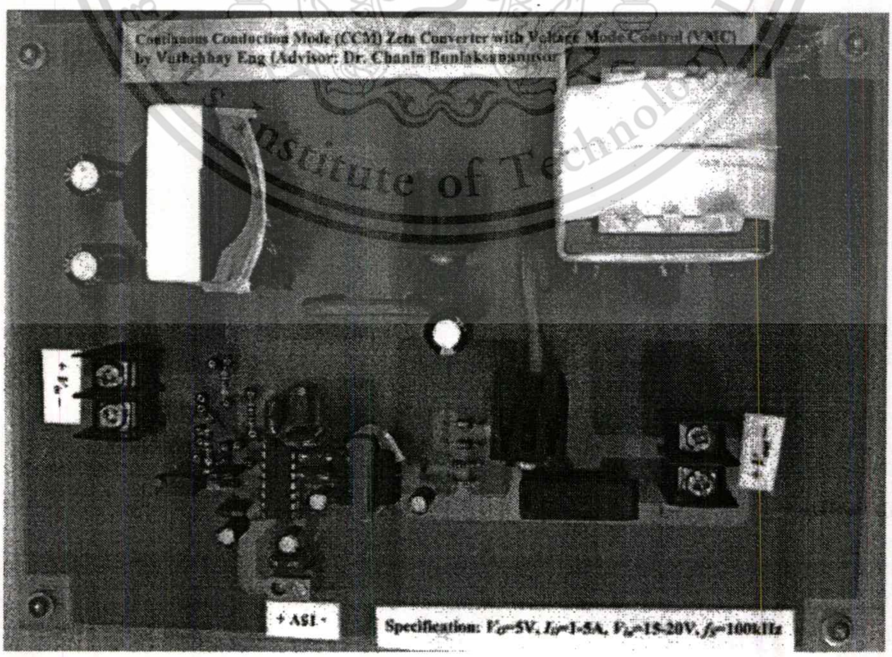

(b)

Fig. 6.9. Prototype CCM Zeta converter with VMC: (a) Circuit schematic and (b) its photo.

6.2.1 Measurement of Converter Waveforms

The experimental setup for measuring waveforms in the prototype Zeta converter is depicted in Fig. 6.10.

The test procedure is as follows:

1. Supply an input voltage, V_g, of 15-20V to power circuit and a voltage of 15V to the control circuit.

2. After the power up in step 1, the output voltage is now regulated at 5V.

3. Varying the load resistor, R, and the input voltage, V_g, measure the value of the output voltage and waveforms of v_{DS}, i_{L1}, and i_{L2}.

TABLE 6.1 shows the measured output voltage as the input voltage and load current varied. It can be seen that the output voltage is regulated at about 5V throughout the entire operating range of converter.

These measured results are the simulated waveforms of V_{DS}, i_{L1}, and i_{L2} produced by PSPICE simulation of the CCM Zeta converter in Fig. 6.11. The waveforms of v_{DS}, i_{L1}, and i_{L2} measured at V_g=15V and I_O=1A (R=5Ω), V_g=15V and I_O=4A (R=1.25Ω), V_g=20V and I_O=1A (R=5Ω), and V_g=20V and I_O=4A (R=1.25Ω) are displayed in Fig. 6.12(a) to Fig. 6.15(a) respectively. The measured results in Fig. 6.12(a) to 6.15(a) agree reasonably well with their simulated counterparts in Fig. 6.12(b) to 6.15(b), proving the accuracy of the CCM Zeta converter design.

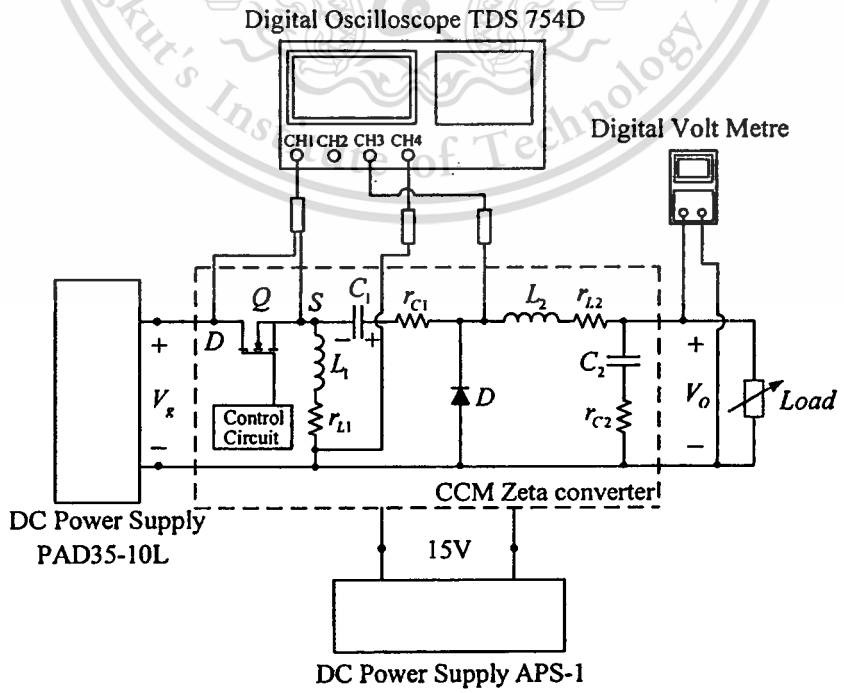

6.10. Experimental setup for measuring v_{DS}, i_{L1}, i_{L2}, and V_O.

TABLE 6.1

The measured values of V_O(V) at different values of V_g and I_O.

V_g (V)	V_O (V)				
	I_O=1A	I_O=2A	I_O=3A	I_O=4A	I_O=5A
15	4.999	4.926	4.887	4.846	4.835
20	4.999	4.915	4.884	4.845	4.831

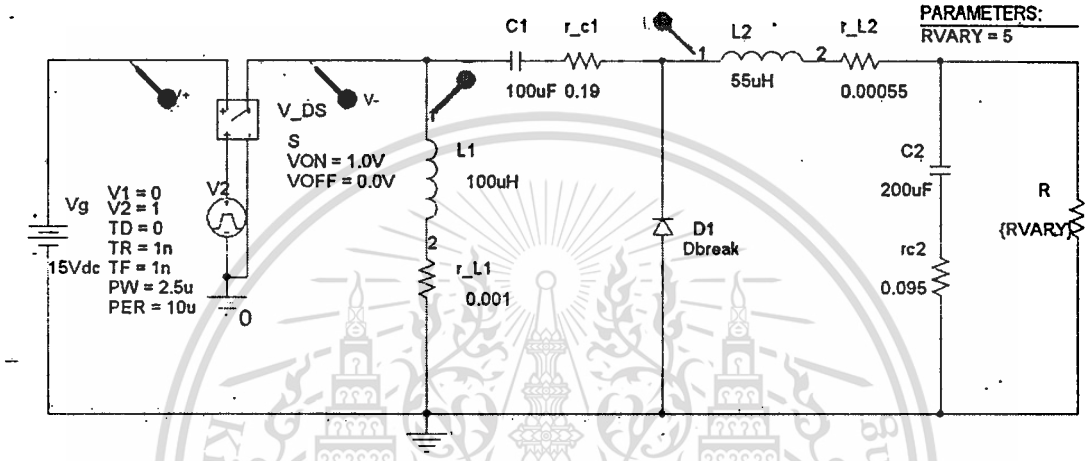

Fig. 6.11. Circuit schematic of CCM Zeta converter for PSPICE simulation.

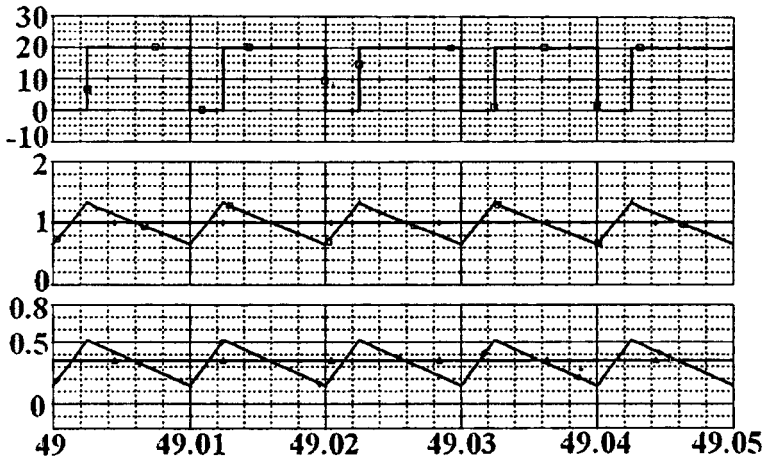

(a) $v_{DS,peak}$=20V, I_{L2}=1A, and I_{L1}=0.35A.

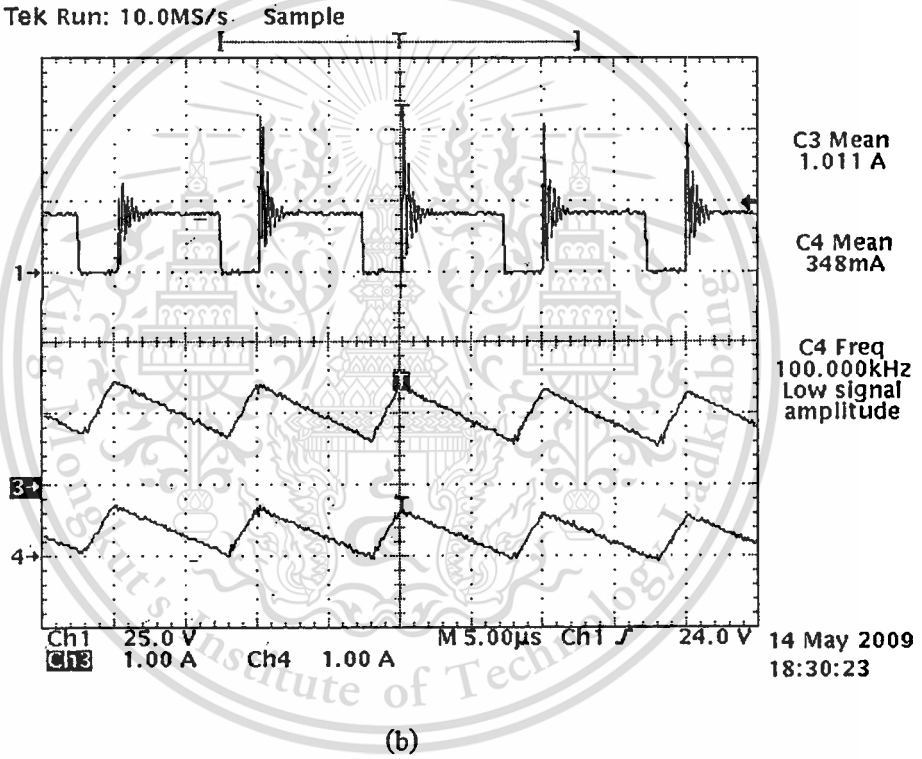

(b)

Fig. 6.12. Waveforms of v_{DS}, i_{L2}, and i_{L1} for V_g=15V and I_O=1A (R=5Ω):

(a) PSPICE simulation and (b) Experiment.

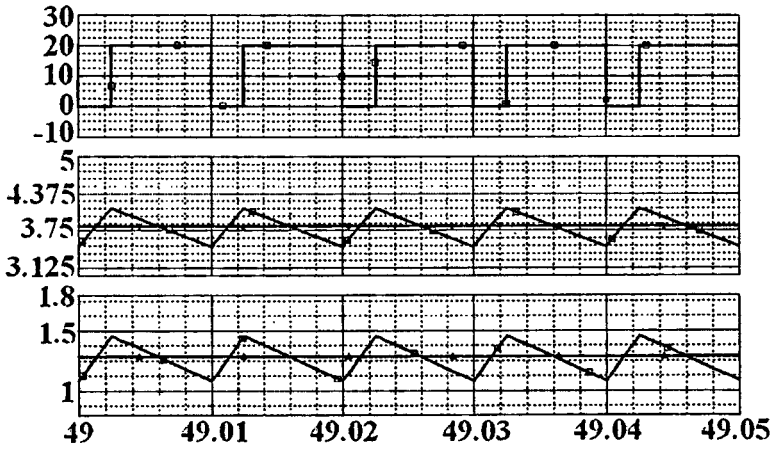

(a) $v_{DS,peak}$=20V, I_{L2}=3.82A, and I_{L1}=1.3A.

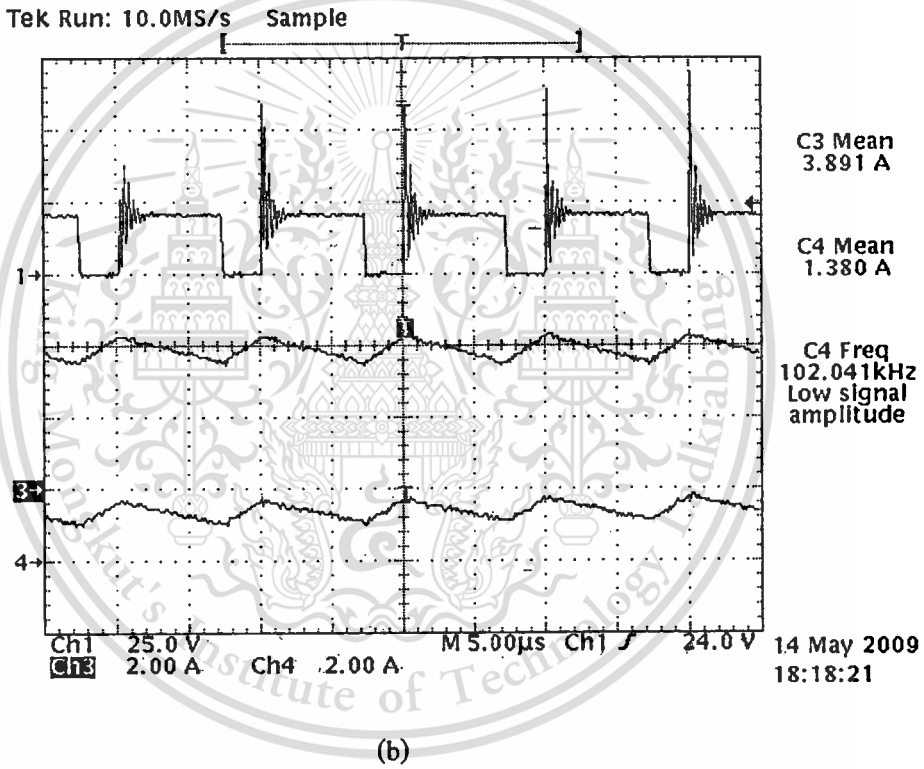

(b)

Fig. 6.13. Waveforms of v_{DS}, i_{L2}, and i_{L1} for V_g=15V and I_O=4A (R=1.25Ω):

(a) PSPICE simulation and (b) Experiment.

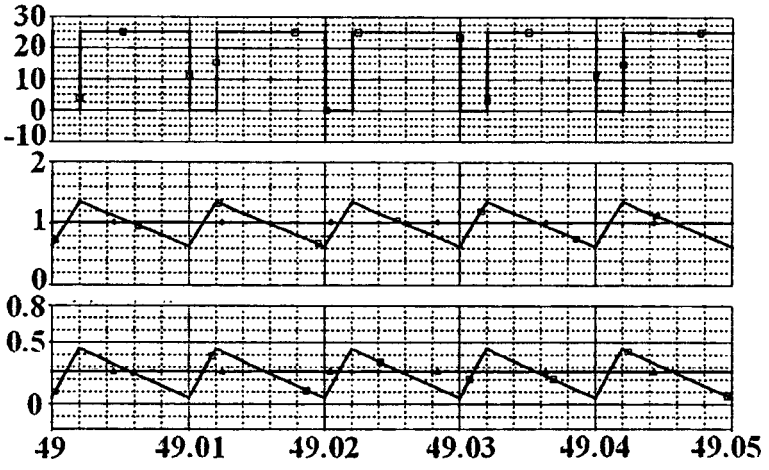

(a) $v_{DS,peak}$=25V, I_{L2}=1A, I_{L1}=0.27A.

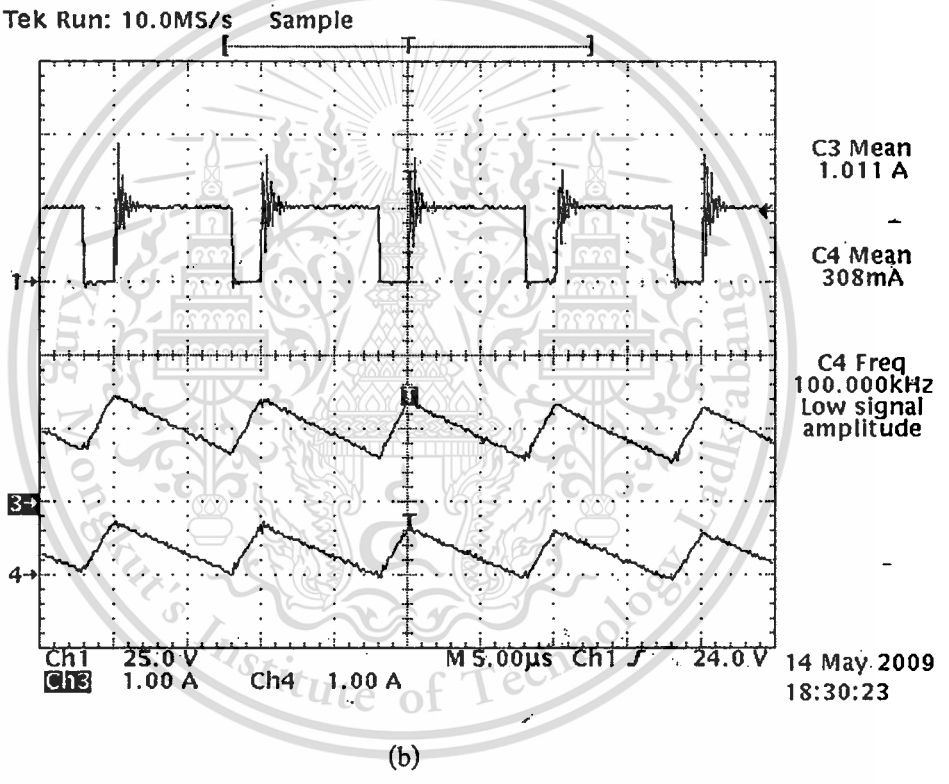

(b)

Fig. 6.14. Waveforms of v_{DS}, i_{L2}, and i_{L1} for V_g=20V and I_O=1A (R=5Ω):

(a) PSPICE simulation and (b) Experiment.

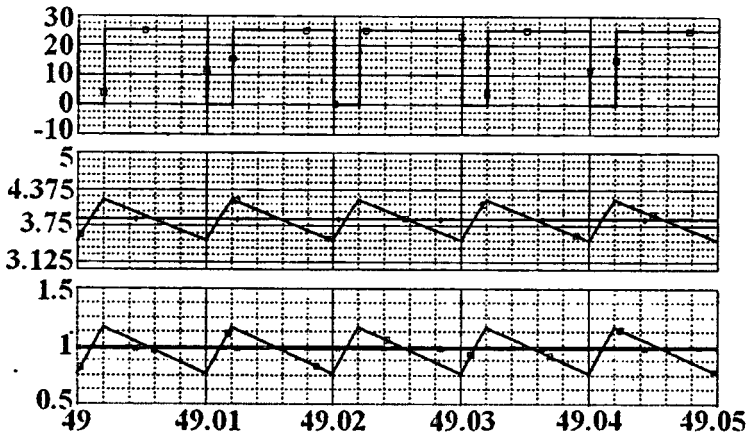

(a) $v_{DS,peak}$=25V, I_{L2}=3.87A, and I_{L1}=1A.

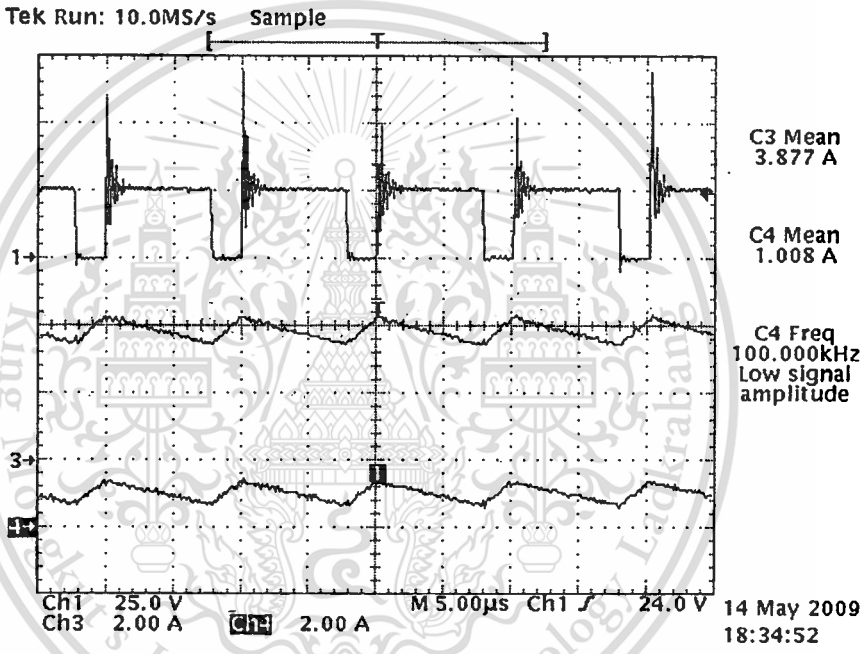

(b)

Fig. 6.15. Waveforms of v_{DS}, i_{L2}, and i_{L1} for V_g=20V and I_O=4A (R=1.25Ω):
(a) PSPICE simulation and (b) Experiment.

6.2.2 Measurement of Output Voltage Response

The experimental setup for measuring the output voltage response due to a step load change is depicted in Fig. 6.16.

The test procedure is as follows:

1. Supply an input voltage, V_g, of 15V to power circuit and a voltage of 15V to the control circuit.

2. After the power up in step 1, the output voltage is now regulated at 5V. The load resistor is 5Ω, so the output current is 1A.

3. Three external 5Ω load resistors are switched in parallel with the existing 5Ω resistor to release the step load change from 1A to 4A.

4. The output voltage of the converter during the step load change is captured by the digital oscilloscope.

Fig. 6.17 shows the captured output voltage response during the step load change from 1A to 4A. The maximum voltage drop during the transient is around 0.4V. It takes approximately 300μs for the output voltage to resettle to 5V after the load change. This result indicates that the designed PI compensator not only makes the converter stable under the load current disturbance, but also yields a fast transient response.

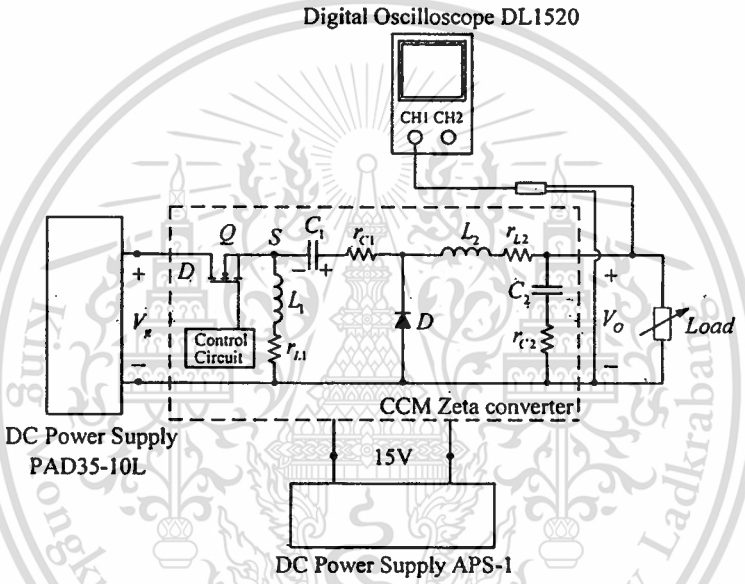

Fig. 6.16. Experimental setup for a step load change.

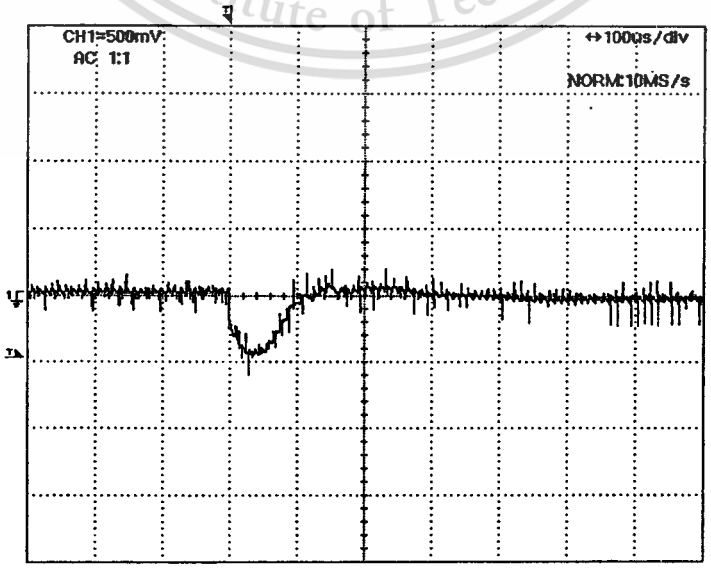

Fig. 6.17. Output voltage response during the step load change from 1A to 4A.

Chapter 7

Conclusion

A DC-DC converter has been widely used in the modern portable electronic equipment and systems. Of many kinds of the DC-DC converters, the converters capable of operating in either step-up or step-down mode, such as SEPIC and Zeta converters, are more attractive for this application. Modeling is of great significance to understand the converters' characteristics and provide a basis for the feedback control design. This thesis has studied dynamic modeling and control of a Zeta converter. To find its model, three well-known modeling methods – SSA technique, PWM-switch model, and Averaged switch model – were applied to explore the converter's model. There are two feasible modes of operation in the Zeta converter: Continuous Conduction Mode (CCM) and Discontinuous Conduction Mode (DCM). Both operational modes have been studied. In CCM, it was observed that the obtained models from the three modeling methods yield the same results. In DCM, it was found that the model derived form SSA technique is a reduced-order one which can predict the converter's characteristic up to the one-tenth of the switching frequency, compared to the models from PWM-switch model and Averaged switch model (full-order models).

Voltage Model Control (VMC) and Peak Current Mode Control (PCMC) were employed to regulate the output voltage of Zeta converter. More importantly, it was found that the accurate region for compensator design of PCMC based on Erickson and Ridley models are consistent with each other up to one-tenth of switching frequency. Feedback compensator design was carried out for four circuit categories; (1) CCM Zeta converter with VMC, (2) DCM Zeta converter with VMC, (3) CCM Zeta converter with PCMC, and (4) DCM Zeta converter with PCMC, to meet the design objective which is to achieve a crossover frequency of 10 KHz and phase of more than 45 degrees. To evaluate the performance of the designed feedback compensators, the Zeta converter in category (1) has been comprehensively simulated for the step load change and start-up transient using the developed SIMULINK model (Fig. 6.1). The results show that the converter is capable of good output regulation when subjecting to these disturbances. Similar results were obtained for the Zeta converter in categories (2), (3), and (4). Finally, the prototype Zeta converter in category (1) was built and tested for output regulation and step load change. It was revealed that the converter possesses tight output voltage regulation (TABLE 6.1) and fast response to a step load change (Fig. 6.17), as predicted by simulation.

References

[1] R. D. Middlebook and S. Cuk, "A General Unified Approach to Modeling Switching-Converter Power Stages," *International Journal of Electronics*, vol. 42, pp. 521-550, June 1977.

[2] S. Cuk and R. D. Middlebrook, "A general unified approach to modeling switching DC-to-DC converters in discontinuous conduction mode," in *Proc. of IEEE PESC'77*, 1977.

[3] L. G. De Vicuna, F. Guinjoan, J. Majo, and L. Martinez, "Discontinuous conduction mode in the SEPIC converter," *Proc. of Electrotechnical Conference on Integrating Research, Industry and Education in Energy and Communication Engineering*, page. 38-42, April 1989.

[4] Vuthchhay E. and Bunlaksananusorn C., "Dynamic Modeling of a Zeta converter with State-Space Averaging Technique," *5th International Conference on Electrical Engineering/Electronics, Computer, Telecommunications and Information Technology 2008 (ECTI-CON 2008)*, May 2008.

[5] Vuthchhay E., Bunlaksananusorn C., and H. Hirata "Dynamic Modeling and Control of a Zeta Converter," *International Symposium on Communications and Information Technologies 2008 (ISCIT 2008)*, Oct. 2008.

[6] E. Vuthchhay, V. Wutti, and C. Bunlaksananusorn, "Modeling of a SEPIC Converter for Feedback Control Design," *Proc. of 31st Electrical Engineering Conference*, Oct. 2008.

[7] Vuthchhay E., Unnat P., and Chanin B., "Modeling of a SEPIC Converter Operating in Continuous Conduction Mode," *6th International Conference on Electrical Engineering/Electronics, Computer, Telecommunications and Information Technology 2009 (ECTI-CON 2009)*, May 2009.

[8] Vuthchhay E. and Chanin B., "Modeling of a SEPIC Converter Operating in Discontinuous Conduction Mode," *6th International Conference on Electrical Engineering/Electronics, Computer, Telecommunications and Information Technology 2009 (ECTI-CON 2009)*, May 2009.

[9] N. Mohan, T. M. Undeland, and W. P. Robbins, *Power Electronics, Converter, Applications, and Design*, 3rd ed., John Wiley and Sons Inc, 2003.

[10] M. H. Rashid, *Power Electronics Handbook: Devices, Circuits, and Applications*, 2nd ed., Elsevier Inc, 2007.

[11] V. Vorperian, "Simplified analysis of PWM converters using model of PWM switch, Part I and Part II: Discontinuous conduction mode," *IEEE trans. on Aerosp. Electron. Syst.*, July 1990.

[12] V. Vorperian, *Fast Analytical Techniques for Electrical and Electronics Circuits*, Cambridge University Press, 2004.

[13] V. Vorpérian, "The Effect of the Magnetizing Inductance on the Small-Signal Dynamics of the Isolated Cuk Converter," *IEEE trans. on aerospace and electronic systems*, July 1996.

[14] V. Vorpérian, "Analysis of the Sepic Converter by Dr. Vatché Vorpérian," *Ridley Engineering Inc*, www.switchingpowermagazine.com, 2006.

[15] R. Ridley, "Analyzing the Sepic Converter," *Power Systems Design Europe Magazine*, pp. 14-18, November 2006.

[16] E. Niculescu, M. C. Niculescu, and D. M. Purcaru, "Modelling the PWM SEPIC converter in discontinuous conduction mode," *Proc. of the 11th WSEAS International Conference on Circuits*, July 2007.

[17] E. Niculescu, M. C. Niculescu, and D. M. Purcaru, " Modelling the PWM Zeta converter in discontinuous conduction mode," *MELECON 2008, Electrotechnical Conference of The 14th IEEE Mediterranean*, May 2008.

[18] R. W. Erickson and D. Maksimovic, *Fundamentals of Power Electronics*, 2nd ed., Kluwer Academic Publishers, 2001.

[19] A. Hren and P. Slibar, "Full Order Dynamic Model of SEPIC Converter," *Proc. of the IEEE International Symposium on Industrial Electronics*, pp. 553-558, June 2005.

[20] Jian Sun, D. M. Mitchell, M. F. Greuel, P. T. Krein, and R. M. Bass, "Averaged modeling of PWM converters operating in discontinuous conduction mode," *IEEE trans. on Power Electronics*, July 2001.

[21] A. J. Forsyth and S. V. Mollov, "Modelling and Control of DC-DC converters," *IEEE Power Engineering Journal*, 1998.

[22] N. Mohan, *First Course on Power Electronics and Drives*, MNPERE, 2003.

[23] R. Ridley, "A new, continuous-time model for current-mode control," *IEEE trans. on Power Electronics*, 1991.

[24] D. W. Hart, *Introduction to Power Electronics*, Prentice Hall Inc, 1997.

[25] B. C. Kuo, *Automatic Control Systems*, 7rd ed., Prentice Hall Inc, 1995.

Appendices

Appendix A

Condition for Zeta Converter Operating in CCM

From Fig. A.1, the averaged inductor currents, I_{L1} and I_{L2}, must be greater than one-half of their ripple components, Δi_{L1} and Δi_{L2}, for the circuit to remain in CCM. The conditions for Zeta converter operating in CCM [24] are:

$$I_{L1} > \frac{\Delta i_{L1}}{2} \tag{A.1-a}$$

$$I_{L2} > \frac{\Delta i_{L2}}{2} \tag{A.1-b}$$

From (2.2.2-1) and (2.2.2-4), we have:

$$\frac{di_{L1}}{dt} = \frac{V_g - r_{L1} i_{L1}}{L_1} \tag{A.2-a}$$

$$I_{L1} = \frac{D^2 V_g}{(1-D)^2 (R + r_{L2}) + r_{L1} D^2 + r_{C1} D(1-D)} \tag{A.2-b}$$

In CCM, with a small-ripple approximation (steady-state operation) [18], equation (A.2-a) yields:

$$\Delta i_{L1} \approx DT \frac{V_g - r_{L1} I_{L1}}{L_1} \tag{A.3}$$

Substitution of (A.3) into (A.1-a) gives:

$$I_{L1} > \frac{DT}{2L_1}(V_g - r_{L1} I_{L1}) \tag{A.4-a}$$

$$\Rightarrow I_{L1}\left(1 + \frac{DTr_{L1}}{2L_1}\right) > \frac{DT}{2L_1} V_g \tag{A.4-b}$$

(A.2-b) and (A.4-b) yields:

$$\frac{D^2 V_g}{(1-D)^2 (R + r_{L2}) + r_{L1} D^2 + r_{C1} D(1-D)} \left(1 + \frac{DTr_{L1}}{2L_1}\right) > \frac{DT}{2L_1} V_g \tag{A.5-a}$$

$$\Rightarrow D + \frac{D^2 T r_{L1}}{2L_1} > \frac{T}{2L_1}[(1-D)^2 (R + r_{L2}) + r_{L1} D^2 + r_{C1} D(1-D)] \tag{A.5-b}$$

$$\Rightarrow D > \frac{T}{2L_1}(1-D)[(1-D)(R + r_{L2}) + r_{C1} D] \tag{A.5-c}$$

$$\Rightarrow D > \frac{RT}{2L_1}(1-D)^2 \left(1 + \frac{r_{L2}}{R} + \frac{r_{C1}}{R}\frac{D}{1-D}\right) \tag{A.5-d}$$

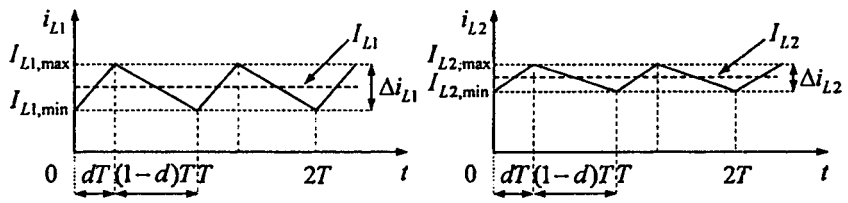

(a) i_{L1} waveform. (b) i_{L2} waveform.

Fig. A.1. Inductor currents' waveforms.

$$\Rightarrow \frac{2L_1}{RT} > \frac{(1-D)^2}{D}\left(1+\frac{r_{L2}}{R}+\frac{r_{C1}}{R}\frac{D}{1-D}\right) \quad \text{(A.5-e)}$$

$$\Rightarrow L_1 > \frac{(1-D)^2 R}{2Df}\left(1+\frac{r_{L2}}{R}+\frac{r_{C1}}{R}\frac{D}{1-D}\right) \quad \text{(A.5-f)}$$

$$\Rightarrow L_1 > L_{1,\min} \quad \text{(A.5-g)}$$

where $L_{1,\min} = \frac{(1-D)^2 R}{2Df}\left(1+\frac{r_{L2}}{R}+\frac{r_{C1}}{R}\frac{D}{1-D}\right)$.

From (2.2.2-1) and (2.2.2-4), we can write:

$$\frac{di_{L2}}{dt} = L_2\left[v_g + v_{C1} - \frac{Rv_{C2}}{R+r_{C2}} - i_{L2}\left(r_{L2}+r_{C1}+\frac{Rr_{C2}}{R+r_{C2}}\right)\right] \quad \text{(A.6-a)}$$

$$I_{L2} = \frac{D(1-D)V_g}{(1-D)^2(R+r_{L2})+r_{L1}D^2+r_{C1}D(1-D)} \quad \text{(A.6-b)}$$

$$V_{C1} = \frac{D[(1-D)(r_{L2}+R)-Dr_{L1}]V_g}{(1-D)^2(R+r_{L2})+r_{L1}D^2+r_{C1}D(1-D)} \quad \text{(A.6-c)}$$

$$V_{C2} = \frac{RD(1-D)V_g}{(1-D)^2(R+r_{L2})+r_{L1}D^2+r_{C1}D(1-D)} \quad \text{(A.6-d)}$$

In CCM, with a small-ripple approximation (steady-state operation) [18], (A.6-a) yields:

$$\Delta i_{L2} \approx \frac{DT}{L_2}\left[V_g + V_{C1} - V_{C2}\frac{R}{R+r_{C2}} - I_{L2}\left(r_{L2}+r_{C1}+\frac{r_{C2}R}{r_{C2}+R}\right)\right] \quad \text{(A.7)}$$

From (A.6-c) and (A.6-d), we can define:

$$V_{C1} - V_{C2}\frac{R}{R+r_{C2}} = \frac{DV_g\left[(1-D)(r_{L2}+R)-Dr_{L1}-\frac{R^2(1-D)}{R+r_{C2}}\right]}{(1-D)^2(R+r_{L2})+r_{L1}D^2+r_{C1}D(1-D)} \quad \text{(A.8)}$$

Substituting (A.7), (A.8), and (A.6-b) into (A.1-b) gives:

$$I_{L2} > \frac{DT}{2L_2}\left[V_g + V_{C1} - V_{C2}\frac{R}{R+r_{C2}} - I_{L2}\left(r_{L2}+r_{C1}+\frac{r_{C2}R}{r_{C2}+R}\right)\right] \quad \text{(A.9-a)}$$

$$\Rightarrow I_{L2}\left[1+\frac{DT}{2L_2}\left(r_{L2}+r_{C1}+\frac{r_{C2}R}{r_{C2}+R}\right)\right] > \frac{DT}{2L_2}\left[V_g + \frac{DV_g\left[(1-D)(r_{L2}+R)-Dr_{L1}-\frac{R^2(1-D)}{R+r_{C2}}\right]}{(1-D)^2(R+r_{L2})+r_{L1}D^2+r_{C1}D(1-D)}\right] \quad \text{(A.9-b)}$$

$$\Rightarrow \frac{D(1-D)V_g}{(1-D)^2(R+r_{L2})+r_{L1}D^2+r_{C1}D(1-D)}\left[1+\frac{DT}{2L_2}\left(r_{L2}+r_{C1}+\frac{r_{C2}R}{r_{C2}+R}\right)\right] > \quad \text{(A.9-c)}$$

$$\frac{DT}{2L_2}\left[V_g + \frac{DV_g\left[(1-D)(r_{L2}+R)-Dr_{L1}-\frac{R^2(1-D)}{R+r_{C2}}\right]}{(1-D)^2(R+r_{L2})+r_{L1}D^2+r_{C1}D(1-D)}\right]$$

$$\Rightarrow (1-D)\left[1+\frac{DT}{2L_2}\left(r_{L2}+r_{C1}+\frac{r_{C2}R}{r_{C2}+R}\right)\right] > \quad \text{(A.9-d)}$$

$$\frac{T}{2L_2}\left[(1-D)^2(R+r_{L2})+r_{L1}D^2+r_{C1}D(1-D)+D\left[(1-D)(r_{L2}+R)-Dr_{L1}-\frac{R^2(1-D)}{R+r_{C2}}\right]\right]$$

$$\Rightarrow 1-D > \frac{T}{2L_2}\left[(1-D)^2(R+r_{L2})+r_{L1}D^2+r_{C1}D(1-D)+D\left[(1-D)(r_{L2}+R)-Dr_{L1}\right.\right. \quad \text{(A.9-e)}$$

$$\left.\left.-\frac{R^2(1-D)}{R+r_{C2}}\right]-D(1-D)\left(r_{L2}+r_{C1}+\frac{r_{C2}R}{r_{C2}+R}\right)\right]$$

$$\Rightarrow 1-D > \frac{T}{2L_2}\left[(1-D)^2(R+r_{L2})+r_{C1}D(1-D)+D(1-D)(r_{L2}+R)-\frac{R^2D(1-D)}{R+r_{C2}}\right. \quad \text{(A.9-f)}$$

$$\left.-D(1-D)(r_{L2}+r_{C1})-D(1-D)\frac{r_{C2}R}{r_{C2}+R}\right]$$

$$\Rightarrow 1-D>\frac{T}{2L_2}[(1-D)^2(R+r_{L2})+D(1-D)(r_{L2}+R)-D(1-D)(r_{L2}+R)] \quad \text{(A.9-g)}$$

$$\Rightarrow 1-D>\frac{T}{2L_2}(1-D)^2(R+r_{L2}) \quad \text{(A.9-h)}$$

$$\Rightarrow L_2>\frac{(1-D)R}{2f}(1+\frac{r_{L2}}{R}) \quad \text{(A.9-i)}$$

$$L_2>L_{2,\min} \quad \text{(A.9-j)}$$

where $L_{2,\min}=\frac{(1-D)R}{2f}(1+\frac{r_{L2}}{R})$.

In short, for CCM operation L_1 and L_2 must satisfy the following conditions:

$$\begin{cases} L_1>\frac{(1-D)^2R}{2Df}(1+\frac{r_{L2}}{R}+\frac{r_{C1}}{R}\frac{D}{1-D}) \\ L_2>\frac{(1-D)R}{2f}(1+\frac{r_{L2}}{R}) \end{cases} \quad \text{(A.10)}$$

Appendix B

State-Space Equations of CCM Zeta Converter

I. State-Space Equations of Zeta converter

I.1 State-Space Equations of Zeta converter for time interval *dT*

Fig. B.1 shows Zeta converter for time interval *dT*, from which apply KVL and KCL; hence, we can define:

$$v_g - L_1\frac{di_{L1}}{dt} - r_{L1}i_{L1} = 0 \qquad \text{(B.I.1-1-a)}$$

$$\Rightarrow \frac{di_{L1}}{dt} = \frac{v_g}{L_1} - \frac{r_{L1}}{L_1}i_{L1} \qquad \text{(B.I.1-1-b)}$$

$$L_2\frac{di_{L2}}{dt} = -i_{L2}r_{L2} - v_{C2} - r_{C2}i_{C2} + v_g + v_{C1} + r_{C1}i_{C1} \qquad \text{(B.I.1-2)}$$

$$i_{C1} = -i_{L2} = -C_1\frac{dv_{C1}}{dt} \qquad \text{(B.I.1-3-a)}$$

$$\Rightarrow \frac{dv_{C1}}{dt} = -\frac{i_{L2}}{C_1} \qquad \text{(B.I.1-3-b)}$$

$$i_{C2} = i_{L2} - i_z - \frac{v_O}{R} = i_{L2} - i_z - \frac{v_{C2} + r_{C2}i_{C2}}{R} \qquad \text{(B.I.1-4-a)}$$

$$\Rightarrow i_{C2} = \frac{R}{R+r_{C2}}i_{L2} - \frac{R}{R+r_{C2}}i_z - \frac{1}{R+r_{C2}}v_{C2} = C_2\frac{dv_{C2}}{dt} \qquad \text{(B.I.1-4-b)}$$

$$\Rightarrow \frac{dv_{C2}}{dt} = \frac{R}{C_2(R+r_{C2})}i_{L2} - \frac{R}{C_2(R+r_{C2})}i_z - \frac{1}{C_2(R+r_{C2})}v_{C2} \qquad \text{(B.I.1-4-c)}$$

Substituting (B.I.1-4-b) into (B.I.1-2) yields:

$$L_2\frac{di_{L2}}{dt} = -i_{L2}r_{L2} - v_{C2} - r_{C2}\left(\frac{Ri_{L2}}{R+r_{C2}} - \frac{Ri_z}{R+r_{C2}} - \frac{v_{C2}}{R+r_{C2}}\right) + v_g + v_{C1} - r_{C1}i_{L2} \qquad \text{(B.I.1-5-a)}$$

$$\Rightarrow \frac{di_{L2}}{dt} = -\frac{i_{L2}}{L_2}\left(r_{L2} + r_{C1} + \frac{Rr_{C2}}{R+r_{C2}}\right) - \frac{Rv_{C2}}{L_2(R+r_{C2})} + \frac{Rr_{C2}i_z}{L_2(R+r_{C2})} + \frac{v_g}{L_2} + \frac{v_{C1}}{L_2} \qquad \text{(B.I.1-5-b)}$$

$$v_o = v_{C2} + r_{C2}i_{C2} \qquad \text{(B.I.1-6-a)}$$

Substituting (B.I.1-4-b) into (B.I.1-6-a) gives:

$$\Rightarrow v_o = v_{C2} + r_{C2}\left(\frac{R}{R+r_{C2}}i_{L2} - \frac{R}{R+r_{C2}}i_z - \frac{1}{R+r_{C2}}v_{C2}\right) \qquad \text{(B.I.1-6-b)}$$

$$\Rightarrow v_o = v_{C2}\frac{R}{R+r_{C2}} + \frac{Rr_{C2}}{R+r_{C2}}i_{L2} - \frac{Rr_{C2}}{R+r_{C2}}i_z \qquad \text{(B.I.1-6-c)}$$

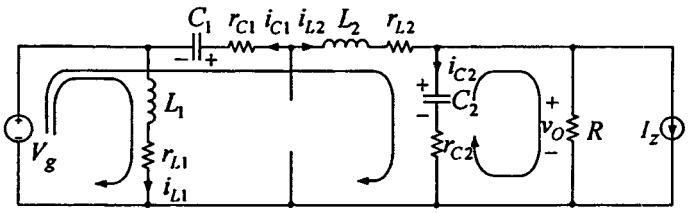

Fig. B.1. Zeta converter for time interval *dT*.

Reorganize (B.I.1-1-b), (B.I.1-5-b), (B.I.1-3-b), (B.I.1-4-c), and (B.I.1-6-c) into a matrix form; then, we obtain the state-space equation for this switch-on position below:

$$\begin{cases} \dfrac{d}{dt}\begin{bmatrix} i_{L1} \\ i_{L2} \\ v_{C1} \\ v_{C2} \end{bmatrix} = \begin{bmatrix} -\dfrac{r_{L1}}{L_1} & 0 & 0 & 0 \\ 0 & \dfrac{-1}{L_2}(r_{L2}+r_{C1}+\dfrac{r_{C2}R}{r_{C2}+R}) & \dfrac{1}{L_2} & \dfrac{-R}{L_2(r_{C2}+R)} \\ 0 & -\dfrac{1}{C_1} & 0 & 0 \\ 0 & \dfrac{R}{C_2(r_{C2}+R)} & 0 & \dfrac{-1}{C_2(r_{C2}+R)} \end{bmatrix}\begin{bmatrix} i_{L1} \\ i_{L2} \\ v_{C1} \\ v_{C2} \end{bmatrix} + \begin{bmatrix} \dfrac{1}{L_1} & 0 \\ \dfrac{1}{L_2} & \dfrac{r_{C2}R}{L_2(r_{C2}+R)} \\ 0 & 0 \\ 0 & \dfrac{-R}{C_2(r_{C2}+R)} \end{bmatrix}\begin{bmatrix} v_g \\ i_z \end{bmatrix} \\ v_O = \begin{bmatrix} 0 & \dfrac{r_{C2}R}{r_{C2}+R} & 0 & \dfrac{R}{r_{C2}+R} \end{bmatrix}\begin{bmatrix} i_{L1} \\ i_{L2} \\ v_{C1} \\ v_{C2} \end{bmatrix} + \begin{bmatrix} 0 & \dfrac{-r_{C2}R}{r_{C2}+R} \end{bmatrix}\begin{bmatrix} v_g \\ i_z \end{bmatrix} \end{cases} \quad \text{(B.I.1-7)}$$

I.2 State-Space Equations of Zeta converter for time interval (1-*d*)*T*

Fig. B.2 illustrates Zeta converter for time interval (1-*d*)*T*, from which apply KVL and KCL; hence, we can write:

$$L_1\frac{di_{L1}}{dt} = -r_{L1}i_{L1} - v_{C1} - r_{C1}i_{C1} \quad \text{(B.I.2-1-a)}$$

$$\Rightarrow \frac{di_{L1}}{dt} = -\frac{r_{L1}+r_{C1}}{L_1}i_{L1} - \frac{v_{C1}}{L_1} \quad \text{(B.I.2-1-b)}$$

$$L_2\frac{di_{L2}}{dt} = -r_{L2}i_{L2} - v_{C2} - r_{C2}i_{C2} \quad \text{(B.I.2-2)}$$

$$i_{C1} = i_{L1} = C_1\frac{dv_{C1}}{dt} \quad \text{(B.I.2-3-a)}$$

$$\Rightarrow \frac{dv_{C1}}{dt} = \frac{i_{L1}}{C_1} \quad \text{(B.I.2-3-b)}$$

$$i_{C2} = i_{L2} - i_z - \frac{v_O}{R} \quad \text{(B.I.2-4)}$$

$$v_O = v_{C2} + r_{C2}i_{C2} \quad \text{(B.I.2-5-a)}$$

$$\Rightarrow v_O = v_{C2} + r_{C2}(i_{L2} - i_z - \frac{v_O}{R}) \quad \text{(B.I.2-5-b)}$$

$$\Rightarrow v_O = \frac{R}{R+r_{C2}}v_{C2} + \frac{Rr_{C2}}{R+r_{C2}}i_{L2} - \frac{Rr_{C2}}{R+r_{C2}}i_z \quad \text{(B.I.2-5-c)}$$

Substitution of (B.I.2-5-c) into (B.I.2-4) yields:

$$i_{C2} = \frac{R}{R+r_{C2}}i_{L2} - \frac{R}{R+r_{C2}}i_z - \frac{1}{R+r_{C2}}v_{C2} = C_2\frac{dv_{C2}}{dt} \quad \text{(B.I.2-6-a)}$$

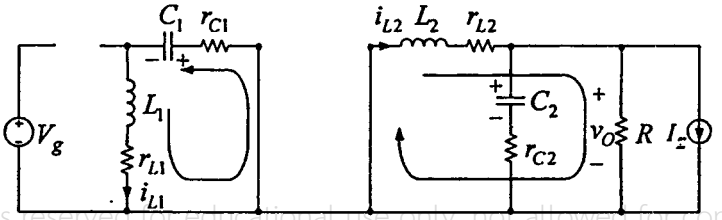

Fig. B.2. Zeta converter for time interval (1-*d*)*T*.

$$\Rightarrow \frac{dv_{C2}}{dt} = \frac{R}{C_2(R+r_{C2})} i_{L2} - \frac{R}{C_2(R+r_{C2})} i_z - \frac{1}{C_2(R+r_{C2})} v_{C2} \quad \text{(B.I.2-6-b)}$$

Substituting (B.I.2-6-a) into (B.I.2-2) produces:

$$L_2 \frac{di_{L2}}{dt} = -r_{L2} i_{L2} - v_{C2} - r_{C2}\left(\frac{R}{R+r_{C2}} i_{L2} - \frac{R}{R+r_{C2}} i_z - \frac{1}{R+r_{C2}} v_{C2}\right) \quad \text{(B.I.2-7-a)}$$

$$\Rightarrow \frac{di_{L2}}{dt} = -\frac{1}{L_2}\left(r_{L2} + \frac{Rr_{C2}}{R+r_{C2}}\right) i_{L2} - \frac{R}{L_2(R+r_{C2})} v_{C2} + \frac{Rr_{C2}}{L_2(R+r_{C2})} i_z \quad \text{(B.I.2-7-b)}$$

From (B.I.2-1-b), (B.I.2-3-b), (B.I.2-5-c), (B.I.2-6-b), and (B.I.2-7-b), we can define a state-space equation during a switch-on position.

$$\begin{cases} \dfrac{d}{dt}\begin{bmatrix} i_{L1} \\ i_{L2} \\ v_{C1} \\ v_{C2} \end{bmatrix} = \begin{bmatrix} -\dfrac{r_{L1}+r_{C1}}{L_1} & 0 & \dfrac{-1}{L_1} & 0 \\ 0 & \dfrac{-1}{L_2}\left(r_{L2} + \dfrac{r_{C2}R}{r_{C2}+R}\right) & 0 & \dfrac{-R}{L_2(r_{C2}+R)} \\ \dfrac{1}{C_1} & 0 & 0 & 0 \\ 0 & \dfrac{R}{C_2(r_{C2}+R)} & 0 & \dfrac{-1}{C_2(r_{C2}+R)} \end{bmatrix} \begin{bmatrix} i_{L1} \\ i_{L2} \\ v_{C1} \\ v_{C2} \end{bmatrix} + \begin{bmatrix} 0 & 0 \\ 0 & \dfrac{r_{C2}R}{L_2(r_{C2}+R)} \\ 0 & 0 \\ 0 & \dfrac{-R}{C_2(r_{C2}+R)} \end{bmatrix} \begin{bmatrix} v_s \\ i_z \end{bmatrix} \\ v_o = \begin{bmatrix} 0 & \dfrac{r_{C2}R}{r_{C2}+R} & 0 & \dfrac{R}{r_{C2}+R} \end{bmatrix} \begin{bmatrix} i_{L1} \\ i_{L2} \\ v_{C1} \\ v_{C2} \end{bmatrix} + \begin{bmatrix} 0 & \dfrac{-r_{C2}R}{r_{C2}+R} \end{bmatrix} \begin{bmatrix} v_s \\ i_z \end{bmatrix} \end{cases} \quad \text{(B.I.2-8)}$$

Appendix C

State-Space Equations of DCM Zeta Converter

I. State-Space Equations of Zeta converter

I.1 State-Space Equations of Zeta converter for time interval d_1T

Fig. C.1 shows Zeta converter for time interval dT, from which recall state-space equation for this interval in (B.I.1-7) by neglecting r_{C1}, r_{C2}, r_{L1} and r_{L2}.

$$\begin{cases} \dfrac{d}{dt}\begin{bmatrix} i_{L1} \\ i_{L2} \\ v_{C1} \\ v_{C2} \end{bmatrix} = \begin{bmatrix} 0 & 0 & 0 & 0 \\ 0 & 0 & 1/L_2 & -1/L_2 \\ 0 & -1/C_1 & 0 & 0 \\ 0 & 1/C_2 & 0 & -1/(C_2R) \end{bmatrix}\begin{bmatrix} i_{L1} \\ i_{L2} \\ v_{C1} \\ v_{C2} \end{bmatrix} + \begin{bmatrix} 1/L_1 \\ 1/L_2 \\ 0 \\ 0 \end{bmatrix}\begin{bmatrix} v_g \end{bmatrix} \\ v_o = \begin{bmatrix} 0 & 0 & 0 & 1 \end{bmatrix}\begin{bmatrix} i_{L1} \\ i_{L2} \\ v_{C1} \\ v_{C2} \end{bmatrix} + \begin{bmatrix} 0 \end{bmatrix}\begin{bmatrix} v_g \end{bmatrix} \end{cases} \quad \text{(C.I.1-1)}$$

I.2 State-Space Equations of Zeta converter for time interval d_2T

Fig. C.2 depicts Zeta converter for time interval d_2T, from which repeat state-space equation for this interval in (B.I.2-8) by excluding r_{C1}, r_{C2}, r_{L1} and r_{L2}.

$$\begin{cases} \dfrac{d}{dt}\begin{bmatrix} i_{L1} \\ i_{L2} \\ v_{C1} \\ v_{C2} \end{bmatrix} = \begin{bmatrix} 0 & 0 & -1/L_1 & 0 \\ 0 & 0 & 0 & -1/L_2 \\ 1/C_1 & 0 & 0 & 0 \\ 0 & 1/C_2 & 0 & -1/(C_2R) \end{bmatrix}\begin{bmatrix} i_{L1} \\ i_{L2} \\ v_{C1} \\ v_{C2} \end{bmatrix} + \begin{bmatrix} 0 \\ 0 \\ 0 \\ 0 \end{bmatrix}\begin{bmatrix} v_g \end{bmatrix} \\ v_o = \begin{bmatrix} 0 & 0 & 0 & 1 \end{bmatrix}\begin{bmatrix} i_{L1} \\ i_{L2} \\ v_{C1} \\ v_{C2} \end{bmatrix} + \begin{bmatrix} 0 \end{bmatrix}\begin{bmatrix} v_g \end{bmatrix} \end{cases} \quad \text{(C.I.2-1)}$$

I.3 State-Space Equations of Zeta converter for time interval d_3T

Fig. C.3 illustrates Zeta converter for time interval d_3T, from which apply KVL and KCL; hence, we can write:

$$v_{C2} + L_2\frac{di_{L2}}{dt} - v_{C1} - L_1\frac{di_{L1}}{dt} = 0 \quad \text{(C.I.3-1)}$$

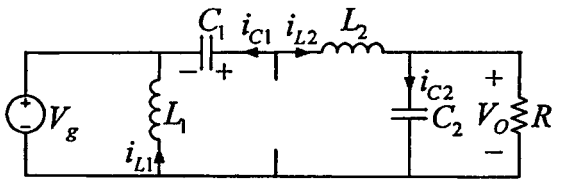

Fig. C.1. Zeta converter during the first state d_1T.

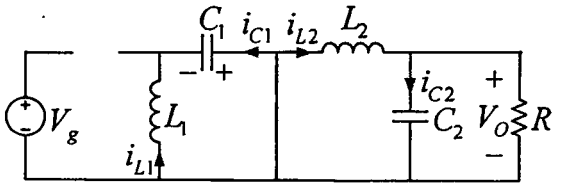

Fig. C.2. Zeta converter during the second state d_2T.

$$i_{C1} = i_{L1} = C_1 \frac{dv_{C1}}{dt} \tag{C.I.3-2-a}$$

$$\Rightarrow \frac{dv_{C1}}{dt} = \frac{i_{L1}}{C_1} \tag{C.I.3-2-b}$$

$$i_{C2} = i_{L2} - \frac{v_{C2}}{R} = C_2 \frac{dv_{C2}}{dt} \tag{C.I.3-3-a}$$

$$\Rightarrow \frac{dv_{C2}}{dt} = \frac{1}{C_2} i_{L2} - \frac{1}{C_2 r_{C2}} v_{C2} \tag{C.I.3-3-b}$$

$$i_{L1} = -i_{L2} \tag{C.I.3-4-a}$$

$$\Rightarrow \frac{di_{L1}}{dt} = -\frac{di_{L2}}{dt} \tag{C.I.3-4-b}$$

From (C.I.3-1) and (C.I.3-4-b), we can write:

$$(L_1 + L_2)\frac{di_{L1}}{dt} = v_{C2} - v_{C1} \tag{C.I.3-5-a}$$

$$\Rightarrow \frac{di_{L1}}{dt} = -\frac{1}{L_1 + L_2} v_{C1} + \frac{1}{L_1 + L_2} v_{C2} \tag{C.I.3-5-b}$$

Rearrange (C.I.3-2-b), (C.I.3-3-b), (C.I.3-4-b), and (C.I.3-5-b) in a matrix form; hence, the state-space equation for the third interval d_3T of the Zeta converter is given by:

$$\begin{cases} \dfrac{d}{dt}\begin{bmatrix} i_{L1} \\ i_{L2} \\ v_{C1} \\ v_{C2} \end{bmatrix} = \begin{bmatrix} 0 & 0 & -1/(L_1+L_2) & 1/(L_1+L_2) \\ 0 & 0 & 1/(L_1+L_2) & -1/(L_1+L_2) \\ 1/C_1 & 0 & 0 & 0 \\ 0 & 1/C_2 & 0 & -1/(C_2R) \end{bmatrix}\begin{bmatrix} i_{L1} \\ i_{L2} \\ v_{C1} \\ v_{C2} \end{bmatrix} + \begin{bmatrix} 0 \\ 0 \\ 0 \\ 0 \end{bmatrix}\begin{bmatrix} v_g \end{bmatrix} \\ v_O = \begin{bmatrix} 0 & 0 & 0 & 1 \end{bmatrix}\begin{bmatrix} i_{L1} \\ i_{L2} \\ v_{C1} \\ v_{C2} \end{bmatrix} + \begin{bmatrix} 0 \end{bmatrix}\begin{bmatrix} v_g \end{bmatrix} \end{cases} \tag{C.I.3-6}$$

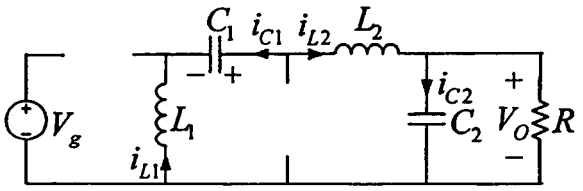

Fig. C.3. Zeta converter during the third state d_3T.

Appendix D

Routh-Hirwitz to Prove All Poles of CCM Zeta Converter Staying in the Left-Half Plane (LHP)

From TABLE 2.1, to facilitate the follow calculation, all parasitic components are supposed to be zero (r_{C1}=0, r_{C2}=0, r_{L1}=0, and r_{L2}=0), so we will obtain:

$$a = L_1C_1L_2C_2R \quad \text{(D-1-a)}$$

$$b = L_1C_1L_2 \quad \text{(D-1-b)}$$

$$c = (1-D)^2L_2C_2R+L_1C_2RD^2+ L_1C_1R \quad \text{(D-1-c)}$$

$$d = L_1 D^2+L_2(1-D)^2 \quad \text{(D-1-d)}$$

$$e = R(1-D)^2 \quad \text{(D-1-e)}$$

So Routh-Hirwitz is used to check the roots of (D-2) to know whether its roots stay on the Left-Half Plan (LHP) or not. The coefficients of (D-2) are first checked, and it can be found that from (D-1) all these coefficients of (D-2) are positive. Then, we go on to find the successive coefficients as follows.

$$as^4+bs^3+cs^2+ds+e = 0 \quad \text{(D-2)}$$

From (D-1), we can define:

$$bc=L_1C_1L_2[(1-D)^2L_2C_2R+L_1C_2RD^2+C_1L_1R] \quad \text{(D-3-a)}$$

$$ad=L_1C_1L_2C_2R[(1-D)^2L_2+L_1D^2] \quad \text{(D-3-b)}$$

$$\Rightarrow A=(bc-ad)/b=[L_1C_1L_2[(1-D)^2L_2RC_2+C_2RL_1D^2+C_1L_1R]-L_1C_1L_2C_2R[(1-D)^2L_2+L_1D^2]]/(L_1C_1L_2) \quad \text{(D-3-c)}$$

$$\Rightarrow A=C_1L_1R>0 \quad \text{(D-3-d)}$$

$$B=e=R(1-D)^2 \quad \text{(D-3-e)}$$

$$A_1=(Ad-Bb)/A=[C_1L_1R[(1-D)^2L_2+L_1D^2]-(1-D)^2RL_1C_1L_2]/(C_1L_1R)=L_1D^2>0 \quad \text{(D-3-f)}$$

$$A_2=A_1=L_1D^2>0 \quad \text{(D-3-g)}$$

From (D-3-e), (D-3-f), (D-3-g), and (D-3-h), these coefficients are positive, so from Routh-Hurwitz criterion, all the roots of (D-2) must stay only in LHP, as in shown TABLE D.

TABLE D

Coefficients of conditions for the LHP zeros.

a	c	e	0
b	d	0	0
$A=(bc-ad)/b$	$B=e$	$C=0$	
$A_1=(Ad-Bb)/A$	$B_1=0$	$C_1=0$	
$A_2=A_1$			

Appendix E

Current Model Control

I - Erickson Model: CCM

Fig. E.1 shows accurate determination of the relationship between the average inductor current $<R_S i(t)>_T$ and v_C [18]. In this figute, the summation of the inductor currents L_1 and L_2 is equal to a current $i(t)$. Therefore, Zeta converter gives:

$$\begin{cases} i_{L1}+i_{L2}=i_Q & ,0<t<dT \\ i_{L1}+i_{L2}=i_D & ,dT<t<T \end{cases} \tag{E-1}$$

$$R_S<i>_T=dR_S<i_L>_{dT}+d'R_S<i_L>_{d'T} \tag{E-2-a}$$

$$R_S<i>_T=(<v_C>_{dT}-\frac{m_a dT}{2}-d\frac{R_S m_1 dT}{2})+(<v_C>_{d'T}-\frac{m_a dT}{2}-d'\frac{R_S m_2 d'T}{2}) \tag{E-2-b}$$

$$R_S<i>_T=<v_C>_T-m_a dT-\frac{R_S m_1 d^2 T}{2}-\frac{R_S m_2 d'^2 T}{2} \tag{E-2-c}$$

A small-signal current mode control is found by perturbation and linearization of (E-2-c). Let $<i(t)>_T=I+\tilde{i}(t)$; $<v_C(t)>_T=V_C+\tilde{v}_C(t)$; $d(t)=D+\tilde{d}(t)$; $m_1(t)=M_1+\tilde{m}_1(t)$; $m_2(t)=M_2+\tilde{m}_2(t)$; $m_a=M_a$; $d'=1-d=1-D-\tilde{d}=D'-\tilde{d}$. Substitute these equations into (E-2-c), we can define:

$$R_S(I+\tilde{i})=(V_C+\tilde{v}_C)-m_a(D+\tilde{d})T-\frac{T}{2}R_S(M_1+\tilde{m}_1)(D+\tilde{d})^2-\frac{T}{2}R_S(M_2+\tilde{m}_2)(D'-\tilde{d})^2 \tag{E-3-a}$$

$$\begin{aligned}\Rightarrow R_S(I+\tilde{i})=&(V_C+\tilde{v}_C)-M_a(D+\tilde{d})T-\frac{T}{2}R_S(M_1+\tilde{m}_1)(D^2+2D\tilde{d}+\tilde{d}^2)\\&-\frac{T}{2}R_S(M_2+\tilde{m}_2)(D'^2-2D'\tilde{d}+\tilde{d}^2)\end{aligned} \tag{E-3-b}$$

From (E-3-b), we can separate DC terms from AC terms respectively, so we can get:

$$R_S I=V_C-M_a DT-\frac{T}{2}R_S(M_1D^2+M_2D'^2) \tag{E-4-a}$$

$$\Rightarrow R_S I=V_C-M_a DT-\frac{T}{2}R_S M_1 D \tag{E-4-b}$$

$$\begin{aligned}R_S\tilde{i}=&\tilde{v}_C-(M_aT+DM_1T-D'M_2T)\tilde{d}-\frac{T}{2}R_S D^2\tilde{m}_1-\frac{T}{2}R_S D'^2\tilde{m}_2-\frac{T}{2}R_S(M_1\tilde{d}^2+2D\tilde{m}_1\tilde{d}+\tilde{m}_1\tilde{d}^2)\\&-\frac{T}{2}R_S(M_2D'^2-2D'\tilde{m}_2\tilde{d}+\tilde{m}_2\tilde{d}^2)\end{aligned} \tag{E-5-a}$$

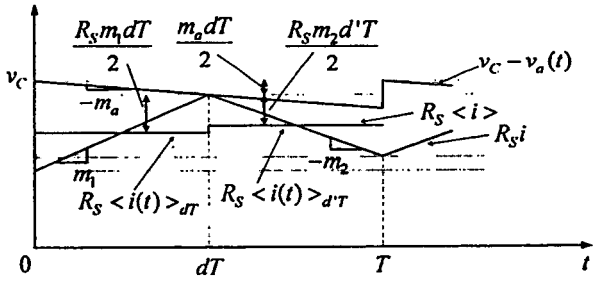

Fig. E.1. Accurate determination of the relationship between the average inductor current $<R_S i(t)>_T$ and v_C.

So the first-order AC terms are:

$$\Rightarrow R_S\tilde{i} = \tilde{v}_C - (M_a T + DM_1 T - D'M_2 T)\tilde{d} - \frac{T}{2}D^2 R_S\tilde{m}_1 - \frac{T}{2}D^2 R_S\tilde{m}_2 \quad \text{(E-5-b)}$$

$$\Rightarrow R_S\tilde{i} = \tilde{v}_C - M_a T\tilde{d} - \frac{TD^2 R_S}{2}\tilde{m}_1 - \frac{TD^2 R_S}{2}\tilde{m}_2 \quad \text{(E-5-c)}$$

where $DM_1 = D'M_2$.

$$\Rightarrow \tilde{d} = \frac{1}{M_a T}(\tilde{v}_C - R_S\tilde{i} - \frac{TD^2 R_S}{2}\tilde{m}_1 - \frac{TD^2 R_S}{2}\tilde{m}_2) \quad \text{(E-5-d)}$$

From (C.I.1-1) and (C.I.2-1), we have:

A- For the interval dT, we can write:

$$\frac{di_{L1}}{dt} = \frac{v_g}{L_1} = m_{L1,1} \quad \text{(E-6-a)}$$

$$\frac{di_{L2}}{dt} = -\frac{v_{C2}}{L_2} + \frac{v_g}{L_2} + \frac{v_{C1}}{L_2} = m_{L2,1} \quad \text{(E-6-b)}$$

$$\Rightarrow \frac{di_{L2}}{dt} = \frac{v_g}{L_2} = m_{L2,1} \quad \text{(E-6-c)}$$

where $v_{C1} \approx v_{C2}$.

$$\Rightarrow \tilde{m}_1 = \tilde{m}_{L1,1} + \tilde{m}_{L2,1} = \tilde{v}_g(\frac{1}{L_1} + \frac{1}{L_2}) = \tilde{v}_g\frac{1}{L_E} \quad \text{(E-6-d)}$$

B- For the interval $(1-d)T$, we can define:

$$\frac{di_{L1}}{dt} = -\frac{v_{C1}}{L_1} = -m_{L1,2} \quad \text{(E-7-a)}$$

$$\frac{di_{L2}}{dt} = -\frac{1}{L_2}v_{C2} = -m_{L2,2} \quad \text{(E-7-b)}$$

where $v_{C1} \approx v_{C2} \approx v_O$.

$$\Rightarrow -\tilde{m}_2 = -\tilde{m}_{L1,2} - \tilde{m}_{L2,2} = -(\frac{1}{L_1} + \frac{1}{L_2})\tilde{v}_O = -\frac{1}{L_E}\tilde{v}_O \quad \text{(E-7-c)}$$

Substituting (E-6-d) and (E-7-c) into (E-5-d) produces:

$$\tilde{d} = \frac{1}{M_a T}(\tilde{v}_C - R_S\tilde{i} - \frac{TD^2 R_S}{2L_E}\tilde{v}_g - \frac{TD^2 R_S}{2L_E}\tilde{v}_O) \quad \text{(E-8-a)}$$

$$\Rightarrow \tilde{d} = \frac{1}{M_a T}(\tilde{v}_C - R_S\tilde{i} - F_g\tilde{v}_g - F_v\tilde{v}_O) \quad \text{(E-8-b)}$$

where $F_g = \frac{TD^2 R_S}{2L_E}$ and $F_v = \frac{TD^2 R_S}{2L_E}$.

II - Ridley Model: CCM

Fig. E.2 illustrates current waveform and its slop compensation. To take the advantage of Ridley model, Zeta converter is first rearranged, as depicted in Fig. E.3, from which, we define $v_{on} = v_g$ and $v_{off} = -v_O$. Hence, we can write:

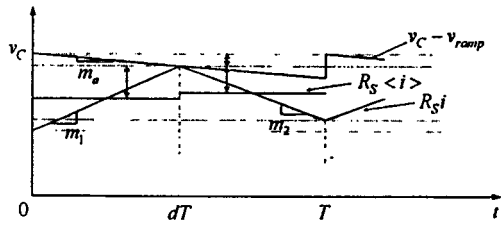

E.2. Current waveform and its slop compensation.

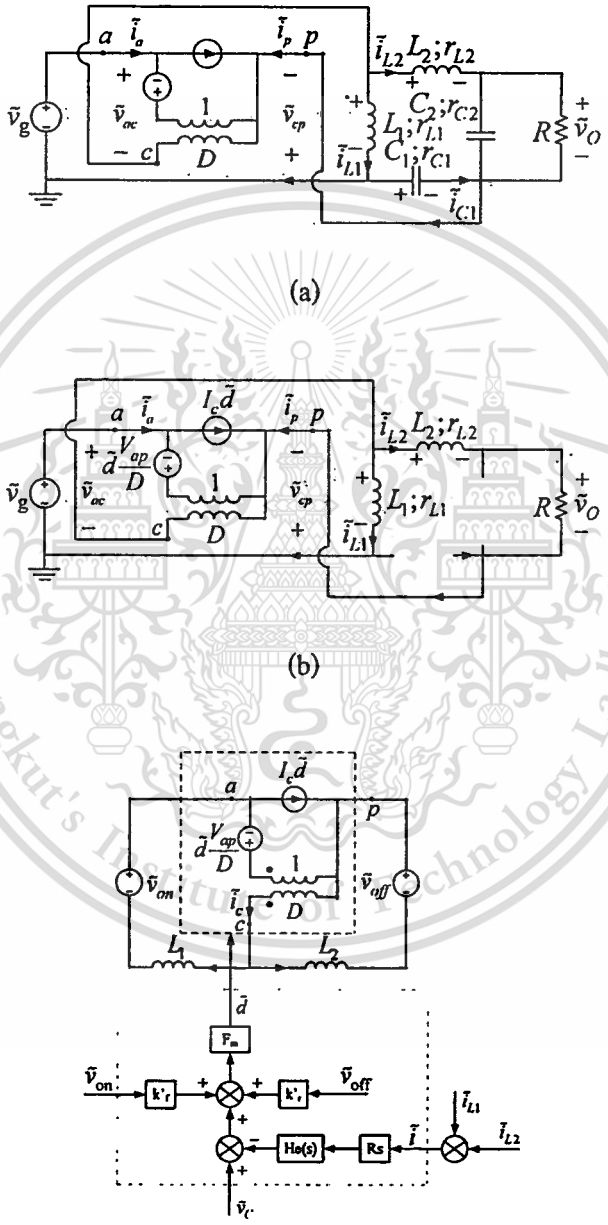

Fig. E.3. Simplified PWM-switch CCM Zeta converter for PCMC analysis.

$$R_s < i > = < v_C > - dTM_a - \frac{m_2 d'T}{2} \quad \text{(E-9)}$$

$$\Delta i = M_1 dT = M_2 d'T \quad \text{(E-10-a)}$$

where $M_1 = v_{on}R_S\left(\frac{1}{L_1}+\frac{1}{L_2}\right)=\frac{v_{on}R_S}{L_E}$, $M_2 = v_{off}R_S\left(\frac{1}{L_1}+\frac{1}{L_2}\right)=\frac{v_{off}R_S}{L_E}$, and $L_E=\frac{L_1L_2}{L_1+L_2}$.

$$\Rightarrow \frac{v_{on}R_S}{L_E}dT=\frac{v_{off}R_S}{L_E}d'T \quad \text{(E-10-b)}$$

$$\Rightarrow v_{on}d=v_{off}d' \quad \text{(E-10-c)}$$

$$\Rightarrow d=\frac{v_{off}}{v_{on}+v_{off}} \quad \text{(E-10-d)}$$

$$\Rightarrow d'=1-d=\frac{v_{on}}{v_{on}+v_{off}} \quad \text{(E-10-e)}$$

Substituting (E-10-d) and (E-10-e) into (E-9) yields:

$$R_S<i>=<v_C>-M_aT\frac{v_{off}}{v_{on}+v_{off}}-\frac{TR_S}{2L_E}\frac{v_{on}v_{off}}{v_{on}+v_{off}} \quad \text{(E-11)}$$

- Find k'_f (Fig. E.4):

$$R_S\frac{\partial<i>}{\partial v_{on}}=\frac{\partial<v_C>}{\partial v_{on}}-M_aT\frac{\partial}{\partial v_{on}}\left(\frac{v_{off}}{v_{on}+v_{off}}\right)-\frac{TR_S}{2L_E}\frac{\partial}{\partial v_{on}}\left(\frac{v_{on}v_{off}}{v_{on}+v_{off}}\right) \quad \text{(E-12-a)}$$

$$\Rightarrow R_S\frac{\partial<i>}{\partial v_{on}}=M_aT\frac{v_{off}}{(v_{on}+v_{off})^2}-\frac{TR_S}{2L_E}v_{off}\frac{v_{on}+v_{off}-v_{on}}{(v_{on}+v_{off})^2} \quad \text{(E-12-b)}$$

$$\Rightarrow R_S\frac{\partial<i>}{\partial v_{on}}=M_aT\frac{v_{off}}{(v_{on}+v_{off})^2}-\frac{TR_S}{2L_E}\frac{v_{off}^2}{(v_{on}+v_{off})^2} \quad \text{(E-12-c)}$$

$$\Rightarrow \frac{\partial<i>}{\partial v_{on}}=\frac{M_aT}{R_S}\frac{v_{off}}{v_{on}+v_{off}}\frac{1}{v_{on}+v_{off}}-\frac{T}{2L_E}\frac{v_{off}^2}{(v_{on}+v_{off})^2} \quad \text{(E-12-d)}$$

$$\Rightarrow \frac{<i>}{v_{on}}=\frac{M_aTD}{R_SV_{ap}}-\frac{TD^2}{2L_E} \quad \text{(E-12-e)}$$

where $d=\frac{v_{off}}{v_{on}+v_{off}}$ and $d'=\frac{v_{on}}{v_{on}+v_{off}}$.

From Fig. E.4, we have:

$$\tilde{d}=F_m(k'_f\tilde{v}_{on}-R_S<\tilde{i}>) \quad \text{(E-13-a)}$$

$$\tilde{v}_{cp}=D\tilde{v}_{ap}+V_{ap}\tilde{d} \quad \text{(E-13-b)}$$

In steady state, we can have $V_{L2}=0$, $V_{cp}=0$, and $\tilde{v}_{ap}=\tilde{v}_{on}$; hence, (E-13-b) will become:

$$\tilde{d}=\frac{-D\tilde{v}_{on}}{V_{ap}} \quad \text{(E-14)}$$

(E-13-a) and (E-14) yields:

$$d\frac{-D\tilde{v}_{on}}{V_{ap}}=F_m(k'_f\tilde{v}_{on}-R_S<\tilde{i}>) \quad \text{(E-15-a)}$$

$$\Rightarrow \frac{-D\tilde{v}_{on}}{V_{ap}}=F_mk'_f\tilde{v}_{on}-F_mR_S<\tilde{i}> \quad \text{(E-15-b)}$$

$$\Rightarrow \frac{<\tilde{i}>}{\tilde{v}_{on}}=\frac{1}{R_S}\left(k'_f+\frac{D}{F_mV_{ap}}\right) \quad \text{(E-15-c)}$$

Matching (E-12-e) and (E-15-c) produces:

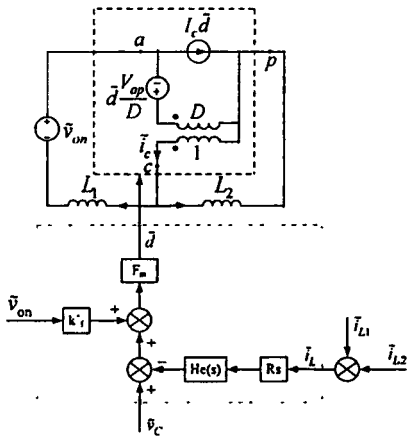

Fig. E.4. Simplification of Fig. E.3 for finding k'_f.

$$\frac{M_a TD}{R_S V_{ap}} - \frac{TD^2}{2L_E} = \frac{1}{R_S}\left(k'_f + \frac{D}{F_m V_{ap}}\right) \tag{E-16-a}$$

$$\Rightarrow k'_f = \frac{M_a TD}{V_{ap}} - \frac{TD^2 R_S}{2L_E} - \frac{D(M_1 + M_a)T}{V_{ap}} \tag{E-16-b}$$

$$\Rightarrow k'_f = -\frac{TD^2 R_S}{2L_E} - \frac{Dm_1 T}{V_{ap}} \tag{E-16-c}$$

$$\Rightarrow k'_f = -\frac{TD^2 R_S}{2L_E} - \frac{DT}{V_{ap}}\frac{D'V_{ap}R_S}{L_E} \tag{E-16-d}$$

where $m_1 = \dfrac{D'V_{ap}R_S}{L_E}$.

$$\Rightarrow k'_f = -\frac{DR_S T}{L_E}\left(\frac{D}{2} + D'\right) = -\frac{DR_S T}{L_E}\left(1 - \frac{D}{2}\right) \tag{E-16-e}$$

- Find k'_r (Fig. E5):

$$R_S \frac{\partial \langle i \rangle}{\partial v_{off}} = \frac{\partial \langle v_C \rangle}{\partial v_{off}} - M_a T \frac{\partial}{\partial v_{off}}\left(\frac{v_{off}}{v_{on} + v_{off}}\right) - \frac{TR_S}{2L_E}\frac{\partial}{\partial v_{off}}\left(\frac{v_{on}v_{off}}{v_{on} + v_{off}}\right) \tag{E-17-a}$$

$$\Rightarrow R_S \frac{\partial \langle i \rangle}{\partial v_{off}} = -M_a T \frac{v_{on} + v_{off} - v_{off}}{(v_{on} + v_{off})^2} - \frac{TR_S}{2L_E} v_{on} \frac{v_{on} + v_{off} - v_{off}}{(v_{on} + v_{off})^2} \tag{E-17-b}$$

$$\Rightarrow R_S \frac{\partial \langle i \rangle}{\partial v_{off}} = -M_a T \frac{v_{on}}{(v_{on} + v_{off})^2} - \frac{TR_S}{2L_E}\frac{v_{on}^2}{(v_{on} + v_{off})^2} \tag{E-17-c}$$

$$\Rightarrow \frac{\partial \langle i \rangle}{\partial v_{off}} = -\frac{M_a T}{R_S}\frac{v_{on}}{v_{on} + v_{off}}\frac{1}{v_{on} + v_{off}} - \frac{T}{2L_E}\frac{v_{on}^2}{(v_{on} + v_{off})^2} \tag{E-17-d}$$

$$\Rightarrow \frac{\langle i \rangle}{v_{off}} = -\frac{M_a T}{R_S}\frac{D'}{V_{ap}} - \frac{T}{2L_E}D'^2 \tag{E-17-e}$$

From Fig. E.5, we have:

$$\tilde{d} = F_m(k'_r \tilde{v}_{off} - R_S H_c(s)\langle \tilde{i}_{L1} + \tilde{i}_{L2} \rangle) \tag{E-18-a}$$

$$\tilde{v}_{cp} = D\tilde{v}_{ap} + V_{ap}\tilde{d} \tag{E-18-b}$$

In steady state: $V_{L2} = 0$, $\tilde{v}_{cp} = \tilde{v}_{ap} = \tilde{v}_{on}$, (E-18-b) can be defined as:

$$\tilde{d} = \frac{D'\tilde{v}_{off}}{V_{ap}} \tag{E-19}$$

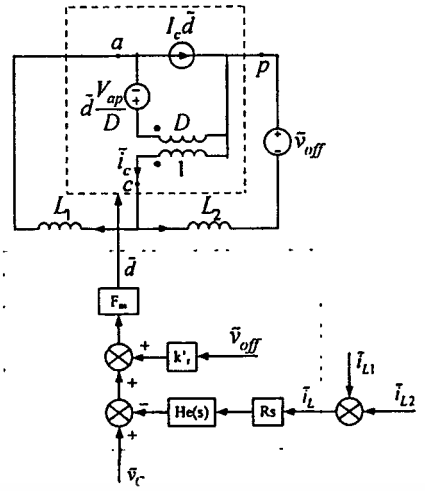

Fig. E.5. Simplification of Fig. 3 for finding k'_r.

Substitution of (E-19) into (E-18-a) yields:

$$\frac{D'\tilde{v}_{off}}{V_{ap}} = F_m(k'_r\tilde{v}_{off} - R_S<\tilde{i}>) \quad \text{(E-20-a)}$$

$$\Rightarrow \frac{D'\tilde{v}_{off}}{V_{ap}} = F_m k'_r\tilde{v}_{off} - F_m R_S<\tilde{i}> \quad \text{(E-20-b)}$$

$$\Rightarrow \frac{<\tilde{i}>}{\tilde{v}_{off}} = \frac{1}{R_S}\left(k'_r - \frac{D'}{V_{ap}F_m}\right) \quad \text{(E-20-c)}$$

Matching (E-17-e) with (E-20-c) gives:

$$-\frac{M_a T}{R_S}\frac{D'}{V_{ap}} - \frac{T}{2L_E}D'^2 = \frac{1}{R_S}\left(k'_r - \frac{D'}{V_{ap}F_m}\right) \quad \text{(E-21-a)}$$

$$\Rightarrow -\frac{M_a TD'}{V_{ap}} - \frac{TD'^2}{2L_E}R_S = k'_r - \frac{D'}{V_{ap}F_m} \quad \text{(E-21-b)}$$

$$\Rightarrow k'_r = -\frac{TD'^2 R_S}{2L_E} - \frac{M_a TD'}{V_{ap}} + \frac{D'(M_1 + M_a)T}{V_{ap}} \quad \text{(E-21-c)}$$

$$\Rightarrow k'_r = -\frac{TD'^2 R_S}{2L_E} + \frac{D'M_1 T}{V_{ap}} \quad \text{(E-21-d)}$$

$$\Rightarrow k'_r = -\frac{TD'^2 R_S}{2L_E} + \frac{D'T}{V_{ap}}\frac{D'V_{ap}R_S}{L_E} \quad \text{(E-21-e)}$$

Where $m_1 = \frac{D'V_{ap}R_S}{L_E}$.

$$\Rightarrow k'_r = -\frac{TD'^2 R_S}{2L_E} + \frac{D'^2 TR_S}{L_E} \quad \text{(E-21-f)}$$

$$\Rightarrow k'_r = \frac{D'^2 TR_S}{2L_E} \quad \text{(E-21-g)}$$

III- Ridley Model: DCM

Fig. E.6 illustrates typical slop compensation waveforms of the DCM DC-DC converter. In DCM operation, the fictitious inductor current, $\tilde{i}$, is zero at the beginning of each

switching period, and only the duty cycle, $\tilde{d}_1$, during the on time is required to function as control signal; that is, $\tilde{v}_{off}$ is neglected [23]. From Fig. E.6, we can hence define:

$$v_C = v_{pk} + m_a d_1 T \tag{E-22-a}$$

$$\Rightarrow v_C = (m_1 + m_a) d_1 T \tag{E-22-b}$$

$$\Rightarrow d_1 = \frac{v_C}{(m_1 + m_a)T} \tag{E-22-c}$$

From (E-22-c), the converter in DCM with a controlled on-time is given by:

$$d_1 = \frac{V_C}{(\frac{v_{on} R_S}{L_E} + M_a)T} \tag{E-22-d}$$

where $m_1 = \frac{v_{on} R_S}{L_E}$.

- Find k'_f:

The on-time slop, m_1, is a function of on-time voltage, inductor value, and current-sense gain value, R_S. The small-signal perturbation due to changes in on-time voltage can therefore be found by taking the partial derivative of equation (E-22-d) with respect to this voltage.

$$\frac{\partial d_1}{\partial v_{on}} = \frac{\partial}{\partial v_{on}} \left(\frac{V_c}{(\frac{v_{on} R_S}{L_E} + M_a)T} \right) \tag{E-23-a}$$

$$\Rightarrow \frac{\partial d_1}{\partial v_{on}} = \frac{V_c}{T} \left(\frac{-R_S}{L} \frac{1}{(\frac{v_{on} R_S}{L_E} + M_a)^2} \right) \tag{E-23-b}$$

$$\Rightarrow \frac{\partial d_1}{\partial v_{on}} = \frac{D_1 (M_1 + M_a) T}{T} \left(\frac{-R_S}{L_E} \frac{1}{(M_1 + M_a)^2} \right) \tag{E-23-c}$$

$$\Rightarrow \frac{d_1}{v_{on}} = \frac{-D_1 R_S}{L_E} \frac{1}{(M_1 + M_a)} \tag{E-23-d}$$

Fig. E.7. depicts Zeta converter's control structure for DCM PCMC, from which we can define:

$$\tilde{d}_1 = F_m k'_f \tilde{v}_{on} \tag{E-24-a}$$

$$\Rightarrow \frac{\tilde{d}_1}{\tilde{v}_{on}} = F_m k'_f \tag{E-24-b}$$

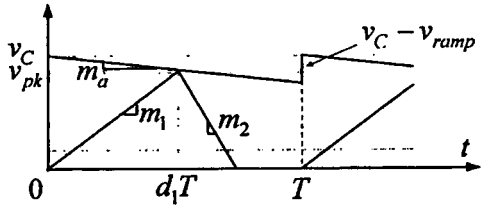

Fig. E.6. Slop compensation waveforms of the DCM DC-DC converter.

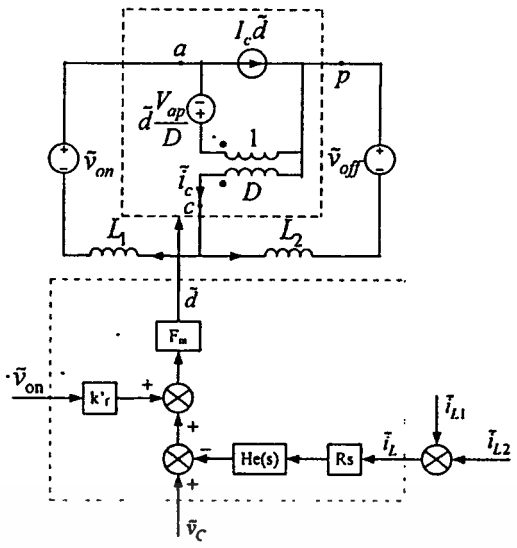

Fig. E.7. Zeta converter's control structure for PCMC in the DCM.

Matching (E-23-d) and (E-24-b) yields:

$$\frac{-D_1 R_S}{L_E}\frac{1}{(M_1+M_a)} = F_m k'_f \tag{E-25-a}$$

$$\Rightarrow k'_f = \frac{1}{F_m}\frac{-D_1 R_S}{L_E}\frac{1}{(M_1+M_a)} \tag{E-25-b}$$

$$\Rightarrow k'_f = \frac{\frac{1}{(M_1+M_a)T}}{\frac{-D_1 R_S}{L_E}\frac{1}{(M_1+M_a)}} \tag{E-25-c}$$

$$\Rightarrow k'_f = \frac{-D_1 R_S T}{L_E} \tag{E-25-d}$$

- Find k'$_r$:

$$\frac{\partial d_1}{\partial v_{off}} = \frac{\partial}{\partial v_{off}}\left(\frac{V_c}{(v_{on}R_S/L_E + M_a)T}\right) = 0 \tag{E-26}$$

$$\Rightarrow k'_r = 0 \tag{E-27}$$

Appendix F

```
%%%%%%%%%%%%%%%%%%%%%%%%%%%%%%%%%%%%%%%%%%%%%%%%%%%%%%%%%%%%%%%%%%%%%%%%%%%%%%%%
% Finding transfer functions of CCM Zeta converter with SSA technique %
%%%%%%%%%%%%%%%%%%%%%%%%%%%%%%%%%%%%%%%%%%%%%%%%%%%%%%%%%%%%%%%%%%%%%%%%%%%%%%%%
function[Gvil,Gvi2,Gdil,Gdi2,Gvv,Gzv,Gdv] = CCMZETASSA(rc1,rc2,rL1,rL2...
    ,C1,C2,L1,L2,R,D,Vg,Iz)
% CCMZETA program is used to find various transfer functions of
...CCM Zeta by SSA technique
% C1, C2, L1, and L2 are capacitors and inductors
% rc1, rc2, rL1, rL2 are ESRs of capacitors and inductors
% Vg is input voltage, Vo is output voltage, Iz is load current,
...D1 is duty ration, and R is a standing load
clc; clear all;
syms rc1 rc2 rL1 rL2 C1 C2 L1 L2 R D Vg Iz I1 I2 V1 V2 s
% The state-space matrices and average matrices
A1 = [-rL1/L1, 0, 0, 0
    0, (1/L2)*(-rL2-rc1-((rc2*R)/(rc2+R))), 1/L2, -R/(L2*(rc2+R))
    0, -1/C1, 0, 0
    0, R/(C2*(rc2+R)), 0, -1/(C2*(rc2+R))];
A2 = [-(rL1+rc1)/L1, 0, -1/L1, 0
    0, -(1/L2)*(rL2+(rc2*R/(rc2+R))), 0,-R/(L2*(rc2+R))
    1/C1, 0, 0, 0
    0, R/(C2*(rc2+R)), 0, -1/(C2*(rc2+R))];
A = A1*D + A2*(1-D);
B1 = [1/L1, 0
    1/L2, rc2*R/(L2*(rc2+R))
    0, 0
    0, -R/(C2*(rc2+R))];
B2 = [0, 0
    0, rc2*R/(L2*(rc2+R))
    0, 0
    0, -R/(C2*(rc2+R))];
B = B1*D + B2*(1-D);
C1 = [0, rc2*R/(rc2+R), 0, R/(rc2+R)];
C2 = [0, rc2*R/(rc2+R), 0, R/(rc2+R)];
C = C1*D + C2*(1-D);
E1 = [0, -rc2*R/(rc2+R)];
E2 = [0, -rc2*R/(rc2+R)];
E = E1*D + E2*(1-D);
% Steady-state equations
U = [Vg; Iz];
X = -inv(A)*B*U;                % where X=[I1; I2; V1; V2];
fprintf('Stead-state equations are: \n')
fprintf('[IL1, IL2, Vc1, Vc2]T = \n')
pretty(simplify(-inv(A)*B))
Vo = C*X+E*U;
fprintf('Vo=: \n')
pretty(simplify(Vo))
% Fiding matrix Bd and Ed
Bd = (A1-A2)*X + (B1-B2)*U;
Ed = (C1-C2)*X + (E1-E2)*U;
I  = eye(4,4);
Bu1=B(:,1); Bu2=B(:,2);
Eu1=E(:,1); Eu2=E(:,2);
C11=[1, 0, 0, 0]; C12=[0, 1, 0, 0]; C13=[0, 0, 1, 0]; C14=[0, 0, 0, 1];
% Various transfer functions
fprintf('Input-voltage-to-inductor-current-L1 transfer function is: \n')
fprintf('Gvil(s)=iL1(s)/vg(s)= \n')
Gvi1 = C11*inv(s*I-A)*Bu1;
simplify(Gvi1); collect(simplify(Gvi1)); pretty(collect(simplify(Gvi1)))
fprintf('Input-voltage-to-inductor-current-L2 transfer function: \n')
fprintf('Gvil(s)=iL2(s)/vg(s)= \n')
Gvi2 = C12*inv(s*I-A)*Bu1;
simplify(Gvi2); collect(simplify(Gvi2)); pretty(collect(simplify(Gvi2)))
Gvv1 = C13*inv(s*I-A)*Bu1;  % Gvv1(s)=vC1(s)/vg(s)
Gvv2 = C14*inv(s*I-A)*Bu1;  % Gvv2(s)=vC2(s)/vg(s)

Gzi1 = C11*inv(s*I-A)*Bu2;  % Gzi1(s)=iL1(s)/iz(s)
Gzi2 = C12*inv(s*I-A)*Bu2;  % Gzi2(s)=iL2(s)/iz(s)
Gzv1 = C13*inv(s*I-A)*Bu2;  % Gzv1(s)=vC1(s)/iz(s)
Gzv2 = C14*inv(s*I-A)*Bu2;  % Gzv2(s)=vC2(s)/iz(s)

fprintf('Duty ratio-to-inductor-current-L1 transfer function: \n')
fprintf('Gvil(s)=iL1(s)/d(s)= \n')
Gdi1 = C11*inv(s*I-A)*Bd;
```

```
simplify(Gdi1); collect(simplify(Gdi1)); pretty(collect(simplify(Gdi1)))
fprintf('Duty ratio-to-inductor-current-L2 transfer function: \n')
fprintf('Gvi2(s)=iL1(s)/d(s)= \n')
Gdi2 = C12*inv(s*I-A)*Bd;
simplify(Gdi2); collect(simplify(Gdi2)); pretty(collect(simplify(Gdi2)))
Gdv1 = C13*inv(s*I-A)*Bd;    % Gdv1(s)=vC1(s)/d(s)
Gdv2 = C14*inv(s*I-A)*Bd;    % Gdv2(s)=vC2(s)/d(s)

fprintf('Input-voltage-to-output-voltage transfer function: \n')
fprintf('Gvv(s)=vo(s)/vg(s)= \n')
Gvv = C*inv(s*I-A)*Bu1+Eu1;
simplify(Gvv); collect(simplify(Gvv)); pretty(collect(simplify(Gvv)))
fprintf('Output impedance transfer function: \n')
fprintf('Gzv(s)=vo(s)/iz(s)= \n')
Gzv = C*inv(s*I-A)*Bu2+Eu2;
simplify(Gzv); collect(simplify(Gzv)); pretty(collect(simplify(Gzv)))
fprintf('Duty-ratio-to-output-voltage transfer function: \n')
fprintf('Gdv(s)=vo(s)/d(s)= \n')
Gdv = C*inv(s*I-A)*Bd+Ed;
simplify(Gdv); collect(simplify(Gdv)); pretty(collect(simplify(Gdv)))
fprintf('Enjoy! \n')
fprintf('Good luck! \n')

%%%%%%%%%%%%%%%%%%%%%%%%%%%%%%%%%%%%%%%%%%%%%%%%%%%%%%%%%%%%%%%%%%%%%%%%%%%%%%%
% Finding transfer functions of DCM Zeta converter with SSA technique %
%%%%%%%%%%%%%%%%%%%%%%%%%%%%%%%%%%%%%%%%%%%%%%%%%%%%%%%%%%%%%%%%%%%%%%%%%%%%%%%
function[Gvv,Gd1v] = DCMZETASSA(C1,C2,L1,L2,R,D1,Vg)
% DCMZETASSA program is used to find various transfer functions of
...DCM Zeta by SSA technique
% C1, C2, L1, and L2 are capacitors and inductors
% Le=L1*L2/(L1+L2);
% T is a period, Vg is input voltage,
...D1 is duty ration, and R is a standing load
clc; clear all;
syms L1 L2 R C1 C2 D1 Vg s T Le
% The state-space matrices
Am = [0; 0, -1/(L1+L2), 1/(L1+L2)
    0, 0, 1/(L1+L2), -1/(L1+L2)
    1/C1, 0, -D1^2*T/(2*C1*L2), D1^2*T/(2*C1*L2)
    -1/C2, 0, D1*T/(2*C2*L2), (-1/C2)*(D1*T/(2*L2)+1/R)];
Bm = [0; 0; -D1^2*T/(2*C1*Le); D1*T/(2*C2*Le)];
Bd1 = [0; 0; -D1*Vg*T/(C1*Le); Vg*T/(2*C2*Le)];
Cm = [0, 0, 0, 1];
Em = [0];
Ed1 = [0];
I = eye(4,4);

fprintf('Input-voltage-to-output-voltage transfer function: \n')
fprintf('Gvv(s)=vo(s)/vg(s)= \n')
Gvv = Cm*inv(s*I-Am)*Bm+Em;
simplify(Gvv); collect(simplify(Gvv)); pretty(collect(simplify(Gvv)))
fprintf('Duty-ratio-to-output-voltage transfer function: \n')
fprintf('Gd1v(s)=vo(s)/d1(s)= \n')
Gd1v = Cm*inv(s*I-Am)*Bd1+Ed1;
simplify(Gd1v); collect(simplify(Gd1v)); pretty(collect(simplify(Gd1v)))
fprintf('Enjoy! \n')
fprintf('Good luck! \n')

%%%%%%%%%%%%%%%%%%%%%%%%%%%%%%%%%%%%%%%%%%%%%%%%%%%%%%%%%%%%%%%%%%%%%%%%%%%%%%%
% Finding transfer functions of DCM Zeta converter with PWM-switch model %
%%%%%%%%%%%%%%%%%%%%%%%%%%%%%%%%%%%%%%%%%%%%%%%%%%%%%%%%%%%%%%%%%%%%%%%%%%%%%%%
% DCMZETAPWM program is used to find various transfer functions of
...CCM Zeta by PWM-switch model
% C1, C2, L1, and L2 are capacitors and inductors
% rc1, rc2, rL1, rL2 are ESRs of capacitors and inductors
% Vg is input voltage, Vo is output voltage,
...D1 is duty ration, and R is a standing load
% where K=D2^2; M=D1/sqrt(K);
% gi=M^2/R; gf=2*M/R; go=1/R; ki=2*M^2*Vg/(R*D1); ko=2*M*Vg/(R*D1);
clc; clear all;
syms gi gf go ki ko s L1 L2 C1 C2 R A Vacd Aac Vcpd Acpg Aacg Aacd Acpd...
     rL1 rL2 rc1 rc2 A B Aacz Acpz

B = go+1/(s*L2+rL2)+(R*(s*C2*rc2+1)/((s*C2*(R+rc2)+1)...
    *(s*L2+rL2)))*(go+s*C1/(s*C1*rc1+1));
A = ((s*C1*rc1+1)/(s*C1))*(gi+(1/(s*L1+rL1))*(1+s*C1*(s*L1+rL1)/(s*C1*rc1+1)));
Aac = gi+gf+1/(s*L1+rL1)+(R*(s*C2*rc2+1)/((s*C2*(R+rc2)+1)...
    *(s*L2+rL2)))*(gf-s*C1/(s*C1*rc1+1))+B*A;
```

```
Aacg = 1/(s*L1+rL1)-(R*(s*C2*rc2+1)/((s*C2*(R+rc2)+1)...
    *(s*L2+rL2)))*(s*C1/(s*C1*rc1+1))+B*((s*C1*rc1+1)/...
    (s*C1*(s*L1+rL1)))*(1+s*C1*(s*L1+rL1)/(s*C1*rc1+1));
Aacd = ki+ko+R*(s*C2*rc2+1)*ko/((s*C2*(R+rc2)+1)*...
    (s*L2+rL2))+B*((s*C1*rc1+1)/(s*C1))*ki;
Aacz = R*(s*C2*rc2+1)/((s*C2*(R+rc2)+1)*(s*L2+rL2));
Acpg = ((s*C1*rc1+1)/(s*C1*(s*L1+rL1)))*(1+s*C1*(s*L1+rL1)...
    /(s*C1*rc1+1))-A*Aacg/Aac;
Acpd = A*Aacd/Aac-(s*C1*rc1+1)*ki/(s*C1);
Acpz = A*Aacz/Aac;

fprintf('Duty-ratio-to-output-voltage transfer function: \n')
fprintf('Gdlv(s)=vo(s)/dl(s)= \n')
%Gdv_dv = (R/(s*C2*(R+rc2)+1))*(ko-(gf-s*C1)*Aacd/Aac-(go+s*C1)*Acpd);
Gdlv = ((s*C2*rc2+1)*R/(s*C2*(R+rc2)+1))*(ko-(gf-s*C1/...
    (s*C1*rc1+1))*Aacd/Aac-(go+s*C1/(s*C1*rc1+1))*Acpd);
simplify(Gdlv); collect(simplify(Gdlv)); pretty(collect(simplify(Gdlv)))

Gvv = ((s*C2*rc2+1)*R/(s*C2*(R+rc2)+1))*((gf-s*C1*(s*C1*rc1+1))...
    *(Aacg/Aac)-(go+s*C1*(s*C1*rc1+1))*Acpg+s*C1*(s*C1*rc1+1));

Gzv = ((s*C2*rc2+1)*R/(s*C2*(R+rc2)+1))*((gf-s*C1/(s*C1*rc1+1))...
    *(Aacz/Aac)+(go+s*C1/(s*C1*rc1+1))*Acpz);
fprintf('Enjoy! \n')
fprintf('Good luck! \n')

%%%%%%%%%%%%%%%%%%%%%%%%%%%%%%%%%%%%%%%%%%%%%%%%%%%%%%%%%%%%%%%%%%%%%%%%%%%
% Finding transfer functions Gvc of CCM Zeta converter in PCMC %
%%%%%%%%%%%%%%%%%%%%%%%%%%%%%%%%%%%%%%%%%%%%%%%%%%%%%%%%%%%%%%%%%%%%%%%%%%%
function[Gvc] = PCMCCCMZETA(rc1,rc2,rL1,rL2...
    ,C1,C2,L1,L2,R,Rs,D,Vg,Iz)
% PCMCCCMZETA program is used to find Gvc of PCMC CCM Zeta
...from Erickson and Ridley model respectively.
% C1, C2, L1, and L2 are capacitors and inductors
% rc1, rc2, rL1, rL2 are ESRs of capacitors and inductors
% Vg is input voltage, Vo is output voltage, Iz is load current,
...D is duty ration, Rs is a sensing resistor
...He is a sampling equation, and P is a standing load.
clc; clear all;
syms rc1 rc2 rL1 rL2 L1 L2 R C1 C2 D Vg Iz I1 I2 V1 V2 s Fm Rs He
% The state-space matrices and average matrices
A1 = [-rL1/L1, 0, 0, 0
    0, (1/L2)*(-rL2-rc1-((rc2*R)/(rc2+R))), 1/L2, -R/(L2*(rc2+R))
    0, -1/C1, 0, 0
    0, R/(C2*(rc2+R)), 0, -1/(C2*(rc2+R))];
A2 = [-(rL1+rc1)/L1, 0, -1/L1, 0
    0, -(1/L2)*(rL2+(rc2*R/(rc2+R))), 0,-R/(L2*(rc2+R))
    1/C1, 0, 0, 0
    0, R/(C2*(rc2+R)), 0, -1/(C2*(rc2+R))];
A = A1*D + A2*(1-D);
B1 = [1/L1, 0
    1/L2, rc2*R/(L2*(rc2+R))
    0, 0
    0, -R/(C2*(rc2+R))];
B2 = [0, 0
    0, rc2*R/(L2*(rc2+R))
    0, 0
    0, -R/(C2*(rc2+R))];
B = B1*D + B2*(1-D);
C1 = [0, rc2*R/(rc2+R), 0, R/(rc2+R)];
C2 = [0, rc2*R/(rc2+R), 0, R/(rc2+R)];
C = C1*D + C2*(1-D);
E1 = [0, -rc2*R/(rc2+R)];
E2 = [0, -rc2*R/(rc2+R)];
E = E1*D + E2*(1-D);
% Steady-state equations
U = [Vg; Iz];
X = -inv(A)*B*U;                % where X=[I1; I2; V1; V2];
fprintf('Stead-state equations are: \n')
fprintf('[IL1, IL2, Vc1, Vc2]T = \n')
pretty(simplify(-inv(A)*B))
Vo = C*X+E*U;
fprintf('Vo=: \n')
pretty(simplify(Vo))
% Fiding matriz Bd and Ed
Bd = (A1-A2)*X + (B1-B2)*U;
Ed = (C1-C2)*X + (E1-E2)*U;
I  = eye(4,4);
Bu1=B(:,1); Bu2=B(:,2);
```

```
Eu1=E(:,1); Eu2=E(:,2);
C11=[1, 0, 0, 0]; C12=[0, 1, 0, 0]; C13=[0, 0, 1, 0]; C14=[0, 0, 0, 1];
% Various transfer functions
Gvi1 = C11*inv(s*I-A)*Bu1;
Gvi2 = C12*inv(s*I-A)*Bu1;
Gvv1 = C13*inv(s*I-A)*Bu1;
Gvv2 = C14*inv(s*I-A)*Bu1;

Gzi1 = C11*inv(s*I-A)*Bu2;
Gzi2 = C12*inv(s*I-A)*Bu2;
Gzv1 = C13*inv(s*I-A)*Bu2;
Gzv2 = C14*inv(s*I-A)*Bu2;

Gdi1 = C11*inv(s*I-A)*Bd;
Gdi2 = C12*inv(s*I-A)*Bd;
Gdv1 = C13*inv(s*I-A)*Bd;
Gdv2 = C14*inv(s*I-A)*Bd;

Gvv = C*inv(s*I-A)*Bu1+Eu1;
Gzv = C*inv(s*I-A)*Bu2+Eu2;
Gdv = C*inv(s*I-A)*Bd+Ed;

fprintf('Control-voltage-to-output-voltage transfer function: \n')
fprintf('Model from Erickson \n')
fprintf('Gvc(s)=vo(s)/vc(s)= \n')
Gvc = Gdv/(Rs*(Gdi1+Gdi2)); collect(simplify(Gvc)); pretty(collect(simplify(Gvc)))
fprintf('Model from Ridley \n')
fprintf('Gvc(s)=vo(s)/vc(s)= \n')
Gvc = (Fm*Gdv)/(1+Fm*Rs*He*(Gdi1+Gdi2));
simplify(Gvc); collect(simplify(Gvc)); pretty(collect(simplify(Gvc)))
fprintf('Enjoy! \n')
fprintf('Good luck! \n')
```

Appendix G

```
%%%%%%%%%%%%%%%%%%%%%%%%%%%%%%%%%%%%%%%%%%%%%%%%%%
% VMC of CCM Zeta converter with SSA technique %
%%%%%%%%%%%%%%%%%%%%%%%%%%%%%%%%%%%%%%%%%%%%%%%%%%
function[] = VMCCCMZETA1()
clc, clear all
disp('To run this proragame (VMCCCMZETA), please type:')
disp('VMCCCMZETA')

function[] = VMCCCMZETA()
% VMCCCMZETA program is used to show the results of
...VMC CCM Zeta by SSA technique
% C1, C2, L1, and L2 are capacitors and inductors
% rc1, rc2, rL1, rL2 are ESRs of capacitors and inductors
% Vg is input voltage, Vo is output voltage, Iz is load current,
...D1 is duty ration, and R is a standing load
clc; clear all;
C1=100*1e-6; rc1=0.19; C2=200*1e-6; rc2=0.095;
L1=100*1e-6; rL1=1*1e-3; L2=55*1e-6; rL2=0.55*1e-3;
Vg=15; Vo=5; D=Vo/(Vo+Vg); R=1; Iz=0;

% The state-space matrices and average matrices
A1 = [-rL1/L1, 0, 0, 0
    0, (1/L2)*(-rL2-rc1-((rc2*R)/(rc2+R))), 1/L2, -R/(L2*(rc2+R))
    0, -1/C1, 0, 0
    0, R/(C2*(rc2+R)), 0, -1/(C2*(rc2+R))];
A2 = [-(rL1+rc1)/L1, 0, -1/L1, 0
    0, -(1/L2)*(rL2+(rc2*R/(rc2+R))), 0,-R/(L2*(rc2+R))
    1/C1, 0, 0, 0
    0, R/(C2*(rc2+R)), 0, -1/(C2*(rc2+R))];
A = A1*D + A2*(1-D);
B1 = [1/L1, 0
    1/L2, rc2*R/(L2*(rc2+R))
    0, 0
    0, -R/(C2*(rc2+R))];
B2 = [0, 0
    0, rc2*R/(L2*(rc2+R))
    0, 0
    0, -R/(C2*(rc2+R))];
B = B1*D + B2*(1-D);
C1 = [0, rc2*R/(rc2+R), 0, R/(rc2+R)];
C2 = [0, rc2*R/(rc2+R), 0, R/(rc2+R)];
C = C1*D + C2*(1-D);
E1 = [0, -rc2*R/(rc2+R)];
E2 = [0, -rc2*R/(rc2+R)];
E = E1*D + E2*(1-D);
% Steady-state equations
U = [Vg; Iz];
X = -inv(A)*B*U;                    % where X=[I1; I2; V1; V2];
Vo = C*X+E*U;
% Fiding matrix Bd and Ed
Bd = (A1-A2)*X + (B1-B2)*U;
Ed = (C1-C2)*X + (E1-E2)*U;
I  = eye(4,4);
Bu1=B(:,1); Bu2=B(:,2);
Eu1=E(:,1); Eu2=E(:,2);
C11=[1, 0, 0, 0]; C12=[0, 1, 0, 0]; C13=[0, 0, 1, 0]; C14=[0, 0, 0, 1];
% Transfer functions
[numvi1, denvi1] = ss2tf(A,Bu1,C11,[0]);
Gvi1 = tf(numvi1,denvi1);
[numvi2, denvi2] = ss2tf(A,Bu1,C12,[0]);
Gvi2 = tf(numvi2,denvi2);
[numvv1, denvv1] = ss2tf(A,Bu1,C13,[0]);
Gvv1 = tf(numvv1,denvv1);
[numvv2, denvv2] = ss2tf(A,Bu1,C14,[0]);
Gvv2 = tf(numvv2,denvv2);

[numzi1, denzi1] = ss2tf(A,Bu2,C11,[0]);
Gzi1 = tf(numzi1,denzi1);
[numzi2, denzi2] = ss2tf(A,Bu2,C12,[0]);
Gzi2 = tf(numzi2,denzi2);
[numzv1, denzv1] = ss2tf(A,Bu2,C13,[0]);
Gzv1 = tf(numzv1,denzv1);
[numzv2, denzv2] = ss2tf(A,Bu2,C14,[0]);
Gzv2 = tf(numzv2,denzv2);
```

```
[numdi1, dendi1] = ss2tf(A,Bd,C11,[0]);
Gdi1 = tf(numdi1,dendi1);
[numdi2, dendi2] = ss2tf(A,Bd,C12,[0]);
Gdi2 = tf(numdi2,dendi2);
[numdv1, dendv1] = ss2tf(A,Bd,C13,[0]);
Gdv1 = tf(numdv1,dendv1);
[numdv2, dendv2] = ss2tf(A,Bd,C14,[0]);
Gdv2 = tf(numdv2,dendv2);
% Transfter funciton
[numv, denv] = ss2tf(A,Bu1,C,Eu1);
Gvv = tf(numv,denv);   %input voltage-to-output voltage transfer function
(Gvv(s)=vo(s)/vg(s))

[numz,denz] = ss2tf(A,Bu2,C,Eu2);
Gzv = tf(numz,denz);   %output impedance transfer function (Gzv(s)=vo(s)/iz(s))

[numd, dend] = ss2tf(A,Bd,C,Ed);
Gdv = tf(numd,dend);   %control-to-output transfer function (Gdv(s)=vo(s)/d(s))
%---------------------
% PWM transfer function
Vref=5; Vm=1.8;          %Vm=1.8 V
Fm = 1/Vm;               %Fm=D/Vc = 1/Vm;
% PI Compensator (PM=52.8 at about f=10kHz)
%Rise time=2*1e-5; setlling time=0.000156; peak magnitude=6.29 and overshoot=25.8%
R1=10*1e3; R2=3.4*1e3; Co1=20*1e-9;
wi=1/(R2*Co1); wz=1/(R1*Co1);
num=[1/wz1, 1]; den=[1/wi, 0]; Gc=tf(num,den);
% Voltage Mode Control (VMC) design
Tu=Gdv*Fm;       % Tu is uncompensated open-loop transfer function
T = Tu*Gc;       % T is compensated open-loop transfer function
Tv = feedback(T,[1]);   % Tv is clsoed-loop transfer function
% Frequency responses of Gc, Tu, and T
figure(1); bode(Gc,':r',Tu,'--g',T,'')
legend('Gc(s)','Tu(s)=Gdv(s).Fm','T(s)=Gdv(s).Fm.Gc(s)',-1);
Tv2=5*Tv;
% Step response of Vo
figure(2); step(Tv2)

%%%%%%%%%%%%%%%%%%%%%%%%%%%%%%%%%%%%%%%%%%%%%%%%%%%%%
% VMC of DCM Zeta converter with PWM-switch model %
%%%%%%%%%%%%%%%%%%%%%%%%%%%%%%%%%%%%%%%%%%%%%%%%%%%%%
function[] = VMCDCMZETAPWM1()
clc, clear all
disp('To run this proragame (VMCDCMZETAPWM), please type:')
disp('VMCDCMZETAPWM')

function[] = VMCDCMZETAPWM()
% VMCDCMZETAPWM program is used to denote the results of
...VMC DCM Zeta by PWM-switch model
% C1, C2, L1, and L2 are capacitors and inductors
% rc1, rc2, rL1, rL2 are ESRs of capacitors and inductors
% Vg is input voltage, Vo is output voltage,
...D1 and D2 are duty ratios, and R is a standing load
clc; clear all;
rc1=0.38; rc2=0.095; rL1=0.001; rL2=0.00022;
C1=47e-6; C2=200e-6; L1=100e-6; L2=22e-6; R=10; Vg=15;
fs=100*1e3; T=1/fs; Le=L1*L2/(L1+L2);
D1=0.2; D2=sqrt(2*Le/(R*T)); D3=1-D1-D2; Vo=Vg*D1/D2;
K=D2^2; M=D1/sqrt(K);
%M=D1/D2;
gi=M^2/R; gf=2*M/R; go=1/R; ki=2*M^2*Vg/(R*D1); ko=2*M*Vg/(R*D1);
adv = C1*L1*((-ko*gi+gf*ki)*rc1-ki-ko);
bdv = (C1*(-ko*rc1*gi-ki-ko+gf*rc1*ki))*rL1+gf*ki*L1-ko*C1*rc1-ko*gi*L1;
cdv = (-ko*gi+gf*ki)*rL1-ko;

a = C2*C1*L2*L1*(gf+go+go*rc1*gi+gi)*(rc2+R);
b = (C2*C1*L2*(gf+go+go*rc1*gi+gi)*(rc2+R))*rL1...
+(C2*C1*L1*(gf+go+go*rc1*gi+gi)*(rc2+R))*rL2+(C1*(go*L2*gi*L1...
+C2*R*gi*L1+go*C2*R*L2+go*C2*rc2*L2+C2*rc2*gi*L1+R*C2*rc2*go*gi*L1))*rc1...
+(C2*(C1*L2+R*go*C1*L1+C1*L1+go*L2*gi*L1+R*C1*gf*L1+R*C1*gi*L1))*rc2...
+gf*C1*L2*L1+gi*C1*L2*L1+go*L2*C1*L1+go*C2*R*L2*gi*L1+C2*R*C1*L1+C1*C2*R*L2;
c = ((C2*C1*(gf+go+go*rc1*gi+gi)*(rc2+R))*rL2+ (gi*C1*(C2*rc2+C2*R+go*L2...
+R*C2*rc2*go))*rc1+(C2*(R*C1*gi+go*L2*gi+C1+R*go*C1+R*C1*gf))*rc2...
+C1*C2*R+gi*C1*L2+gf*C1*L2+go*L2*C1+go*C2*R*L2*gi)*rL1...
+((go*C1*(gi*L1+C2*R+C2*rc2))*rc1+(C2*(go*gi*L1+C1))*rc2+gf*C1*L1+C1*C2*R...
+go*C2*R*gi*L1+gi*C1*L1+go*C1*L1)*rL2+(C1*(gi*L1+R*go*gi*L1+R*C2*rc2*go...
+C2*R+C2*rc2+go*L2))*rc1+(C2*(R*C1+gi*L1+go*L2+R*go*gi*L1))*rc2+go*L2*gi*L1...
+C1*L2+R*C1*gf*L1+R*C1*gi*L1+go*C2*R*L2+C1*L1+C2*R*gi*L1+R*go*C1*L1;
d = ((go*C2*rc2*gi+go*C1+go*C2*R*gi+go*C1*rc1*gi+gf*C1+gi*C1)*rL2+C1*rc1*gi...
```

```
+go*L2*gi+R*C2*rc2*go*gi+C1+R*C1*gf+R*go*C1+R*C1*gi+C2*rc2*gi+C2*R*gi...
+R*go*C1*rc1*gi)*rL1+(go*C2*rc2+go*C2*R+go*gi*L1+C1+go*C1*rc1)*rL2...
+(C1+R*go*C1)*rc1+C2*rc2+R*go*gi*L1+R*C2*rc2*go+C2*R+go*L2+R*C1+gi*L1;
e = (1+gi*rL1)*(R*go+1+go*rL2);
% Transfer functions
num1 = [C2*rc2, 1];
den1 = [0, 1];
Gdv1 = tf(num1,den1);
num2 = [adv, bdv, cdv];
den2 = [a, b, c, d, e];
Gdv2 = tf(num2,den2);
%Gdv = -R*Gdv1*Gdv2;
n = -R*conv(num1,num2);
d = conv(den1,den2);
Gdv = tf(n,d);
% VMC - Open-loop transfer function
Vref=5; Vm=1.8;          %Vm=1.8 V
Fm = 1/Vm;               %Fm=D/Vc = 1/Vm;
Tu=Gdv*Fm;
% One-zero-and-two-pole compensator
% PM=58.2
% Rise time=1.95*1e-5; setlling time=0.000228; peak magnitude=6.19 and
overshoot=23.7%
R1=0.12*1e3; R2=0.12*1e3; Co2=5*1e-9; Co1=44*1e-9;
wi=1/(R2*(Co1+Co2)); wz1=1/(R1*Co1); wp1=1/(R1*((Co1*Co2)/(Co1+Co2)));
n1=[0, 1]; d1=[1/wi, 0];
n2=[1/wz1, 1]; d2=[1/wp1, 1];
Gc1=tf(n1,d1);
Gc2=tf(n2,d2);
Gc=series(Gc1,Gc2);
% Closed-loop transfer function
T = Tu*Gc;
Tv = feedback(T,[1]);
figure(1); bode(Gc,'.:r',Tu,'.--g',T,'.-')
legend('Gc(s)','Tu(s)=Gdv(s).Fm','T(s)=Gdv(s).Fm.Gc(s)',-1);
Tv2=5*Tv;
figure(2); step(Tv2)

%%%%%%%%%%%%%%%%%%%%%%%%%%%%%
% PCMC of CCM Zeta converter %
%%%%%%%%%%%%%%%%%%%%%%%%%%%%%
function[] = PCMCCCMZETAERICKSON1()
clc, clear all
disp('To run this proragame (PCMCCCMZETAERICKSON), please type:')
disp('PCMCCCMZETAERICKSON')

function[] = PCMCCCMZETAERICKSON()
% PCMCCCMZETAERICKSON program is to show the results of PCMC CCM Zeta converter
...from Erickson model
% C1, C2, L1, and L2 are capacitors and inductors
% rc1, rc2, rL1, rL2 are ESRs of capacitors and inductors
% Vg is input voltage, Vo is output voltage,
...D1 is duty ratio, and R is a standing load
clc; clear all;
C1=100*1e-6; rc1=0.19; C2=200*1e-6; rc2=0.095;
L1=100*1e-6; rL1=1*1e-3; L2=55*1e-6; rL2=0.55*1e-3;
Vg=15; Vo=5; D=Vo/(Vo+Vg); R=1; Iz=0;
Le=L1*L2/(L1+L2); fs=100*1e3; Rs=0.1;       % Rs is a sensing resistor
% The state-space matrices and average matrices
A1 = [-rL1/L1, 0, 0, 0
    0, (1/L2)*(-rL2-rc1-((rc2*R)/(rc2+R))), 1/L2, -R/(L2*(rc2+R))
    0, -1/C1, 0, 0
    0, R/(C2*(rc2+R)), 0, -1/(C2*(rc2+R))];
A2 = [-(rL1+rc1)/L1, 0, -1/L1, 0
    0, -(1/L2)*(rL2+(rc2*R/(rc2+R))), 0,-R/(L2*(rc2+R))
    1/C1, 0, 0, 0
    0, R/(C2*(rc2+R)), 0, -1/(C2*(rc2+R))];
A = A1*D + A2*(1-D);
B1 = [1/L1, 0
    1/L2, rc2*R/(L2*(rc2+R))
    0, 0
    0, -R/(C2*(rc2+R))];
B2 = [0, 0
    0, rc2*R/(L2*(rc2+R))
    0, 0
    0, -R/(C2*(rc2+R))];
B = B1*D + B2*(1-D);
C1 = [0, rc2*R/(rc2+R), 0, R/(rc2+R)];
C2 = [0, rc2*R/(rc2+R), 0, R/(rc2+R)];
```

```
C = C1*D + C2*(1-D);
E1 = [0, -rc2*R/(rc2+R)];
E2 = [0, -rc2*R/(rc2+R)];
E = E1*D + E2*(1-D);
%-------------------------------------
U = [Vg; Iz];
%X  = [I1; I2; V1; V2];
X = -inv(A)*B*U;                % steady-state relations
%Vo = C*X+E*U ;                 % steady-state relations
%-------------------------------------
Bd = (A1-A2)*X + (B1-B2)*U;
Ed = (C1-C2)*X + (E1-E2)*U;
I  = eye(4,4);
Bu1=B(:,1); Bu2=B(:,2);
Eu1=E(:,1); Eu2=E(:,2);
C11=[1, 0, 0, 0]; C12=[0, 1, 0, 0]; C13=[0, 0, 1, 0]; C14=[0, 0, 0, 1];
% Transfer functions
[numvi1, denvi1] = ss2tf(A,Bu1,C11,[0]);
Gvi1 = tf(numvi1,denvi1);
[numvi2, denvi2] = ss2tf(A,Bu1,C12,[0]);
Gvi2 = tf(numvi2,denvi2);
[numvv1, denvv1] = ss2tf(A,Bu1,C13,[0]);
Gvv1 = tf(numvv1,denvv1);
[numvv2, denvv2] = ss2tf(A,Bu1,C14,[0]);
Gvv2 = tf(numvv2,denvv2);

[numzi1, denzi1] = ss2tf(A,Bu2,C11,[0]);
Gzi1 = tf(numzi1,denzi1);
[numzi2, denzi2] = ss2tf(A,Bu2,C12,[0]);
Gzi2 = tf(numzi2,denzi2);
[numzv1, denzv1] = ss2tf(A,Bu2,C13,[0]);
Gzv1 = tf(numzv1,denzv1);
[numzv2, denzv2] = ss2tf(A,Bu2,C14,[0]);
Gzv2 = tf(numzv2,denzv2);

[numdi1, dendi1] = ss2tf(A,Bd,C11,[0]);
Gdi1 = tf(numdi1,dendi1);
[numdi2, dendi2] = ss2tf(A,Bd,C12,[0]);
Gdi2 = tf(numdi2,dendi2);
[numdv1, dendv1] = ss2tf(A,Bd,C13,[0]);
Gdv1 = tf(numdv1,dendv1);
[numdv2, dendv2] = ss2tf(A,Bd,C14,[0]);
Gdv2 = tf(numdv2,dendv2);
% Transfter funciton
[numv, denv] = ss2tf(A,Bu1,C,Eu1);
Gvv = tf(numv,denv);   %input voltage-to-output voltage transfer function
(Gvv(s)=vo(s)/vg(s))

[numz,denz] = ss2tf(A,Bu2,C,Eu2);
Gzv = tf(numz,denz);   %output impedance transfer function (Gzv(s)=vo(s)/iz(s))

[numd, dend] = ss2tf(A,Bd,C,Ed);
Gdv = tf(numd,dend);   %control-to-output transfer function (Gdv(s)=vo(s)/d(s))
% Model from Erickson
Fm=1;
num_vc = numd;
den_vc = numdi1+numdi2;
Gvc_cpm = tf(num_vc,den_vc);
Gvc = (1/Rs)*Gvc_cpm;                %Gvc_cpm_0 = Gdv/((Gdi1+Gdi2)*Rs);
minreal(Gvc)
% One-zero-and-two-pole compesnator design
R1=5.31*1e3; R2=2.7*1e3; Co1=3*1e-9; Co2=2*1e-9;
wi=1/(R2*(Co1+Co2)); wz1=1/(R1*Co1); wp1=1/(R1*((Co1*Co2)/(Co1+Co2)));
n1=[0, 1]; d1=[1/wi, 0]; Gc1=tf(n1,d1);
n2=[1/wz1, 1]; d2=[1/wp1, 1]; Gc2=tf(n2,d2);
Gc=series(Gc1,Gc2);
num=conv(n1,n2); den=conv(d1,d2); Gvcc=Gvc*Gc;
Tc1=feedback(Gvcc,[1]);
figure(1), bode(Gvc,'--',Gc,'+-',Gvcc,'')
legend('G_v_c','G_c','G_v_cG_c',-1)
figure(2), step(5*Tc1)

function[] = PCMCCCMZETARIDLEY1()
clc, clear all
disp('To run this proragame (PCMCCCMZETARIDLEY), please type:')
disp('PCMCCCMZETARIDLEY')
```

```
function[] = PCMCCCMZETARIDLEY()
% PCMCCCMZETARIDLEY program is to indicate the results of PCMC CCM Zeta converter
...from Ridley model, excluding He (sampling equation)
% C1, C2, L1, and L2 are capacitors and inductors
% rc1, rc2, rL1, rL2 are ESRs of capacitors and inductors
% Vg is input voltage, Vo is output voltage,
...D1 is duty ratio, and R is a standing load
clc; clear all;
C1=100*1e-6; rc1=0.19; C2=200*1e-6; rc2=0.095;
L1=100*1e-6; rL1=1*1e-3; L2=55*1e-6; rL2=0.55*1e-3;
Vg=15; Vo=5; D=Vo/(Vo+Vg); R=1; Iz=0;
Le=L1*L2/(L1+L2); fs=100*1e3; Rs=0.1;       % Rs is a sensing resistor
% The state-space matrices and average matrices
A1 = [-rL1/L1, 0, 0, 0
    0, (1/L2)*(-rL2-rc1-((rc2*R)/(rc2+R))), 1/L2, -R/(L2*(rc2+R))
    0, -1/C1, 0, 0
    0, R/(C2*(rc2+R)), 0, -1/(C2*(rc2+R))];
A2 = [-(rL1+rc1)/L1, 0, -1/L1, 0
    0, -(1/L2)*(rL2+(rc2*R/(rc2+R))), 0,-R/(L2*(rc2+R))
    1/C1, 0, 0, 0
    0, R/(C2*(rc2+R)), 0, -1/(C2*(rc2+R))];
A = A1*D + A2*(1-D);
B1 = [1/L1, 0
    1/L2, rc2*R/(L2*(rc2+R))
    0, 0
    0, -R/(C2*(rc2+R))];
B2 = [0, 0
    0, rc2*R/(L2*(rc2+R))
    0, 0
    0, -R/(C2*(rc2+R))];
B = B1*D + B2*(1-D);
C1 = [0, rc2*R/(rc2+R), 0, R/(rc2+R)];
C2 = [0, rc2*R/(rc2+R), 0, R/(rc2+R)];
C = C1*D + C2*(1-D);
E1 = [0, -rc2*R/(rc2+R)];
E2 = [0, -rc2*R/(rc2+R)];
E = E1*D + E2*(1-D);
%-----------------------------------------
U = [Vg; Iz];
%X  = [I1; I2; V1; V2];
X = -inv(A)*B*U;                % steady-state relations
%Vo = C*X+E*U ;                 % steady-state relations
%-----------------------------------------
Bd = (A1-A2)*X + (B1-B2)*U;
Ed = (C1-C2)*X + (E1-E2)*U;
I  = eye(4,4);
Bu1=B(:,1); Bu2=B(:,2);
Eu1=E(:,1); Eu2=E(:,2);
C11=[1, 0, 0, 0]; C12=[0, 1, 0, 0]; C13=[0, 0, 1, 0]; C14=[0, 0, 0, 1];
% Transfer functions
[numvi1, denvi1] = ss2tf(A,Bu1,C11,[0]);
Gvi1 = tf(numvi1,denvi1);
[numvi2, denvi2] = ss2tf(A,Bu1,C12,[0]);
Gvi2 = tf(numvi2,denvi2);
[numvv1, denvv1] = ss2tf(A,Bu1,C13,[0]);
Gvv1 = tf(numvv1,denvv1);
[numvv2, denvv2] = ss2tf(A,Bu1,C14,[0]);
Gvv2 = tf(numvv2,denvv2);

[numzi1, denzi1] = ss2tf(A,Bu2,C11,[0]);
Gzi1 = tf(numzi1,denzi1);
[numzi2, denzi2] = ss2tf(A,Bu2,C12,[0]);
Gzi2 = tf(numzi2,denzi2);
[numzv1, denzv1] = ss2tf(A,Bu2,C13,[0]);
Gzv1 = tf(numzv1,denzv1);
[numzv2, denzv2] = ss2tf(A,Bu2,C14,[0]);
Gzv2 = tf(numzv2,denzv2);

[numdi1, dendi1] = ss2tf(A,Bd,C11,[0]);
Gdi1 = tf(numdi1,dendi1);
[numdi2, dendi2] = ss2tf(A,Bd,C12,[0]);
Gdi2 = tf(numdi2,dendi2);
[numdv1, dendv1] = ss2tf(A,Bd,C13,[0]);
Gdv1 = tf(numdv1,dendv1);
[numdv2, dendv2] = ss2tf(A,Bd,C14,[0]);
Gdv2 = tf(numdv2,dendv2);
% Transfter funciton
[numv, denv] = ss2tf(A,Bu1,C,Eu1);
```

```
Gvv = tf(numv,denv);   %input voltage-to-output voltage transfer function
(Gvv(s)=vo(s)/vg(s))
[numz,denz] = ss2tf(A,Bu2,C,Eu2);
Gzv = tf(numz,denz);   %output impedance transfer function (Gzv(s)=vo(s)/iz(s))

[numd, dend] = ss2tf(A,Bd,C,Ed);
Gdv = tf(numd,dend);   %control-to-output transfer function (Gdv(s)=vo(s)/d(s))
% Model from Ridley: excludes sampling equation (or He=1).
num_e=[0, 1]; den_e=[0, 1]; He=tf(num_e,den_e);
M1=Vg*Rs/Le; Fm=fs/M1;
num_vc=Fm*numd;
den_vc=dend+Fm*Rs*(numdi1+numdi2);
Gvc=tf(num_vc,den_vc);
minreal(Gvc)
% One-zero-and-two-pole compesnator design
R1=5.31*1e3; R2=2.7*1e3; Co1=3*1e-9; Co2=2*1e-9;
wi=1/(R2*(Co1+Co2)); wz1=1/(R1*Co1); wp1=1/(R1*((Co1*Co2)/(Co1+Co2)));
n1=[0, 1]; d1=[1/wi, 0]; Gc1=tf(n1,d1);
n2=[1/wz1, 1]; d2=[1/wp1, 1]; Gc2=tf(n2,d2);
Gc=series(Gc1,Gc2);
num=conv(n1,n2); den=conv(d1,d2); Gvcc=Gvc*Gc;
Tc1=feedback(Gvcc,[1]);
figure(1), bode(Gvc,'--',Gc,'+-',Gvcc,'')
legend('G_v_c','G_c','G_v_cG_c',-1)
figure(2), step(5*Tc1)

function[] = PCMCCCMZETARIDLEYHE1()
clc, clear all
disp('To run this proragame (PCMCCCMZETARIDLEYHE), please type:')
disp('PCMCCCMZETARIDLEYHE')

function[] = PCMCCCMZETARIDLEYHE()
% PCMCCCMZETARIDLEY program is to show the results of PCMC CCM Zeta converter
...from Ridley model, including He (sampling equation)
% C1, C2, L1, and L2 are capacitors and inductors
% rc1, rc2, rL1, rL2 are ESRs of capacitors and inductors
% Vg is input voltage, Vo is output voltage,
...D1 is duty ratio, and R is a standing load
clc; clear all;
C1=100*1e-6; rc1=0.19; C2=200*1e-6; rc2=0.095;
L1=100*1e-6; rL1=1*1e-3; L2=55*1e-6; rL2=0.55*1e-3;
Vg=15; Vo=5; D=Vo/(Vo+Vg); R=1; Iz=0;
Le=L1*L2/(L1+L2); fs=100*1e3; Rs=0.1;        % Rs is a sensing resistor
% The state-space matrices and average matrices
A1 = [-rL1/L1, 0, 0, 0
    0, (1/L2)*(-rL2-rc1-((rc2*R)/(rc2+R))), 1/L2, -R/(L2*(rc2+R))
    0, -1/C1, 0, 0
    0, R/(C2*(rc2+R)), 0, -1/(C2*(rc2+R))];
A2 = [-(rL1+rc1)/L1, 0, -1/L1, 0
    0, -(1/L2)*(rL2+(rc2*R/(rc2+R))), 0,-R/(L2*(rc2+R))
    1/C1, 0, 0, 0
    0, R/(C2*(rc2+R)), 0, -1/(C2*(rc2+R))];
A = A1*D + A2*(1-D);
B1 = [1/L1, 0
    1/L2, rc2*R/(L2*(rc2+R))
    0, 0
    0, -R/(C2*(rc2+R))];
B2 = [0, 0
    0, rc2*R/(L2*(rc2+R))
    0, 0
    0, -R/(C2*(rc2+R))];
B = B1*D + B2*(1-D);
C1 = [0, rc2*R/(rc2+R), 0, R/(rc2+R)];
C2 = [0, rc2*R/(rc2+R), 0, R/(rc2+R)];
C = C1*D + C2*(1-D);
E1 = [0, -rc2*R/(rc2+R)];
E2 = [0, -rc2*R/(rc2+R)];
E = E1*D + E2*(1-D);
%---------------------------------------
U = [Vg; Iz];
%X  = [I1; I2; V1; V2];
X = -inv(A)*B*U;              % steady-state relations
%Vo = C*X+E*U ;               % steady-state relations
%---------------------------------------
Bd = (A1-A2)*X + (B1-B2)*U;
Ed = (C1-C2)*X + (E1-E2)*U;
I  = eye(4,4);
Bu1=B(:,1); Bu2=B(:,2);
Eu1=E(:,1); Eu2=E(:,2);
```

```
C11=[1, 0, 0, 0]; C12=[0, 1, 0, 0]; C13=[0, 0, 1, 0]; C14=[0, 0, 0, 1];
% Transfer functions
[numvi1, denvi1] = ss2tf(A,Bu1,C11,[0]);
Gvi1 = tf(numvi1,denvi1);
[numvi2, denvi2] = ss2tf(A,Bu1,C12,[0]);
Gvi2 = tf(numvi2,denvi2);
[numvv1, denvv1] = ss2tf(A,Bu1,C13,[0]);
Gvv1 = tf(numvv1,denvv1);
[numvv2, denvv2] = ss2tf(A,Bu1,C14,[0]);
Gvv2 = tf(numvv2,denvv2);

[numzi1, denzi1] = ss2tf(A,Bu2,C11,[0]);
Gzi1 = tf(numzi1,denzi1);
[numzi2, denzi2] = ss2tf(A,Bu2,C12,[0]);
Gzi2 = tf(numzi2,denzi2);
[numzv1, denzv1] = ss2tf(A,Bu2,C13,[0]);
Gzv1 = tf(numzv1,denzv1);
[numzv2, denzv2] = ss2tf(A,Bu2,C14,[0]);
Gzv2 = tf(numzv2,denzv2);

[numdi1, dendi1] = ss2tf(A,Bd,C11,[0]);
Gdi1 = tf(numdi1,dendi1);
[numdi2, dendi2] = ss2tf(A,Bd,C12,[0]);
Gdi2 = tf(numdi2,dendi2);
[numdv1, dendv1] = ss2tf(A,Bd,C13,[0]);
Gdv1 = tf(numdv1,dendv1);
[numdv2, dendv2] = ss2tf(A,Bd,C14,[0]);
Gdv2 = tf(numdv2,dendv2);
% Transfter funciton
[numv, denv] = ss2tf(A,Bu1,C,Eu1);
Gvv = tf(numv,denv);   %input voltage-to-output voltage transfer function
(Gvv(s)=vo(s)/vg(s))

[numz,denz] = ss2tf(A,Bu2,C,Eu2);
Gzv = tf(numz,denz);   %output impedance transfer function (Gzv(s)=vo(s)/iz(s))

[numd, dend] = ss2tf(A,Bd,C,Ed);
Gdv = tf(numd,dend);   %control-to-output transfer function (Gdv(s)=vo(s)/d(s))
% Model from Ridley: includes sampling equation (or He differs from 1).
wn=pi*fs; Qz=-2/pi;
num_e=[1/wn^2, 1/(wn*Qz), 1]; den_e=[0, 1]; He=tf(num_e,den_e);
M1=Vg*Rs/Le; Fm=fs/M1;
num_vc=Fm*numd;
dend1=[0, 0, dend];
den_vc=dend1+Fm*Rs*conv(num_e,numdi1+numdi2);
Gvc=tf(num_vc,den_vc);
minreal(Gvc)
% One-zero-and-two-pole compesnator design
R1=5.31*1e3; R2=2.7*1e3; Co1=3*1e-9; Co2=2*1e-9;
wi=1/(R2*(Co1+Co2)); wz1=1/(R1*Co1); wp1=1/(R1*((Co1*Co2)/(Co1+Co2)));
n1=[0, 1]; d1=[1/wi, 0]; Gc1=tf(n1,d1);
n2=[1/wz1, 1]; d2=[1/wp1, 1]; Gc2=tf(n2,d2);
Gc=series(Gc1,Gc2);
num=conv(n1,n2); den=conv(d1,d2); Gvcc=Gvc*Gc;
Tc1=feedback(Gvcc,[1]);
figure(1), bode(Gvc,'--',Gc,'+-',Gvcc,'')
legend('G_v_c','G_c','G_v_cG_c',-1)
figure(2), step(5*Tc1)

%%%%%%%%%%%%%%%%%%%%%%%%%%%%%%%%
% PCMC of DCM Zeta converter %
%%%%%%%%%%%%%%%%%%%%%%%%%%%%%%%%
function[] = PCMCDCMZETARIDLEY1()
clc, clear all
disp('To run this proragame (PCMCDCMZETARIDLEY), please type:')
disp('PCMCDCMZETARIDLEY')

function[] = PCMCDCMZETARIDLEY()
% PCMCDCMZETARIDLEY program is to show the results of PCMC DCM Zeta converter
...from Ridley model
% C1, C2, L1, and L2 are capacitors and inductors
% rc1, rc2, rL1, rL2 are ESRs of capacitors and inductors
% Vg is input voltage, Vo is output voltage,
...D1 and D2 are duty ratios, and R is a standing load
clc; clear all;
L1=100e-6; L2=22e-6; C1=47e-6; C2=200e-6; R=10; Vg=15;
rL1=0.001; rL2=0.00022; rc1=0.38; rc2=0.095;
fs=100*1e3; T=1/fs; Le=L1*L2/(L1+L2);
D1=0.2; D2=sqrt(2*Le/(R*T)); D3=1-D1-D2;
```

```
Vo=Vg*D1/D2; K=D2^2; M=D1/sqrt(K);          %M=D1/D2;
gi=M^2/R; gf=2*M/R; go=1/R; ki=2*M^2*Vg/(R*D1); ko=2*M*Vg/(R*D1);
T=1/fs; Le=L1*L2/(L1+L2); Rs=0.1; fs=100*1e3;
% coefficients of transfer fucniton
adv = C1*L1*((-ko*gi+gf*ki)*rc1-ki-ko);
bdv = (C1*(-ko*rc1*gi-ki-ko+gf*rc1*ki))*rL1+gf*ki*L1-ko*C1*rc1-ko*gi*L1;
cdv = (-ko*gi+gf*ki)*rL1-ko;

adi1 = L2*C1*C2*(ki+ko+ki*go*rc1)*(R+rc2);
bdi1 = (C1*C2*(ki+ko+ki*go*rc1)*(R+rc2))*rL2+(ki*C1*(go*L2+R*C2*rc2*go...

+C2*R+C2*rc2))*rc1+(C2*(R*ko*C1+ki*go*L2+ki*R*C1))*rc2+L2*(ki*C1+ko*C1+ki*go*C2*R);
cdi1 = (ki*C1+ki*go*C2*R+ki*go*C1*rc1+ko*C1+ki*go*C2*rc2)*rL2...
    +ki*(C2*rc2+C1*rc1)*(1+R*go)+(L2*go+R*C2+R*C1)*ki+R*ko*C1;
ddi1 = ki*(go*rL2+1+R*go);

adi2 = C1*L1*(gi*rc1*ko-gf*rc1*ki+ki+ko);
bdi2 = (C1*(gi*rc1*ko-gf*rc1*ki+ki+ko))*rL1+C1*rc1*ko-ki*gf*L1+gi*L1*ko;
cdi2 = ko*gi*rL1+ko-gf*ki*rL1;
ddi2 = C2*(rc2+R);

a = C2*C1*L2*L1*(gf+go+go*rc1*gi+gi)*(rc2+R);
b =
(C2*C1*L2*(gf+go+go*rc1*gi+gi)*(rc2+R))*rL1+(C2*C1*L1*(gf+go+go*rc1*gi+gi)*(rc2...
+R))*rL2+(C1*(go*L2*gi*L1+C2*R*gi*L1+go*C2*R*L2+go*C2*rc2*L2+C2*rc2*gi*L1+...
R*C2*rc2*go*gi*L1))*rc1+(C2*(C1*L2+R*go*C1*L1+C1*L1+go*L2*gi*L1+R*C1*gf*L1+...
R*C1*gi*L1))*rc2+gf*C1*L2*L1+gi*C1*L2*L1+go*L2*C1*L1+go*C2*R*L2*gi*L1+...
C2*R*C1*L1+C1*C2*R*L2;
c = ((C2*C1*(gf+go+go*rc1*gi+gi)*(rc2+R))*rL2+(gi*C1*(C2*rc2+C2*R+go*L2+...
R*C2*rc2*go))*rc1+(C2*(R*C1*gi+go*L2*gi+C1+R*go*C1+R*C1*gf))*rc2+C1*C2*R+gi*C1*L2...
+gf*C1*L2+go*L2*C1+go*C2*R*L2*gi)*rL1+((go*C1*(gi*L1+C2*R+C2*rc2))*rc1+...
(C2*(go*gi*L1+C1))*rc2+gf*C1*L1+C1*C2*R+go*C2*R*gi*L1+gi*C1*L1+go*C1*L1)*rL2...
+(C1*(gi*L1+R*go*gi*L1+R*C2*rc2*go+C2*R+C2*rc2+go*L2))*rc1+(C2*(R*C1+gi*L1+...
go*L2+R*go*gi*L1))*rc2+go*L2*gi*L1+C1*L2+R*C1*gf*L1+R*C1*gi*L1+go*C2*R*L2+C1*L1...
+C2*R*gi*L1+R*go*C1*L1;
d = ((go*C2*rc2*gi+go*C1+go*C2*R*gi+go*C1*rc1*gi+gf*C1+gi*C1)*rL2+C1*rc1*gi+...
go*L2*gi+R*C2*rc2*go*gi+C1+R*C1*gf+R*go*C1+R*C1*gi+C2*rc2*gi+C2*R*gi+...
R*go*C1*rc1*gi)*rL1+(go*C2*rc2+go*C2*R+go*gi*L1+C1+go*C1*rc1)*rL2+(C1+R*go*C1)*rc1...
+C2*rc2+R*go*gi*L1+R*C2*rc2*go+C2*R+go*L2+R*C1+gi*L1;
e = (1+gi*rL1)*(R*go+1+go*rL2);
% Transfer functions
num1 = [C2*rc2, 1]; den1 = [0, 1]; Gdv1 = tf(num1,den1);
num2 = [adv, bdv, cdv]; den2 = [a, b, c, d, e]; Gdv2 = tf(num2,den2);
nun_dv = -R*conv(num1,num2); den_dv = conv(den1,den2); Gdv = tf(nun_dv,den_dv);
num_di1 = [adi1, bdi1, cdi1, ddi1]; Gdi1 = tf(num_di1,den_dv);
num_di21 = [adi2, bdi2, cdi2]; num_di22 = [ddi2, 1];
num_di2 = conv(num_di21, num_di22); Gdi2 = tf(num_di2,den_dv);
%%%% Model from Ridley
M1=Vg*Rs/Le; Fm=fs/M1;
Gvc=Fm*Gdv;
% One-zero-and-two-pole compesnator design
R1=2.2*1e3; R2=2*1e3; Co1=4.7*1e-9; Co2=2*1e-9;
wi=1/(R2*(Co1+Co2)); wz1=1/(R1*Co1); wp1=1/(R1*((Co1*Co2)/(Co1+Co2)));
n1=[0, 1]; d1=[1/wi, 0]; Gc1=tf(n1,d1);
n2=[1/wz1, 1]; d2=[1/wp1, 1]; Gc2=tf(n2,d2);
Gc=series(Gc1,Gc2); Gvcc=Gvc*Gc;
figure(1), bode(Gvc,'--',Gc,'+-',Gvc*Gc,''), legend('G_v_c','G_c','G_v_cG_c',-1)
Tc1 = feedback(Gvcc,[1]);
figure(2), step(Tc1)
```

Appendix H

List of Publication

[1] Vuthchhay E. and Chanin B., "Dynamic Modeling of a Zeta converter with State-Space Averaging Technique," *5th International Conference on Electrical Engineering/Electronics, Computer, Telecommunications and Information Technology 2008 (ECTI-CON 2008)*, May 2008.

[2] Vuthchhay E., Chanin B., and H. Hirata "Dynamic Modeling and Control of a Zeta Converter," *International Symposium on Communications and Information Technologies 2008 (ISCIT 2008)*, Oct. 2008.

[3] Vuthchhay E., V. Wutti, and Chanin B., "Modeling of a SEPIC Converter for Feedback Control Design," *Proc. of 31st Electrical Engineering Conference*, Oct. 2008.

[4] Vuthchhay E., Unnat P., and Chanin B., "Modeling of a SEPIC Converter Operating in Continuous Conduction Mode," *6th International Conference on Electrical Engineering/Electronics, Computer, Telecommunications and Information Technology 2009 (ECTI-CON 2009)*, May 2009.

[5] Vuthchhay E. and Chanin B., "Modeling of a SEPIC Converter Operating in Discontinuous Conduction Mode," *6th International Conference on Electrical Engineering/Electronics, Computer, Telecommunications and Information Technology 2009 (ECTI-CON 2009)*, May 2009.

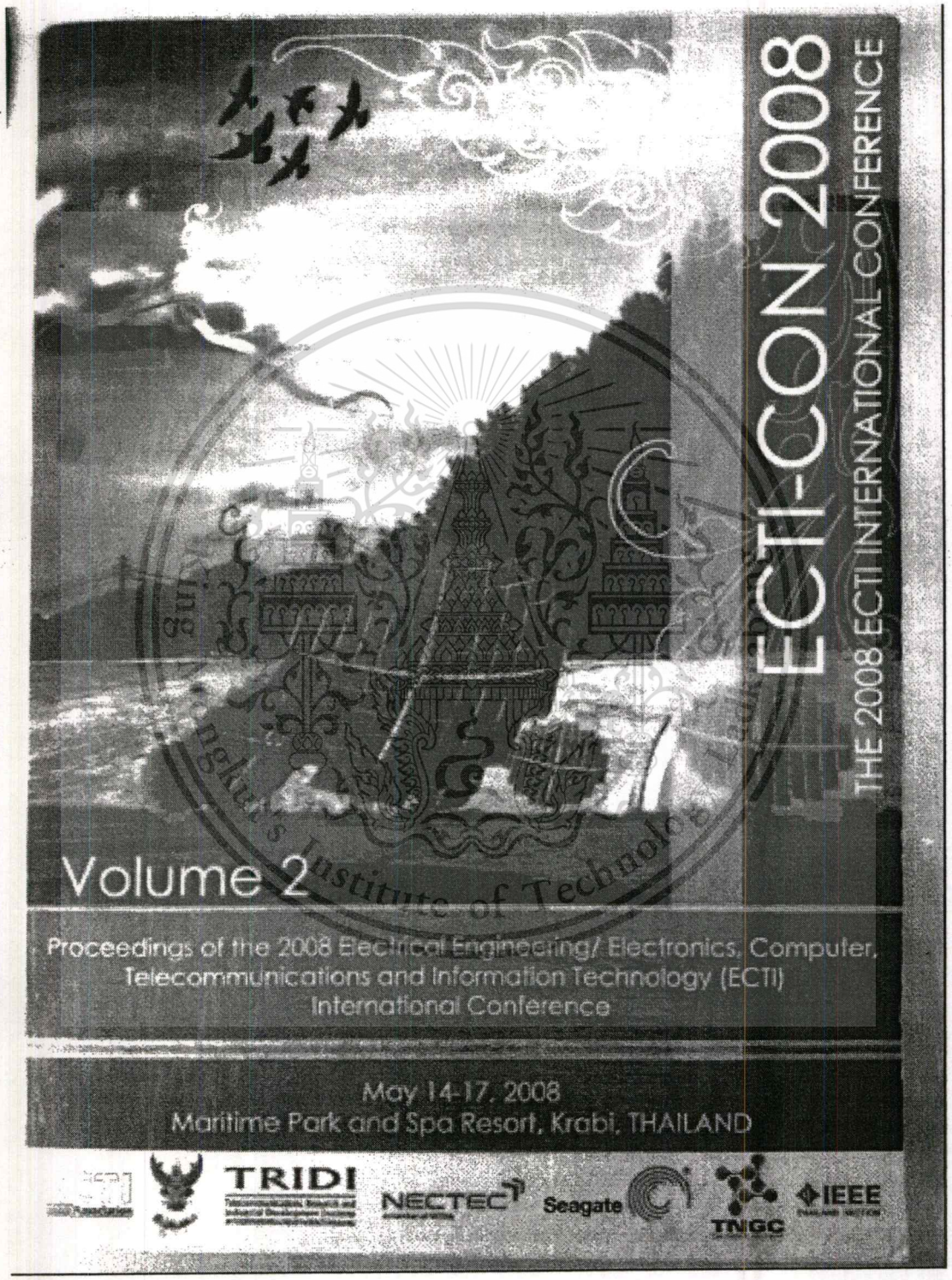

Proceedings of ECTI-CON 2008

Dynamic Modeling of a Zeta Converter with State-Space Averaging Technique

Eng Vuthchhay and Chanin Bunlaksananusorn
Faculty of Engineering, King Mongkut's Institute of Technology Ladkrabang (KMITL),
Chalongkrung Rd. Ladkrabang, Bangkok 10520

Abstract- **A Zeta converter is a fourth-order DC-DC converter made up of two inductors and two capacitors and capable of operating in either step-up or step-down mode. Compared with a Cuk or Sepic converters, the Zeta converter has received the least attention and its dynamic properties have never been reported before in the literature. This paper presents dynamic modeling of a Zeta converter with State-Space averaging (SSA) technique. The modeling leads to a small-signal linear dynamic model of the converter, from which the transfer functions used for feedback control design can be determined. Simulation results are presented to verify the accuracy of the obtained model.**

I. Introduction

Nowadays, a DC-DC converter is widely used as a power supply in electronic systems. The converter incorporates feedback control to maintain the constant output voltage. However, changes in an input voltage and/or load current will cause the converter's output voltage to deviate from the desired value. It is a task of the feedback control to correct this error and quickly bring the output voltage back into the regulated level. Modeling plays a key role in revealing the insight of the converter's dynamic behavior as well as providing a basis for feedback control design. In the last two decades, there has been a continually active research on DC-DC converters; as a consequence, several modeling methods have been proposed [1]. Among them, the State-Space Averaging (SSA) technique [2] is one of the best-known methods. It provides a systematic way to model the converter and gains widespread acceptance. The SSA modeling consists of three stages: (1) Formulation of state-space equations of the converter for each subinterval in a switching cycle, (2) Average of these equations to get a single averaged state-space equation, and (3) Perturbation of the averaged equation to get a linear small-signal state-space equation, from which various transfer functions can be determined. Since the SSA is a matrix-based technique, i.e. all the steps described above are done in a matrix form, formal matrix treatment can be applied to facilitate the modeling process.

The SSA technique is commonly used to model the second-order converters such as buck, boost, and buck-boost converters [1- 4]. Modeling of the fourth-order converters such as Cuk and Sepic converters has also been studied [5- 7]; however, the techniques used were based on circuit averaging approach rather than the SSA. Like Cuk and Sepic converters, a Zeta converter is the fourth-order converter made up of two inductors and two capacitors and capable of working in either step-up or step-down mode. Its dynamic characteristics, however, have never been reported before in the literatures. This paper presents dynamic modeling of a Zeta converter with the SSA technique. The paper is organized as follows. The SSA technique is reviewed in Section II. Modeling of the Zeta converter with the SSA technique is demonstrated in Section III. Simulation results are presented in Section IV. Section V gives a conclusion of this work.

II. Overview Of SSA Technique

For the DC-DC converters operating in Continuous Conduction Mode (CCM), there exist two power circuit states within one switching period, T. One is when the MOSFET is turned on for an interval dT, and another is when the MOSFET is turned off for an interval (1-d)T, where d is a duty cycle. The state-space equations for these two circuit states are:

$$\begin{cases} \dfrac{d\mathbf{x}(t)}{dt} = \mathbf{A}_1\mathbf{x}(t) + \mathbf{B}_1\mathbf{u}(t) \\ \mathbf{y}(t) = \mathbf{C}_1\mathbf{x}(t) + \mathbf{E}_1\mathbf{u}(t) \end{cases} \quad (1)$$

$$\begin{cases} \dfrac{d\mathbf{x}(t)}{dt} = \mathbf{A}_2\mathbf{x}(t) + \mathbf{B}_2\mathbf{u}(t) \\ \mathbf{y}(t) = \mathbf{C}_2\mathbf{x}(t) + \mathbf{E}_2\mathbf{u}(t) \end{cases} \quad (2)$$

To find the averaged behavior of the converter over one switching period, (1) and (2) are weighed average by the duty cycle as:

$$\begin{cases} \dfrac{d\mathbf{x}(t)}{dt} = \mathbf{A}_s\mathbf{x}(t) + \mathbf{B}_s\mathbf{u}(t) \\ \mathbf{y}(t) = \mathbf{C}_s\mathbf{x}(t) + \mathbf{E}_s\mathbf{u}(t) \end{cases} \quad (3)$$

where

$\mathbf{A}_s = \mathbf{A}_1 d + \mathbf{A}_2(1-d)$, $\mathbf{B}_s = \mathbf{B}_1 d + \mathbf{B}_2(1-d)$, $\mathbf{C}_s = \mathbf{C}_1 d + \mathbf{C}_2(1-d)$, and $\mathbf{E}_s = \mathbf{E}_1 d + \mathbf{E}_2(1-d)$.

Equation (3) is a nonlinear continuous-time equation. It can be linearized by small-signal perturbation with $\mathbf{x} = \mathbf{X} + \tilde{\mathbf{x}}$, $\mathbf{y} = \mathbf{Y} + \tilde{\mathbf{y}}$, $\mathbf{u} = \mathbf{U} + \tilde{\mathbf{u}}$, and $d = D + \tilde{d}$, where the $\tilde{}$ symbol represents a small signal, and the capital letter a DC value. It should be noted that $\mathbf{X} >> \tilde{\mathbf{x}}$, $\mathbf{Y} >> \tilde{\mathbf{y}}$, $\mathbf{U} >> \tilde{\mathbf{u}}$, and $D >> \tilde{d}$. The perturbation yields the steady-state and linear small-signal state-space equations in (4) and (5) respectively.

$$\begin{cases} \dfrac{d\mathbf{X}}{dt} = \mathbf{AX} + \mathbf{BU} = 0 \\ \mathbf{Y} = \mathbf{CX} + \mathbf{EU} \end{cases} \quad (4)$$

$$\begin{cases} \dfrac{d\tilde{\mathbf{x}}(t)}{dt} = \mathbf{A}\tilde{\mathbf{x}}(t) + \mathbf{B}\tilde{\mathbf{u}}(t) + \mathbf{B}_d\tilde{d}(t) \\ \tilde{\mathbf{y}}(t) = \mathbf{C}\tilde{\mathbf{x}}(t) + \mathbf{E}\tilde{\mathbf{u}}(t) + \mathbf{E}_d\tilde{d}(t) \end{cases} \quad (5)$$

978-1-4244-2101-5/08/$25.00 ©2008 IEEE

where

$\mathbf{A} = \mathbf{A}_1 D + \mathbf{A}_2(1-D)$, $\mathbf{B} = \mathbf{B}_1 D + \mathbf{B}_2(1-D)$, $\mathbf{C} = \mathbf{C}_1 D + \mathbf{C}_2(1-D)$,

$\mathbf{E} = \mathbf{E}_1 D + \mathbf{E}_2(1-D)$, $\mathbf{B}_d = (\mathbf{A}_1 - \mathbf{A}_2)\mathbf{X} + (\mathbf{B}_1 - \mathbf{B}_2)\mathbf{U}$, and

$\mathbf{E}_d = (\mathbf{C}_1 - \mathbf{C}_2)\mathbf{X} + (\mathbf{E}_1 - \mathbf{E}_2)\mathbf{U}$.

The steady-state solution of the converter can be found by solving (4) which gives:

$$\begin{cases} \mathbf{X} = -\mathbf{A}^{-1}\mathbf{B}\mathbf{U} \\ \mathbf{Y} = (-\mathbf{C}\mathbf{A}^{-1}\mathbf{B} + \mathbf{E})\mathbf{U} \end{cases} \tag{6}$$

The small-signal transfer function of the converter can be found by applying the Laplace transform to (5). In a matrix form, we get:

$$\begin{cases} \tilde{\mathbf{x}}(s) = \begin{bmatrix} (s\mathbf{I}-\mathbf{A})^{-1}\mathbf{B} & (s\mathbf{I}-\mathbf{A})^{-1}\mathbf{B}_d \end{bmatrix} \begin{bmatrix} \tilde{\mathbf{u}}(s) \\ \tilde{d}(s) \end{bmatrix} \\ \tilde{\mathbf{y}}(s) = \begin{bmatrix} \mathbf{C}(s\mathbf{I}-\mathbf{A})^{-1}\mathbf{B} + \mathbf{E} & \mathbf{C}(s\mathbf{I}-\mathbf{A})^{-1}\mathbf{B}_d + \mathbf{E}_d \end{bmatrix} \begin{bmatrix} \tilde{\mathbf{u}}(s) \\ \tilde{d}(s) \end{bmatrix} \end{cases} \tag{7}$$

In DC-DC converters, the input variable $\tilde{\mathbf{u}}$ usually contains the input voltage and load current. Hence, $\tilde{\mathbf{u}}$ is express as $\tilde{\mathbf{u}} = [u_1\ u_2]^T$, the matrix B as $\mathbf{B}=[\mathbf{B}_{u1}\ \mathbf{B}_{u2}]$, and the matrix E as $\mathbf{E}=[\mathbf{E}_{u1}\ \mathbf{E}_{u2}]$. Therefore,

$$\begin{cases} \tilde{\mathbf{x}}(s) = \begin{bmatrix} (s\mathbf{I}-\mathbf{A})^{-1}\mathbf{B}_{u1} & (s\mathbf{I}-\mathbf{A})^{-1}\mathbf{B}_{u2} & (s\mathbf{I}-\mathbf{A})^{-1}\mathbf{B}_d \end{bmatrix} \begin{bmatrix} \tilde{u}_1(s) \\ \tilde{u}_2(s) \\ \tilde{d}(s) \end{bmatrix} \\ \tilde{\mathbf{y}}(s) = \begin{bmatrix} \mathbf{C}(s\mathbf{I}-\mathbf{A})^{-1}\mathbf{B}_{u1} + \mathbf{E}_{u1} & \mathbf{C}(s\mathbf{I}-\mathbf{A})^{-1}\mathbf{B}_{u2} + \mathbf{E}_{u2} & \mathbf{C}(s\mathbf{I}-\mathbf{A})^{-1}\mathbf{B}_d + \mathbf{E}_d \end{bmatrix} \begin{bmatrix} \tilde{u}_1(s) \\ \tilde{u}_2(s) \\ \tilde{d}(s) \end{bmatrix} \end{cases} \tag{8}$$

For the fourth-order converter, $(s\mathbf{I}-\mathbf{A})^{-1}\mathbf{B}_{u1}$, $(s\mathbf{I}-\mathbf{A})^{-1}\mathbf{B}_{u2}$, and $(s\mathbf{I}-\mathbf{A})^{-1}\mathbf{B}_d$ are the matrices that have four rows and one column. So the above equations can be extended into:

$$\begin{cases} \tilde{\mathbf{x}}(s) = \begin{bmatrix} G_{iu_1}(s) & G_{iu_2}(s) & G_{id}(s) \\ G_{vu_1}(s) & G_{vu_2}(s) & G_{dv}(s) \\ G_{wu_1}(s) & G_{wu_2}(s) & G_{dw}(s) \end{bmatrix} \begin{bmatrix} \tilde{u}_1(s) \\ \tilde{u}_2(s) \\ \tilde{d}(s) \end{bmatrix} \\ \tilde{\mathbf{y}}(s) = \begin{bmatrix} G_{vu}(s) & G_{iu}(s) & G_{dv}(s) \end{bmatrix} \begin{bmatrix} \tilde{u}_1(s) \\ \tilde{u}_2(s) \\ \tilde{d}(s) \end{bmatrix} \end{cases} \tag{9}$$

where

$G_{iu_1}(s) = [(s\mathbf{I}-\mathbf{A})^{-1}\mathbf{B}_{u1}]_{11}$, $G_{iu_2}(s) = [(s\mathbf{I}-\mathbf{A})^{-1}\mathbf{B}_{u2}]_{11}$, $G_{id}(s) = [(s\mathbf{I}-\mathbf{A})^{-1}\mathbf{B}_d]_{11}$,

$G_{vu_1}(s) = [(s\mathbf{I}-\mathbf{A})^{-1}\mathbf{B}_{u1}]_{21}$, $G_{vu_2}(s) = [(s\mathbf{I}-\mathbf{A})^{-1}\mathbf{B}_{u2}]_{21}$, $G_{dv}(s) = [(s\mathbf{I}-\mathbf{A})^{-1}\mathbf{B}_d]_{21}$,

$G_{wu_1}(s) = [(s\mathbf{I}-\mathbf{A})^{-1}\mathbf{B}_{u1}]_{31}$, $G_{wu_2}(s) = [(s\mathbf{I}-\mathbf{A})^{-1}\mathbf{B}_{u2}]_{31}$, $G_{dw}(s) = [(s\mathbf{I}-\mathbf{A})^{-1}\mathbf{B}_d]_{31}$,

$G_{vu}(s) = [(s\mathbf{I}-\mathbf{A})^{-1}\mathbf{B}_{u1}]_{41}$, $G_{iu_1}(s) = [(s\mathbf{I}-\mathbf{A})^{-1}\mathbf{B}_{u2}]_{41}$, $G_{dv}(s) = [(s\mathbf{I}-\mathbf{A})^{-1}\mathbf{B}_d]_{41}$,

$G_{vu}(s) = \mathbf{C}(s\mathbf{I}-\mathbf{A})^{-1}\mathbf{B}_{u1} + \mathbf{E}_{u1}$, $G_{iu}(s) = \mathbf{C}(s\mathbf{I}-\mathbf{A})^{-1}\mathbf{B}_{u2} + \mathbf{E}_{u2}$, and

$G_{dv}(s) = \mathbf{C}(s\mathbf{I}-\mathbf{A})^{-1}\mathbf{B}_d + \mathbf{E}_d$

III. Modeling Of A Zeta Converter By SSA Technique

A Zeta converter shown in Fig. 1(a) is made up of the MOSFET switch (Q), diode (D), two inductors (L_1 and L_2), and two capacitors (C_1 and C_2). The resistor R is a standing load, while r_{C1} and r_{C2} are Equivalent Series Resistances (ESR) of the capacitors C_1 and C_2 respectively. The current source, I_z, models the load current.

In CCM, the converter exhibits two circuit states. The first state is when the MOSFET switch is turned on (Fig. 1(b)). During this interval (dT), the currents through L_1 and L_2 are supplied by V_g, and hence i_{L1} and i_{L2} increase linearly as shown in Fig. 2. This interval is called the *charging* mode. The second state exists when the MOSFET switch is turned off (Fig. 1(c)). During this interval ((1-d)T), L_1 and L_2 release the stored energy to C_1 and the output section. Thus, i_{L1} and i_{L2} decrease linearly as shown in Fig. 2. This interval is known as the *discharging* mode.

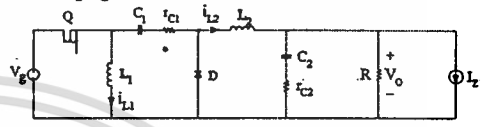

(a) Zeta converter.

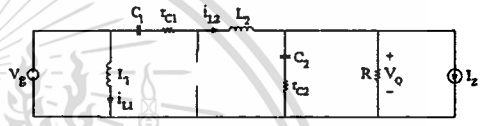

(b) Zeta converter when MOSFET is turned on.

(c) Zeta converter when MOSFET is turned off.

Fig. 1. Operation of Zeta converter.

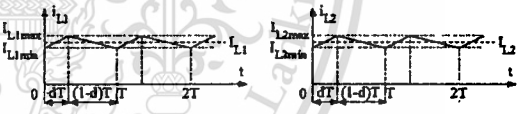

(a) i_{L1} waveform (b) i_{L2} waveform

Fig. 2. Current waveforms.

A. State-Space Description

Following (1) and (2), the state-space equations of the Zeta converter for the on and off states of the switch can be written from Fig. 1(b) and (c) respectively, given:

$$\begin{aligned} \frac{di_{L1}}{dt} &= \frac{r_{C1}}{L_1}(\delta-1)i_{L1} + \frac{v_o}{L_1}(\delta-1) + \frac{V_g}{L_1}\delta \\ \frac{di_{L2}}{dt} &= \frac{-1}{L_2}(r_{C1}\delta + \frac{r_{C1}R}{r_{C1}+R})i_{L2} + \frac{v_o}{L_2}\delta - \frac{R}{L_2(r_{C1}+R)}v_{C1} + \frac{V_g}{L_2}\delta + \frac{r_{C1}R}{L_2(r_{C1}+R)}I_z \\ \frac{dv_{C1}}{dt} &= \frac{i_{L2}}{C_1}(1-\delta) - \frac{i_{L1}}{C_1}\delta \\ \frac{dv_{C2}}{dt} &= \frac{R}{C_2(r_{C2}+R)}i_{L2} - \frac{1}{C_2(r_{C2}+R)}v_{C2} - \frac{R}{C_2(r_{C2}+R)}I_z \\ v_o &= \frac{r_{C2}R}{r_{C2}+R}i_{L2} + \frac{R}{r_{C2}+R}v_{C2} - \frac{r_{C2}R}{r_{C2}+R}I_z \end{aligned} \tag{10}$$

It should be noted that the equations are expressed in a compact form using the switching function, δ. When the switch is on, δ =1, (10) will then become the on-state equation.

When the switch is off, $\delta = 0$, (10) will then become the off-state equation. From (4) and (5), the averaged matrices for the steady-state equations and the linear small-signal state-space equations are:

$$\mathbf{A} = \mathbf{A}_1 D + \mathbf{A}_2(1-D) = \begin{bmatrix} \frac{-r_{C1}}{L_1}(1-D) & 0 & \frac{-1}{L_1}(1-D) & 0 \\ 0 & \frac{-1}{L_2}(r_{C1}D + \frac{r_{C2}R}{r_{C2}+R}) & \frac{D}{L_2} & \frac{-R}{L_2(r_{C2}+R)} \\ \frac{1}{C_1}(1-D) & \frac{-D}{C_1} & 0 & 0 \\ 0 & \frac{R}{C_2(r_{C2}+R)} & 0 & \frac{-1}{C_2(r_{C2}+R)} \end{bmatrix} \quad (11)$$

$$\mathbf{B} = \mathbf{B}_1 D + \mathbf{B}_2(1-D) = \begin{bmatrix} \frac{1}{L_1}D & 0 \\ \frac{1}{L_2}D & \frac{r_{C2}R}{L_2(r_{C2}+R)} \\ 0 & 0 \\ 0 & \frac{-R}{C_2(r_{C2}+R)} \end{bmatrix} \quad (12)$$

$$\mathbf{C} = \mathbf{C}_1 D + \mathbf{C}_2(1-D) = \begin{bmatrix} 0 & \frac{r_{C2}R}{r_{C2}+R} & 0 & \frac{R}{r_{C2}+R} \end{bmatrix} \quad (13)$$

$$\mathbf{E} = \mathbf{E}_1 D + \mathbf{E}_2(1-D) = \begin{bmatrix} 0 & \frac{-r_{C2}R}{r_{C2}+R} \end{bmatrix} \quad (14)$$

$$\mathbf{B}_d = (\mathbf{A}_1 - \mathbf{A}_2)\mathbf{X} + (\mathbf{B}_1 - \mathbf{B}_2)\mathbf{U} = \begin{bmatrix} \frac{V_g}{(1-D)L_1} \\ \frac{R(r_{C1}I_2 - V_g)}{L_2[(Dr_{C1} + R(1-D)]} \\ \frac{-DV_g - RI_2(1-D)}{[Dr_{C1} + R(1-D)](1-D)C_1} \\ 0 \end{bmatrix} \quad (15)$$

$$\mathbf{E}_d = (\mathbf{C}_1 - \mathbf{C}_2)\mathbf{X} + (\mathbf{E}_1 - \mathbf{E}_2)\mathbf{U} = [0] \quad (16)$$

B. Steady-State Equations

Given the averaged matrices (11) to (16), the steady-state solution of the converter can be obtained from (6):

$$\begin{cases} \begin{bmatrix} I_{L1} \\ I_{L2} \\ V_{C1} \\ V_{C2} \end{bmatrix} = \frac{RD}{r_{C1}D + R(1-D)} \begin{bmatrix} \frac{D}{R(1-D)} & 1 \\ \frac{1}{R} & \frac{1-D}{D} \\ 1 & -r_{C1} \\ 1 & -r_{C1} \end{bmatrix} \begin{bmatrix} V_g \\ I_2 \end{bmatrix} \\ V_o = \frac{(V_g - r_{C1}I_2)DR}{Dr_{C1} + R(1-D)} \end{cases} \quad (17)$$

If r_{C1} and r_{C2} are assumed to be zero, the conversion ratio of the Zeta converter will become $\frac{V_o}{V_g} = \frac{D}{1-D}$, which is the same as Cuk and Sepic converters.

C. Linear Small-Signal State-Space Equations

Given the averaged matrices (11) to (16), the linear small-signal state-space equations of the Zeta converter can be formulated as given in (5):

$$\frac{d}{dt}\begin{bmatrix} \tilde{i}_{L1}(t) \\ \tilde{i}_{L2}(t) \\ \tilde{v}_{C1}(t) \\ \tilde{v}_{C2}(t) \end{bmatrix} = \begin{bmatrix} \frac{-r_{C1}}{L_1}(1-D) & 0 & \frac{-1}{L_1}(1-D) & 0 \\ 0 & \frac{-1}{L_2}(r_{C1}D + \frac{r_{C2}R}{r_{C2}+R}) & \frac{D}{L_2} & \frac{-R}{L_2(r_{C2}+R)} \\ \frac{1}{C_1}(1-D) & \frac{-D}{C_1} & 0 & 0 \\ 0 & \frac{R}{C_2(r_{C2}+R)} & 0 & \frac{-1}{C_2(r_{C2}+R)} \end{bmatrix} \begin{bmatrix} \tilde{i}_{L1}(t) \\ \tilde{i}_{L2}(t) \\ \tilde{v}_{C1}(t) \\ \tilde{v}_{C2}(t) \end{bmatrix} + \begin{bmatrix} \frac{D}{L_1} & 0 & \frac{V_g}{(1-D)L_1} \\ \frac{D}{L_2} & \frac{r_{C2}R}{L_2(r_{C2}+R)} & \frac{R(r_{C1}I_2 - V_g)}{L_2[(Dr_{C1} + R(1-D)]} \\ 0 & 0 & \frac{-DV_g - RI_2(1-D)}{[Dr_{C1} + R(1-D)](1-D)C_1} \\ 0 & \frac{-R}{C_2(r_{C2}+R)} & 0 \end{bmatrix} \begin{bmatrix} \tilde{v}_g(t) \\ \tilde{i}_2(t) \\ \tilde{d}(t) \end{bmatrix} \quad (18)$$

$$\tilde{v}_o(t) = \begin{bmatrix} 0 & \frac{r_{C1}R}{r_{C1}+R} & 0 & \frac{R}{r_{C2}+R} \end{bmatrix} \begin{bmatrix} \tilde{i}_{L1}(t) \\ \tilde{i}_{L2}(t) \\ \tilde{v}_{C1}(t) \\ \tilde{v}_{C2}(t) \end{bmatrix} + \begin{bmatrix} 0 & \frac{-r_{C2}R}{r_{C2}+R} & 0 \end{bmatrix} \begin{bmatrix} \tilde{v}_g(t) \\ \tilde{i}_2(t) \\ \tilde{d}(t) \end{bmatrix} \quad (19)$$

D. Finding Transfer Functoins

From (9), there are altogether fifteen transfer functions that can be determined from (18) and (19). However, only a few of them are significant for feedback control design purpose. These transfer functions are:

The duty ratio-to-output voltage transfer function

$$G_{dv}(s) = \frac{\tilde{v}_o(s)}{\tilde{d}(s)} = \mathbf{C}(s\mathbf{I} - \mathbf{A})^{-1}\mathbf{B}_d + \mathbf{E}_d = \frac{R}{(1-D)\{(Dr_{C1} + (1-D)R\}} \frac{(a_1 s^3 + b_1 s + c_1)(d_1 s + 1)}{a_2 s^4 + b_2 s^3 + c_2 s^2 + d_2 s + e_2} \quad (20)$$

The input voltage-to-output voltage transfer function

$$G_{vv}(s) = \frac{\tilde{v}_o(s)}{\tilde{v}_g(s)} = \mathbf{C}(s\mathbf{I} - \mathbf{A})^{-1}\mathbf{B}_{u1} + \mathbf{E}_{u1} = DR\frac{(a_1' s^2 + b_1' s + c_1')(d_1' s + 1)}{a_2 s^4 + b_2 s^3 + c_2 s^2 + d_2 s + e_2} \quad (21)$$

The output impedance transfer function

$$G_{zv}(s) = \frac{\tilde{v}_o(s)}{\tilde{i}_g(s)} = \mathbf{C}(s\mathbf{I} - \mathbf{A})^{-1}\mathbf{B}_{u2} + \mathbf{E}_{u2} = -R\frac{a_1'' s^4 + b_1'' s^3 + c_1'' s^2 + d_1'' s + e_1''}{a_2 s^4 + b_2 s^3 + c_2 s^2 + d_2 s + e_2} \quad (22)$$

The coefficients in (20) to (22) are listed in TABLE I.

TABLE I
COEFFICIENTS OF $G_{dv}(s)$, $G_{zv}(s)$, AND $G_{vv}(s)$.

$a_1 = (V_g - r_{C1}I_2)(1-D)RL_1C_1$, $c_1 = (V_g - r_{C1}I_2)(1-D)^2R$, $d_1 = C_2r_{C2}$, $b_1 = [C_1Rr_{C1}(1-D)^2 - L_1D^2]V_g - [(L_1D + C_1r_{C1}^2(1-D))(1-D)RI_2$.
$a_1' = L_1C_1$, $b_1' = r_{C1}C_1(1-D)$, $c_1' = 1-D$, $d_1' = C_2r_{C2}$.
$a_1'' = L_1C_1L_2C_2r_{C2}$, $b_1'' = L_1C_1(L_2 + r_{C1}r_{C2}C_2D) + r_{C1}r_{C2}C_1L_2C_2(1-D)$, $c_1'' = [r_{C2}L_2C_2(1-D) + r_{C1}C_1L_2 + r_{C1}^2r_{C2}C_1C_2D](1-D) + L_1D(r_{C1}C_1 + r_{C2}C_2D)$, $d_1'' = L_2(1-D)^2 + L_1D^2 + (r_{C1}C_1 + r_{C2}C_2)r_{C1}D(1-D)$, $e_1'' = r_{C1}D(1-D)$.
$a_2 = (R + r_{C2})L_1C_1L_2C_2$, $e_2 = [(1-D)R + Dr_{C1}](1-D)$, $b_2 = (r_{C2} + R)(1-D)r_{C1}C_1L_2C_2 + L_1C_1[L_2 + Rr_{C2}C_2 + (R + r_{C2})r_{C1}C_2D]$, $c_2 = [L_2C_2(R + r_{C2})(1-D) + r_{C1}C_1L_2 + C_1C_2r_{C1}^2r_{C2}D + C_1C_2Rr_{C1}r_{C2} + C_1C_2Rr_{C1}^2D](1-D) + [(R + Dr_{C1})C_1 + (R + r_{C2})C_2D^2]L_1$, $d_2 = [(r_{C2}RC_2 + L_2)(1-D) + (r_{C2} + R)r_{C1}C_1D + (R + r_{C1}D)r_{C2}C_2](1-D) + L_1D^2$.

IV. SIMULATION RESULTS

Fig. 3 shows Bode plots of $G_{dv}(s)$ in (20), $G_{vv}(s)$ in (21), and $G_{zv}(s)$ in (22) generated with MATLAB. To plot these transfer functions, the following converter parameters are used: L_1=100μH, C_1=100μF, r_{C1}=0.19Ω, L_2=55μH, C_2=200μF, r_{C2}=0.095Ω, V_g=15V, V_O=5V, I_Z=0, and R=1Ω. All the three transfer functions have the same four complex poles: $p_{1,2}$=(2.5234±9.4385i)x10^3 and $p_{3,4}$=(1.7028±7.0112i)x10^3. $G_{dv}(s)$ has one real and two complex zeros: z_1= 5.2632x10^4 and $z_{2,3}$=(0.0301±0.8655i)x10^4. $G_{vv}(s)$ has one real and two complex zeros: z_1= 5.2632x10^4 and $z_{2,3}$=(0.0717±0.8630i)x10^4. $G_{zv}(s)$ has two real and two complex zeros: z_1= 5.2632x10^4, z_2= 0.0969x10^4, and $z_{3,4}$=(0.0670±0.8193i)x10^4.

Fig. 4(a) shows a start-up transient of the converter simulated with MATLAB using (18) and (19). The output voltage is settled to about 5V, approximately 4ms after V_g was applied. This result agrees well with the PSPICE simulation result of the Zeta converter using an ideal switch shown in Fig. 4(b), confirming the accuracy of the derived model.

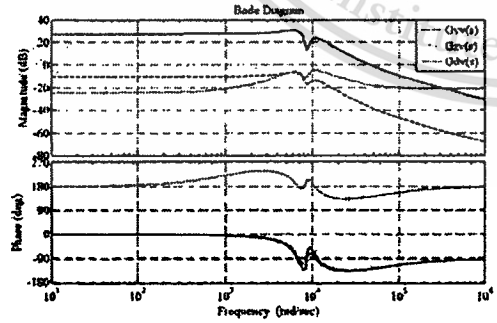

Fig. 3. Frequency responses of $G_{vv}(s)$, $G_{zv}(s)$, and $G_{dv}(s)$.

V. CONCLUSION

In this paper, dynamic modeling of a Zeta converter has been performed with the State-Space Averaging (SSA) technique. The results yield an insight into the steady-state and small-signal dynamic properties of the converter as shown by (17), (18), and (19) respectively. To provide a basis for feedback control design, three relevant transfer functions ($G_{dv}(s)$, $G_{vv}(s)$, and $G_{zv}(s)$) were derived and their Bode plots presented. Finally, simulation results are given to validate the small-signal dynamic model of the Zeta converter.

REFERENCES

[1] R. W. Erickson and D. Maksimović, *Fundamentals of Power Electronics*, 2nd ed., Kluwer Academic Publishers, 2001.

[2] R. D. Middlebook and S. Cuk, "A General Unified Approach to Modeling Switching-Converter Power Stages," *International Journal of Electronics*, vol. 42, pp. 521-550, June 1977.

[3] N. Mohan, T. M. Undeland, and W. P. Robbins, *Power Electronics, Converter, Applications, and Design*, 3rd ed., John Wiley and Sons Inc, 2003.

[4] M. H. Rashid, *Power Electronics Handbook: Devices, Circuits, and Applications*, 2nd ed., Elsevier Inc, 2007.

[5] R. Ridley, "Analyzing the Sepic Converter," *Power Systems Design Europe Magazine*, pp. 14-18, November 2006.

[6] A. Hren and P. Slibar, "Full Order Dynamic Model of SEPIC Converter," *Proc. of the IEEE International Symposium on Industrial Electronics*, pp. 553-558, June 2005.

[7] P. R. K. Chetty, "Modeling and Analysis of Cuk Converter Using Current-Injected Equivalent Circuit Approach," *IEEE trans. on Industrial Electronics*, pp. 56-59, February 1983.

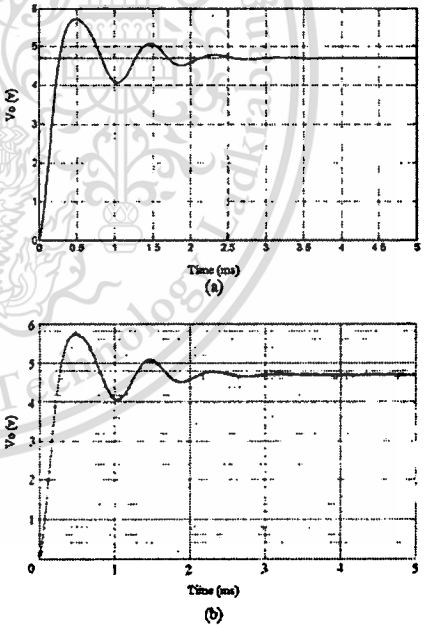

Fig. 4. Output voltage start-up transient simulation: (a) MATLAB and (b) PSPICE.

Dynamic Modeling and Control of a Zeta Converter

E. Vuthchhay[1], C. Bunlaksananusorn[1], and H. Hirata[2]

[1] Faculty of Engineering, King Mongkut's Institute of Technology Ladkrabang (KMITL), Bangkok 10520, Thailand
[2] Department of Applied Computer Engineering, Tokai University, Kanagawa 259-1292, Japan

***Abstract*— A Zeta converter is a fourth-order dc-dc converter made up of two inductors and two capacitors and capable of operating in either step-up or step-down mode. Compared with other converters in the same class, such as Cuk and Sepic converters, the Zeta converter has received the least attention, and more importantly, its dynamic modeling and control have never been reported before in the literature. This paper presents dynamic modeling and control of a Zeta converter. The State-Space Averaging (SSA) technique is applied to find small-signal linear dynamic model of the converter, whereby various transfer functions of the converter can be determined. Based on the control-to-output transfer function, the compensator in PWM feedback loop can be designed to regulate the output voltage. Simulation results show that the converter exhibits good performance during a start-up and step load change.**

I. Introduction

Nowadays, a dc-dc converter is widely used as a power supply in electronic systems. The converter incorporates feedback control to regulate its output voltage. However, the changes in an input voltage and/or load current will cause the converter's output voltage to deviate from the desired value. It is a task of the feedback control to correct this error and quickly bring the output voltage back into the regulated level. Modeling plays a key role in revealing the insight of the converter's dynamic behavior as well as providing a basis for feedback control design. In the last two decades, there has been a continually active research on dc-dc converters; as a consequence, several modeling methods have been proposed [1]. Among them, State-Space Averaging (SSA) technique [2] is one of the best-known methods. It provides a systematic way to model the converter and has gained widespread acceptance. The SSA modeling technique consists of three stages: (1) Formulation of the state-space equations of the converter for each subinterval in a switching cycle, (2) Average of these equations to get a single averaged state-space equation, and (3) Perturbation of the averaged equation to get a linear small-signal state-space equation, from which various transfer functions of the converter can be determined. Since the SSA is a matrix-based technique, i.e. all the steps above are carried out in a matrix form, formal matrix treatment can be applied to facilitate the modeling process.

The SSA technique was commonly used to model the second-order converters such as buck, boost, and buck-boost converters [2-4]. The modeling of the fourth-order converters such as Cuk and Sepic converters has also been studied [5-7]; however, the used techniques were based on circuit averaging. Like Cuk and Sepic converters, a Zeta converter is the fourth-order converter made up of two inductors and two capacitors and capable of working in either step-up or step-down mode. So far, the dynamic modeling and control of the Zeta converter have never been reported before in the literature. This paper, therefore, presents dynamic modeling and control of a Zeta converter. The SSA technique [2] is applied to find small-signal linear dynamic model of the converter, whereby the various transfer functions of the converter can be determined. Of these, the control-to-output transfer function is used for feedback control design. This transfer function has two pairs of the complex poles on the left half plane and a pair of the complex zeros which can locate either on the left or right half plane, depending on the circuit parameters. The Right-Half-Plane (RHP) zeros are undesirable because they cause extra 360 degrees phase-lag to the control-to-output transfer function. In this paper, the condition to avoid the RHP zeros is established. Finally, based on the control-to-output transfer function, the compensator in PWM feedback loop is designed to regulate an output voltage of the converter.

II. Overview of SSA Technique

For dc-dc converters operating in Continuous Conduction Mode (CCM), there exist two circuit states within one switching period, T. One is when the MOSFET is turned on for an interval dT, and another is when the MOSFET is turned off for an interval (1-d)T, where d is a duty cycle. The state-space equations for these two circuit states are represented by:

$$\begin{cases} \dfrac{d\mathbf{x}(t)}{dt} = \mathbf{A}_1\mathbf{x}(t) + \mathbf{B}_1\mathbf{u}(t) \\ \mathbf{y}(t) = \mathbf{C}_1\mathbf{x}(t) + \mathbf{E}_1\mathbf{u}(t) \end{cases} \quad (1)$$

$$\begin{cases} \dfrac{d\mathbf{x}(t)}{dt} = \mathbf{A}_2\mathbf{x}(t) + \mathbf{B}_2\mathbf{u}(t) \\ \mathbf{y}(t) = \mathbf{C}_2\mathbf{x}(t) + \mathbf{E}_2\mathbf{u}(t) \end{cases} \quad (2)$$

To find the averaged behavior of the converter over one switching period, (1) and (2) are weighed average by the duty cycle:

$$\begin{cases} \dfrac{d\mathbf{x}(t)}{dt} = \mathbf{A}_s\mathbf{x}(t) + \mathbf{B}_s\mathbf{u}(t) \\ \mathbf{y}(t) = \mathbf{C}_s\mathbf{x}(t) + \mathbf{E}_s\mathbf{u}(t) \end{cases} \quad (3)$$

where

$\mathbf{A}_s = \mathbf{A}_1 d + \mathbf{A}_2(1-d)$, $\mathbf{B}_s = \mathbf{B}_1 d + \mathbf{B}_2(1-d)$, $\mathbf{C}_s = \mathbf{C}_1 d + \mathbf{C}_2(1-d)$, and $\mathbf{E}_s = \mathbf{E}_1 d + \mathbf{E}_2(1-d)$.

Equation (3) is a nonlinear continuous-time equation. It can be linearized by small-signal perturbation with $\mathbf{x} = \mathbf{X} + \tilde{\mathbf{x}}$, $\mathbf{y} = \mathbf{Y} + \tilde{\mathbf{y}}$, $\mathbf{u} = \mathbf{U} + \tilde{\mathbf{u}}$, and $d = D + \tilde{d}$, where the ~ symbol

978-1-4244-2336-1/08/$25.00 © 2008 IEEE

represents a small signal value and the capital letter a dc value. It should be noted that $X >> \tilde{x}$, $Y >> \tilde{y}$, $U >> \tilde{u}$, and $D >> \tilde{d}$. The perturbation yields the steady-state and linear small-signal state-space equations in (4) and (5) respectively.

$$\begin{cases} \dfrac{dX}{dt} = AX + BU = 0 \\ Y = CX + EU \end{cases} \tag{4}$$

$$\begin{cases} \dfrac{d\tilde{x}(t)}{dt} = A\tilde{x}(t) + B\tilde{u}(t) + B_d\tilde{d}(t) \\ \tilde{y}(t) = C\tilde{x}(t) + E\tilde{u}(t) + E_d\tilde{d}(t) \end{cases} \tag{5}$$

where

$A = A_1D + A_2(1-D)$, $B = B_1D + B_2(1-D)$, $C = C_1D + C_2(1-D)$,

$E = E_1D + E_2(1-D)$, $B_d = (A_1 - A_2)X + (B_1 - B_2)U$, and

$E_d = (C_1 - C_2)X + (E_1 - E_2)U$.

The steady-state solution of the converter can be found by solving (4), which gives:

$$\begin{cases} X = -A^{-1}BU \\ Y = (-CA^{-1}B + E)U \end{cases} \tag{6}$$

The small-signal transfer function of the converter can be found by applying the Laplace transform to (5). In a matrix form, we get:

$$\begin{cases} \tilde{x}(s) = \left[(sI - A)^{-1}B \quad (sI - A)^{-1}B_d\right]\begin{bmatrix} \tilde{u}(s) \\ \tilde{d}(s) \end{bmatrix} \\ \tilde{y}(s) = \left[C(sI - A)^{-1}B + E \quad C(sI - A)^{-1}B_d + E_d\right]\begin{bmatrix} \tilde{u}(s) \\ \tilde{d}(s) \end{bmatrix} \end{cases} \tag{7}$$

In the dc-dc converters, the input variable $\tilde{u}$ usually contains the input voltage and load current. Hence, $\tilde{u}$ is express as $\tilde{u} = [u_1 \; u_2]^T$, the matrix B as $B = [B_{u1} \; B_{u2}]$, and the matrix E as $E = [E_{u1} \; E_{u2}]$. Therefore, (7) becomes:

$$\begin{cases} \tilde{x}(s) = \left[(sI - A)^{-1}B_{u1} \quad (sI - A)^{-1}B_{u2} \quad (sI - A)^{-1}B_d\right]\begin{bmatrix} \tilde{u}_1(s) \\ \tilde{u}_2(s) \\ \tilde{d}(s) \end{bmatrix} \\ \tilde{y}(s) = \left[C(sI - A)^{-1}B_{u1} + E_{u1} \quad C(sI - A)^{-1}B_{u2} + E_{u2} \quad C(sI - A)^{-1}B_d + E_d\right]\begin{bmatrix} \tilde{u}_1(s) \\ \tilde{u}_2(s) \\ \tilde{d}(s) \end{bmatrix} \end{cases} \tag{8}$$

For the fourth-order converter, $(sI–A)^{-1}B_{u1}$, $(sI–A)^{-1}B_{u2}$, and $(sI–A)^{-1}B_d$ are the matrices that have four rows and one column. So, (8) can be expanded into:

$$\begin{cases} \tilde{x}(s) = \begin{bmatrix} G_{vd_1}(s) & G_{vi_1}(s) & G_{di_1}(s) \\ G_{vd_2}(s) & G_{vi_2}(s) & G_{di_2}(s) \\ G_{vv_1}(s) & G_{iv_1}(s) & G_{di_1}(s) \\ G_{vv_2}(s) & G_{iv_2}(s) & G_{di_2}(s) \end{bmatrix}\begin{bmatrix} \tilde{u}_1(s) \\ \tilde{u}_2(s) \\ \tilde{d}(s) \end{bmatrix} \\ \tilde{y}(s) = \left[G_{vv}(s) \quad G_{iv}(s) \quad G_{dv}(s)\right]\begin{bmatrix} \tilde{u}_1(s) \\ \tilde{u}_2(s) \\ \tilde{d}(s) \end{bmatrix} \end{cases} \tag{9}$$

where

$G_{vd_1}(s) = [(sI - A)^{-1}B_{u1}]_{11}$, $G_{vi_1}(s) = [(sI - A)^{-1}B_{u2}]_{11}$, $G_{di_1}(s) = [(sI - A)^{-1}B_d]_{11}$,

$G_{vd_2}(s) = [(sI - A)^{-1}B_{u1}]_{21}$, $G_{vi_2}(s) = [(sI - A)^{-1}B_{u2}]_{21}$, $G_{di_2}(s) = [(sI - A)^{-1}B_d]_{21}$,

$G_{vv_1}(s) = [(sI - A)^{-1}B_{u1}]_{31}$, $G_{iv_1}(s) = [(sI - A)^{-1}B_{u2}]_{31}$, $G_{dv_1}(s) = [(sI - A)^{-1}B_d]_{31}$,

$G_{vv_2}(s) = [(sI - A)^{-1}B_{u1}]_{41}$, $G_{iv_2}(s) = [(sI - A)^{-1}B_{u2}]_{41}$, $G_{dv_2}(s) = [(sI - A)^{-1}B_d]_{41}$,

$G_{vv}(s) = C(sI - A)^{-1}B_{u1} + E_{u1}$, $G_{iv}(s) = C(sI - A)^{-1}B_{u2} + E_{u2}$, and

$G_{dv}(s) = C(sI - A)^{-1}B_d + E_d$

III. Modeling of a Zeta Converter By SSA Technique

A Zeta converter is shown in Fig. 1(a). It is comprised of the MOSFET switch (Q), diode (D), two capacitors (C_1 and C_2), and two inductors (L_1 and L_2). The resistor, R, represents a standing load, and the current source, I_z, models the load current. The resistors, r_{C1}, r_{C2}, r_{L1}, and r_{L2}, are an equivalent series resistance of the capacitors and inductors respectively. Their values are usually very small, compared to R. In the ideal converter, these equivalent series resistance will be zero.

In CCM, the converter exhibits two circuit states. The first state is when the MOSFET switch is turned on (Fig. 1(b)). During this interval (dT), the inductors L_1 and L_2 are in a charging phase, and hence i_{L1} and i_{L2} increase linearly as shown in Fig. 2. The second state is when the MOSFET switch is turned off (Fig. 1(c)). During this interval ((1-d)T), L_1 and L_2 are in a discharging phase; L_1 discharges the stored energy to C_1, and L_2 discharges the stored energy to output section. Thus, i_{L1} and i_{L2} decrease linearly as shown in Fig. 2.

The output voltage, V_O, is a dc voltage that contains small ripple due to the switching action. For the ideal Zeta converter, the relationship between V_O and V_g is given by:

$$M = \frac{V_o}{V_g} = \frac{D}{1-D} \tag{10}$$

where M is a voltage conversion ratio. It can be seen that V_O could be larger or smaller than V_g, depending on the duty cycle. From Fig. 2., the averaged inductor currents, I_{L1} and I_{L2}, must be greater than one-half of their ripple components, Δi_{L1} and Δi_{L2}, for the circuit to remain in CCM [8]. It can be shown that for CCM operation L_1 and L_2 must satisfy the following conditions:

$$\begin{cases} L_1 > \dfrac{(1-D)^2 R}{2Df}\left(1 + \dfrac{r_{L2}}{R} + \dfrac{r_{C1}}{R}\dfrac{D}{1-D}\right) \\ L_2 > \dfrac{(1-D)R}{2f}\left(1 + \dfrac{r_{L2}}{R}\right) \end{cases} \tag{11}$$

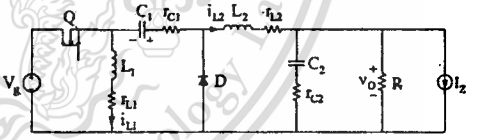

(a) Zeta converter.

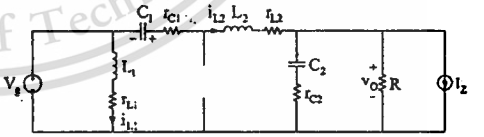

(b) Zeta converter when MOSFET is turned on.

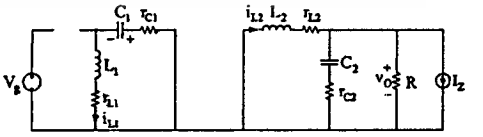

(c) Zeta converter when MOSFET is turned off.

Fig. 1. Operation of Zeta converter.

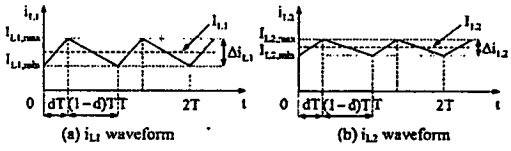

Fig. 2. Current waveforms.

A. State-Space Description

The state-space equations of the Zeta converter for the on and off states of the switch can be written from Fig. 1(b) and (c) respectively, which is given in (12):

$$\begin{aligned}
\frac{di_{L1}}{dt} &= \frac{r_{C1}}{L_1}(\delta-1)i_{L1} - \frac{r_{L1}}{L_1}+\frac{v_{C1}}{L_1}(\delta-1)+\frac{V_g}{L_1}\delta \\
\frac{di_{L2}}{dt} &= \frac{-1}{L_2}(r_{L1}-r_{C1}\delta+\frac{r_{C2}R}{r_{C2}+R})i_{L2}+\frac{v_{C1}}{L_2}\delta-\frac{R}{L_2(r_{C2}+R)}v_{C1}+\frac{V_g}{L_2}\delta+\frac{r_{C2}R}{L_2(r_{C2}+R)}I_Z \\
\frac{dv_{C1}}{dt} &= \frac{i_{L1}}{C_1}(1-\delta)-\frac{i_{L2}}{C_1}\delta \\
\frac{dv_{C2}}{dt} &= \frac{R}{C_2(r_{C2}+R)}i_{L2}-\frac{1}{C_2(r_{C2}+R)}v_{C2}-\frac{R}{C_2(r_{C2}-R)}I_Z \\
v_O &= \frac{r_{C2}R}{r_{C2}+R}i_{L2}+\frac{R}{r_{C2}-R}v_{C2}-\frac{r_{C2}R}{r_{C2}+R}I_Z
\end{aligned} \tag{12}$$

Note that the equations are expressed in a compact form using the switching function, δ. When the switch is on, δ =1, (12) will become the on-state equation. When the switch is off, δ =0, (12) will become the off-state equation.

The averaged matrices for the steady-state and the linear small-signal state-space equations can be written according to (4) and (5).

$$\mathbf{A}=\begin{bmatrix}
-\frac{r_{C1}(1-D)+r_{L1}}{L_1} & 0 & -\frac{1-D}{L_1} & 0 \\
0 & -\frac{(r_{C2}+R)(Dr_{C1}+r_{L2})+r_{C2}R}{L_2(r_{C2}+R)} & \frac{D}{L_2} & \frac{-R}{L_2(r_{C2}+R)} \\
\frac{1-D}{C_1} & \frac{-D}{C_1} & 0 & 0 \\
0 & \frac{R}{C_2(r_{C2}-R)} & 0 & \frac{-1}{C_2(r_{C2}-R)}
\end{bmatrix} \tag{13}$$

$$\mathbf{B}=\begin{bmatrix}
\frac{D}{L_1} & 0 \\
\frac{D}{L_2} & \frac{r_{C2}R}{L_2(r_{C2}+R)} \\
0 & 0 \\
0 & \frac{-R}{C_2(r_{C2}+R)}
\end{bmatrix} \tag{14}$$

$$\mathbf{C}=\begin{bmatrix} 0 & \frac{r_{C2}R}{r_{C2}+R} & 0 & \frac{r_{C2}R}{r_{C2}+R} \end{bmatrix} \tag{15}$$

$$\mathbf{E}=\begin{bmatrix} 0 & \frac{-r_{C2}R}{r_{C2}+R} \end{bmatrix} \tag{16}$$

$$\mathbf{B}_d=\frac{\eta}{R(1-D)^2}\begin{bmatrix}
\frac{1}{L_1}[V_g[(1-D)(R+r_{L2})+Dr_{C1}]-I_Z Dr_{L1}R] \\
\frac{1}{L_2}[V_g(r_{L2}+R)(1-D)-[r_{C1}(1-D)+Dr_{L1}]RI_Z] \\
\frac{-1}{C_1}[DV_g+RI_Z(1-D)] \\
0
\end{bmatrix} \tag{17}$$

$$\mathbf{E}_d=[0] \tag{18}$$

B. Steady-State Equations

Given the averaged matrices from (13) to (18), the steady-state solution of the converter can be obtained from (6):

$$\begin{cases}
\begin{bmatrix} I_{L1} \\ I_{L2} \\ V_{C1} \\ V_{C2} \end{bmatrix} = M\eta\begin{bmatrix}
\frac{D}{R(1-D)} & 1 \\
\frac{1}{R} & \frac{1}{M} \\
1+\frac{r_{L2}}{R}-\frac{r_{L1}}{R}M & -(r_{C1}+r_{L1}\frac{1}{1-D}) \\
1 & -(r_{C1}+r_{L1}M+r_{L2}\frac{1}{M})
\end{bmatrix}\begin{bmatrix} V_g \\ I_Z \end{bmatrix} \\
V_O=[V_g-I_Z(r_{C1}+r_{L1}M+r_{L2}\frac{1}{M})]M\eta
\end{cases} \tag{19}$$

where $\eta=\dfrac{1}{1+\frac{r_{L2}}{R}+\frac{r_{C1}}{R}M+\frac{r_{L1}}{R}M^2}$ and $M=\dfrac{D}{1-D}$.

Notice that if r_{C1}, r_{C2}, r_{L1}, and r_{L2} are assumed to be zero, the output equation in (19) will be reduced to $M=V_O/V_g=D/(1-D)$, the same as the expression for the ideal converter in (10).

C. Linear Small-Signal State-Space Equations

Given the averaged matrices (13) to (18), the linear small-signal state-space equations of the Zeta converter can be formulated in according with (5):

$$\begin{aligned}
\frac{d}{dt}\begin{bmatrix} \tilde{i}_{L1}(t) \\ \tilde{i}_{L2}(t) \\ \tilde{v}_{C1}(t) \\ \tilde{v}_{C2}(t) \end{bmatrix} &= \begin{bmatrix}
-\frac{r_{C1}(1-D)+r_{L1}}{L_1} & 0 & -\frac{1-D}{L_1} & 0 \\
0 & -\frac{(r_{C2}+R)(Dr_{C1}+r_{L2})+r_{C2}R}{L_2(r_{C2}+R)} & \frac{D}{L_2} & \frac{-R}{L_2(r_{C2}+R)} \\
\frac{1-D}{C_1} & -\frac{D}{C_1} & 0 & 0 \\
0 & \frac{R}{C_2(r_{C2}+R)} & 0 & \frac{1}{C_2(r_{C2}+R)}
\end{bmatrix}\begin{bmatrix} \tilde{i}_{L1}(t) \\ \tilde{i}_{L2}(t) \\ \tilde{v}_{C1}(t) \\ \tilde{v}_{C2}(t) \end{bmatrix} + \\
&\begin{bmatrix}
\frac{D}{L_1} & 0 & \frac{\eta[V_g[(1-D)(R+r_{L2})+Dr_{C1}]-I_Z Dr_{L1}R]}{L_1R(1-D)^2} \\
\frac{D}{L_2} & \frac{r_{C2}R}{L_2(r_{C2}+R)} & \frac{\eta[V_g(r_{L2}+R)(1-D)-I_Z R[r_{C1}(1-D)+Dr_{L1}]]}{L_2R(1-D)^2} \\
0 & 0 & \frac{-\eta[DV_g+RI_Z(1-D)]}{C_1R(1-D)^2} \\
0 & -\frac{R}{C_2(r_{C2}+R)} & 0
\end{bmatrix}\begin{bmatrix} \tilde{v}_g(t) \\ \tilde{i}_Z(t) \\ \tilde{d}(t) \end{bmatrix}
\end{aligned} \tag{20}$$

$$\tilde{v}_O(t)=\begin{bmatrix} 0 & \frac{r_{C2}R}{r_{C2}+R} & 0 & \frac{r_{C2}R}{r_{C2}+R} \end{bmatrix}\begin{bmatrix} \tilde{i}_{L1}(t) \\ \tilde{i}_{L2}(t) \\ \tilde{v}_{C1}(t) \\ \tilde{v}_{C2}(t) \end{bmatrix}+\begin{bmatrix} 0 & \frac{-r_{C2}R}{r_{C2}+R} & 0 \end{bmatrix}\begin{bmatrix} \tilde{v}_g(t) \\ \tilde{i}_Z(t) \\ \tilde{d}(t) \end{bmatrix}$$

D. Finding Transfer Functions

Referring to (9), fifteen transfer functions can be determined from (20). However, only a few of them are useful for feedback control design. These transfer functions are:

The duty ratio-to-output voltage transfer function

$$\begin{aligned}
G_{dv}(s)&=\frac{\tilde{v}_O(s)}{\tilde{d}(s)}=\mathbf{C}(s\mathbf{I}-\mathbf{A})^{-1}\mathbf{B}_d+\mathbf{E}_d \\
&=\frac{\eta}{(1-D)^2}\frac{(a_{dv}s^2+b_{dv}s+c_{dv})(d_{dv}s+1)}{as^4+bs^3+cs^2+ds+e}
\end{aligned} \tag{21}$$

The input voltage-to-output voltage transfer function

$$\begin{aligned}
G_{vv}(s)&=\frac{\tilde{v}_O(s)}{\tilde{v}_g(s)}=\mathbf{C}(s\mathbf{I}-\mathbf{A})^{-1}\mathbf{B}_{v1}+\mathbf{E}_{v1} \\
&=DR\frac{(a_{vv}s^2+b_{vv}s+c_{vv})(d_{vv}s+1)}{as^4+bs^3+cs^2+ds+e}
\end{aligned} \tag{22}$$

The output impedance transfer function

$$\begin{aligned}
G_{zv}(s)&=\frac{\tilde{v}_O(s)}{\tilde{i}_Z(s)}=\mathbf{C}(s\mathbf{I}-\mathbf{A})^{-1}\mathbf{B}_{v2}+\mathbf{E}_{v2} \\
&=-R\frac{(a_{zv}s^2+b_{zv}s+c_{zv})(d_{zv}s+1)}{as^4+bs^3+cs^2+ds+e}
\end{aligned} \tag{23}$$

The coefficients in (21) to (23) are listed in TABLE I.

TABLE I
COEFFICIENTS OF $G_{dv}(s)$, $G_{zv}(s)$, AND $G_{vv}(s)$.

$a_{dv} = L_1C_1[V_g(1-D)(R+r_{L2}) - I_2R\{(1-D)r_{C1} + Dr_{L1}\}$, $b_{dv} = -V_g[L_1D^2 - C_1(1-D)(R+r_{L2})\{(1-D)r_{C1} + r_{L1}\}]$ $-I_2R[L_1D(1-D) + r_{C1}^2C_1(1-D)^2 + r_{L1}C_1\{r_{C1} + r_{L1}D - D^2r_{C1}\})]$, $c_{dv} = V_g[(1-D)^2(R+r_{L2}) - D^2r_{L1}] - I_2R(1-D)\{2Dr_{L1} + r_{C1}(1-D)\}$, $d_{dv} = C_2r_{C2}$.
$a_{zv} = C_1L_1$, $b_{zv} = C_1\{r_{L1} + r_{C1}(1-D)\}$, $c_{zv} = 1-D$, $d_{zv} = C_2r_{C2}$.
$a_{vv} = L_1L_2C_1C_2r_{C2}$, $e_{vv} = r_{C1}D(1-D) + r_{L1}D^2 + r_{L2}(1-D)^2$, $b_{vv} = L_1C_1(L_2 + Dr_{C2}r_{C1}C_2) + (1-D)r_{C1}r_{C2}L_1C_1C_2 + (L_1r_{L2} + L_2r_{L1})r_{C2}C_1C_2$, $c_{vv} = (1-D)[(1-D)r_{C2}L_2C_2 + r_{C1}C_1\{L_2 + Dr_{C1}r_{C2}C_2 + r_{C2}r_{L2}C_2\}] + L_1D\{Dr_{C2}C_2 + r_{C1}C_1\}$ $+C_1\{r_{L1}r_{C2}C_2(r_{C1}D + r_{L1}) + r_{L1}L_2 + r_{L2}L_1\}$, $d_{vv} = L_1D^2 + (1-D)[(1-D)\{L_2 + r_{C2}r_{L2}C_2\} + Dr_{C1}(r_{C1}C_1 + r_{C2}C_2) + r_{C1}r_{L2}C_1$ $+r_{L1}\{C_1r_{L2} + C_1Dr_{C1} + r_{C2}D^2C_2\}$.
$a = L_1C_1L_2C_2(R + r_{C2})$, $e = (1-D)^2(R + r_{L2}) + r_{C1}D(1-D) + r_{L1}D^2$, $b = L_1C_1(L_2 + r_{C2}C_2R) + C_1(R + r_{C2})[r_{C1}L_2C_2(1-D) + Dr_{C1}L_1C_2 + C_2(r_{L2}L_1 + r_{L1}L_2)]$ $c = (1-D)[\{(1-D)I_2 + (Dr_{C1} + r_{L2})r_{C1}C_1\}\{r_{C2} + R\}C_2 + r_{C1}C_1(r_{C2}C_2R + I_2)]$ $+C_2(r_{C2} + R)[L_1D^2 + (Dr_{C1} + r_{L2})r_{L1}C_1] + C_1[L_1(Dr_{C1} + R) + r_{L1}L_2 + r_{L2}L_1 + r_{L1}r_{C2}C_2R]$, $d = L_1D^2 + (1-D)^2[L_2 + r_{C2}C_2R + r_{L2}C_2(R + r_{C2})] + [r_{C1}(1-D) + r_{L1}D]\{R + r_{C2}\}DC_2$ $+\{(1-D)r_{C1} + r_{L2}\}\{r_{L2} + Dr_{C1} + R\}C_1$.

IV. PWM FEEDBACK CONTROL

A. Description of PWM Feedback Control

Fig. 3 (a) shows feedback control of a Zeta converter with PWM technique. The output voltage, v_O, is fed back and compared with the reference voltage, V_{ref}. The resulting error voltage is processed by a controller, $G_C(s)$, which produces the control voltage, v_C, to compare with the sawtooth voltage, v_{saw}, at the PWM comparator. As shown in Fig. 3 (b), the MOSFET is turned on when v_C is larger than v_{saw}, and turned off when v_C is smaller than v_{saw}. If v_O is changed, feedback control will respond by adjusting v_C and the duty cycle of the MOSFET until v_O is again equal to V_{ref}.

Fig. 4 shows a small-signal block diagram of the converter in Fig. 3 (a) The power stage is represented by the three transfer functions: $G_{dv}(s)$, $G_{vv}(s)$, and $G_{zv}(s)$ derived earlier. The transfer function of the PWM comparator can be derived from the waveform in Fig. 3 (b). It is given by:

$$F_M = \frac{\tilde{d}(s)}{\tilde{v}_C(s)} = \frac{1}{V_M} \tag{24}$$

where V_M is an amplitude of the sawtooth voltage. $G_C(s)$ is a controller or compensator. From Fig. 4, the open loop transfer function is defined as:

$$T(s) = G_C(s)G_{dv}(s)F_M \tag{25}$$

Given $G_{dv}(s)$ in (21) and F_M in (24), we can design the compensator $G_C(s)$ by appropriately selecting its poles and zeros so that (25) has high dc gain and reasonable crossover frequency, while possessing sufficient amount of phase margin [1].

Before proceeding to design the compensator, it is worthwhile to firstly examine the transfer function $G_{dv}(s)$ in (21), which has three zeros and four poles. It can be proved by the Routh-Hurwitz criterion [9] that all the poles of $G_{dv}(s)$ are located on the left half plane. The $d_{dv}s+1$ term on the numerator always gives the Left-Half-Plane (LHP) zero since d_{dv} is positive. However, there is a possibility that the quadratic term, $a_{dv}s^2+b_{dv}s+c_{dv}$ can yield a pair of Right-Half-Plane (RHP) zeros. The RHP zeros are undesirable because they contribute additional 360 degrees phase-lag to $G_{dv}(s)$, making feedback loop compensation very difficult. The LHP zeros from the quadratic term are given by:

$$s_{z1,2} = \frac{-b_{dv} \pm \sqrt{b_{dv}^2 - 4a_{dv}c_{dv}}}{2a_{dv}} < 0 \tag{26}$$

It can be proved that (26) yields only a complex conjugate, not real number. Hence, to avoid the RHP zeros, the following conditions must be satisfied:

$$\begin{cases} b_{dv}^2 < 4a_{dv}c_{dv} \\ b_{dv} > 0 \end{cases} \tag{27}$$

where

$a_{dv} = L_1C_1V_g(1-D)(R+r_{L2})$, $c_{dv} = V_g[(1-D)^2(R+r_{L2}) - D^2r_{L1}]$, and $b_{dv} = -V_g[L_1D^2 - C_1(1-D)(R+r_{L2})\{(1-D)r_{C1} + r_{L1}\}]$.

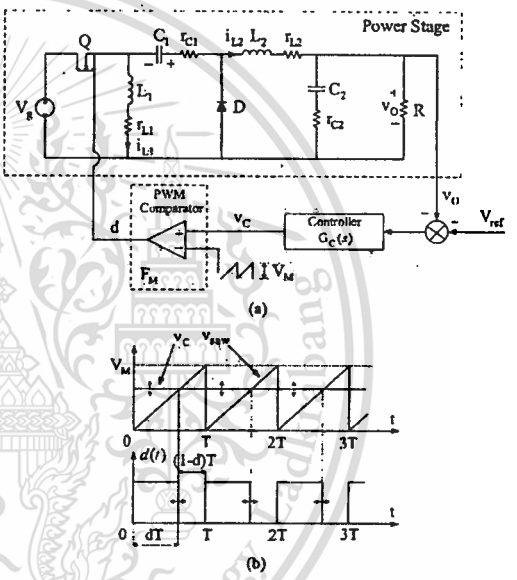

Fig. 3 (a) Zeta converter with PWM feedback control
(b) Waveforms of PWM comparator.

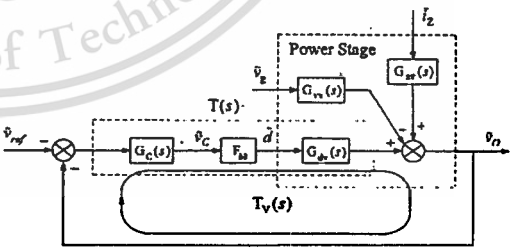

Fig. 4. Small-signal block diagram of Zeta converter with PWM feedback control.

B. *Feedback Loop Compensation*

The compensator design is illustrated with the Zeta converter whose circuit parameters are as shown in Table II. It should be noted that these parameters satisfy both the condition for CCM in (11) and the condition for LHP zeros in (27). Since both the input voltage and load current can vary, the design is performed for the worst case condition, which occurs when Vg = 15V and R = 1Ω. Substituting the relevant parameters from TABLE II into (21) and (24), the product $T_U(s)=F_M G_{dv}(s)$ can be found:

$$T_U(s)=\frac{1.648\text{x}10^4 s^3+8.774\text{x}10^8 s^2+1.758\text{x}10^{12}s+6.505\text{x}10^{16}}{s^4+8452s^3+1.647\text{x}10^8 s^2+5.878\text{x}10^{11}s+4.969\text{x}10^{15}} \quad (28)$$

A PI compensator shown in Fig. 5 has been selected to compensate $T_U(s)$ in (29). Its transfer function is given by:

$$G_C(s)=\frac{z_2}{z_1}=\frac{\omega_o}{s}\left(\frac{s}{\omega_z}+1\right) \quad (29)$$

where $\omega_o=\frac{1}{R_1C_1}$ and $\omega_z=\frac{1}{R_2C_1}$.

The pole at the origin helps increase the low frequency gain of the open-loop transfer function, T(s). The zero, ω_Z, and gain, ω_O, can be tuned to give T(s) the desirable crossover frequency and phase margin respectively.

The design objective here is to achieve T(s) with the crossover frequency of 10kHz and phase margin of more than 45 degrees. To achieve this, the zero of $G_C(s)$ has been set at ω_Z=3x10^{3}rad/s and the gain at ω_O=8.65x10^3 rad/s. Based on these values, PI compensator's component values are calculated, getting: R_1=15KΩ, R_2=43KΩ, and C_1=4.7nF. Substitution of the component values into (30) gives:

$$G_C(s)=\frac{8.65\text{x}10^3}{s}\left(\frac{s}{3\text{x}10^5}+1\right) \quad (30)$$

Fig. 6 shows the bode plots of $G_C(s)$ (dotted line), $T_U(s)$ (dashed line), and T(s) (solid line). It can be seen that T(s) has the phase margin of 53 degrees and crossover frequency of 10KHz, meeting the design objective.

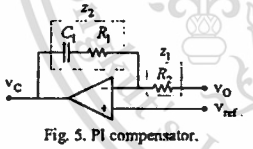

Fig. 5. PI compensator.

TABLE II
CONVERTER PARAMETERS.

Circuit Parameters	Values
V_g	15-20V
V_O	5V
R	1-5Ω
C_1	100μF
C_2	200μF
r_{C1}	0.19Ω
r_{C2}	0.095Ω
L_1	100μH
L_2	55μH
r_{L1}	1mΩ
r_{L2}	0.55mΩ
I_Z	0
V_M	1.8V
T=1/f	10μs

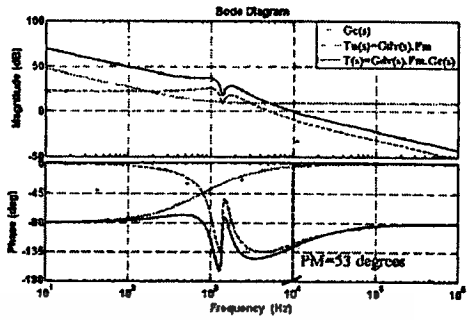

Fig. 6. Bode Plots of $G_C(s)$, $T_U(s)$, and T(s).

V. RESULTS

A SIMULINK model of a PWM controlled Zeta converter is depicted in Fig. 7. The linear small-signal state-space equations in (20), F_M in (24), and $G_C(s)$ in (30) are inputted into the power stage, PWM comparator, and compensator blocks respectively. The mux block combines three input signals (V_g, I_Z, and d) into vector form for using in the power stage block.

Fig. 8 shows the simulated output voltage start-up transient. The output voltage settles to 5V after about 160μs, with the maximum voltage overshoot of 6.3V. Fig. 9 shows the simulated output voltage response, when the load current is switched back and forth between 1A and 3A. The maximum voltage drop/raise during the transient is around 0.28V. The feedback control is able to keep the output voltage at 5V after the transient which lasts about 100μs.

VI. CONCLUSION

In this paper, dynamic modeling and control of a Zeta converter have been presented. The State-Space Averaging (SSA) technique was applied to find the small-signal linear dynamic model of the converter (equation (20)), from which the transfer functions $G_{dv}(s)$ in (21), $G_{vv}(s)$ in (22), and $G_{zv}(s)$ in (23) were derived. $G_{dv}(s)$ was particularly important for feedback control design. The quadratic term on the numerator of $G_{dv}(s)$ could yield the RHP zeros and; to prevent this, the condition in (27) was establish. Based on $G_{dv}(s)$, the compensator in PWM feedback loop was designed to regulate the output voltage. Simulation results show that the converter exhibited good performance during a start-up and step load change.

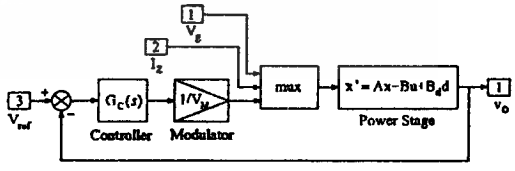

Fig. 7. SIMULINK model of Zeta converter with PWM feedback control.

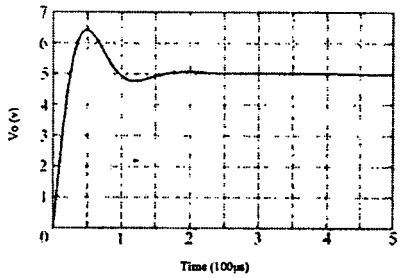

Fig. 8. Output voltage response during a start-up.

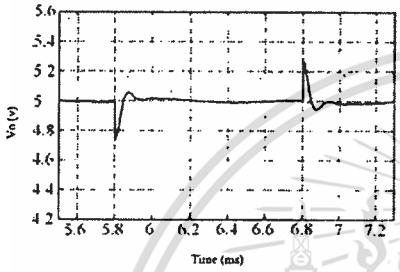

Fig. 9. Output voltage response during the load current back and forth between 1A and 3A.

REFERENCES

[1] R. W. Erickson and D. Maksimović, *Fundamentals of Power Electronics*, 2nd ed., Kluwer Academic Publishers, 2001.

[2] R. D. Middlebook and S. Cuk, "A General Unified Approach to Modeling Switching-Converter Power Stages," *International Journal of Electronics*, vol. 42, pp. 521-550, June 1977.

[3] N. Mohan, T. M. Undeland, and W. P. Robbins, *Power Electronics, Converter, Applications, and Design*, 3rd ed., John Wiley and Sons Inc, 2003.

[4] M. H. Rashid, *Power Electronics Handbook: Devices, Circuits, and Applications*, 2nd ed., Elsevier Inc, 2007.

[5] V. Vorpérian, "The Effect of the Magnetizing Inductance on the Small-Signal Dynamics of the Isolated Cuk Converter," *IEEE trans. on aerospace and electronic systems*, July 1996.

[6] R. Ridley, "Analyzing the Sepic Converter," *Power Systems Design Europe Magazine*, pp. 14-18, November 2006.

[7] A. Hren and P. Slibar, "Full Order Dynamic Model of SEPIC Converter," *Proc. of the IEEE International Symposium on Industrial Electronics*, pp. 553-558, June 2005.

[8] D. W. Hart, *Introduction to Power Electronics*, Prentice Hall Inc, 1997.

[9] B. C. Kuo, *Automatic Control Systems*, 7rd ed., Prentice Hall Inc, 1995.

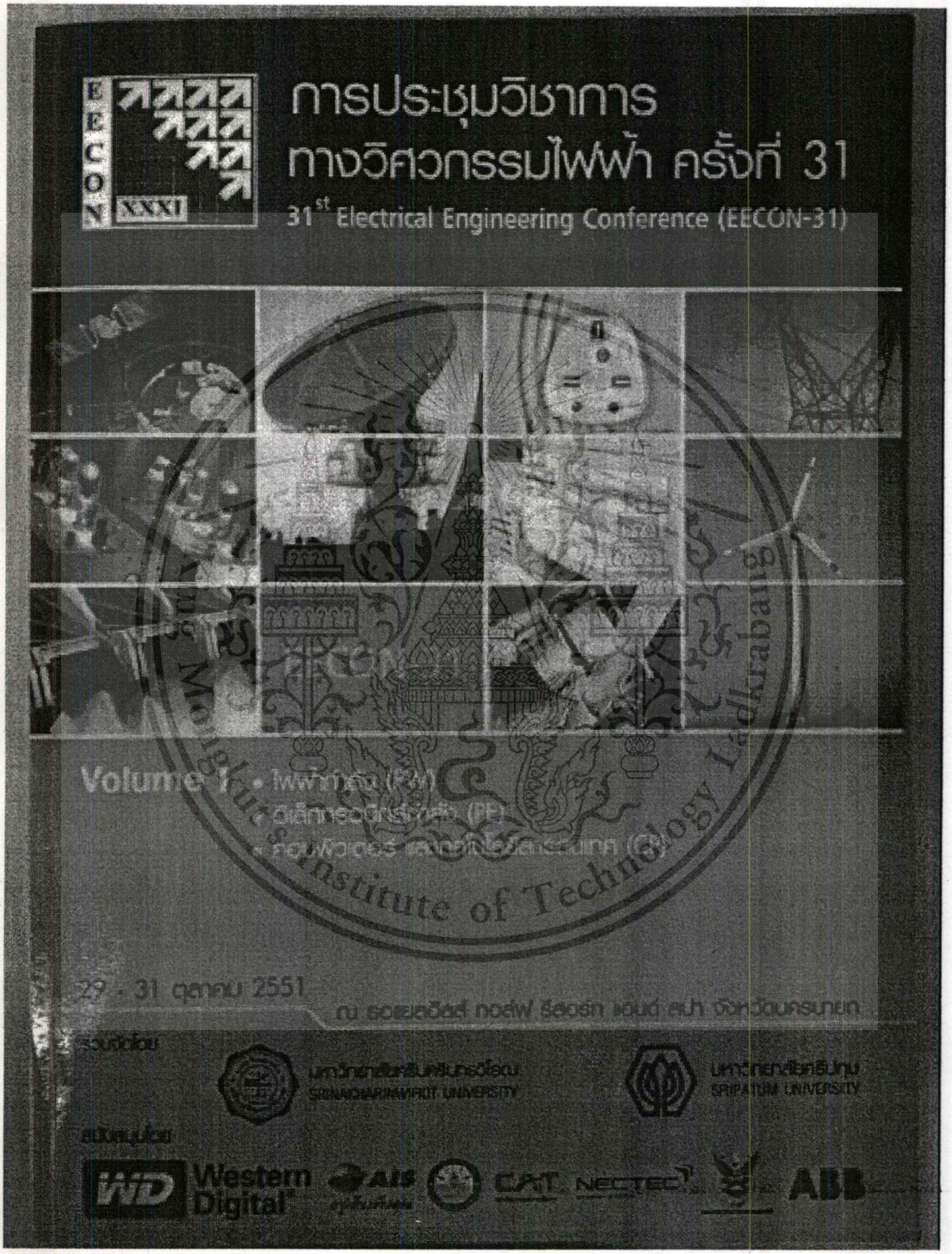

Modeling of a SEPIC Converter for Feedback Control Design

E. Vuthchhay, V. Wutti, and C. Bunlaksananusorn
Faculty of Engineering, King Mongkut's Institute of Technology Ladkrabang (KMITL), Bangkok 10520, Thailand

Abstract

A SEPIC (Single-Ended Primary Inductor Converter) DC-DC converter is capable of operating in either step-up or step-down mode and widely used in battery-operated equipment. Recently, modeling of the SEPIC converter has been performed by replacing the nonlinear switches (i.e. MOSFET and diode) with the PWM switch model [1, 2] and by averaged switch model [3]. This paper presents an alternative method to model the SEPIC converter using the State-Space Averaging (SSA) technique. The modeling leads to a small-signal linear model of the converter, from which the transfer functions used for feedback control design can be determined. Simulation results are presented to verify the accuracy of the obtained model.

1. Introduction

Nowadays, the use of a DC-DC converter is widespread in modern portable electronic equipment and systems. In battery-operated portable devices, when not connected to the AC mains, the battery provides an input voltage to the converter, which then converts it into the output voltage suitable for use by the electronic load. The battery voltage can vary over a wide range, depending on a charge level. At the low charge level, it may drop below the load voltage. Hence, to continue supplying the constant load voltage over the entire battery voltage range, the converter must be able to work in both buck and boost modes. The DC-DC converters that meet this operational requirement are Buck-boost, Cuk, and SEPIC converters. However, the Buck-boost and Cuk converters, in their basic form, produce the output voltage, whose polarity is reversed from the input voltage. The problem can be corrected by incorporating an isolation transformer into the circuits, but this will inevitably lead to the increased size and cost of the converters. On the other hands, the SEPIC (Single-Ended Primary Inductor Converter) converter is capable of operating in both step-up and step-down modes and does not suffer from the polarity reversal problem. It is therefore attractive for the aforementioned application.

The SEPIC converter consists of an active power switch, a diode, two inductors, and two capacitors and is thus a fourth-order nonlinear system. Feedback control is usually incorporated into the converter's circuit to regulate its output voltage, typically by means of Pulse Width Modulation (PWM). To facilitate the feedback controller design or system stability analysis, the linear model of the converter is needed. Recently, modeling of the SEPIC converter has been carried out by some researchers. The linear converter models were found by substitution of the power switch and diode of the converter by the so called small-signal PWM switch model [1, 2] and small-signal averaged switch model [3, 4] respectively. The resulting linear equivalent circuits of the SEPIC converter, however, appeared to be rather complicated. Much effort had to be spent to manipulate and analyze the circuit to find the transfer function of this interest. This paper presents modeling of a SEPIC converter with the State-Space Averaging (SSA) technique [4, 5]. Unlike the PWM and averaged switch model methods, the SSA technique is performed via matrix; hence formal matrix treatment can be applied to facilitate the modeling process. The objective of this paper is to show that the SSA technique is an effective tool to model the SEPIC converter.

2. Overview of SSA Technique

For DC-DC converters operating in Continuous Conduction Mode (CCM), there exist two circuit states within one switching period, T. One is when the MOSFET is turned on for an interval dT, and another is when the MOSFET is turned off for an interval (1-d)T, where d is a duty cycle. The state-space equations for these two circuit states are represented by:

$$\begin{cases} \dfrac{dx(t)}{dt} = A_1 x(t) + B_1 u(t) \\ y(t) = C_1 x(t) + E_1 u(t) \end{cases} \quad (1)$$

$$\begin{cases} \dfrac{dx(t)}{dt} = A_2 x(t) + B_2 u(t) \\ y(t) = C_2 x(t) + E_2 u(t) \end{cases} \quad (2)$$

To find the averaged behavior of the converter over one switching period, (1) and (2) are weighed average by the duty cycle:

$$\begin{cases} \dfrac{dx(t)}{dt} = A_s x(t) + B_s u(t) \\ y(t) = C_s x(t) + E_s u(t) \end{cases} \quad (3)$$

where

$A_s = A_1 d + A_2 (1-d)$, $B_s = B_1 d + B_2 (1-d)$, $C_s = C_1 d + C_2 (1-d)$, and $E_s = E_1 d + E_2 (1-d)$.

Equation (3) is a nonlinear continuous-time equation. It can be linearized by small-signal perturbation with $\mathbf{x} = \mathbf{X} + \tilde{\mathbf{x}}$, $\mathbf{y} = \mathbf{Y} + \tilde{\mathbf{y}}$, $\mathbf{u} = \mathbf{U} + \tilde{\mathbf{u}}$, and $d = D + \tilde{d}$, where the ~ symbol represents a small signal value and the capital letter a dc value. It should be noted that $\mathbf{X} >> \tilde{\mathbf{x}}$, $\mathbf{Y} >> \tilde{\mathbf{y}}$, $\mathbf{U} >> \tilde{\mathbf{u}}$, and $D >> \tilde{d}$. The perturbation yields the steady-state and linear small-signal state-space equations in (4) and (5) respectively.

$$\begin{cases} \dfrac{d\mathbf{X}}{dt} = \mathbf{AX} + \mathbf{BU} = 0 \\ \mathbf{Y} = \mathbf{CX} + \mathbf{EU} \end{cases} \quad (4)$$

$$\begin{cases}\dfrac{d\tilde{\mathbf{x}}(t)}{dt}=\mathbf{A}\tilde{\mathbf{x}}(t)+\mathbf{B}\tilde{\mathbf{u}}(t)+\mathbf{B}_d\tilde{d}(t)\\ \tilde{\mathbf{y}}(t)=\mathbf{C}\tilde{\mathbf{x}}(t)+\mathbf{E}\tilde{\mathbf{u}}(t)+\mathbf{E}_d\tilde{d}(t)\end{cases} \quad (5)$$

where

$\mathbf{A}=\mathbf{A}_1D+\mathbf{A}_2(1-D)$, $\mathbf{B}=\mathbf{B}_1D+\mathbf{B}_2(1-D)$, $\mathbf{C}=\mathbf{C}_1D+\mathbf{C}_2(1-D)$, $\mathbf{E}=\mathbf{E}_1D+\mathbf{E}_2(1-D)$, $\mathbf{B}_d=(\mathbf{A}_1-\mathbf{A}_2)\mathbf{X}+(\mathbf{B}_1-\mathbf{B}_2)\mathbf{U}$, and $\mathbf{E}_d=(\mathbf{C}_1-\mathbf{C}_2)\mathbf{X}+(\mathbf{E}_1-\mathbf{E}_2)\mathbf{U}$.

The steady-state solution of the converter can be found by solving (4), which gives:

$$\begin{cases}\mathbf{X}=-\mathbf{A}^{-1}\mathbf{B}\mathbf{U}\\ \mathbf{Y}=(-\mathbf{C}\mathbf{A}^{-1}\mathbf{B}+\mathbf{E})\mathbf{U}\end{cases} \quad (6)$$

The small-signal transfer function of the converter can be found by applying the Laplace transform to (5). In a matrix form, we get:

$$\begin{cases}\tilde{\mathbf{x}}(s)=\begin{bmatrix}(s\mathbf{I}-\mathbf{A})^{-1}\mathbf{B} & (s\mathbf{I}-\mathbf{A})^{-1}\mathbf{B}_d\end{bmatrix}\begin{bmatrix}\tilde{\mathbf{u}}(s)\\ \tilde{d}(s)\end{bmatrix}\\ \tilde{\mathbf{y}}(s)=\begin{bmatrix}\mathbf{C}(s\mathbf{I}-\mathbf{A})^{-1}\mathbf{B}+\mathbf{E} & \mathbf{C}(s\mathbf{I}-\mathbf{A})^{-1}\mathbf{B}_d+\mathbf{E}_d\end{bmatrix}\begin{bmatrix}\tilde{\mathbf{u}}(s)\\ \tilde{d}(s)\end{bmatrix}\end{cases} \quad (7)$$

In the DC-DC converters, the input variable $\tilde{\mathbf{u}}$ usually contains the input voltage and load current. Hence, $\tilde{\mathbf{u}}$ is express as $\tilde{\mathbf{u}}=[u_1\ u_2]^T$, the matrix B as $\mathbf{B}=[\mathbf{B}_{u1}\ \mathbf{B}_{u2}]$, and the matrix E as $\mathbf{E}=[\mathbf{E}_{u1}\ \mathbf{E}_{u2}]$. Therefore, (7) becomes:

$$\begin{cases}\tilde{\mathbf{x}}(s)=\begin{bmatrix}(s\mathbf{I}-\mathbf{A})^{-1}\mathbf{B}_{u1} & (s\mathbf{I}-\mathbf{A})^{-1}\mathbf{B}_{u2} & (s\mathbf{I}-\mathbf{A})^{-1}\mathbf{B}_d\end{bmatrix}\begin{bmatrix}\tilde{u}_1(s)\\ \tilde{u}_2(s)\\ \tilde{d}(s)\end{bmatrix}\\ \tilde{\mathbf{y}}(s)=\begin{bmatrix}\mathbf{C}(s\mathbf{I}-\mathbf{A})^{-1}\mathbf{B}_{u1}+\mathbf{E}_{u1} & \mathbf{C}(s\mathbf{I}-\mathbf{A})^{-1}\mathbf{B}_{u2}+\mathbf{E}_{u2} & \mathbf{C}(s\mathbf{I}-\mathbf{A})^{-1}\mathbf{B}_d+\mathbf{E}_d\end{bmatrix}\begin{bmatrix}\tilde{u}_1(s)\\ \tilde{u}_2(s)\\ \tilde{d}(s)\end{bmatrix}\end{cases} \quad (8)$$

For the fourth-order converter, $(s\mathbf{I}-\mathbf{A})^{-1}\mathbf{B}_{u1}$, $(s\mathbf{I}-\mathbf{A})^{-1}\mathbf{B}_{u2}$, and $(s\mathbf{I}-\mathbf{A})^{-1}\mathbf{B}_d$ are the matrices that have four rows and one column. So, (8) can be expanded into:

$$\begin{cases}\tilde{\mathbf{x}}(s)=\begin{bmatrix}G_{vi_1}(s) & G_{zi_1}(s) & G_{di_1}(s)\\ G_{vi_2}(s) & G_{zi_2}(s) & G_{di_2}(s)\\ G_{vv_1}(s) & G_{zv_1}(s) & G_{dv_1}(s)\\ G_{vv_2}(s) & G_{zv_2}(s) & G_{dv_2}(s)\end{bmatrix}\begin{bmatrix}\tilde{u}_1(s)\\ \tilde{u}_2(s)\\ \tilde{d}(s)\end{bmatrix}\\ \tilde{\mathbf{y}}(s)=\begin{bmatrix}G_{vv}(s) & G_{zv}(s) & G_{dv}(s)\end{bmatrix}\begin{bmatrix}\tilde{u}_1(s)\\ \tilde{u}_2(s)\\ \tilde{d}(s)\end{bmatrix}\end{cases} \quad (9)$$

where

$G_{vi_1}(s)=[(s\mathbf{I}-\mathbf{A})^{-1}\mathbf{B}_{u1}]_{11}$, $G_{zi_1}(s)=[(s\mathbf{I}-\mathbf{A})^{-1}\mathbf{B}_{u2}]_{11}$, $G_{di_1}(s)=[(s\mathbf{I}-\mathbf{A})^{-1}\mathbf{B}_d]_{11}$,
$G_{vi_2}(s)=[(s\mathbf{I}-\mathbf{A})^{-1}\mathbf{B}_{u1}]_{21}$, $G_{zi_2}(s)=[(s\mathbf{I}-\mathbf{A})^{-1}\mathbf{B}_{u2}]_{21}$, $G_{di_2}(s)=[(s\mathbf{I}-\mathbf{A})^{-1}\mathbf{B}_d]_{21}$,
$G_{vv_1}(s)=[(s\mathbf{I}-\mathbf{A})^{-1}\mathbf{B}_{u1}]_{31}$, $G_{zv_1}(s)=[(s\mathbf{I}-\mathbf{A})^{-1}\mathbf{B}_{u2}]_{31}$, $G_{dv_1}(s)=[(s\mathbf{I}-\mathbf{A})^{-1}\mathbf{B}_d]_{31}$,
$G_{vv_2}(s)=[(s\mathbf{I}-\mathbf{A})^{-1}\mathbf{B}_{u1}]_{41}$, $G_{zv_2}(s)=[(s\mathbf{I}-\mathbf{A})^{-1}\mathbf{B}_{u2}]_{41}$, $G_{dv_2}(s)=[(s\mathbf{I}-\mathbf{A})^{-1}\mathbf{B}_d]_{41}$,
$G_{vv}(s)=\mathbf{C}(s\mathbf{I}-\mathbf{A})^{-1}\mathbf{B}_{u1}+\mathbf{E}_{u1}$, $G_{zv}(s)=\mathbf{C}(s\mathbf{I}-\mathbf{A})^{-1}\mathbf{B}_{u2}+\mathbf{E}_{u2}$, and
$G_{dv}(s)=\mathbf{C}(s\mathbf{I}-\mathbf{A})^{-1}\mathbf{B}_d+\mathbf{E}_d$.

3. Modeling of a SEPIC converter by SSA Technique

A SEPIC converter is shown in Fig. 1(a). It is comprised of the MOSFET switch (Q), diode (D), two capacitors (C_1 and C_2), and two inductors (L_1 and L_2). The resistor, R, represents a standing load, and the current source, I_Z, models the load current. The resistors, r_{C1}, r_{C2}, r_{L1}, and r_{L2}, are an equivalent series resistance of the capacitors and inductors respectively. Their values are usually very small compared to R. In the ideal converter, these equivalent series resistance are zero. In CCM, the converter exhibits two circuit states. The first state is when the MOSFET switch is turned on (Fig. 1(b)). During this interval (dT), L_1 is charged by the source, V_g, and L_2 by the capacitor C_1. Hence i_{L1} and i_{L2} increase linearly as shown in Fig. 2. The second state is when the MOSFET switch is turned off (Fig. 1(c)). During this interval ((1-d)T), L_1 and L_2 are in a discharging phase; L_1 and L_2 release the stored energy to the capacitors and load respectively. Thus, i_{L1} and i_{L2} decrease linearly as shown in Fig. 2.

The output voltage, V_O, is a DC voltage that contains small ripple due to the switching action. For ideal SEPIC converter, the relationship between V_O and V_g is given by:

$$M=\frac{V_O}{V_g}=\frac{D}{1-D} \quad (10)$$

where M is a voltage conversion ratio. It can be seen that V_O could be larger or smaller than V_g, depending on the duty cycle. From Fig. 2, the averaged inductor currents, I_{L1} and I_{L2}, must be greater than one-half of their ripple components, Δi_{L1} and Δi_{L2}, for the circuit to remain in CCM. It can be shown that for CCM operation L_1 and L_2 must satisfy the following conditions:

$$\begin{cases}L_1>\dfrac{(1-D)^2R}{2Df}\left(\dfrac{1}{\frac{r_{C2}}{R}+1}+\dfrac{1}{1-D}\dfrac{R_g}{R}+\dfrac{Mr_{C1}}{R}+\dfrac{r_{L2}}{R}\right)\\ L_2>\dfrac{(1-D)R}{2f}\left(\dfrac{1}{\frac{r_{C2}}{R}+1}+\dfrac{1}{1-D}\dfrac{r_{L2}+R_g}{R}+\dfrac{Mr_{C1}}{R}+M\dfrac{r_{C1}+r_{L2}}{R}\right)\end{cases} \quad (11)$$

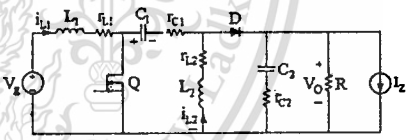

(a) SEPIC converter.

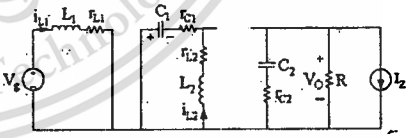

(b) SEPIC converter when MOSFET is turned on.

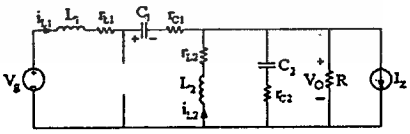

(c) SEPIC converter when MOSFET is turned off.

Fig. 1. Operation of SEPIC converter.

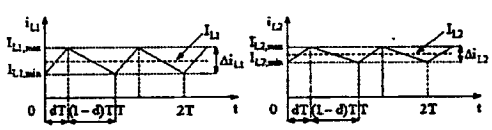

(a) i_{L1} waveform. (b) i_{L2} waveform.

Fig. 2. Current waveforms.

3.1 State-Space Description of SEPIC Converter

The state-space equations of the SEPIC converter for the on and off states of the switch can be written from Figs. 1(b) and (c) respectively, which are given by:

$$\begin{aligned}
\frac{di_{L1}}{dt} &= \frac{-i_{L1}}{L_1}[r_{L1}+(1-\delta)(r_{C1}+R_g)]-(1-\delta)(\frac{R_g i_{L2}}{L_1}+\frac{v_{C1}}{L_1}+\frac{R_g v_{C2}}{r_{C2}L_1}-\frac{R_g I_z}{L_1})+\frac{V_g}{L_1}\\
\frac{di_{L2}}{dt} &= (1-\delta)(\frac{I_z}{L_2}-\frac{i_{L1}}{L_2}-\frac{v_{C2}}{r_{C2}L_2})R_g-\frac{i_{L2}}{L_2}[r_{C1}\delta+r_{L2}+(1-\delta)R_g]+\frac{v_{C1}\delta}{L_2}\\
\frac{dv_{C1}}{dt} &= \frac{i_{L1}}{C_1}(1-\delta)-\frac{i_{L2}}{C_1}\delta\\
\frac{dv_{C2}}{dt} &= \frac{1-\delta}{C_2 r_{C2}}(i_{L1}+i_{L2})R_g-\frac{R_g}{C_2 r_{C2} R}v_{C2}-\frac{R_g}{C_2 r_{C2}}I_z\\
v_O &= (1-\delta)(i_{L1}+i_{L2})R_g+\frac{R_g}{r_{C2}}v_{C2}-R_g I_z
\end{aligned} \tag{12}$$

Note that the equations are expressed in a compact form using the switching function, δ. When the switch is on, δ =1, (12) will become the on-state equation. When the switch is off, δ =0, (12) will become the off-state equation.

The averaged matrices for the steady-state and the linear small-signal state-space equations can be written according to (4) and (5).

$$\mathbf{A}=\begin{bmatrix}
\frac{r_{L1}+(r_{C1}+R_g)(D-1)}{L_1} & \frac{D-1}{L_1}R_g & \frac{D-1}{L_1} & \frac{D-1}{L_1 r_{C2}}R_g\\
\frac{(D-1)R_g}{L_2} & \frac{r_{L2}+Dr_{C1}+R_g(1-D)}{L_2} & \frac{D}{L_2} & \frac{D-1}{L_2 r_{C2}}R_g\\
\frac{1-D}{C_1} & \frac{-D}{C_1} & 0 & 0\\
\frac{1-D}{C_2 r_{C2}}R_g & \frac{1-D}{C_2 r_{C2}}R_g & 0 & \frac{-1}{C_2(r_{C2}+R)}
\end{bmatrix} \tag{13}$$

$$\mathbf{B}=\begin{bmatrix}
\frac{1}{L_1} & \frac{1-D}{L_1}R_g\\
0 & \frac{1-D}{L_2}R_g\\
0 & 0\\
0 & \frac{-R_g}{C_2 r_{C2}}
\end{bmatrix} \tag{14}$$

$$\mathbf{C}=\begin{bmatrix}(1-D)R_g & (1-D)R_g & 0 & \frac{R_g}{r_{C2}}\end{bmatrix} \tag{15}$$

$$\mathbf{E}=\begin{bmatrix}0 & -R_g\end{bmatrix} \tag{16}$$

$$\mathbf{B_d}=\begin{bmatrix}
\frac{V_g[R_g(Mr_{C1}+r_{L1}+\frac{R}{1-D})-MR^2]-Mr_{L1}RR_gI_z}{\eta(1-D)r_{C2}R^3L_1}\\
\frac{V_g[R_g(r_{L2}+\frac{R}{1-D})-MR^2]-(r_{C1}+Mr_{L1})RR_gI_z}{\eta(1-D)r_{C2}R^3L_2}\\
\frac{-R_g[MV_g+RI_z]}{\eta(1-D)r_{C2}C_1R^3}\\
\frac{-MV_g-RI_z}{\eta(1-D)RC_2}
\end{bmatrix} \tag{17}$$

$$\mathbf{E_d}=\frac{-MV_g-RI_z}{\eta(1-D)R}r_{C2} \tag{18}$$

3.2 Steady-State Equations

Given the averaged matrices in (13) to (18), the steady-state solution of converter is obtained from (6):

$$\begin{aligned}
\begin{bmatrix}I_{L1}\\I_{L2}\\V_{C1}\\V_{C2}\end{bmatrix} &= \frac{M}{\eta}\begin{bmatrix}
\frac{r_{C2}M}{R_gR} & & & \frac{r_{C1}}{R_g}\\
\frac{r_{C1}}{R_gR} & & & \frac{r_{C2}}{MR_g}\\
\frac{r_{C2}}{R_gR}(r_{C1}+\frac{1}{M}\frac{r_{L2}+R}{1-D})-1 & & & \frac{(r_{L2}-Mr_{L1})r_{C1}}{MR_g}\\
\frac{r_{C2}}{R_g} & & -\frac{r_{C1}}{R_g}(Mr_{L1}+r_{C1}+\frac{r_{L1}}{M})-\frac{r_{C2}}{1-D} &
\end{bmatrix}\\
V_O &= \frac{Mr_{C2}}{\eta R_g}[V_g+(\frac{r_{L1}r_{C1}R}{MR_g}\frac{1}{1-D}-R_g-r_{C1}-r_{L1}M)I_z]
\end{aligned} \tag{19}$$

where $R_g=\frac{r_{C2}R}{r_{C2}+R}$, $R_T=R+r_{C2}$, $n=(1+\frac{r_{C2}}{R})(\frac{r_{L2}}{R}+M\frac{r_{C1}}{R}+M^2\frac{r_{L1}}{R})$, $\eta=1+n+\frac{r_{C2}}{(1-D)R}$, $M=\frac{D}{1-D}=\frac{D}{D'}$, and $L_T=L_1+L_2$.

Notice that if r_{C1}, r_{C2}, r_{L1}, and r_{L2} are assumed to be zero, the output equation in (19) will be reduced to $M=V_O/V_g=D/(1-D)$, the same as the expression for the ideal SEPIC converter in (10).

3.3 Linear Small-Signal State-Space Equations

Given the averaged matrices (13) to (18), the linear small-signal state-space equations of the SEPIC converter can be formulated in accordance with (5):

$$\begin{aligned}
\frac{d}{dt}\begin{bmatrix}\tilde{i}_{L1}(t)\\\tilde{i}_{L2}(t)\\\tilde{v}_{C1}(t)\\\tilde{v}_{C2}(t)\end{bmatrix} &= \begin{bmatrix}
\frac{r_{L1}+(r_{C1}+R_g)(D-1)}{L_1} & \frac{D-1}{L_1}R_g & \frac{D-1}{L_1} & \frac{D-1}{L_1 r_{C2}}R_g\\
\frac{(D-1)R_g}{L_2} & \frac{r_{L2}+Dr_{C1}+R_g(1-D)}{L_2} & \frac{D}{L_2} & \frac{D-1}{L_2 r_{C2}}R_g\\
\frac{1-D}{C_1} & \frac{-D}{C_1} & 0 & 0\\
\frac{1-D}{C_2 r_{C2}}R_g & \frac{1-D}{C_2 r_{C2}}R_g & 0 & \frac{-1}{C_2(r_{C2}+R)}
\end{bmatrix}\begin{bmatrix}\tilde{i}_{L1}(t)\\\tilde{i}_{L2}(t)\\\tilde{v}_{C1}(t)\\\tilde{v}_{C2}(t)\end{bmatrix}+\\
&\begin{bmatrix}
\frac{1}{L_1} & \frac{1-D}{L_1}R_g & \frac{V_g[R_g(Mr_{C1}+r_{L2}+\frac{R}{1-D})-MR^2]-Mr_{L1}RR_gI_z}{\eta(1-D)r_{C2}R^3L_1}\\
0 & \frac{1-D}{L_2}R_g & \frac{V_g[R_g(r_{L2}+\frac{R}{1-D})-MR^2]-(r_{C1}+Mr_{L1})I_zRR_g}{\eta(1-D)r_{C2}R^3L_2}\\
0 & 0 & \frac{-R_g[MV_g+RI_z]}{\eta(1-D)r_{C2}C_1R^3}\\
0 & \frac{-R_g}{C_2 r_{C2}} & \frac{-MV_g-RI_z}{\eta(1-D)RC_2}
\end{bmatrix}\begin{bmatrix}\tilde{v}_g(t)\\\tilde{i}_z(t)\\\tilde{d}(t)\end{bmatrix}
\end{aligned} \tag{20}$$

$$\tilde{v}_O(t)=\begin{bmatrix}(1-D)R_g & (1-D)R_g & 0 & \frac{R_g}{r_{C2}}\end{bmatrix}\begin{bmatrix}\tilde{i}_{L1}(t)\\\tilde{i}_{L2}(t)\\\tilde{v}_{C1}(t)\\\tilde{v}_{C2}(t)\end{bmatrix}+\begin{bmatrix}0 & -R_g & \frac{-MV_g-RI_z}{\eta(1-D)R}r_{C2}\end{bmatrix}\begin{bmatrix}\tilde{v}_g(t)\\\tilde{i}_z(t)\\\tilde{d}(t)\end{bmatrix}$$

3.4 Finding Transfer Functions

Referring to (9), fifteen transfer functions can be determined from (20). However, only a few of them are useful for feedback control design. These transfer functions are:

The duty ratio-to-output voltage transfer function

$$\begin{aligned}
G_{dv}(s) &= \frac{\tilde{v}_O(s)}{\tilde{d}(s)} = \mathbf{C}(s\mathbf{I}-\mathbf{A})^{-1}\mathbf{B_d}+\mathbf{E_d}\\
&= K_D\frac{a_{dv}s^4+b_{dv}s^3+c_{dv}s^2+d_{dv}s+e_{dv}}{as^4+bs^3+cs^2+ds+e}
\end{aligned} \tag{21}$$

where $K_D=\frac{1}{R_T D'+R(n-M)D'^2}$

The input voltage-to-output voltage transfer function

$$\begin{aligned}
G_{vv}(s) &= \frac{\tilde{v}_O(s)}{\tilde{v}_g(s)} = \mathbf{C}(s\mathbf{I}-\mathbf{A})^{-1}\mathbf{B_{d1}}+\mathbf{E_{d1}}\\
&= RD'\frac{a_{vv}s^3+b_{vv}s^2+c_{vv}s+d_{vv}}{as^4+bs^3+cs^2+ds+e}
\end{aligned} \tag{22}$$

The output impedance transfer function

$$\begin{aligned}
G_{zv}(s) &= \frac{\tilde{v}_O(s)}{\tilde{i}_Z(s)} = \mathbf{C}(s\mathbf{I}-\mathbf{A})^{-1}\mathbf{B_{d2}}+\mathbf{E_{d2}}\\
&= R\frac{a_{zv}s^4+b_{zv}s^3+c_{zv}s^2+d_{zv}s+e_{zv}}{as^4+bs^3+cs^2+ds+e}
\end{aligned} \tag{23}$$

The coefficients in (21) to (23) are listed in TABLE I.

4. Simulation Results

To validate the accuracy of the SEPIC converter model, $G_{dv}(s)$ in (21) is plotted and compared with the Ridley's result [2], using the same circuit parameters: L_1=100μH, r_{L1}=1mΩ, L_2=100μH, r_{L2}=1mΩ, C_1=680μF, r_{C1}=3mΩ, C_2=2200μF, r_{C2}=1mΩ, V_g=10V, V_O=15V,

I_Z=0, and R=1Ω. The result is shown in Fig. 3. Fig. 4 also gives the same result, using circuit block CCM1 of the averaged switch model [4]. The plotted $G_{dv}(s)$ has four complex poles at $p_{1,2}$=(−0.0158±2.7771i)x10^3 and $p_{3,4}$=(−0.2403±1.1578i)x10^3; and two real zeros at z_1=−4.5455x10^5, z_2=0.0510x10^5 and two complex zeros at $z_{3,4}$=(0.0010±0.0277i)x10^5. This result is exactly the same as that in [1- 3], validating the accuracy of the derived model with the SSA technique.

Fig. 5(a) shows a start-up transient of the SEPIC converter simulated with (20). V_g=10V was applied at t=0s, and D=0.6. It takes about 120ms for V_O to settle to 15V. This result agrees well with the PSPICE simulation result of the SEPIC converter simulated using an ideal switch shown in Fig. 5(b).

5. Conclusions

In this paper, modeling of a SEPIC converter has been performed with the State-Space Averaging (SSA) technique. The results yield an insight into the steady-state and small-signal dynamic properties of the converter in (19) and (20) respectively. To provide a basis for feedback control design, three relevant transfer functions ($G_{dv}(s)$, $G_{vv}(s)$, and $G_{zv}(s)$) were derived. The derived $G_{dv}(s)$ was found to be the same as that in [1- 3]. The results in (20) and (21) were highly consistent with that from PSPICE simulation, proofing the accuracy of the derived model.

TABLE I
Coefficients of $G_{dv}(s)$, $G_{vv}(s)$ and $G_{zv}(s)$

$a_{dv}=-r_{C2}L_1C_1L_2C_2R_T^2(DV_g+RD'I_Z)$,

$b_{dv}=[D^2r_{C2}L_TC_2R_T-DL_2(r_{l1}r_{C2}C_2+L_1)-r_{C2}C_2DL_1(Dr_{C1}+r_{l2})]R_T^2C_1V_g$
$-D'C_1RR_TI_Z[r_{C2}C_2L_2[R_T(Dr_{l1}+r_{C1})+r_{C2}RD']$
$+R_TL_1(r_{C2}r_{l2}C_2+L_2)+r_{C2}L_2C_2(r_{l1}-Dr_{C1})]]$,

$c_{dv}=R_T^2V_g[D^2[C_1(r_{l2}+R)[C_2(r_{l2}r_{C2}+r_{C2}r_{C1}+r_{l1}r_{C2})+L_T]$
$-D^2r_{C2}C_2L_1]-C_1D(Dr_{C1}+r_{l2})(L_1+r_{l1}r_{C2}C_2)+DL_2r_{l1}]-$
$D'R_T^2RI_Z[C_1[D'r_{C1}+(1+D)r_{l1}][r_{C2}C_2(r_{l2}+r_{C1})+L_2]+L_1C_1(r_{l2}+r_{C1})+$
$DL_1(r_{l1}C_1+r_{C2}C_2)+Dr_{l1}^2r_{C2}C_1C_2+D'C_1R_T[L_T+(r_{l2}+r_{C1}+r_{l1})C_2r_{C2}]]$,

$d_{dv}=-D'RR_TI_Z[R_T[D(L_1-r_{C1}r_{l2}C_1+2r_{C2}r_{l2}C_2)+C_1r_{l2}(r_{l1}+r_{C1})]$
$+(r_{C2}RD'+r_{l1}R_TD)(r_{l1}+r_{l2})C_1+(r_{C1}R_T+r_{C2}R)(r_{C1}C_1+r_{C2}C_2)D']$
$+R_T^2V_g[D^2[C_1R(r_{l1}+r_{l2})+r_{l2}C_1(r_{l2}-r_{l1})+(r_{C1}C_1+C_2r_{C2})(R+r_{l2})]$
$-r_{l1}D^3(r_{C1}C_1+r_{C2}C_2)-L_1D^2-Dr_{l2}r_{l1}C_1]$,

$e_{dv}=V_gR_T^2[D^3(R+r_{l2})-D^2r_{l1}]-D'R_TRI_Z[2DR_Tr_{l1}+D'(r_{C1}R_T+r_{C2}R)]$.

$a_{vv}=r_{C2}L_2C_1C_2R_T$, $b_{vv}=C_1R_T[r_{C2}C_2(Dr_{C1}+r_{l2})+L_2]$, $d_{vv}=DR_T$,
$c_{vv}=R_T[(r_{C1}C_1+r_{C2}C_2)D+r_{l2}C_1]$.

$a_{zv}=-r_{C2}L_1C_1L_2C_2R_T$, $e_{zv}=-R_T(D^2r_{l1}-D^2r_{l2})-DD'(r_{C1}R_T+r_{C2}R)$,
$b_{zv}=C_1L_1L_2-r_{C2}C_1C_2[r_{C2}RL_TDD'+R_T(L_2r_{l1}+L_1r_{l2}+r_{C1}L_1D+r_{C1}L_2D')]$,
$c_{zv}=-r_{C2}C_1RDD'[L_T+C_2(r_{l1}r_{C2}+r_{C1}r_{C2}+r_{l2})]-R_T[r_{C1}C_1(L_1D+L_2D')+$
$r_{C2}C_2(L_1D^2+L_2D^2)]-C_1R_T[r_{C2}C_2(Dr_{C1}+r_{l2})(r_{l1}+r_{C1}D')+r_{l1}L_2+r_{l2}L_1]$,
$d_{zv}=-(C_1r_{C1}r_{l2}+C_1r_{C2}r_{l2}+C_2r_{C2}^2)RDD'-R_T[(D'r_{C1}+r_{l1})(Dr_{C1}+r_{l2})C_1$
$+L_1D^2+L_2D^2]-(r_{l2}C_1RD+r_{C1}C_2DD'+r_{l1}C_2D^2+r_{l2}C_2D^2)r_{C2}R_T$.

$a=L_1C_1L_2C_2R_T^2$, $e=R_T(D^2r_{l1}+D^2r_{l2}+DD'r_{C1})+(D'R+r_{C1})D'R$,
$b=C_1R_T[C_2R_T[L_2r_{l1}+L_1(r_{l2}+Dr_{C1})]+C_2D'(r_{C1}L_2R_T+r_{C2}L_TR)+L_1L_2]$,
$c=C_1R_T[D'r_{C2}C_2R(r_{l1}+r_{l2}+r_{C1})+r_{C1}D'L_2+L_1(Dr_{C1}+r_{l2})+r_{l1}L_2]+$
$R_T^2C_2[C_1(Dr_{C1}+r_{l2})(r_{l1}+r_{C1}D')+D^2L_2+L_1D^2]+(RD'+r_{C2})D'RC_1L_T$,
$d=R_T[C_1(Dr_{C1}+r_{l2})(r_{l1}+r_{C1}D')+r_{C2}C_2RD'+L_1D^2+L_2D^2]$
$+(r_{l1}D^2+r_{l2}D^2+r_{C1}DD')R_T^2C_2+(RD'+r_{C2})(r_{l1}+r_{l2}+r_{C1})RC_1D'$.

References

[1] V. Vorpérian, "Analysis of the Sepic Converter by Dr. Vatché Vorpérian," *Ridley Engineering Inc*, www.switchingpowermagazine.com, 2006.

[2] R. Ridley, "Analyzing the Sepic Converter," *Power Systems Design Europe Magazine*, pp. 14-18, November 2006.

[3] A. Hren and P. Slibar, "Full Order Dynamic Model of SEPIC Converter," *Proc. of the IEEE International Symposium on Industrial Electronics*, pp. 553-558, June 2005.

[4] R. W. Erickson and D. Maksimović, *Fundamentals of Power Electronics*, 2nd ed., Kluwer Academic Publishers, 2001.

[5] R. D. Middlebook and S. Cuk, "A General Unified Approach to Modeling Switching-Converter Power Stages," *International Journal of Electronics*, vol. 42, pp. 521-550, June 1977.

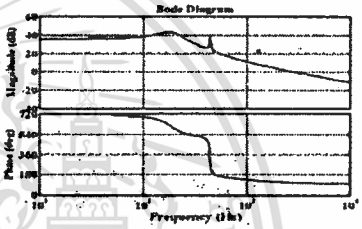

Fig. 3. Frequency responses of $G_{dv}(s)$ with Matlab.

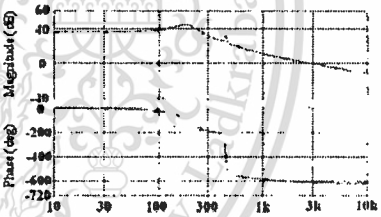

Fig. 4. Frequency responses of $G_{dv}(s)$ with circuit block CCM1.

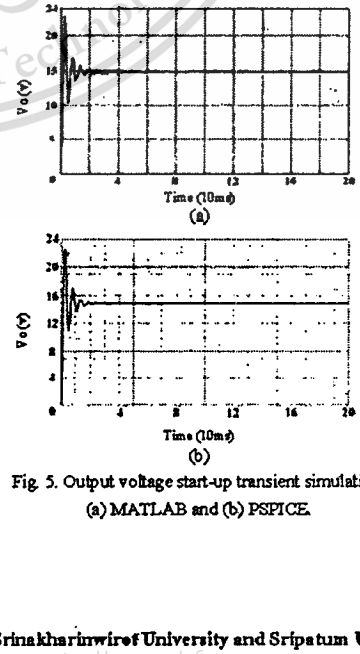

Fig. 5. Output voltage start-up transient simulation: (a) MATLAB and (b) PSPICE.

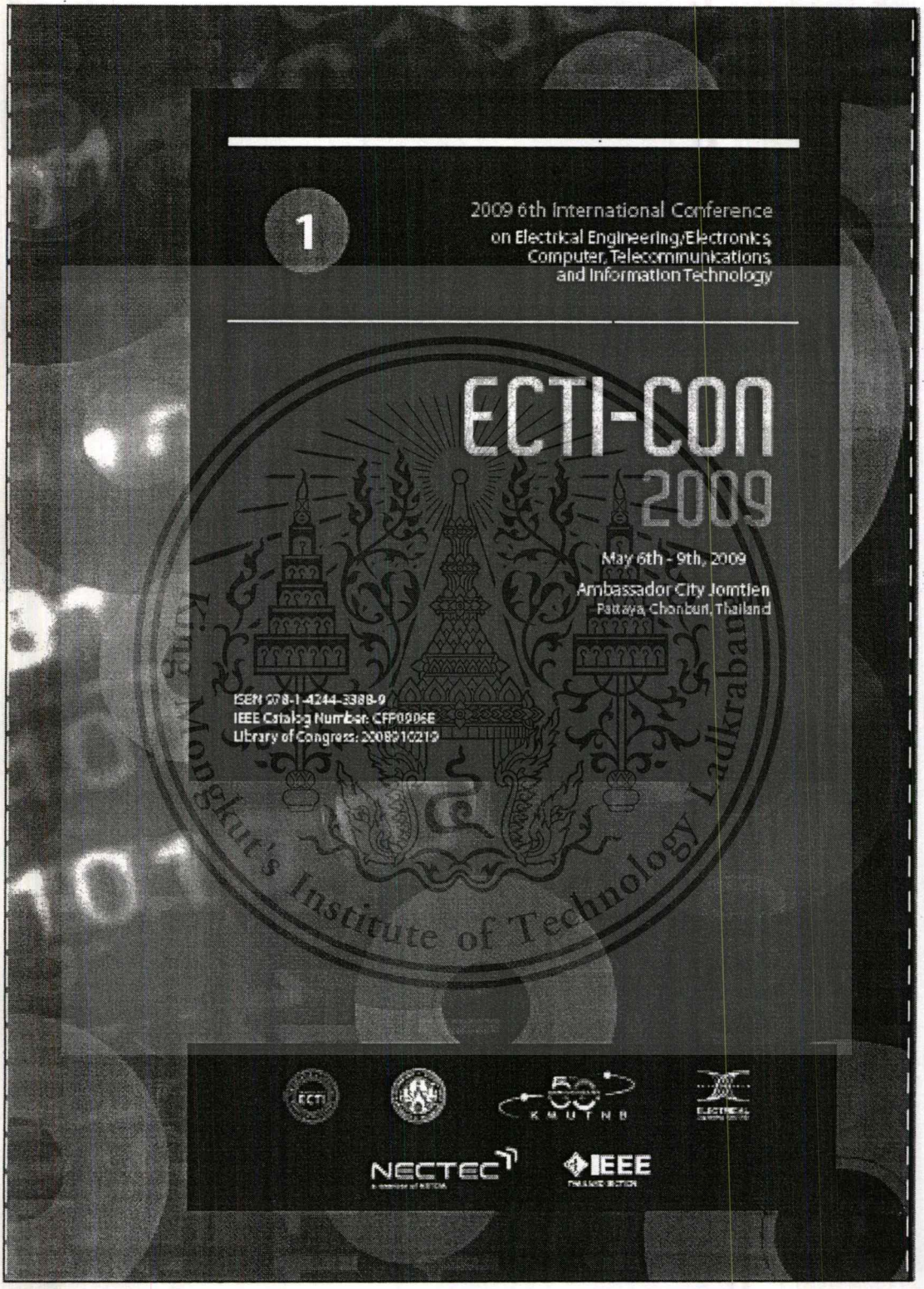

Modeling of a SEPIC Converter Operating in Continuous Conduction Mode

Vuthchhay Eng, Unnat Pinsopon, and Chanin Bunlaksananusorn
Faculty of Engineering, King Mongkut's Institute of Technology Ladkrabang (KMITL),
Chalongkrung Rd. Ladkrabang, Bangkok 10520
vouthchhay_oeung@yahoo.com and kbchanin@kmitl.ac.th

Abstract - **A SEPIC (Single-Ended Primary Inductor Converter) DC-DC converter is capable of operating in either step-up or step-down mode and widely used in battery-operated equipment. There are two possible modes of operation in the SEPIC converter: Continuous Conduction Mode (CCM) and Discontinuous Conduction Mode (DCM). This paper presents modeling of a SEPIC converter operating in CCM using the State-Space Averaging (SSA) technique. The modeling leads to a small-signal linear model of the converter, from which the transfer functions used for feedback control design can be determined. Results are presented to verify the accuracy of the obtained model.**

I. Introduction

Nowadays, the use of a DC-DC converter is widespread in modern portable electronic equipment and systems. In battery-operated portable devices, when not connected to the AC mains, the battery provides an input voltage to the converter, which then converts it into the output voltage suitable for use by the electronic load. The battery voltage can vary over a wide range, depending on a charge level. At the low charge level, it may drop below the load voltage. Hence, to continue supplying the constant load voltage over the entire battery voltage range, the converter must be able to work in both buck and boost modes. The DC-DC converters that meet this operational requirement are Buck-boost, Cuk, and SEPIC converters. However, the Buck-boost and Cuk converters, in their basic form, produce the output voltage, whose polarity is reversed from the input voltage. The problem can be corrected by incorporating an isolation transformer into the circuits, but this will inevitably lead to the increased size and cost of the converters. On the other hands, the SEPIC (Single-Ended Primary Inductor Converter) converter is capable of operating in both step-up and step-down modes and does not suffer from the polarity reversal problem. It is therefore attractive for the aforementioned application.

The SEPIC converter consists of an active power switch, a diode, two inductors, and two capacitors and is thus a fourth-order nonlinear system. Feedback control is usually incorporated into the converter's circuit to regulate its output voltage, typically by means of Pulse Width Modulation (PWM). To facilitate the feedback controller design or system stability analysis, the linear model of the converter is needed. Recently, modeling of the SEPIC converter has been carried out by some researchers. The linear converter models were found by substitution of the power switch and diode of the converter by the so called small-signal PWM switch model [1, 2] and small-signal averaged switch model [3, 4]. This paper presents an alternative modeling method for a SEPIC converter, using the State-Space Averaging (SSA) technique [4, 5]. Unlike the PWM and averaged switch model methods which are based on equivalent circuit manipulation, the SSA technique is performed via matrix; hence, formal matrix treatment can be applied to facilitate the modeling process.

II. Overview of SSA Technique

For DC-DC converters operating in Continuous Conduction Mode (CCM), there exist two circuit states within one switching period, T. One is when the MOSFET is turned on for an interval dT, and another is when the MOSFET is turned off for an interval $(1-d)T$, where d is a duty cycle. The state-space equations for these two circuit states are represented by:

$$\begin{cases} d\mathbf{x}/dt = \mathbf{A}_1\mathbf{x} + \mathbf{B}_1\mathbf{u} \\ \mathbf{y} = \mathbf{C}_1\mathbf{x} + \mathbf{E}_1\mathbf{u} \end{cases} \quad (1)$$

$$\begin{cases} d\mathbf{x}/dt = \mathbf{A}_2\mathbf{x} + \mathbf{B}_2\mathbf{u} \\ \mathbf{y} = \mathbf{C}_2\mathbf{x} + \mathbf{E}_2\mathbf{u} \end{cases} \quad (2)$$

To find the averaged behavior of the converter over one switching period, (1) and (2) are weighed average by the duty cycle:

$$\begin{cases} d\mathbf{x}/dt = \mathbf{A}_s\mathbf{x} + \mathbf{B}_s\mathbf{u} \\ \mathbf{y} = \mathbf{C}_s\mathbf{x} + \mathbf{E}_s\mathbf{u} \end{cases} \quad (3)$$

where $\mathbf{A}_s = \mathbf{A}_1 d + \mathbf{A}_2(1-d)$, $\mathbf{B}_s = \mathbf{B}_1 d + \mathbf{B}_2(1-d)$, $\mathbf{C}_s = \mathbf{C}_1 d + \mathbf{C}_2(1-d)$, and $\mathbf{E}_s = \mathbf{E}_1 d + \mathbf{E}_2(1-d)$.

Equation (3) is a nonlinear continuous-time equation. It can be linearized by small-signal perturbation with $\mathbf{x} = \mathbf{X} + \tilde{\mathbf{x}}$, $\mathbf{y} = \mathbf{Y} + \tilde{\mathbf{y}}$, $\mathbf{u} = \mathbf{U} + \tilde{\mathbf{u}}$, and $d = D + \tilde{d}$, where the ~ symbol represents a small-signal value and the capital letter a DC value. It should be noted that $\mathbf{X} >> \tilde{\mathbf{x}}$, $\mathbf{Y} >> \tilde{\mathbf{y}}$, $\mathbf{U} >> \tilde{\mathbf{u}}$, and $D >> \tilde{d}$. The perturbation yields the steady-state and linear small-signal state-space equations in (4) and (5) respectively.

$$\begin{cases} d\mathbf{X}/dt = \mathbf{A}\mathbf{X} + \mathbf{B}\mathbf{U} = \mathbf{0} \\ \mathbf{Y} = \mathbf{C}\mathbf{X} + \mathbf{E}\mathbf{U} \end{cases} \quad (4)$$

$$\begin{cases} d\tilde{\mathbf{x}}/dt = \mathbf{A}\tilde{\mathbf{x}} + \mathbf{B}\tilde{\mathbf{u}} + \mathbf{B}_d\tilde{d} \\ \tilde{\mathbf{y}} = \mathbf{C}\tilde{\mathbf{x}} + \mathbf{E}\tilde{\mathbf{u}} + \mathbf{E}_d\tilde{d} \end{cases} \quad (5)$$

978-1-4244-3388-9/09/$25.00 ©2009 IEEE

where $\mathbf{A}=\mathbf{A}_1D+\mathbf{A}_2(1-D)$, $\mathbf{B}=\mathbf{B}_1D+\mathbf{B}_2(1-D)$, $\mathbf{C}=\mathbf{C}_1D+\mathbf{C}_2(1-D)$ $\mathbf{E}=\mathbf{E}_1D+\mathbf{E}_2(1-D)$, $\mathbf{B}_d=(\mathbf{A}_1-\mathbf{A}_2)\mathbf{X}+(\mathbf{B}_1-\mathbf{B}_2)\mathbf{U}$, and $\mathbf{B}_d=(\mathbf{A}_1-\mathbf{A}_2)\mathbf{X}+(\mathbf{B}_1-\mathbf{B}_2)\mathbf{U}$.

The steady-state solution of the converter can be found by solving (4), which gives:

$$\begin{cases}\mathbf{X}=-\mathbf{A}^{-1}\mathbf{B}\mathbf{U}\\ \mathbf{Y}=(-\mathbf{C}\mathbf{A}^{-1}\mathbf{B}+\mathbf{E})\mathbf{U}\end{cases} \tag{6}$$

The small-signal transfer function of the converter can be found by applying Laplace transform to (5). In a matrix form, we get:

$$\begin{cases}\tilde{\mathbf{x}}(s)=\begin{bmatrix}(s\mathbf{I}-\mathbf{A})^{-1}\mathbf{B} & (s\mathbf{I}-\mathbf{A})^{-1}\mathbf{B}_d\end{bmatrix}\begin{bmatrix}\tilde{\mathbf{u}}(s) & \tilde{d}(s)\end{bmatrix}^T\\ \tilde{\mathbf{y}}(s)=\begin{bmatrix}\mathbf{C}(s\mathbf{I}-\mathbf{A})^{-1}\mathbf{B}+\mathbf{E} & \mathbf{C}(s\mathbf{I}-\mathbf{A})^{-1}\mathbf{B}_d+\mathbf{E}_d\end{bmatrix}\begin{bmatrix}\tilde{\mathbf{u}}(s) & \tilde{d}(s)\end{bmatrix}^T\end{cases} \tag{7}$$

In the DC-DC converters, the input variable $\tilde{u}$ usually contains the input voltage and load current. Hence, $\tilde{u}$ is express as $\tilde{u}=[u_1\ u_2]^T$, the matrix B as $\mathbf{B}=[\mathbf{B}_{u1}\ \mathbf{B}_{u2}]$, and the matrix E as $\mathbf{E}=[\mathbf{E}_{u1}\ \mathbf{E}_{u2}]$. Therefore, (7) becomes:

$$\begin{cases}\tilde{\mathbf{x}}(s)=\begin{bmatrix}(s\mathbf{I}-\mathbf{A})^{-1}\mathbf{B}_{u1} & (s\mathbf{I}-\mathbf{A})^{-1}\mathbf{B}_{u2} & (s\mathbf{I}-\mathbf{A})^{-1}\mathbf{B}_d\end{bmatrix}\begin{bmatrix}\tilde{u}_1(s) & \tilde{u}_2(s) & \tilde{d}(s)\end{bmatrix}^T\\ \tilde{\mathbf{y}}(s)=\begin{bmatrix}\mathbf{C}(s\mathbf{I}-\mathbf{A})^{-1}\mathbf{B}_{u1}+\mathbf{E}_{u1} & \mathbf{C}(s\mathbf{I}-\mathbf{A})^{-1}\mathbf{B}_{u2}+\mathbf{E}_{u2} & \mathbf{C}(s\mathbf{I}-\mathbf{A})^{-1}\mathbf{B}_d+\mathbf{E}_d\end{bmatrix}\begin{bmatrix}\tilde{u}_1(s) & \tilde{u}_2(s) & \tilde{d}(s)\end{bmatrix}^T\end{cases} \tag{8}$$

For the fourth-order converter, $(s\mathbf{I}-\mathbf{A})^{-1}\mathbf{B}_{u1}$, $(s\mathbf{I}-\mathbf{A})^{-1}\mathbf{B}_{u2}$, and $(s\mathbf{I}-\mathbf{A})^{-1}\mathbf{B}_d$ are the matrices that have four rows and one column. So, (8) can be expanded into:

$$\begin{cases}\tilde{\mathbf{x}}(s)=\begin{bmatrix}G_{vi_1}(s) & G_{zi_1}(s) & G_{di_1}(s)\\ G_{vi_2}(s) & G_{zi_2}(s) & G_{di_2}(s)\\ G_{vv_1}(s) & G_{zv_1}(s) & G_{dv_1}(s)\\ G_{vv_2}(s) & G_{zv_2}(s) & G_{dv_2}(s)\end{bmatrix}\begin{bmatrix}\tilde{u}_1(s) & \tilde{u}_2(s) & \tilde{d}(s)\end{bmatrix}^T\\ \tilde{\mathbf{y}}(s)=\begin{bmatrix}G_{vv}(s) & G_{zv}(s) & G_{dv}(s)\end{bmatrix}\begin{bmatrix}\tilde{u}_1(s) & \tilde{u}_2(s) & \tilde{d}(s)\end{bmatrix}^T\end{cases} \tag{9}$$

where

$G_{vi_1}(s)=[(s\mathbf{I}-\mathbf{A})^{-1}\mathbf{B}_{u1}]_{11}$, $G_{di_1}(s)=[(s\mathbf{I}-\mathbf{A})^{-1}\mathbf{B}_{u2}]_{11}$, $G_{di_1}(s)=[(s\mathbf{I}-\mathbf{A})^{-1}\mathbf{B}_d]_{11}$,
$G_{vi_2}(s)=[(s\mathbf{I}-\mathbf{A})^{-1}\mathbf{B}_{u1}]_{21}$, $G_{zi_2}(s)=[(s\mathbf{I}-\mathbf{A})^{-1}\mathbf{B}_{u2}]_{21}$, $G_{di_2}(s)=[(s\mathbf{I}-\mathbf{A})^{-1}\mathbf{B}_d]_{21}$,
$G_{vv_1}(s)=[(s\mathbf{I}-\mathbf{A})^{-1}\mathbf{B}_{u1}]_{31}$, $G_{zv_1}(s)=[(s\mathbf{I}-\mathbf{A})^{-1}\mathbf{B}_{u2}]_{31}$, $G_{dv_1}(s)=[(s\mathbf{I}-\mathbf{A})^{-1}\mathbf{B}_d]_{31}$,
$G_{vv_2}(s)=[(s\mathbf{I}-\mathbf{A})^{-1}\mathbf{B}_{u1}]_{41}$, $G_{zv_2}(s)=[(s\mathbf{I}-\mathbf{A})^{-1}\mathbf{B}_{u2}]_{41}$, $G_{dv_2}(s)=[(s\mathbf{I}-\mathbf{A})^{-1}\mathbf{B}_d]_{41}$,
$G_{vv}(s)=\mathbf{C}(s\mathbf{I}-\mathbf{A})^{-1}\mathbf{B}_{u1}+\mathbf{E}_{u1}$, $G_{zv}(s)=\mathbf{C}(s\mathbf{I}-\mathbf{A})^{-1}\mathbf{B}_{u2}+\mathbf{E}_{u2}$, and
$G_{dv}(s)=\mathbf{C}(s\mathbf{I}-\mathbf{A})^{-1}\mathbf{B}_d+\mathbf{E}_d$.

III. Modeling Of SEPIC Converter By SSA Technique

A SEPIC converter is shown in Fig. 1(a). It is comprised of the MOSFET switch (Q), diode (D), two capacitors (C_1 and C_2), and two inductors (L_1 and L_2). The resistor, R, represents a standing load, and the current source, I_Z, models the load current. The resistors, r_{C1}, r_{C2}, r_{L1}, and r_{L2}, are equivalent series resistances (ESRs) of the capacitors and inductors respectively. Their values are usually very small compared to R. In the ideal converter, these ESRs are zero. In CCM, the converter exhibits two circuit states. The first state is when Q is turned on (Fig. 1(b)). During this interval (dT), L_1 is charged by the source, V_g, and L_2 by the capacitor C_1. Hence i_{L1} and i_{L2} increase linearly as shown in Fig. 2. The second state is when Q is turned off (Fig. 1(c)). During this interval ($(1-d)T$), L_1 and L_2 are in a discharging phase; L_1 and L_2 release the stored energy to the capacitors and load respectively. Thus, i_{L1} and i_{L2} decrease linearly as shown in Fig. 2.

The output voltage, V_O, is a DC voltage that contains small ripple due to the switching action. For ideal SEPIC converter, the relationship between V_O and V_g is given by:

$$M=V_O/V_g=D/(1-D) \tag{10}$$

where M is a voltage conversion ratio. It can be seen that V_O could be larger or smaller than V_g, depending on the duty cycle. From Fig. 2, the averaged inductor currents, I_{L1} and I_{L2}, must be greater than one-half of their ripple components, Δi_{L1} and Δi_{L2}, for the circuit to remain in CCM. It can be shown that for CCM operation L_1 and L_2 must satisfy the following conditions:

$$\begin{cases}L_1>\dfrac{(1-D)^2R}{2Df}\left(\dfrac{1}{\frac{r_{C2}}{R}+1}+\dfrac{1}{1-D}\dfrac{R_g}{R}+\dfrac{Mr_{C1}}{R}+\dfrac{r_{L1}}{R}\right)\\ L_2>\dfrac{(1-D)R}{2f}\left(\dfrac{1}{\frac{r_{C2}}{R}+1}+\dfrac{1}{1-D}\dfrac{r_{L2}+R_g}{R}+\dfrac{Mr_{C1}}{R}-M\dfrac{r_{C1}+r_{L1}}{R}\right)\end{cases} \tag{11}$$

where $R_g=r_{C2}R/(r_{C2}+R)$.

A. State-Space Description of SEPIC Converter

The state-space equations of the SEPIC converter for the on and off states of the switch can be written from Figs. 1(b) and (c) respectively, which are given by:

$$\begin{aligned}\frac{di_{L1}}{dt}&=\frac{-I_{L1}}{L_1}[r_{L1}+(1-\delta)(r_{C1}+R_g)]-(1-\delta)\left(\frac{R_gI_{L2}}{L_1}+\frac{v_{C1}}{L_1}+\frac{R_gv_{C2}}{r_{C2}L_1}-\frac{R_gI_Z}{L_1}\right)+\frac{V_g}{L_1}\\ \frac{di_{L2}}{dt}&=(1-\delta)\left(\frac{I_Z}{L_2}-\frac{I_{L1}}{L_2}-\frac{v_{C2}}{r_{C2}L_2}\right)R_g-\frac{I_{L2}}{L_2}[r_{C1}\delta+r_{L2}+(1-\delta)R_g]+\frac{v_{C1}}{L_2}\delta\\ \frac{dv_{C1}}{dt}&=\frac{I_{L1}}{C_1}(1-\delta)-\frac{I_{L2}}{C_1}\delta\\ \frac{dv_{C2}}{dt}&=\frac{1-\delta}{C_2r_{C2}}(I_{L1}+I_{L2})R_g-\frac{R_g}{C_2r_{C2}R}v_{C2}-\frac{R_g}{C_2r_{C2}}I_Z\\ v_O&=(1-\delta)(I_{L1}+I_{L2})R_g+\frac{R_g}{r_{C2}}v_{C2}-R_gI_Z\end{aligned} \tag{12}$$

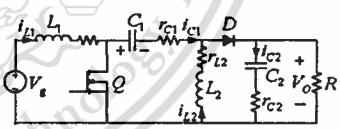

(a). SEPIC converter.

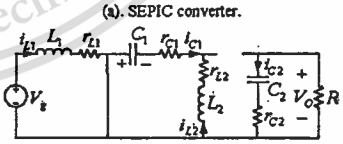

(b) SEPIC converter during the first state d_1T.

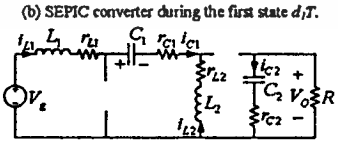

(c) SEPIC converter during the second state d_2T.

Fig. 1. Operation of the SEPIC converter in CCM.

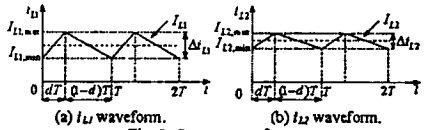

(a) i_{L1} waveform. (b) i_{L2} waveform.

Fig. 2. Current waveforms.

Note that the equations are expressed in a compact form using the switching function, δ. When the switch is on, δ =1, (12) will become the on-state equation. When the switch is off, δ =0, (12) will become the off-state equation.

The averaged matrices for the steady-state and the linear small-signal state-space equations can be written according to (4) and (5).

$$\mathbf{A}=\begin{bmatrix} [r_{L1}+(r_{C1}+R_g)(D-1)]/L_1 & (D-1)R_g/L_1 & (D-1)/L_1 & (D-1)R_g/(L_1r_{C2}) \\ (D-1)R_g/L_2 & [Dr_{C1}+R_g(1-D)-r_{L2}]/L_2 & D/L_2 & (D-1)R_g/(L_2r_{C2}) \\ (1-D)/C_1 & -D/C_1 & 0 & 0 \\ (1-D)R_g/(C_2r_{C2}) & (1-D)R_g/(C_2r_{C2}) & 0 & -1/[C_2(r_{C2}+R)] \end{bmatrix} \quad (13)$$

$$\mathbf{B}=\begin{bmatrix} 1/L_1 & (1-D)R_g/L_1 \\ 0 & (1-D)R_g/L_2 \\ 0 & 0 \\ 0 & -R_g/(C_2r_{C2}) \end{bmatrix} \quad (14)$$

$$\mathbf{C}=\begin{bmatrix} (1-D)R_g & (1-D)R_g & 0 & R_g/r_{C2} \end{bmatrix} \quad (15)$$

$$\mathbf{E}=\begin{bmatrix} 0 & -R_g \end{bmatrix} \quad (16)$$

$$\mathbf{B}_d=\begin{bmatrix} \dfrac{V_g[R_g[Mr_{C1}+r_{L2}+R/(1-D)]-MR^2]-Mr_{L1}RR_gI_z}{\eta(1-D)r_{C2}R^2L_1} \\ \dfrac{V_g[R_g[r_{L2}+R/(1-D)]-MR^2]-(r_{C1}+Mr_{L1})RR_gI_z}{\eta(1-D)r_{C2}R^2L_2} \\ -R_g(MV_g+RI_z)/[(1-D)\eta r_{C2}C_2R^2] \\ -(MV_g+RI_z)/[(1-D)\eta RC_2] \end{bmatrix} \quad (17)$$

$$\mathbf{E}_d=-r_{C2}(MV_g+RI_z)/[\eta R(1-D)] \quad (18)$$

B. Steady-State Equations

Given the averaged matrices in (13) to (18), the steady-state solution of converter is obtained from (6):

$$\begin{bmatrix} I_{L1} \\ I_{L2} \\ V_{C1} \\ V_{C2} \end{bmatrix}=\frac{M}{\eta}\begin{bmatrix} r_{C2}M/(R_gR) & (r_{C2}/R_g \\ r_{C2}/(R_gR) & (r_{C2}/MR_g) \\ \dfrac{r_{C2}}{R_gR}(r_{C1}+\dfrac{1}{M}\dfrac{r_{L2}+R}{1-D})-1 & \dfrac{(r_{L2}-Mr_{L1})r_{C2}}{MR_g} \\ r_{C2}/R_g & -(r_{C1}+Mr_{L1}+r_{L2}/M)r_{C2}/R_g-r_{C2}/(1-D) \end{bmatrix} \quad (19)$$

$$V_o=[V_g+[r_{L2}r_{C2}R/[MR_g(1-D)]-R_g-r_{C1}-r_{L1}M]I_z]Mr_{C2}/(\eta R_g)$$

where $R_g=r_{C2}R/(r_{C2}+R)$, $L_T=L_1+L_2$, $R_T=R+r_{C2}$, $M=D/(1-D)=D/D'$, $\eta=1+n+r_{C2}/[(1-D)R]$, and $n=(1+r_{C2}/R)(r_{L2}/R+Mr_{C1}/R+M^2r_{L1}/R)$.

Note that if r_{C1}, r_{C2}, r_{L1}, and r_{L2} are assumed to be zero, the equation (19) will be reduced to $M=V_O/V_g=D/(1-D)$, the same as the expression for the ideal SEPIC converter in (10).

C. Linear Small-Signal State-Space Equations

Given the averaged matrices (13) to (18), the linear small-signal state-space equations of the SEPIC converter can be formulated in accordance with (5):

$$\frac{d}{dt}\begin{bmatrix} \tilde{i}_{L1} \\ \tilde{i}_{L2} \\ \tilde{v}_{C1} \\ \tilde{v}_{C2} \end{bmatrix}=\begin{bmatrix} \dfrac{r_{L1}+(r_{C1}+R_g)(D-1)}{L_1} & \dfrac{D-1}{L_1}R_g & \dfrac{D-1}{L_1} & \dfrac{D-1}{L_1r_{C2}}R_g \\ \dfrac{(D-1)R_g}{L_2} & -\dfrac{r_{L2}+Dr_{C1}+R_g(1-D)}{L_2} & \dfrac{D}{L_2} & \dfrac{D-1}{L_2r_{C2}}R_g \\ \dfrac{1-D}{C_1} & -\dfrac{D}{C_1} & 0 & 0 \\ \dfrac{1-D}{C_2r_{C2}}R_g & \dfrac{1-D}{C_2r_{C2}}R_g & 0 & \dfrac{-1}{C_2(r_{C2}+R)} \end{bmatrix}\begin{bmatrix} \tilde{i}_{L1} \\ \tilde{i}_{L2} \\ \tilde{v}_{C1} \\ \tilde{v}_{C2} \end{bmatrix}+$$

$$\begin{bmatrix} \dfrac{1}{L_1} & \dfrac{1-D}{L_1}R_g & \dfrac{V_g[R_g(Mr_{C1}+r_{L2}+\frac{R}{1-D})-MR^2]-Mr_{L1}RR_gI_z}{\eta(1-D)r_{C2}R^2L_1} \\ 0 & \dfrac{1-D}{L_2}R_g & \dfrac{V_g[R_g(r_{L2}+\frac{R}{1-D})-MR^2]-(r_{C1}+Mr_{L1})I_zRR_g}{\eta(1-D)r_{C2}R^2L_2} \\ 0 & 0 & \dfrac{-R_g[MV_g+RI_z]}{\eta(1-D)r_{C1}C_2R^2} \\ 0 & \dfrac{-R_g}{C_2r_{C2}} & \dfrac{-MV_g-RI_z}{\eta(1-D)RC_2} \end{bmatrix}\begin{bmatrix} \tilde{v}_g \\ \tilde{i}_z \\ d \end{bmatrix} \quad (20)$$

$$\tilde{v}_o=\begin{bmatrix} (1-D)R_g & (1-D)R_g & 0 & \dfrac{R_g}{r_{C2}} \end{bmatrix}\begin{bmatrix} \tilde{i}_{L1} \\ \tilde{i}_{L2} \\ \tilde{v}_{C1} \\ \tilde{v}_{C2} \end{bmatrix}+\begin{bmatrix} 0 & -R_g & \dfrac{-MV_g-RI_z}{\eta(1-D)R}r_{C2} \end{bmatrix}\begin{bmatrix} \tilde{v}_g \\ \tilde{i}_z \\ d \end{bmatrix}$$

D. Finding Transfer Functions

Referring to (9), fifteen transfer functions can be determined from (20). However, only a few of them are useful for feedback control design. These transfer functions are:

The duty ratio-to-output voltage transfer function

$$G_{dv}(s)=\tilde{v}_o(s)/\tilde{d}(s)=\mathbf{C}(s\mathbf{I}-\mathbf{A})^{-1}\mathbf{B}_d+\mathbf{E}_d$$
$$=K_D(a_{dv}s^4+b_{dv}s^3+c_{dv}s^2+d_{dv}s+e_{dv})/\Delta \quad (21)$$

where $K_D=1/R_TD'+R(n-M)D'^2$.

The input voltage-to-output voltage transfer function

$$G_{vv}(s)=\tilde{v}_o(s)/\tilde{v}_g(s)=\mathbf{C}(s\mathbf{I}-\mathbf{A})^{-1}\mathbf{B}_{d1}+\mathbf{E}_{d1}$$
$$=RD'(a_{vv}s^3+b_{vv}s^2+c_{vv}s+d_{vv})/\Delta \quad (22)$$

The output impedance transfer function

$$G_{zv}(s)=\tilde{v}_o(s)/\tilde{i}_z(s)=\mathbf{C}(s\mathbf{I}-\mathbf{A})^{-1}\mathbf{B}_{d2}+\mathbf{E}_{d2}$$
$$=R(a_{zv}s^4+b_{zv}s^3+c_{zv}s^2+d_{zv}s+e_{zv})/\Delta \quad (23)$$

where $\Delta=as^4+bs^3+cs^2+ds+e$

The coefficients in (21) to (23) are listed in TABLE I.

IV. Results

To validate the accuracy of the SEPIC converter model, $G_{dv}(s)$ in (21) is plotted and compared with the results from the other two methods, PWM switch model [1, 2] and averaged switch model [3, 4]. They are shown in Fig. 3(a) to Fig. 3(c) respectively. The following circuit parameters are used to create these plots: L_1 = 100μH, r_{L1} = 1mΩ, L_2 = 100μH, r_{L2} = 1mΩ, C_1 = 680μF, r_{C1} = 3mΩ, C_2 = 2200μF, r_{C2} = 1mΩ, V_g = 10V, V_O = 15V, I_z = 0, and R = 1Ω. The plotted $G_{dv}(s)$ in Fig 3(a) has four complex poles at $p_{1,2}$ = (-0.0158±2.7771i)x10^3 and $p_{3,4}$ = (-0.2403±1.1578i)x10^3; and two real zeros at z_1 = -4.5455x10^5, z_2 = 0.0510x10^5 and two complex zeros at $z_{3,4}$ = (0.0010±0.0277i)x10^5. It can be seen from Fig. 3(a) to Fig. 3(c) that $G_{dv}(s)$ derived by the SSA technique is exactly the same as the other two methods, validating the accuracy of the model derived by the SSA technique.

TABLE I
COEFFICIENTS OF $G_{dv}(s)$, $G_{zv}(s)$, AND $G_{vv}(s)$.

$a_{dv}=-r_{C2}L_1C_1L_2C_2R_T^2(DV_g+RD'I_g)$,

$b_{dv}=[D'^2r_{C2}I_gC_2R_T-DI_2(r_{L1}r_{C2}C_2+L_1)-r_{C2}C_2DL_1(Dr_{C1}+r_{L1})]R_T^2C_1V_g$
$-D'C_1RR_TI_g[r_{C2}C_2I_gR_T(Dr_{L1}+r_{C1})+r_{C2}RD']$
$+R_gI_1(r_{C2}r_{L2}C_2+L_2)+r_{C2}L_2C_2(r_{L1}-Dr_{C1})]$,

$c_{dv}=R_T^2V_g[D'^2[C_1(r_{L2}+R)\{C_2(r_{L2}r_{C2}+r_{C2}r_{C1}+r_{L1}r_{C2})+L_T$
$-D'^2r_{C2}C_2I_1]-C_2D(Dr_{C1}+r_{L2})(L_1+r_{L1}r_{C2}C_2)+DI_2r_{L1}]-$
$D'R_T^2RI_g[C_1\{D'^2r_{C1}+(1+D)r_{L1}\}[r_{C2}C_2(r_{L2}+r_{C1})+L_2]+L_1C_1(r_{L2}+r_{C1})+$
$DI_1(r_{L1}C_1+r_{C2}C_2)+Dr_{L1}^2r_{C2}C_1C_2+D'C_1R_g[L_T+(r_{L2}+r_{C1}+r_{L1})C_2r_{C2}]]$,

$d_{dv}=-D'RR_TI_g[R_T[D(I_1-r_{C1}r_{L2}C_1+2r_{C2}r_{L2}C_2)+C_1r_{L2}(r_{L1}+r_{C1})]$
$+(r_{C2}RD'+r_{L1}R_TD)(r_{L1}+r_{L2})C_1+(r_{C1}R_T+r_{C2}R)(r_{C1}C_1+r_{C2}C_2)D']$
$+R_T^2V_g[D'^2[C_1R(r_{L1}+r_{L2})+r_{L2}C_1(r_{L2}-r_{L1})+(r_{C1}C_1+C_2r_{C2})(R+r_{L2})]$
$-r_{L1}D^3(r_{C1}C_1+r_{C2}C_2)-L_1D^2-Dr_{L2}r_{L1}C_1]$,

$e_{dv}=V_gR_T^2[D'^2(R+r_{L2})-D^2r_{L1}]-D'R_TRI_g[2DR_Tr_{L1}+D'(r_{C1}R_T+r_{C2}R)]$.

$a_{vv}=r_{C2}L_2C_1C_2R_T$, $b_{vv}=C_1R_T[r_{C2}C_2(Dr_{C1}+r_{L2})+L_2]$, $d_{vv}=DR_T$,
$c_{vv}=R_T[(r_{C1}C_1+r_{C2}C_2)D+r_{L2}C_1]$.

$a_{zv}=-r_{C2}I_1C_1L_2C_2R_T$, $c_{zv}=-R_T(D^2r_{L1}-D'^2r_{L2})-DD'(r_{C1}R_T+r_{C2}R)$,
$b_{zv}=C_1I_1I_2-r_{C2}C_1C_2[r_{C2}RI_gDD'+R_T(I_2r_{L1}+I_1r_{L2}+r_{C1}I_1D+r_{C1}I_2D')]$,
$c_{zv}=-r_{C2}C_2RDD'[L_T+C_1(r_{L1}r_{C2}+r_{C1}r_{C2}+r_{L2})]-R_T[r_{C1}C_1(I_1D+I_2D')+$
$r_{C2}C_2(I_1D^2+I_2D'^2)]-C_1R_T[r_{C2}C_2(Dr_{C1}+r_{L2})(r_{L1}+r_{C1}D')+r_{L1}L_2+r_{L2}L_1]$,
$d_{zv}=-(C_1r_{C1}r_{C2}+C_1r_{C2}r_{L2}+C_2r_{C2}^2)RDD'-R_T[(D'r_{C1}+r_{L1})(Dr_{C1}+r_{L2})C_1$
$+L_1D'^2+L_2D^2]-(r_{L1}C_1RD+r_{C1}C_2DD'+r_{L1}C_1D'^2+r_{L2}C_2D'^2)r_{C2}R_T$.

$a=I_gC_1L_2C_2R_T^2$, $e=R_T(D^2r_{L1}+D'^2r_{L2}+DD'r_{C1})+(D'R+r_{C2})D'R_I$,
$b=C_1R_T[C_2R_T\{I_gr_{C1}+L_1(r_{L2}+Dr_{C1})\}+C_2D'(r_{C1}I_gR_T+r_{C2}I_gR)+L_1I_g]$,
$c=C_1R_T[D'r_{C2}C_2R(r_{L1}+r_{L2}+r_{C1})+r_{C1}D'I_g+L_1(Dr_{C1}+r_{L2})+r_{L1}I_g]+$
$R_T^2C_1[C_1(Dr_{C1}+r_{L1})(r_{L1}+r_{C1}D')+D'^2L_g+L_1D^2]+(RD'+r_{C1})D'RC_1I_g$,
$d=R_T[C_1(Dr_{C1}+r_{L2})(r_{L1}+r_{C1}D')+r_{C2}C_2RD'+L_1D^2+I_gD'^2]$
$+(r_{L1}D^2+r_{L2}D'^2+r_{C1}DD')R_T^2C_2+(RD'+r_{C2})(r_{L1}+r_{L2}+r_{C1})RC_1D'$.

V. CONCLUSION

In this paper, modeling of a SEPIC converter in CCM has been performed with the State-Space Averaging (SSA) technique. The results yield an insight into the steady-state and small-signal dynamic properties of the converter, as given in (19) and (20) respectively. To provide a basis for feedback control design, three relevant transfer functions ($G_{dv}(s)$, $G_{vv}(s)$, and $G_{zv}(s)$) were derived. The derived transfer function, $G_{dv}(s)$, was verified to be accurate as shown in Fig. 3, where the frequency responses of the derived $G_{dv}(s)$ were seen to be identical to the AC simulation results by PSPICE of the SEPIC converter employing the PWM-switch model (Fig. 3(b)) and averaged switch model (Fig. 3(c)). Though not shown in the paper, other derived transfer functions, $G_{vv}(s)$ and $G_{zv}(s)$, have been found to be accurate as well.

REFERENCES

[1] V. Vorpérian, "Analysis of the Sepic Converter by Dr. Vatché Vorpérian," *Ridley Engineering Inc*, www.switchingpowermagazine.com, 2006.

[2] R. Ridley, "Analyzing the Sepic Converter," *Power Systems Design Europe Magazine*, pp. 14-18, November 2006.

[3] A. Hren and P. Slibar, "Full Order Dynamic Model of SEPIC Converter," *Proc. of the IEEE International Symposium on Industrial Electronics*, pp. 553-558, June 2005.

[4] R. W. Erickson and D. Maksimović, *Fundamentals of Power Electronics*, 2nd ed., Kluwer Academic Publishers, 2001.

[5] R. D. Middlebook and S. Cuk, "A General Unified Approach to Modeling Switching-Converter Power Stages," *International Journal of Electronics*, vol. 42, pp. 521-550, June 1977.

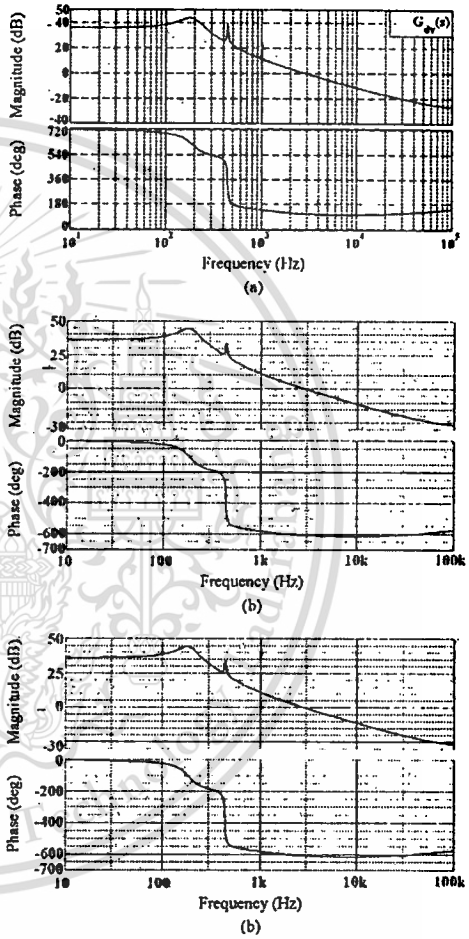

Fig. 3 Frequency responses of $G_{dv}(s)$ from: (a) SSA technique, (b) PWM-switch model, and (c) Averaged switch model.

Modeling of a SEPIC Converter Operating in Discontinuous Conduction Mode

Vuthchhay Eng and Chanin Bunlaksananusorn
Faculty of Engineering, King Mongkut's Institute of Technology Ladkrabang (KMITL),
Chalongkrung Rd. Ladkrabang, Bangkok 10520
vouthchhay_oeung@yahoo.com and kbchanin@kmitl.ac.th

Abstract **- A SEPIC (Single-Ended Primary Inductor Converter) DC-DC converter is capable of operating in either step-up or step-down mode and widely used in battery-operated equipment. There are two possible modes of operation in the SEPIC converter: Continuous Conduction Mode (CCM) and Discontinuous Conduction Mode (DCM). This paper presents modeling of a SEPIC converter operating in DCM using the State-Space Averaging (SSA) technique. The modeling leads to a small-signal linear model of the converter, from which the transfer functions used for feedback control design can be determined. It is found that the derived model is a reduced-order model, which can accurately predict the converter's characteristics up to one-tenth of the switching frequency.**

I. Introduction

A SEPIC (Single Ended Primary Inductor Converter) converter is a fourth-order dc-dc converter capable of delivering an output voltage which can be greater or lower than an input voltage. There are two possible modes of operation in the SEPIC converter: Continuous Conduction Mode (CCM) and Discontinuous Conduction Mode (DCM). Although the converter may have been designed for the CCM operation, it can plunge into the DCM operation at light loads. In some cases, the converter is even intentionally designed to operate in DCM because of the faster dynamic response compared with the CCM [1, 2]. Recently, the small-signal dynamic characteristics of the DCM SEPIC converter have been modeled [3]. In this work, the active switch and passive diode of the SEPIC converter were substituted by the PWM-switch model [4]. Transfer functions of interest, e.g. duty ratio-to-output or input-to-output transfer function, were then derived from the resulting equivalent circuit. However, the modeling process in [3] had assumed the converter is being ideal and neglected the Equivalent Series Resistance (ESR) of the capacitors. The ESR affects the value of zeros in the final transfer functions - excluding it from the modeling process only adds to the inaccuracy in the final model.

This papers presents modeling of the DCM SEPIC converter with State-Space Averaging (SSA) technique [1], taking into account the effect of the capacitors' ESR. The transfer functions for feedback control design are derived and compared with the results from the DCM averaged switch model [2]. It is found that the derived model is a reduced-order model, which can accurately predict the converter's characteristics up to one-tenth of the switching frequency.

II. Overview of SSA Technique in DCM

A SEPIC converter is shown in Fig. 1(a). Due to the switching action of the MOSFET, Q, and diode, D, the converter will exhibit three different circuit states in one switching period, T, when operating in DCM. The first state exists when Q is turned on for a time interval d_1T (Fig. 1(b)), the second state when Q is turned off (i.e. D turned on) for a time interval d_2T (Fig. 1(c)), and the third state when both Q and D are turned off for the rest of the time period d_3T (Fig. 1(d)). Note that d_1 and d_2 are the duty cycle of Q and D respectively, and d_3 equals $1-d_1-d_2$. The general state-space equations for these three circuit states are:

$$\begin{cases} dx/dt = \mathbf{A}_1\mathbf{x} + \mathbf{B}_1\mathbf{u} \\ \mathbf{y} = \mathbf{C}_1\mathbf{x} + \mathbf{E}_1\mathbf{u} \end{cases} \quad \text{for time interval } d_1T \tag{1-a}$$

$$\begin{cases} dx/dt = \mathbf{A}_2\mathbf{x} + \mathbf{B}_2\mathbf{u} \\ \mathbf{y} = \mathbf{C}_2\mathbf{x} + \mathbf{E}_2\mathbf{u} \end{cases} \quad \text{for time interval } d_2T \tag{1-b}$$

$$\begin{cases} dx/dt = \mathbf{A}_3\mathbf{x} + \mathbf{B}_3\mathbf{u} \\ \mathbf{y} = \mathbf{C}_3\mathbf{x} + \mathbf{E}_3\mathbf{u} \end{cases} \quad \text{for time interval } d_3T \tag{1-c}$$

Since the SEPIC converter is made up of two inductors L_1 and L_2 and two capacitors C_1 and C_2, the state vector $\mathbf{x}$, thus, comprises of i_{L1}, i_{L2}, v_{C1}, and v_{C2}. The input voltage v_g is typically assigned as the input vector $\mathbf{u}$, and the output voltage v_O as the output vector $\mathbf{y}$. To find the averaged behavior of the converter over one switching period, T, equations (1-a) to (1-c) are weighed average by the duty cycles as:

$$\begin{cases} dx/dt = \mathbf{A}\mathbf{x} + \mathbf{B}\mathbf{u} \\ \mathbf{y} = \mathbf{C}\mathbf{x} + \mathbf{E}\mathbf{u} \end{cases} \tag{2}$$

where $\mathbf{A}=\mathbf{A}_1d_1+\mathbf{A}_2d_2+\mathbf{A}_3d_3$, $\mathbf{B}=\mathbf{B}_1d_1+\mathbf{B}_2d_2+\mathbf{B}_3d_3$, $\mathbf{C}=\mathbf{C}_1d_1+\mathbf{C}_2d_2+\mathbf{C}_3d_3$, and $\mathbf{E}=\mathbf{E}_1d_1+\mathbf{E}_2d_2+\mathbf{E}_3d_3$.

Equation (2) is a nonlinear continuous-time equation. It can be linearized by small-signal perturbation with $\mathbf{x}=\mathbf{X}+\tilde{\mathbf{x}}$, $\mathbf{y}=\mathbf{Y}+\tilde{\mathbf{y}}$, $\mathbf{u}=\mathbf{U}+\tilde{\mathbf{u}}$, $d_1=D_1+\tilde{d}_1$, $d_2=D_2+\tilde{d}_2$, and $d_3=D_3+\tilde{d}_1-\tilde{d}_2$ where the tilde symbol " ~ " represents a small-signal value and the capital letter a DC value. It should be noted that $\mathbf{X}>>\tilde{\mathbf{x}}$, $\mathbf{Y}>>\tilde{\mathbf{y}}$, $\mathbf{U}>>\tilde{\mathbf{u}}$, $D_1>>\tilde{d}_1$, $D_2>>\tilde{d}_2$, and $D_3>>\tilde{d}_3$. The perturbation yields the steady-state and linear small-signal state-space equations in (3) and (4) respectively.

$$\begin{cases} dX/dt = \mathbf{A}\mathbf{X} + \mathbf{B}\mathbf{U} = 0 \\ \mathbf{Y} = \mathbf{C}\mathbf{X} + \mathbf{E}\mathbf{U} \end{cases} \tag{3}$$

978-1-4244-3388-9/09/$25.00 ©2009 IEEE

$$\begin{cases} d\tilde{\mathbf{x}}/dt = \mathbf{A}\tilde{\mathbf{x}} + \mathbf{B}\tilde{\mathbf{u}} + \mathbf{B}_{e1}\tilde{d}_1 + \mathbf{B}_{e2}\tilde{d}_2 \\ \tilde{\mathbf{y}} = \mathbf{C}\tilde{\mathbf{x}} + \mathbf{E}\tilde{\mathbf{u}} + \mathbf{E}_{e1}\tilde{d}_1 + \mathbf{E}_{e2}\tilde{d}_2 \end{cases} \quad (4)$$

where $\mathbf{A}=\mathbf{A}_1D_1+\mathbf{A}_2D_2+\mathbf{A}_3D_3$, $\mathbf{B}=\mathbf{B}_1D_1+\mathbf{B}_2D_2+\mathbf{B}_3D_3$, $\mathbf{C}=\mathbf{C}_1D_1+\mathbf{C}_2D_2+\mathbf{C}_3D_3$, $\mathbf{E}=\mathbf{E}_1D_1+\mathbf{E}_2D_2+\mathbf{E}_3D_3$, $\mathbf{B}_{e1}=(\mathbf{A}_1-\mathbf{A}_3)\mathbf{X}+(\mathbf{B}_1-\mathbf{B}_3)\mathbf{U}$, $\mathbf{B}_{e2}=(\mathbf{A}_2-\mathbf{A}_3)\mathbf{X}+(\mathbf{B}_2-\mathbf{B}_3)\mathbf{U}$, $\mathbf{E}_{e1}=(\mathbf{C}_1-\mathbf{C}_3)\mathbf{X}+(\mathbf{E}_1-\mathbf{E}_3)\mathbf{U}$, and $\mathbf{E}_{e2}=(\mathbf{C}_2-\mathbf{C}_3)\mathbf{X}+(\mathbf{E}_2-\mathbf{E}_3)\mathbf{U}$.

Equations (1) to (4) provide a systematic way to model the DC-DC converters in DCM. When applied to the DCM SEPIC converter, the direct solution of (3) and (4) will not produce correct results because the chosen state variables, i_{L1} and i_{L2}, are actually not independent from each other. Hence, only one of these currents can be said to be a true state variable. If both i_{L1} and i_{L2} are to remain as a state variable as in equations (2) to (4), some constraints must be imposed on them. As shown in [1], the steady-state and linear small-signal state-space equations in (3) and (4) are subject to the following constraints:

$$I = i(V_g, V_O, L_1, L_2, T) \quad (5\text{-a})$$

where $I = I_{L1} + I_{L2}$.

$$\begin{cases} d\tilde{i}/dt = 0 \\ \tilde{i} = (\partial i/\partial v_g)\tilde{v}_g + (\partial i/\partial v_O)\tilde{v}_O + (\partial i/\partial d)\tilde{d}_1 \end{cases} \quad (5\text{-b})$$

wehre $\tilde{i} = \tilde{i}_{L1} + \tilde{i}_{L2}$.

To find the steady-state solution, due to the reason above, the relationship between I_{L1} and I_{L2} must be first established before the other unknown, such as V_{C1} V_{C2}, and V_O, can be found by solving (3):

$$\begin{cases} \mathbf{X} = -\mathbf{A}^{-1}\mathbf{B}\mathbf{U} \\ \mathbf{Y} = (-\mathbf{C}\mathbf{A}^{-1}\mathbf{B} + \mathbf{E})\mathbf{U} \end{cases} \quad (6)$$

The constraints in (5) will result in $\tilde{d}_2$ and one inductor current be eliminated from the linear small-signal state-space equations in (4). The disappearance of one inductor current means the system's order has been reduced by one. For this reason, the converter's model derived by the SSA technique in DCM is known as a reduced-order model [3, 5]. Consequently, the linear small-signal state-space can be rewritten as:

$$\begin{cases} d\tilde{\mathbf{x}}/dt = \mathbf{A}_m\tilde{\mathbf{x}} + \mathbf{B}_m\tilde{v}_g + \mathbf{B}_{me1}\tilde{d}_1 \\ \tilde{\mathbf{y}} = \mathbf{C}_m\tilde{\mathbf{x}} + \mathbf{E}_m\tilde{v}_g + \mathbf{E}_{me1}\tilde{d}_1 \end{cases} \quad (7)$$

Finally, by applying the Laplace transform to (7), transfer functions for feedback control design, e.g. duty ratio-to-output or input-to-output transfer function, can be derived.

III. Modeling of SEPIC Converter in DCM

In Fig. 1(a), the resistances r_{C1} and r_{C2} are Equivalent Series Resistances (ESRs) of the capacitors C_1 and C_2 respectively. Although their values are small, these ESRs cannot be neglected in the modeling process as they have a direct impact on the accuracy of the final model. Fig. 2 depicts the current waveforms i_{L1} and i_{L2} of the converter, when operating in DCM. The currents i_{L1} and i_{L2} are increasing during the time interval d_1T and decreasing during the time interval d_2T. During the time interval d_3T, these currents have a constant value, with the amplitude of i_{L1} and i_{L2} being equal but flowing on the opposite direction (Fig. 1(d)); that is, $i_{L1} = -i_{L2}$. The equality in the amplitude of i_{L1} and i_{L2} is always true during the time interval d_3T, and this essentially makes i_{L1} and i_{L2} depend on each other.

A. State-Space Description

Chosen $\mathbf{x} = [i_{L1}\ i_{L2}\ v_{C1}\ v_{C2}]^T$, $\mathbf{u} = v_g$, and $\mathbf{y} = v_O$, the matrices $\mathbf{A}_1$, $\mathbf{A}_2$, $\mathbf{A}_3$, $\mathbf{B}_1$, $\mathbf{B}_2$, $\mathbf{B}_3$, $\mathbf{C}_1$, $\mathbf{C}_2$, $\mathbf{C}_3$, $\mathbf{E}_1$, $\mathbf{E}_2$, and $\mathbf{E}_3$ in (1) are determined from the circuits in Figs. 1(b) to 1(d).

$$\mathbf{A}_1 = \begin{bmatrix} 0 & 0 & 0 & 0 \\ 0 & -r_{C1}/L_2 & 1/L_2 & 0 \\ 0 & -1/C_1 & 0 & 0 \\ 0 & 0 & 0 & -R_g/(C_2r_{C2}R) \end{bmatrix} \quad (8\text{-a})$$

$$\mathbf{A}_2 = \begin{bmatrix} (R_g - r_{C1})/L_1 & -R_g/L_1 & -1/L_1 & -R_g/(L_1r_{C2}) \\ -R_g/L_2 & -R_g/L_2 & 0 & -R_g/(L_2r_{C2}) \\ 1/C_1 & 0 & 0 & 0 \\ R_g/(C_2r_{C2}) & R_g/(C_2r_{C2}) & 0 & -R_g/(C_2r_{C2}R) \end{bmatrix} \quad (8\text{-b})$$

$$\mathbf{A}_3 = \begin{bmatrix} r_{C1}/(L_1+L_2) & 0 & -1/(L_1+L_2) & 0 \\ -r_{C1}/(L_1+L_2) & 0 & 1/(L_1+L_2) & 0 \\ 1/C_1 & 0 & 0 & 0 \\ 0 & 0 & 0 & -R_g/(C_2r_{C2}R) \end{bmatrix} \quad (8\text{-c})$$

$$\mathbf{B}_1 = [1/L_1\ 0\ 0\ 0]^T \quad (8\text{-d})$$

$$\mathbf{B}_2 = [1/L_1\ 0\ 0\ 0]^T \quad (8\text{-e})$$

$$\mathbf{B}_3 = [1/(L_1+L_2)\ \ -1/(L_1+L_2)\ \ 0\ \ 0]^T \quad (8\text{-f})$$

$$\mathbf{C}_1 = [0\ 0\ 0\ R_g/r_{C2}] \quad (8\text{-g})$$

$$\mathbf{C}_2 = [R_g\ R_g\ 0\ R_g/r_{C2}] \quad (8\text{-h})$$

$$\mathbf{C}_3 = [0\ 0\ 0\ R_g/r_{C2}] \quad (8\text{-i})$$

$$\mathbf{E}_1 = \mathbf{E}_2 = \mathbf{E}_3 = [0] \quad (8\text{-j})$$

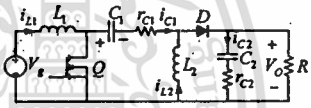

(a) SEPIC converter.

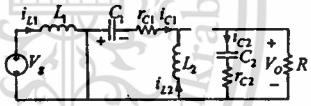

(b) SEPIC converter during the first state d_1T.

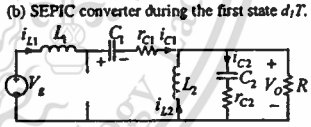

(c) SEPIC converter during the second state d_2T.

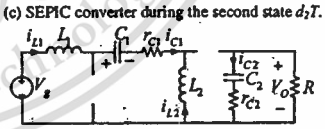

(d) SEPIC converter during the third state d_3T.

Fig. 1. Operation of the SEPIC converter in DCM.

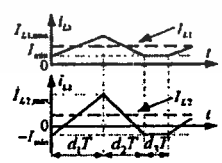

Fig. 2. Current waveform of i_{L1} and i_{L2}.

Referring back to (3) and (4), the matrices for the steady-state equations and the linear small-signal state-space equations are determined from (8):

$$\mathbf{A}=\begin{bmatrix} \frac{r_{C1}D_1}{L_1+L_2} & \frac{(r_{C1}+R_E)D_2}{L_1} & \frac{-R_ED_1}{L_1} & -K_{34} & \frac{-R_ED_2}{L_1r_{C2}} \\ \frac{-R_ED_2}{L_2} & \frac{r_{C1}D_1}{L_1+L_2} & \frac{-r_{C1}D_1-R_ED_2}{L_2} & K_{34} & \frac{-R_ED_2}{L_2r_{C2}} \\ \frac{D_2+D_1}{C_1} & & \frac{-D_1}{C_1} & 0 & 0 \\ \frac{R_ED_2}{C_2r_{C2}} & & \frac{R_ED_1}{C_2r_{C2}} & 0 & \frac{-R_E}{C_2r_{C2}R} \end{bmatrix} \quad (9\text{-a})$$

$$\mathbf{B}=\begin{bmatrix}(D_1+D_2)/L_1+D_2/(L_1+L_2) & -D_1/(L_1+L_2) & 0 & 0\end{bmatrix}^T \quad (9\text{-b})$$

$$\mathbf{C}=\begin{bmatrix}R_ED_2 & R_ED_2 & 0 & R_E/r_{C2}\end{bmatrix} \quad (9\text{-c})$$

$$\mathbf{E}=[0] \quad (9\text{-d})$$

$$\mathbf{B}_{d1}=\begin{bmatrix} -r_{C1}I_{L1}/(L_1+L_2)+V_g/L_1 \\ r_{C1}I_{L1}/(L_1+L_2)+(V_{C1}-r_{C1}I_{L2})/L_1 \\ -(I_{L1}+I_{L2})/C_1 \\ 0 \end{bmatrix} \quad (9\text{-e})$$

$$\mathbf{B}_{d2}=\begin{bmatrix} -[(r_{C1}+R_E)/L_1+r_{C1}/(L_1+L_2)]I_{L1}-(I_{L2}+V_{C2}/r_{C2})R_E/L_1 \\ [r_{C1}/(L_1+L_2)-R_E/L_2]I_{L1}-(I_{L2}+V_{C2}/r_{C2})R_E/L_2 \\ 0 \\ R_E(I_{L1}+I_{L2})/(C_2r_{C2}) \end{bmatrix} \quad (9\text{-f})$$

$$\mathbf{E}_{d1}=[0] \quad (9\text{-g})$$

$$\mathbf{E}_{d2}=[R_E(I_{L1}+I_{L2})] \quad (9\text{-h})$$

B. Steady-state equations

As stated above, the relationship between the steady-state inductor currents, I_{L1} and I_{L2}, must be determined before other steady-state values can be found. This is done by averaging the capacitor current i_{C1} in Fig. 3 over a switching period, T. In Fig. 3, i_{C1} can be expressed as:

$$i_{C1}=-i_{L2} \quad \text{for time interval } d_1T \quad (10\text{-a})$$

$$i_{C1}=i_{L1} \quad \text{for time interval } d_2T \quad (10\text{-b})$$

$$i_{C1}=i_{L1}=-i_{L2} \quad \text{for time interval } d_3T \quad (10\text{-c})$$

Average of i_{C1} over a switching period, T, gives:

$$I_{C1}=I_{min}-(I_{L2}+I_{min})D_1/(D_1+D_2)+(I_{L1}-I_{min})D_2/(D_1+D_2) \quad (11)$$

In steady-state, I_{C1} is equal to zero. Thus the relationship between I_{L1} and I_{L2} is obtained as:

$$I_{L2}=I_{L1}D_2/D_1 \quad (12)$$

Given the averaged matrices in (9-a) to (9-d) and the relationship in (12), the steady-state solution of converter can be obtained by using (5).

$$\begin{bmatrix} I_{L1} \\ I_{L2} \\ V_{C1} \\ V_{C2} \end{bmatrix}=V_g\begin{bmatrix} (D_1/D_2)^2\eta/R \\ \eta D_1/(RD_2) \\ 1 \\ \eta D_1/D_2 \end{bmatrix} \quad (13)$$

where $\eta=1/[1+R_ED_1/(RD_2)+[L_1+L_2(1-D_1)/D_2]r_{C1}D_1/[RD_2(L_1+L_2)]]$

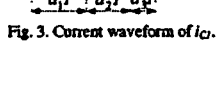

Fig. 3. Current waveform of i_{C1}.

From Fig. 2, the average value of I_{L1} and I_{L2} are expressed as:

$$I_{L1}=D_1T(D_1+D_2)V_g/(2L_1)+I_{min} \quad (14\text{-a})$$

$$I_{L2}=D_1T(D_1+D_2)V_g/(2L_2)-I_{min} \quad (14\text{-b})$$

Matching the summation of I_{L1} and I_{L2} in (13) to those in (14), D_2 can be defined as:

$$D_2=\sqrt{2\eta L_E/(RT)} \quad (15)$$

where $L_E=(L_1+L_2)/(L_1L_2)$ and $R_E=(R+r_{C2})/(Rr_{C2})$.

C. Linear Small-Signal State-Space Equations

Referring to (7), linear small-signal state-space equation is:

$$\begin{cases} \frac{d}{dt}\begin{bmatrix}\tilde{i}_{L1} & \tilde{i}_{L2} & \tilde{v}_{C1} & \tilde{v}_{C2}\end{bmatrix}^T=\mathbf{A}_m\begin{bmatrix}\tilde{i}_{L1} & \tilde{i}_{L2} & \tilde{v}_{C1} & \tilde{v}_{C2}\end{bmatrix}^T+\mathbf{B}_m\tilde{v}_g+\mathbf{B}_{md1}\tilde{d}_1 \\ \tilde{v}_O=\mathbf{C}_m\begin{bmatrix}\tilde{i}_{L1} & \tilde{i}_{L2} & \tilde{v}_{C1} & \tilde{v}_{C2}\end{bmatrix}^T+\mathbf{E}_m\tilde{v}_g+\mathbf{E}_{md1}\tilde{d}_1 \end{cases} \quad (16)$$

where

$$\mathbf{A}_m=\begin{bmatrix} r_{C1}(K_{33}-K_{23}K_{12}/n) & 0 & -K_{23}K_{12}/n-TD_1K_E/(2L_2)-K_{34} & D_2[K_{23}/(nL_E)-1/L_1] \\ r_{C1}(K_{23}K_{12}/n-K_{23}) & 0 & K_{23}K_{12}/n+TD_1K_E/(2L_2)+K_{34} & -D_2[K_{23}/(nL_E)-1/L_1] \\ 1/C_1 & 0 & -TD_1^2/(2L_2C_1) & 0 \\ r_{C1}K_{12}/(nC_2) & 0 & (D_2-IR_{ln}/n)TD_1/(2L_2C_2)+IK_{12}/(nC_2) & -[1/R+ID_1/(nL_E)]/C_2 \end{bmatrix}$$

$$\mathbf{B}_m=\begin{bmatrix} (D_1+D_2)/L_1+D_2/(L_1+L_2)-K_{23}(D_1+D_2)/(nL_1)-TD_1K_E/(2L_1) \\ -(D_1+D_2)/L_1-D_2/(L_1+L_2)+K_{23}(D_1+D_2)/(nL_2)+TD_1K_E/(2L_2) \\ -TD_1^2/(2L_1C_1) \\ (D_1+D_2)I/(nL_1C_2)+(D_2-IR_{ln}/n)TD_1/(2L_2C_2) \end{bmatrix}$$

$$\mathbf{C}_m=\begin{bmatrix}r_{C1}R_EIK_{12}/n & 0 & R_E[IK_{12}/n+(D_2-IR_{ln}/n)TD_1/(2L_2)] & 1-IR_ED_1/(nL_E)\end{bmatrix}$$

$$\mathbf{E}_m=\begin{bmatrix}R_EI(D_1+D_2)/(nL_1)+(D_2-IR_{ln}/n)TD_1R_E/(2L_1)\end{bmatrix}$$

$$\mathbf{B}_{md1}=\begin{bmatrix} V_g[1/L_1-K_{23}/(nL_E)]+r_{C1}[K_{23}I_{L2}/(nL_2)-I_{L1}(L_1+L_2)]-K_TIK_E/D_1 \\ -V_g[1/L_1-K_{23}/(nL_E)]-r_{C1}[K_{23}I_{L2}/(nL_2)-I_{L1}(L_1+L_2)]+K_TIK_E/D_1 \\ -2I/C_1 \\ (V_g/L_E-r_{C1}I_{L2}/L_2)I/(nC_2)+(D_2-IR_{ln}/n)I/(D_1C_2) \end{bmatrix}$$

$$\mathbf{E}_{md1}=\begin{bmatrix}(V_g/L_E-r_{C1}I_{L2}/L_2)R_EI/n+(D_2-IR_{ln}/n)R_EI/D_1\end{bmatrix}$$

$K_{12}=D_1/L_2-D_2/L_1$, $K_{23}=D_2/(L_1+L_2)-D_1/L_1$, $K_{34}=D_2/L_1+D_2/(L_1+L_2)$, $K_E=R_ED_2/L_1-K_{23}R_E/n$, $K_{23}=R_EI/L_1+V_{C2}/L_1$, $n=(R_EI+V_{C2})/L_E$, $\eta=1$, $K_T=1/[1+TD_1r_{C1}/(2L_2)]=1$, $I=D_1TV_g/(2L_E)$, and $R_{ln}=r_{C1}D_1/L_2+R_ED_2/L_E$.

D. Finding Transfer Function

Applying the Laplace transform to (16), various transfer functions can be derived for the converter. Due to the limited space, only two important transfer functions are presented: the duty ratio-to-output voltage and input-to-output transfer functions, $G_{d1v}(s)$ and $G_{vv}(s)$, respectively.

$$G_{d1v}(s)=\tilde{v}_O(s)/\tilde{d}_1(s)=\mathbf{C}(s\mathbf{I}-\mathbf{A})^{-1}\mathbf{B}_{d1}+\mathbf{E}_{d1}$$
$$=\frac{[TD_2V_g/(L_EC_2)](a_{d1v}s^3+b_{d1v}s^2+c_{d1v}s+d_{d1v})}{[as+[2+R_E/(RD_2)]/(C_2R)](s^2+bs+c)} \quad (17)$$

$$G_{vv}(s)=\tilde{v}_O(s)/\tilde{v}_g(s)=\mathbf{C}(s\mathbf{I}-\mathbf{A})^{-1}\mathbf{B}_{v1}+\mathbf{E}_{v1}$$
$$=\frac{[TD_2/(4L_1^2L_2C_2C_2)](a_{vv}s^3+b_{vv}s^2+c_{vv}s+d_{vv})}{[as+[2+R_E/(RD_2)]/(C_2R)](s^2+bs+c)} \quad (18)$$

Coefficients of $G_{d1v}(s)$ and $G_{vv}(s)$ are listed in TABLE I.

IV. Results

Fig 4(a) shows a frequency response of $G_{d1v}(s)$ in (17). The plot is generated by MATLAB using the SEPIC converter's circuit parameters in TABLE II (these values cause the converter

to operate in DCM). Fig. 4(b) shows the same plot from PSPICE simulation using the DCM averaged switch model [2]. Generally accepted as being accurate, this PSPICE result is used to validate $G_{d1v}(s)$ in (17). The two results are closely agreed at frequencies below 10 KHz, i.e. one-tenth of switching frequency, beyond which the result from (17) starts to diverse from its PSPICE counterparts. The discrepancy occurs due to the fact that the former is a reduced-order model, while the latter is a full-order model [2, 5]. $G_{d1v}(s)$ in (17) being a reduced-order model is evident in (16), where all elements in the second column of $\mathbf{A_m}$ matrix are zero, which literally means i_{L2} is no longer a state variable, thus reducing the system's order by one.

TABLE I
COEFFICIENTS OF $G_{d1v}(s)$ AND $G_{vv}(s)$.

$$a_{dv}=C_2R_E[1-TD_1r_{C1}/(4L_1)-D_1L_Er_{C1}/(2D_2L_2R)]$$

$$b_{dv}=(1+R_E/R)[1-TD_1r_{C1}/(4L_2)]+\{D_2/L_1-D_1/L_2+TD_1^2r_{C1}/(4L_2^2)\}TD_1C_2R_E/(2C_1)$$
$$\frac{D_1L_2C_2R_E^2r_{C1}}{2D_2^2L_2L_1R}\{\frac{D_1L_1-D_2L_2}{L_1+L_2}\{(\frac{TD_1R}{2L_E}+1)D_2+D_1\}+\frac{D_1L_E(2D_2-1)}{L_2}\{\frac{TD_1R}{2L_E}+1\}\}$$
$$-\{[TD_1^2L_1/(4D_2L_2C_1R)+1]C_1/L_1+D_1(R+R_E)/(2D_2R^2R_E)-2C_1(D_1+D_2)/L_1\}L_ER_Er_{C1}/L_2$$

$$c_{dv}=\frac{TD_1}{2C_1}(1+\frac{R_E}{R})(\frac{D_2}{L_1}-\frac{D_1}{L_2})+\frac{r_{C1}(R+R_E)}{R}\{\frac{T^2D_1^3}{8L_2^2C_1}+\frac{1}{L_1+L_2}(1-2D_2-\frac{TD_1^2L_1}{4D_2L_2C_1R})\}$$
$$\frac{D_1L_2C_1R_Er_{C1}}{2D_2C_1R(L_1+L_2)^2}+\frac{C_1R_E}{C_1(L_1+L_2)}\{1-[L_1+D_2L_2-4D_2(L_1D_1-L_2D_2)]\frac{TD_1r_{C1}}{4L_2L_1}\}$$
$$+\frac{D_1r_{C1}(D_1-D_2)}{2D_2C_1R(L_1+L_2)^2}\{\frac{C_1R_E}{D_2}(D_1L_2-2D_2L_1)-\frac{r_{C1}}{2R}\{TD_1^2C_1RR_E+2L_2C_1(R+R_E)\}\}$$
$$+\frac{D_1r_{C1}^2}{L_1+L_2}\{\frac{-T}{8L_2^2L_1C_1}(2L_1C_1-TD_1^2C_2R_E)(D_2L_2+D_1L_1+2L_1D_2-L_2)-\frac{D_1^2L_1(R+R_E)}{2D_2^2R^2(L_1+L_2)}$$
$$\frac{L_2D_1(2D_2-1+D_1)}{4D_2^2L_2R^2}\{\frac{TRR_E}{C_1L_1}(D_1^2L_1C_1+D_1L_1C_1+D_2L_2C_1)+2R+2R_E\}$$
$$\frac{T}{4L_1R^2}\{\frac{D_1^2C_1L_1^2(D_2-1)}{D_2^2L_2C_1(L_1+L_2)}+D_2R_E\}\}$$

$$d_{dv}=\frac{(1+R_E/R)}{C_1(L_1+L_2)}\{1-\frac{TD_1r_{C1}}{4L_1L_2}(L_1+D_2L_2)+\frac{D_1r_{C1}}{4D_2L_2^2R}\{\frac{TD_1^2r_{C1}}{2L_1}(L_1-D_1L_1-D_2L_2$$
$$-2D_2L_1)(2L_E-TD_1R)+\{TD_1^2r_{C1}+2L_2(D_1D_2-D_1^2-D_2)\}L_E/D_2\}$$
$$+\frac{D_1r_{C1}L_E(D_1L_2-D_2L_1)}{4L_1^2L_2D_2^2R}\{L_1(2D_1L_2-2D_2L_2+TD_1^2r_{C1})-4TD_2^2D_2R(L_1+L_2)\}\}$$

$$a_{vv}=L_1C_2r_{C2}R_E[2L_2(2D_2+D_2)-D_2^2Tr_{C1}]$$

$$b_{vv}=\{2L_1L_2C_1(1+R_E/R)(2D_1+D_2)+TD_1^2D_2C_2R_E(L_1+L_2)$$
$$+(2D_2L_1-L_2+D_1L_1+D_2L_2)TD_1^2C_1C_2R_Er_{C1}^2/(L_1+L_2)$$
$$+L_1C_1r_{C1}[D_2L_1+2L_2(2D_1+D_2-1)(D_1+D_2)]2C_1R_E/(L_1+L_2)-(R+R_E)TD_1^2/R]\}$$

$$c_{vv}=(1+R_E/R)[TD_1^2D_2(L_1+L_2)+\{2(D_1+D_2)(2D_1+D_2-1)L_2+D_1L_1\}2L_1C_1r_{C1}(L_1+L_2)$$
$$-(2D_2L_1+D_1L_1-L_2+D_2L_2)TD_1^2C_1r_{C1}^2/(L_1+L_2)\}$$
$$+4D_1L_1C_1R_E[D_1L_1-L_1-D_2L_2-2D_2L_2D_2]TD_1r_{C1}/(4L_1L_2)+1]$$

$$d_{vv}=(1+R_E/R)\{4D_1L_1+\{D_1L_1-L_1-D_2L_2-2D_2L_2D_2\}TD_1^2r_{C1}/L_2\}$$

$$a=1+\frac{R_ETD_1}{2L_E},\quad b=\frac{(1-2D_2)r_{C1}}{L_1+L_2}+\frac{D_1^2T}{2L_2C_1},\quad c=\frac{1}{C_1(L_1+L_2)}(1-\frac{D_1^2TDr_{C1}}{L_2})$$

TABLE II
CONVERTER PARAMETERS

Circuit Parameters	Values
V_g / V_o	15 / 5V
C_1 / C_2	47 / 200μF
r_{C1} / r_{C2}	0.38 / 0.095Ω
R	10Ω
L_1 / L_2	100/ 30μH

V. CONCLUSION

In this paper, modeling of a DCM SEPIC converter with State-Space Averaging (SSA) technique has been presented. The modeling yielded a steady-state and linear small-signal equations of the converter in (13) and (16) respectively. From (16), the transfer functions $G_{d1v}(s)$ and $G_{vv}(s)$, which provide a basis for feedback control design, were derived. The obtained $G_{d1v}(s)$ was compared against the result from the DCM averaged switch model [2]. Good consistency between the two results was observed only at frequencies below 10kHz, or one tenth of the switching frequency. Above this frequency, the derived $G_{d1v}(s)$ became invalid. Due to this limitation, if the derived models in (17) and (18) were to be used in feedback control design, a crossover frequency must be selected in the frequency region where these models are legitimate.

REFERENCES

[1] S. Cuk and R. D. Middlebrook, "A general unified approach to modeling switching DC-to-DC converters in discontinuous conduction mode," in *Proc.* IEEE PESC'77, 1977.

[2] R. W. Erickson and D. Maksimović, *Fundamentals of Power Electronics*, 2nd ed., Kluwer Academic Publishers, 2001.

[3] L. G. De Vicuna, F. Guinjoan, J. Majo, and L. Martinez, "Discontinuous conduction mode in the SEPIC converter," *Proc. of Electrotechnical Conference on Integrating Research, Industry and Education in Energy and Communication Engineering*, page. 38-42, April 1989.

[4] E. Niculescu, M. C. Niculescu, and D. M. Purcaru, "Modelling the PWM SEPIC converter in discontinuous conduction mode," *Proc. of the 11th WSEAS International Conference on Circuits*, July 2007.

[5] Jian Sun, D. M. Mitchell, M. F. Greuel, P. T. Krein, and R. M. Bass, "Averaged modeling of PWM converters operating in discontinuous conduction mode," *IEEE trans. on Power Electronics*, July 2001.

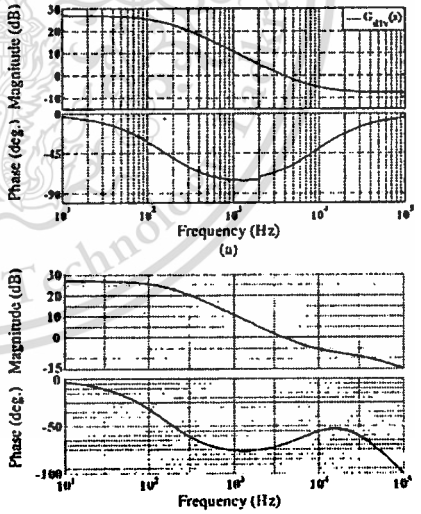

Fig. 4 (a) Frequency response of $G_{d1v}(s)$: (a) with MATLAB and (b) with PSPICE.